AD_____

Award Number: **W81XWH-10-1-0771**

TITLE: **Characterizing and Targeting Androgen Receptor Pathway-Independent Prostate Cancer**

PRINCIPAL INVESTIGATOR: **Peter S. Nelson, MD**

CONTRACTING ORGANIZATION: **Fred Hutchinson Cancer Research Center**
Seattle, WA 98109

REPORT DATE: November 2013

TYPE OF REPORT: **Final**

PREPARED FOR: U.S. Army Medical Research and Materiel Command
Fort Detrick, Maryland 21702-5012

REPORT DOCUMENTATION PAGE

Form Approved
OMB No. 0704-0188

1. REPORT DATE	2. REPORT TYPE	3. DATES COVERED
01 November 2013	FINAL	1 Sep 2010 – 31 Aug 2013

4. TITLE AND SUBTITLE
Characterizing and Targeting Androgen Receptor Pathway-Independent Prostate Cancer

5a. CONTRACT NUMBER

5b. GRANT NUMBER
W81XWH-10-1-0771

5c. PROGRAM ELEMENT NUMBER

6. AUTHOR(S)
Peter S. Nelson

E-Mail: pnelson@fhcrc.org

5d. PROJECT NUMBER

5e. TASK NUMBER

5f. WORK UNIT NUMBER

7. PERFORMING ORGANIZATION NAME(S) AND ADDRESS(ES)
Fred Hutchinson Cancer Research Center
Seattle, WA 98109-1024

8. PERFORMING ORGANIZATION REPORT NUMBER

9. SPONSORING / MONITORING AGENCY NAME(S) AND ADDRESS(ES)
U.S. Army Medical Research and Materiel Command
Fort Detrick, Maryland 21702-5012

10. SPONSOR/MONITOR'S ACRONYM(S)

11. SPONSOR/MONITOR'S REPORT NUMBER(S)

12. DISTRIBUTION / AVAILABILITY STATEMENT
Approved for Public Release; Distribution Unlimited

13. SUPPLEMENTARY NOTES

14. ABSTRACT

In this proposal, we aimed to test the hypothesis that complete AR pathway inhibition selects for subpopulations of tumor cells that are completely independent of AR signaling and further, that these resistant cells will have activated---and be dependent upon---a limited set of specific survival and growth regulatory pathways that can be identified and targeted. The proposal comprised three Specific Aims: Aim 1 will define the genomic alterations and transcript variants that comprise 'states' of ARIPC. Aim 2 will determine if targeting/inhibiting the survival pathway(s) that emerge following AR pathway ablation will restrain tumor growth. Aim 3 will determine if simultaneously co-targeting the AR pathway and ARIPC survival pathway(s) in AR sensitive prostate cancers will augment tumor responses and delay/prevent recurrences. During this funding period we have: (i) completed laser capture microdissection of CRPC prostate cancers to acquire RNA and DNA; (ii) completed transcript profiling for 196 CRPC metastasis; (iii) completed genomic analyses for 196 prostate cancer metastasis; (iv) identified a program of AR-repressed genes that may influence the development of CRPC; (v) completed preclinical studies of three putative AR-bypass pathways; (vi) completed an integrated molecular analysis of AR bypass pathways; and (vii) completed a preclinical trial co-targeting residual AR signaling with AR bypass that suppressed the growth of advanced prostate cancer.

15. SUBJECT TERMS
prostate cancer, androgens, androgen receptor, molecular profiles

16. SECURITY CLASSIFICATION OF:			17. LIMITATION OF ABSTRACT	18. NUMBER OF PAGES	19a. NAME OF RESPONSIBLE PERSON
a. REPORT	b. ABSTRACT	c. THIS PAGE			USAMRMC
U	U	U	UU	94	19b. TELEPHONE NUMBER *(include area code)*

Table of Contents

Introduction

The objective of this project was to exploit data generated in the Nelson and Febbo groups demonstrating that although most CRPC tumors exhibit androgen receptor (AR) activity, there is significant heterogeneity in the level of AR activity within tumors, and some cancers appear to have trivial or no AR activity ("AR-null"). Importantly, even in patients that demonstrate global continued AR activity following AR-targeted therapies, there are infrequent tumor deposits with no AR expression. Thus, with the application of increasingly potent blockade of the androgen axis, resistant clones/tumors exhibiting an "AR-null" signature have emerged and a greater percentage of patients have AR-null CRPC. However, at this time, it is unclear what phenotypes, genotypes, and attendant dominant growth and survival pathways will be operative to "drive" an AR-null prostate malignancy.

The objective of this proposal was to test the hypothesis that complete AR pathway inhibition selects for subpopulations of tumor cells that are completely independent of AR signaling and further, that these resistant cells will have activated---and be dependent upon---a limited set of specific survival and growth regulatory pathways (stemming from genomic alterations in specific oncogene networks) that can be identified and targeted. The research plan comprised 3 Specific Aims to test these hypotheses. Aim 1 was designed to define the genomic alterations and transcript variants that comprise 'states' of ARIPC. Aim 2 was designed to determine if targeting/inhibiting the survival pathway(s) that emerge following AR pathway ablation would restrain tumor growth. Aim 3 was designed to determine if simultaneously co-targeting the AR pathway and ARIPC survival pathway(s) in *AR-sensitive prostate cancers* would augment tumor responses and delay/prevent recurrences.

Body

This proposal was designed as a "synergy" project between the laboratories of Dr. Phil Febbo at the University of California, San Francisco (UCSF) and Dr. Peter Nelson in the Division of Human Biology at the Fred Hutchinson Cancer Research Center (FHCRC). Because these are separate awards to the two investigators, this progress report is specific to tasks from the statement of work (SOW) assigned to the Nelson Lab only (or to progress within the Nelson Lab for joint tasks). As per the instructions, progress is reported in association with each of the relevant tasks listed in the SOW. To complete the Project Aims, we have divided the proposed studies into discrete Tasks. We have numbered these Tasks (e.g. Task 1, Task 2, etc) and have designed them as **N** for Nelson lab, **F** for Febbo lab, and **NF** for Nelson and Febbo joint task. The time frame for the Task is noted as Year (Y1-3) and Quarter (Q1-4). Progress:

Task 1. Animal protocol administration (see previous progress reports)

*1a: Submit established animal protocol to DOD for review (Y1Q1)-**N***

Task completed.

*1b Respond to comments from DOD Review (Y1Q1)—**N***

Task completed and protocols were approved.

*1c Submit revised final animal protocol to Institutional IACUC approval (Y1Q1)—**N***

Task completed and protocols were approved.

*1d Respond to comments from IACUC (Months 7) (Y1Q2)—**N***

Task completed and protocols amended.

*Milestone #1: IACUC Approval of amended animal protocol (Y1Q3)-**N***
Milestone completed and protocol approved. FHCRC IACUC #1775

*Milestone #2: Activate Amended Animal Protocol (Y1Q3)-**N***
Milestone completed and protocol activated.

*1f. Amend/renew animal protocol to include testing of novel pathways (Y2Q2)—**N***
Milestone completed and protocols activated.

*1g. Annual renewal of animal protocol (Y3Q3)—**N***
Milestone completed and protocols activated.

Task 2: Analysis of scientific aim 1: Integration of genome-scale bioinformatics-based approaches with quantitative assessments of gene expression measurements to define the pathways associated with ARIPC

*2a. Laser Capture Microdissection of 150 CRPC specimens (Y1Q3)—**NF***
We have focused this task on 150 CRPC metastatic prostate cancer samples. These were acquired primarily through the rapid tissue acquisition necropsy program and represent single or multiple metastasis from the same patient. During the course of the study, we expanded this aim to include 196 prostate cancer metastasis and primary tumors. Laser Capture Microdissections were performed on each of these 196 tissues to enrich for tumors and appropriate matched cell counterparts and exclude benign components (see details in previous progress report). High quality RNA and DNA was obtained from 196 samples and used for molecular profiling (see tasks below).
Task completed.

*2b. (Revised) Splice variant analysis of 150 CRPC specimens (Y1Q4)—**F***
Task to Dr. Febbo.

*2c. (Revised) SNP/Genomic Copy Number analysis of 150 CRPC specimens (Y1Q4)—**N***
We completed array CGH analyses of 196 tumors and matched benign (constitutional) DNA to determine copy number variation across the prostate cancer genome and followed this up with targeted sequencing to determine single nucleotide polymorphism (SNP) and mutation status. Figure 1 shows the results of the copy number variation analysis (loss/gain) across the 196 prostate samples (included in Y2 progress report). Recurrent high frequency alterations in several loci are shown including amplification of the androgen receptor (AR) and alterations in several genes that may contribute to AR Pathway Independent Prostate Cancer (ARIPC) (**Figure 1**).
Task completed.

*Milestone #3: Complete processing of 150 CRPC specimens (Y1Q4)--**N***
Milestone completed. See above.

*2d. (Revised) Classify each CRPC with respect to AR splice variation (Y1Q3)---**F***
Task to Dr. Febbo.

*2e. (Revised) Classify each CRPC with respect to AR amplification (Y1Q3)---**F***
Task to Dr. Febbo.

*2f. (Revised) Classify each CRPC with respect to AR activity, androgen levels, AR splice variation, and AR copy number (Y1Q4)--**F***

Task to Dr. Febbo.

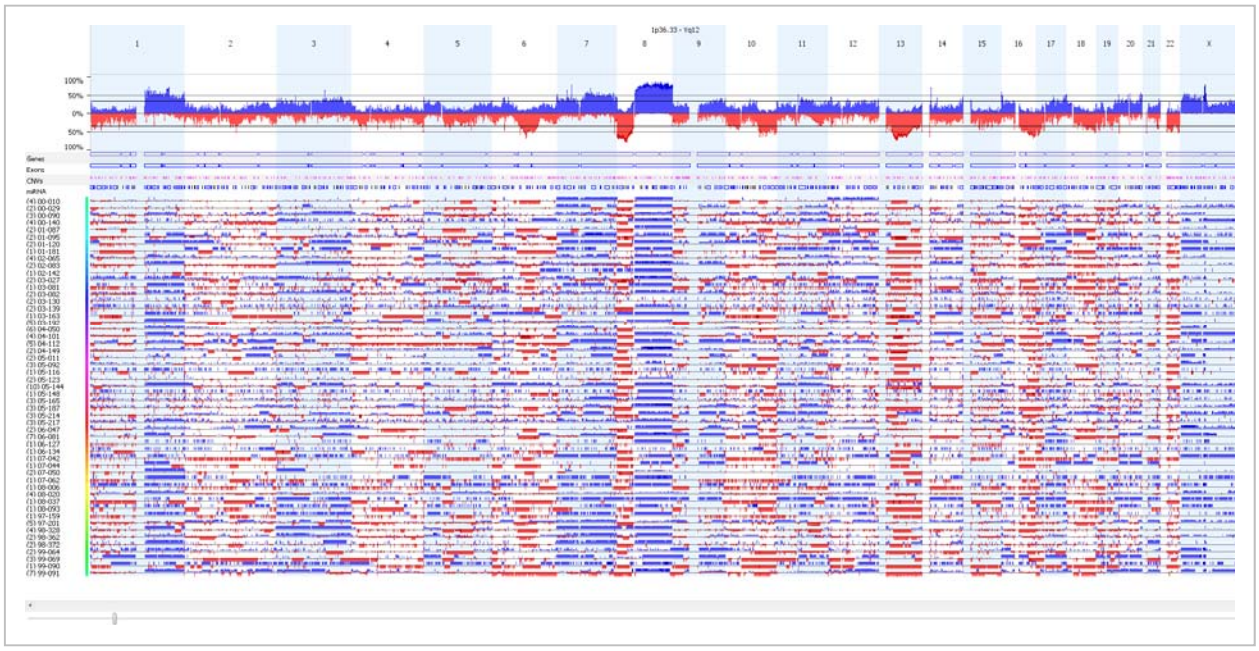

Figure 1. Copy number analyses of prostate cancer metastasis. Red depicts chromosomal regions with copy number gain and Blue depicts regions with copy number loss. X-axis (columns) of figure the full human genome ordered by chromosome (1-X,Y). The Y-Axis (Rows) are individual patients with multiple tumors per patient. Note amplification of chromosome 8 (MYC locus) and X (AR locus). Regions of loss or gain represents a potential pathway promoting ARIPC.

Milestone #4:(Revised) Impact of AR splice variation and AR genetic amplification on classification of CRPC specimens into AR-specific states (Y1Q4)

As described in the Y1 and Y2 progress reports, we have classified the prostate cancer metastasis based on gene expression profiles into AR activity categories and subsequently subdivided the AR activity 'high' category, representing the >90% of the tumors, into subcategories based in AR splice variant status and AR amplification status. The results indicate that most tumors in the AR activity 'high' category has AR amplification, ~70%. Further, ~30% have evidence of one or more splice variants of the AR (V7 or V567) (see Reportable Outcomes: Yu et al 2014). We identified a small number of tumors, ~1% that do not exhibit a neuroendocrine/small cell phenotype and do not express AR or AR target genes. In addition to the microarray classifications, we are including immunohistochemical studies to rule-out neuroendocrine differentiation. **Figure 2** demonstrates ARIPC tumors that are AR-null and that do not exhibit NE differentiation as determined by lack of chromogranin and synaptophysin expression. Milestone Complete

2g. Associate additional pathways with ARIPC. (Y1Q4)—Task to Dr. Febbo

In addition to studies conducted by Dr. Febbo in defining additional pathways associated with ARIPC, we reported in the Y1 Progress Report the identification of a pathway involving LSD1 and H3K4me1,2 demethylation in modulating AR activity. This pathway may represent a

ligand-independent subtype of CRPC, still dependent on AR signaling, but does not appear to promote or represent a driver of ARIPC (see Reportable Outcomes Cai et al 2011).

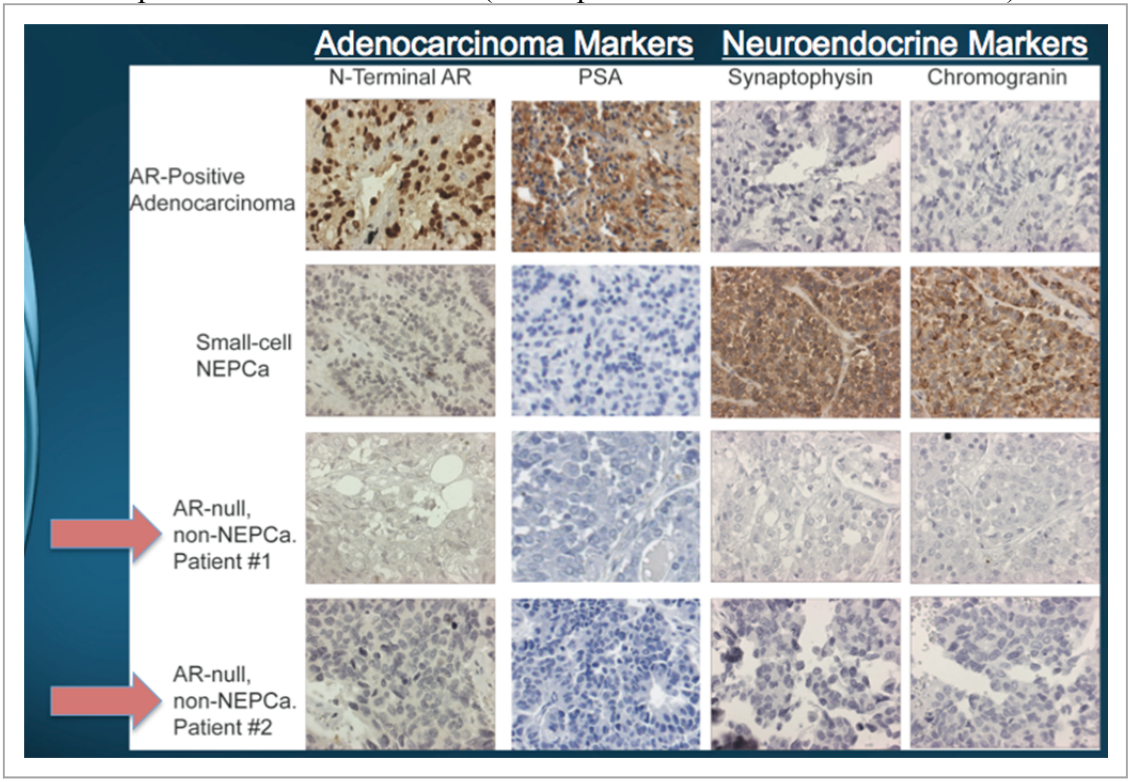

Figure 2. IHC of metastatic prostate cancers showing AR and PSA expression (AR activity) and NE-cell differentiation.

As described in the Y2 progress report, we performed a high-throughput RNAi screen (HTRS) using two androgen-sensitive prostate cancer cell lines; LNCaP and VCaP to identify genes capable of promoting the growth of prostate cancer cells in the absence of exogenous AR ligands,. We hypothesized that a subset of genes and gene networks could confer a castration-resistant phenotype in prostate cancer cells previously dependent upon androgen-mediated signaling for growth and survival.

Briefly, cells were cultured in charcoal-dextran stripped fetal bovine serum (CSS) in order to simulate androgen deprivation therapy.

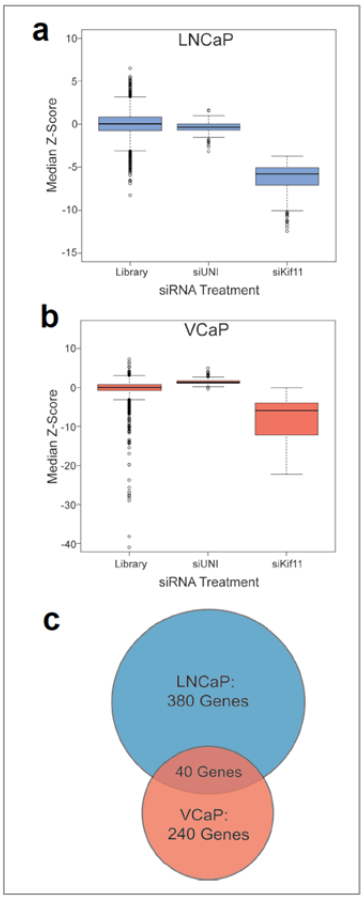

Figure 3. High throughput RNAi screening identifies suppressors of CRPC growth. Pools of siRNAs targeting 6650 genes (Library) were used to knockdown individual gene targets in LNCaP and VCaP cells grown in androgen-depleted medium. HTRS Z-score results are plotted for the LNCaP (a) and VCaP (b) cell lines. siUNI is a non-targeting scrambled control siRNA. siKif11 is a positive control cell death-inducing siRNA targeting Kif11.
(c) In the library screen, 380 siRNAs and 240 siRNAs induced castration-resistant growth in LNCaP or VCaP, respectively. Of these, 40 genes induced growth in androgen depleted conditions in both cell lines (Significance threshold: Z≥1.96).

A library of siRNAs designed to inhibit the translation of 6650 individual genes (designated the 'druggable genome') was used in an arrayed screening strategy whereby a pool of three siRNAs targeting each specific gene was separately introduced into replicate cell cultures (one gene per well) in 384-well culture plates. After 96 hours of growth, cell numbers were estimated using the Cell Titer-Glo luminescence reagent. Raw luminescence signal intensity from the HTRS screen was transformed into Z-scores within each plate, and median standardized Z-scores for each gene were used in downstream analysis. To prioritize genes for further study, we arbitrarily set a significance threshold of $Z \geq 1.96$. At this cut-point, suppression of 380 unique genes in LNCaP and 240 unique genes in VCaP induced cell growth in the absence of exogenous androgens (**Figure 3**), of which 40 induced growth in both cell lines. Of the 40 genes whose suppression induced growth in both LNCaP and VCaP cells, 2 encoded components of the PP2A serine and threonine phosphatase complex: PPP2R2C and PPP2R1A.

*2h. Validate additional pathways with ARIPC (Y2Q4)—**NF***

As detailed in the Y2 progress report, we prioritized HTRS hits exhibiting potential tumor-suppressor expression patterns by cross-referencing the screen results with transcript abundance levels determined by microarray measurements of laser-capture microdissected benign prostate epithelia (n=15), ADT-resistant primary prostate tumors (n=14), and CRPC metastases (n=54). Out of the 40 proliferation-suppressor genes identified in the *in vitro* HTRS, 14 genes were significantly downregulated in primary and metastatic CRPC samples compared to benign prostate epithelia, including PPP2R2C and PPP2RA1 (See Y2 Progress Report). Specifically, the mean expression of PPP2R2C in these primary and metastatic cancers was 3.85-fold lower (P=0.034) and 5.69-fold lower (P<0.001) than benign prostate epithelia, respectively. PPP2R1A expression was also decreased in metastatic prostate tumors (1.55-fold, P<0.001).

We next evaluated HTRS experimental results and human prostate gene expression data for evidence of other PP2A components behaving as tumor suppressors. Previous studies have

Figure 4 (Right). Genes with significant growth suppressing effects in the context of CRPC. Suppression of these genes with siRNA promoted the growth of prostate cancer cells in the absence of AR ligands.

Genes Promoting ARIPC Growth.

Official Gene Symbol	Gene ID	Gene Name	Median Z-Score	
			LNCaP	VCaP
APOB	338	Apolipoprotein B (including Ag(x) antigen)	2.43	1.97
AQP8	343	Aquaporin 8	2.40	2.26
ART4	420	ADP-ribosyltransferase 4	2.03	2.72
CAPN13	92291	Calpain 13	2.11	2.29
CYP2A6	1548	Cytochrome P450, family 2, subfamily A, polypeptide 6	2.19	2.15
DNAJB2	3300	DnaJ (Hsp40) homolog, subfamily B, member 2	3.79	2.09
DPEP1	1800	Dipeptidase 1	3.22	2.14
ESRRB	2103	Estrogen-related receptor beta	2.51	2.81
GABRA2	2555	Gamma-aminobutyric acid A receptor, alpha 2	2.44	2.53
GBP7	388646	Guanylate binding protein 7	3.07	2.86
IDS	3423	Iduronate 2-sulfatase	2.00	2.25
KCND2	3751	Potassium voltage-gated channel, Shal-related subfamily, 2	2.20	3.07
KCTD5	54442	Potassium channel tetramerisation domain containing 5	3.13	2.47
KCTD12	115207	potassium channel tetramerisation domain containing 12	3.54	3.81
KIF2C	11004	Kinesin family member 2C	2.01	2.01
KLHL3	26249	Kelch-like 3	2.39	2.54
KLHL13	90293	Kelch-like 13	3.16	2.42
LAMB2	3913	Laminin, beta 2	3.48	3.46
MGC26694	284439	Hypothetical protein MGC26694	3.49	7.26
MIPEP	4285	Mitochondrial intermediate peptidase	2.27	2.67
NPM2	10361	Nucleophosmin/nucleoplasmin, 2	2.26	2.43
NR2F1	7025	Nuclear receptor subfamily 2, group F, member 1	2.34	3.45
PAFAH1B1	5048	Platelet-activating factor acetylhydrolase, isoform Ib, alpha	2.70	2.20
PAQR4	124222	Progestin and adipoQ receptor family member IV	2.38	2.25
PLOD2	5352	Procollagen-lysine, 2-oxoglutarate 5-dioxygenase 2	2.32	3.09
PPP2R1A	5518	Protein phosphatase 2 regulatory subunit A (PR65 alpha)	2.20	3.29
PPP2R2C	5522	Protein phosphatase 2 regulatory subunit B (PR55 gamma)	2.81	2.10
PYGM	5837	Phosphorylase, glycogen; muscle	3.29	2.25
RAD23A	5886	RAD23 homolog A	3.21	2.04
RARG	5916	Retinoic acid receptor, gamma	2.04	2.05
RHD	6007	Rhesus blood group, D antigen	2.41	2.03
RNF20	56254	Ring finger protein 20	3.01	2.03
RNF144	9781	Ring finger protein 144	2.39	2.77
SRM	6723	Spermidine synthase	2.34	2.07
TNXB	7148	Tenascin XB	2.32	2.57
TOPBP1	11073	Topoisomerase (DNA) II binding protein	2.48	2.22
UBA6	55236	Ubiquitin-like modifier activating enzyme 6	2.01	2.09
UNC5C	8633	Unc-5 homolog C	3.68	3.18
USP21	27005	Ubiquitin specific protease 21	2.13	2.17
ZFAND3	60685	Zinc finger, AN1-type domain 3	3.83	3.65

reported that suppression of the PP2A constituents PPP2CA and PPP2R2A can promote castration-resistant prostate cancer cell growth. However, transcripts encoding these PP2A subunits were not down-regulated in the primary prostate cancers we evaluated. Further, transcripts encoding PPP2CA were significantly higher in metastatic CRPC (1.9-fold, $p<0.001$. In the HTRS experiments, siRNAs targeting PPP2CA or PPP2R2A did not induce significant castration-resistant growth in either LuCAP or VCaP cells.

Milestone #5: Identifications of additional pathways associated with ARIPC (Y2Q2)

Through the gene expression profiling studies and the RNAi screening studies we have identified several genes and pathways with the potential to modulate ARIPC growth. These include MYC, HDACs, LSD1, PPP2R2C, Fibroblast growth factors (FGFs), 3BHSD1 and others listed in **Figure 4** (see Reportable Outcomes Chang et al 2013). Confirmation of the effects of modulating components of these pathways was conducted under Task 3 (below).

Milestone Complete.

Task 3: Analysis of scientific aim 2: To determine if targeting/inhibiting the pathway(s) associated with ARIPC will restrain prostate tumor growth.

3a.(Revised) Determine the impact of inhibiting MYC in ARIPC (Y2Q4)-N

Our preliminary studies indicated that Myc expression can promote the growth of prostate cancer cells in the absence of AR ligands (**Figure 5**). We further determined that AR suppression also suppresses Myc-target genes further supporting the interaction of these signaling programs (**Figure 6**). We further investigated the effects of Myc-pathway antagonisms on the growth of ligand-independent prostate cancer and found that Myc suppression markedly reduced the growth of androgen-independent prostate cancers (see Task 3d and appended manuscript: Gao et al PLOS One 2013). Ongoing experiments are evaluating whether Myc can completely bypass the requirement of AR and whether Myc suppression can suppress the growth of ARIPC.

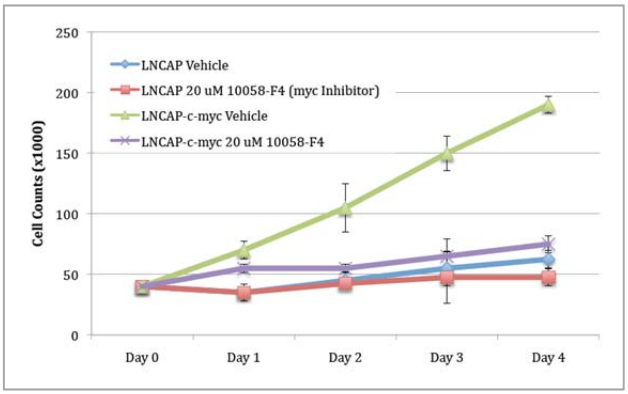

Figure 5. Myc expression promotes the growth of AR ligand dependent prostate cancer cells in the absence of AR ligands. The effect is blocked by the addition of the Myc inhibitor, 10058-F4.

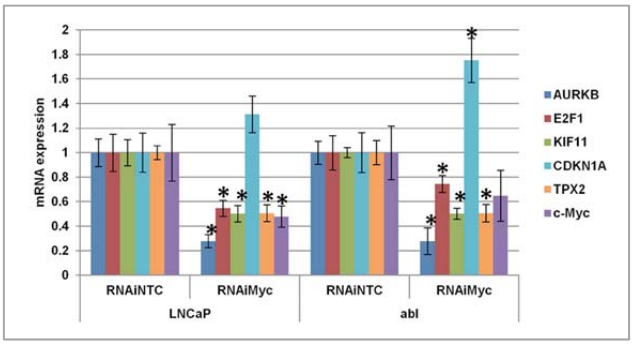

Figure 6. AR suppression recapitulates the effect of c-Myc suppression on c-Myc target gene expression. LNCaP and abl cells were transfected with 50 nM of non-targeted control (NTC) c-Myc RNAi oligonucleotides. Cells were switched to charcoal-stripped serum on the day of transfection and harvested 96 hours later. QRT-PCR was performed to determine the levels of the indicated c-Myc target genesrelative to actin. *denotes p,0.05 compared to NTC.

*3b. (Revised) Determine the impact of targeting HDAC family members in ARIPC (Y2Q4)—**F***
Task to Dr. Febbo.

*Milestone #6: (Revised) Results demonstrating the impact of MYC and HDAC inhibition on ARIPC xenografts (Y2Q4)-**F***
Task to Dr. Febbo.

3c. Determine the impact on ARIPC growth of inhibition of candidate pathway #1 identified during Tasks 2g and 2h-(Y3Q3)NF

As detailed in the Y2 progress report, as four of the 16 PP2A subunits tested in the HTRS experiments induced AR ligand-independent proliferation in at least one cell line, we sought to further assess the mechanism(s) by which PP2A activity contributes to this phenotype. We selected PPP2R2C for further investigation based on the findings that PPP2R2C induced significant castration-resistant proliferation in both cell lines evaluated, and PPP2R2C was the HTRS hit found to be most down-regulated in castration-resistant metastatic prostate cancer compared to benign epithelium.

Because the HTRS experiments were performed using pools of three siRNAs targeting each gene, we evaluated individual siRNA efficacy by transfecting LNCaP and VCaP with the deconvoluted pool of PPP2R2C siRNAs, designated siRNA #1-3. Suppression of PPP2R2C by gene-specific siRNA was confirmed by qRT-PCR and correlated with assays of cell proliferation. PPP2R2C knockdown by si#2 and si#3 were confirmed at the protein level in both cell lines (**Figure**

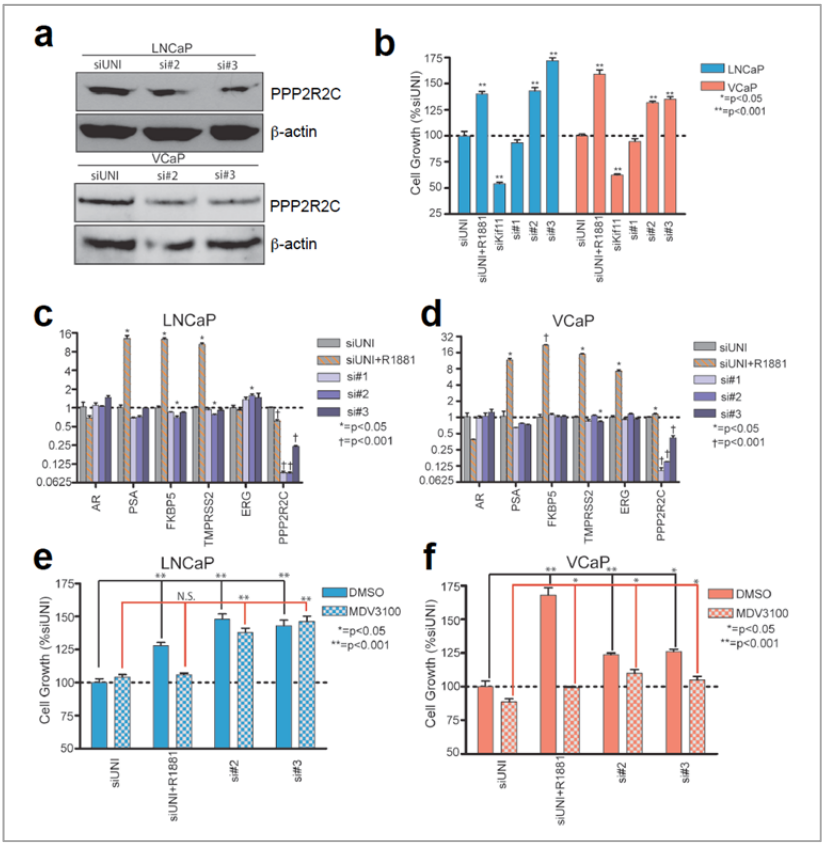

Figure 7. siRNA knockdown of PPP2R2C induces growth in LNCaP and VCaP through pathways independent of the Androgen Receptor. LNCaP and VCaP were transfected with PPP2R2C siRNAs (si#1-3), in addition to a scrambled control (siUNI) and a positive control for transfection (siKif11). siUNI + 1nM R1881 is a positive control for androgen-induced cell growth and gene expression. (a) Western immunoblot analysis of PPP2R2C protein with siRNAs targeting PPP2R2C. (b) Growth of LNCaP and VCaP cells in androgen-depleted medium is induced by PPP2R2C-targeted siRNA (c – d) qRT-PCR analysis of cDNA collected from LNCaP (c) and VCaP (d) demonstrates successful suppression of PPP2R2C expression. PPP2R2C knockdown does not increase the expression of AR or AR-regulated genes (PSA, FKBP5, TMPRSS2, ERG). Co-treatment with non-targeting siRNA + 1nM R1881 induced AR-regulated gene expression. Statistical comparisons of gene expression were performed between siUNI and gene-specific siRNA within each cell line. (e – f) LNCaP (e) and VCaP (f) were transfected with non-targeting siRNA or siRNA targeting PPP2R2C and co-treated with 5μM MDV3100.

7a). Scrambled control siRNAs (siUNI) did not alter PPP2R2C expression or influence cell proliferation (**Figure 7b**). The positive control for cell death, siKiff11, substantially reduced the number of tumor cells in both LNCaP and VCaP experiments (**Figure 7b**). As expected, exposing LNCaP or VCaP cells to androgen (R1881) stimulated proliferation and induced the AR target genes PSA, FKBP5, TMRPSS2, and ERG (in VCaP; **Figure 7b-d**). siRNA#1 suppressed PPP2R2C transcripts by 10-fold in both cell lines, but did not influence cell proliferation in either line. However, both siRNA #2 and siRNA #3 reduced PPP2R2C mRNAs in LNCaP by 11.1-fold and 4.2-fold (P<0.001), respectively (**Figure 7b-c**), and induced cell proliferation in androgen-depleted medium by 42% (siRNA #2, P<0.001) and 72% (siRNA #3, P<0.001). This increase in cell number approximated the influence of adding the androgen R1881 (**Figure 7b**). In VCaP cells PPP2R2C transcripts were reduced 6.7-fold by siRNA #2 and 4.2-fold by siRNA #3 (P<0.001; **Figure 7d**), and these siRNAs increased cell proliferation by approximately 33% in androgen depleted growth conditions (P<0.001; **Figure 7b**). PPP2R2C suppression did not alter AR or PSA expression in either cell line (**Figure 7c-d)**. Suppression of PPP2R2C with siRNA #2 in LNCaP cells did slightly decrease the expression of FKBP5 (1.4-fold, P=0.02) and TMPRSS2 (1.3-fold, P=0.02) and resulted in a 1.6-fold increase in ERG expression (P=0.01; **Figure 7c**). Suppression of PPP2R2C with siRNA #3 in VCaP resulted in decreased TMPRSS2 expression (1.2-fold, P=0.01; **Figure 7d**). PPP2R2C downregulated with si#3 in LNCaP and si#2 in VCaP did not affect androgen-regulated gene expression. These data indicate that the growth advantages attained from PPP2R2C knockdown were not mediated by an increase in canonical AR transcriptional activity.

To further assess the potential role of the AR in PPP2R2C mediated prostate cancer cell growth in the context of androgen depletion, LNCaP and VCaP cells were treated with the AR antagonist MDV3100. In the absence of exogenous androgens, MDV3100 had a slight effect in reducing VCaP cell numbers after 96 hours (12%, p=0.05) and no discernable effect on LNCaP growth (**Figure 7e-f**). As expected, MDV3100 effectively suppressed the proliferative effects induced by the synthetic androgen R1881 in both lines (**Figure 7e-f**). Suppression of PPP2R2C induced cell proliferation in VCaP cells (si#2: 24%, p<0.001; si#3: 18%, p=0.002) and LNCaP cells (si#2: 32%, p<0.001; si#3: 40%, p<0.001) in androgen-depleted medium despite treatment with MDV3100 (**Figure 7e-f**). Collectively, these experiments confirm that PPP2R2C loss is sufficient to induce AR pathway-independent proliferation in prostate cancer cells.

Task Completed

3d. Determine the impact on ARIPC growth of inhibition of candidate pathway #2 identified during Tasks 2g and 2h--(Y3Q4) NF

Results of the gene expression profiling studies comparing ARIPC tumors with those expressing an active AR signaling program identified the FGF/FGFR signaling axis as a potential mediator of ARIPC progression. Our studies confirmed that autocrine FGF contributes to the proliferation of $LNCaP^{APIPC}$ cells and also promotes the growth of parental LNCaP cells in the absence of androgens (**Figure 8**). In contrast to previous studies demonstrating a reciprocal feedback loop involving PI3K signaling in the context of AR pathway suppression, we found minimal activity of the PI3K pathway in APIPC cells in the complete absence of AR (**Figure 8B**), but substantial activity of the MAPK pathway (**Figure 8C**). The MAPK pathway was activated in parental LNCaP cells by exogenous FGF8b, and MAPK activity and cell proliferation were each inhibited in both parental LNCaP and APIPC cells after exposure to the fibroblast growth factor receptor (FGFR) inhibitor PD173074 (**Figure 8D,E**). Expression of FGF8b promoted the growth

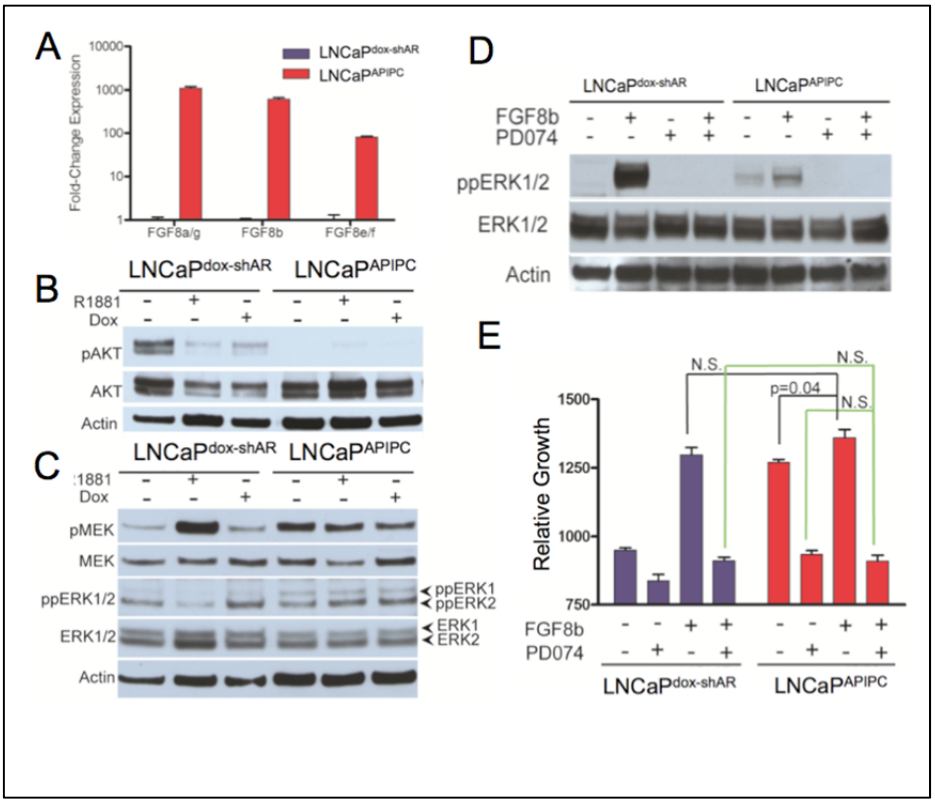

Figure 8: FGF8 signaling functions as an autocrine growth pathway in APIPC. (A) qRT-PCR confirms FGF8 is upregulated in APIPC cells relative to the parental LNCaP line. (B) The AKT pathway is not activated in APIPC cells. (C) The MEK pathway is hyper-activated in APIPC cells in the absence of androgen (R1881) or AR (Dox-induced suppression). (D) Exogenous FGF8b activates MAPK pathway signaling in parental LNCaP cells and further induces MAPK activity in APIPC cells. MAPK activity is suppressed by the FGFR inhibitor PD173074 (PD074). (E) FGF8 promotes the proliferation of parental LNCaP cells in the absence of androgens, an effect that was blocked by the co-treatment with PD173074, and suppresses the growth of APIPC cells.

of LNCaP cells in the absence of androgens (**Figure 9**). Further, in short-term growth experiments, LNCaP cells with doxycycline-inducible AR^{shRNA} exposed to FGF8b were able to proliferate following AR knockdown, and transition to an APIPC phenotype (**Figure 9**). Though these experiments provide support for our hypotheses, longer-term studies are required to confirm that autocrine FGF signaling can consistently bypass AR and sustain AR-independent growth.

Task Completed

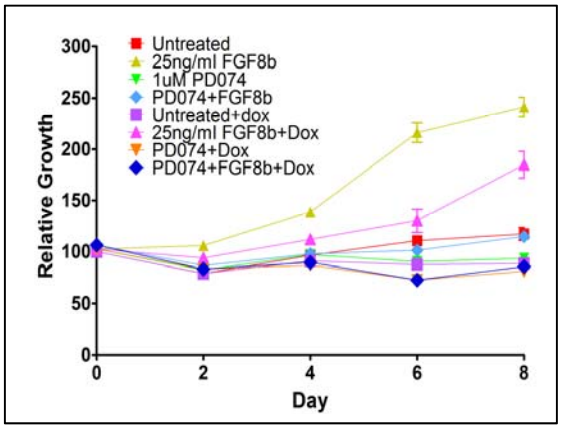

Figure 9. FGF8b allows LNCaP cells to bypass the requirement for AR activity in maintaining proliferation. Shown are growth curves of LNCaP cells expressing a doxycycline-inducible shRNA targeting AR. Exogenous FGF8b maintains cell growth after the addition of Dox to suppress AR (pink triangle). The FGF8 effects are blocked by the FGFR inhibitor PD173074.

*3e. Determine the impact on ARIPC growth of inhibition of candidate pathway #3 identified during Tasks 2g and 2h--(Y3Q4)---**NF***

We have completed studies of three other candidates, RAC1, RAC2, and HSD3B1 that emerged from the initial screens and molecular profiling studies of ARIPC cell growth or assessments of mutation and gene expression alterations in CRPC. RAC1, a member of the rho family of small GTP binding proteins, has been shown to promote androgen ligand-independent growth in LNCaP cells by stimulating the atypical protein kinase C (aPKC) pathway leading to

proliferation. Our studies confirmed this result and determined that RAC2 also confers this phenotype (***Figure 10***). RAC1 inhibitors are currently in development for clinical effects as anticancer agents. HSD3B1 is a steroid metabolic enzyme identified through detailed studies of androgen metabolism by our collaborator Dr Nima Sharifi. Knockdown of HSD3B1 severely impaired the growth of LNCaP prostate cancer cells growing in medium devoid of testosterone or DHT but supplemented with the precursor hormone DHEA (***Figure 11***).

Task Completed.

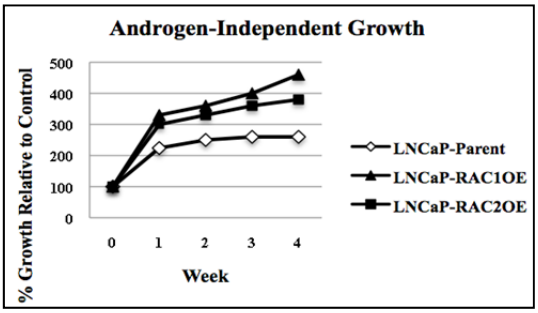

Figure 10. LNCaP cells transduced with RAC1 or RAC2 ORF constructs proliferate in androgen-depleted growth medium.

*Milestone #7: Results demonstrating the impact of inhibition of candidate pathways #1, #2, and #3 on ARIPC xenografts -(Y3Q4)---**N***

We completed studies of agents that inhibit candidate survival pathways in ARIPC xenografts. Individually, we did not observe a substantial effect on growth suppression/improvement in survival. We tested Dasatinib, DNP, metformin, and dutasteride and the combination of metformin with dutasteride. A representative example of the results of the effects of targeting the ARIPC xenograft LuCaP35V with metformin and dutasteride is shown in **Figure 12**. The improvement in survival did not reach statistical significance.

Task Completed.

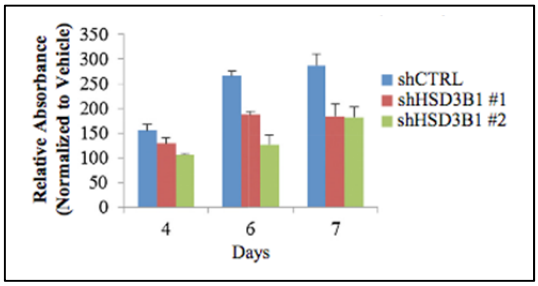

Figure 11. LNCaP cell growth in DHEA-supplemented medium with (shHSD3B1) or without (shCTRL) HSD3B1 suppression.

Task 4: Analysis of scientific aim 3: To determine if simultaneously co-targeting the AR pathway and ARIPC survival pathway(s) in AR-sensitive prostate cancers will augment tumor responses and delay/prevent recurrences.

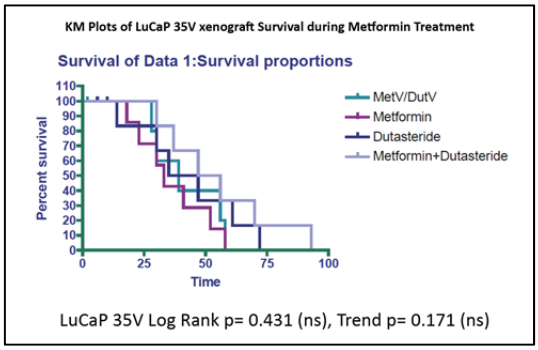

Figure 12. Survival curve of the ARIPC LuCaP35V xenograft treated with vehicle control (MetV/DutV) or the indicated agent.

4a.(Revised) Determine the impact of co-targeting AR and the most promising pathways out of SRC, MYC, OxPhos or HDAC in castration sensitive prostate cancers. (Y2Q4)-N

We have completed experiments co-targeting SRC (with Dasatinib) in two CRPC prostate cancer xenografts. Briefly, CB17-SCID mice were castrated at eight weeks of age. After two weeks recovery, these mice were subcutaneously implanted with a LuCaP 35V or LuCaP49 tumor fragments. Mice were measured daily for tumor growth. When a mouse with a tumor achieved a volume of 200 mm^3, it was enrolled into Vehicle, or Dasatinib treatment groups. Treatments were administered once daily by oral gavage and tumor measurements were conducted every other day. Tumors were harvested from mice when they had a volume greater than 800

mm^3. Paired t-test analysis indicates that there was no significant difference between Vehicle and Dasatinib treatment. Though there was evidence of growth suppression in the LuCaP49 tumors, the overall suppression of CRPC tumor growth is quite modest and unlikely to represent a clinically-meaningful response in these two tumor types (LuCaP35V and LuCaP49) (**Figure 13**).

Task Complete.

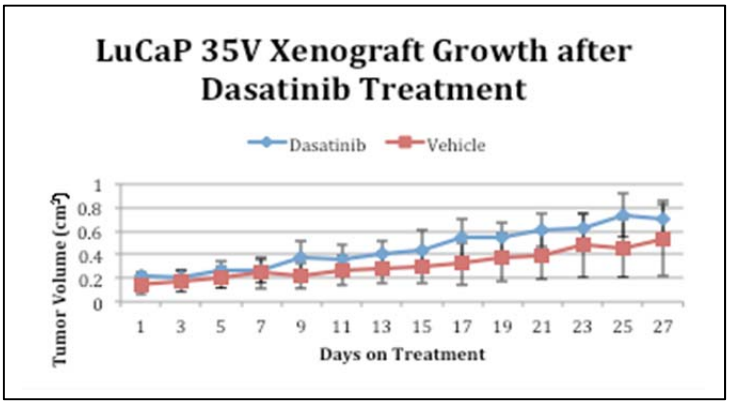

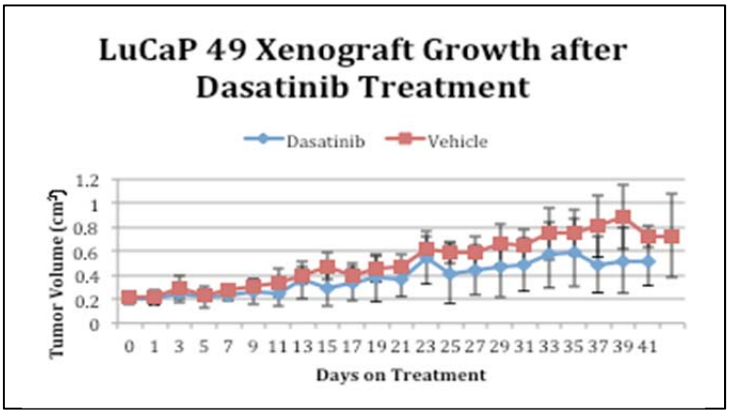

Figure 13. Effect of Dasatinib treatment on the growth of prostate cancer xenografts.

4b. (Revised) Determine the impact of co-targeting the second most promising pathways out of SRC, MYC, OxPhos or HDAC in castration sensitive prostate cancers.- (Y2Q4)---N

We have completed experiments co-targeting the OxPhos pathway (with DNP) in two CRPC prostate cancer xenografts. Briefly, CB17-SCID mice were castrated at eight weeks of age. After two weeks recovery, these mice were subcutaneously implanted with a LuCaP 35V or LuCaP49 tumor fragments. Mice were measured daily for tumor growth. When a mouse with a tumor achieved a volume of 200 mm^3, it was enrolled into Vehicle or DNP treatment groups. Treatments were administered once daily by oral gavage and tumor measurements were conducted every other day. Tumors were harvested from mice when they had a volume greater than 800 mm^3. Paired t-test analysis indicates that there was no significant difference between Vehicle and DNP treatment duration. The overall alteration of CRPC tumor growth is quite modest and unlikely to represent a clinically-meaningful response in these two tumor types (LuCaP35V and LuCaP49) (***Figure 14***).

Task Complete.

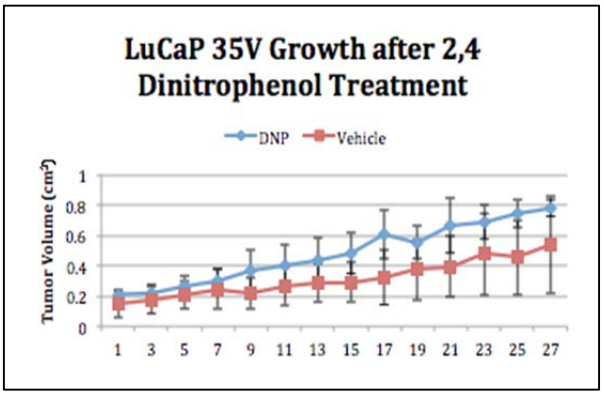

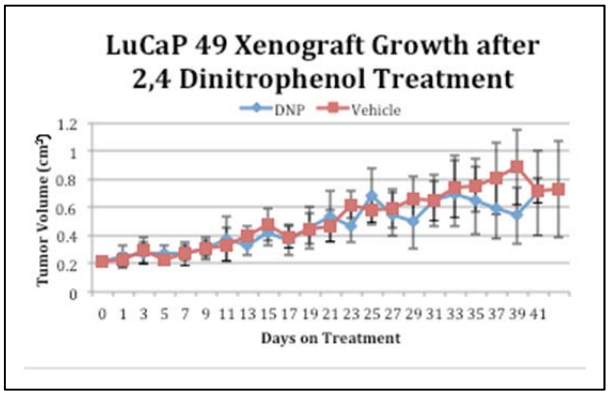

Figure 14. Effect of DNP treatment on the growth of prostate cancer xenografts.

*Milestone #8:(Revised) Results demonstrating the impact of cotargeting AR and either MYC or HDAC inhibition on prostate cancer xenografts. (Y2Q4). -**F***

The *in vitro* studies co-targeting MYC and AR are complete (see Figure 5 above). The xenograft studies were to be conducted by Dr. Febbo. Task to Dr. Febbo.

*4c. Determine the impact on hormone naïve prostate cancer xenograft growth of co-targeting candidate pathway #1 and AR (Y3Q3) --- **NF***

We carried out studies using the androgen sensitive cell line/xenograft VCaP. We co-targeted the AR pathway with castration and the SRC resistance pathway with Dasatinib. Castrate CB17 SCID mice were injected with 1 x 10^6 VCaP cells mixed with matrigel/RPMI media in a 50:50 ratio. Treatments were started when the tumor volume was 0.2 cm^3. The treatments were administered by oral gavage fives times a week. Measurements were taken every two days. Dasatinib dosage was at 15mg/kg/day. No significant differences in tumor growth were observed with Dasatinib treatment (**Figure 15**).

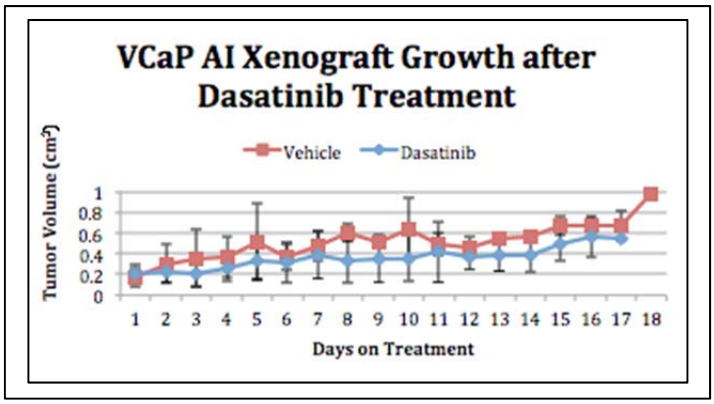

Figure 15. Effects on Dasatinib and androgen suppression on VCaP xenograft growth.

Task Complete.

*4d. Determine the impact on hormone naïve prostate cancer xenograft growth of co-targeting candidate pathway #2 and AR (Y3Q4)--- **NF***

We carried out studies using the androgen sensitive cell line/xenograft VCaP. We co-targeted the AR pathway with castration and the Metabolic resistance pathway with DNP. Castrate CB17 SCID mice were injected with 1 x 10^6 VCaP cells mixed with matrigel/RPMI media in a 50:50 ratio. Treatments were started when the tumor volume was 0.2 cm^3. The treatments were administered by oral gavage fives times a week. Measurements were taken every two days. Dinitrophenol dosage was at 10 mg/kg/day. There were at least four tumors in each treatment group. A significant, but modest growth suppression effect was observed with DNP treatment (**Figure 16**).

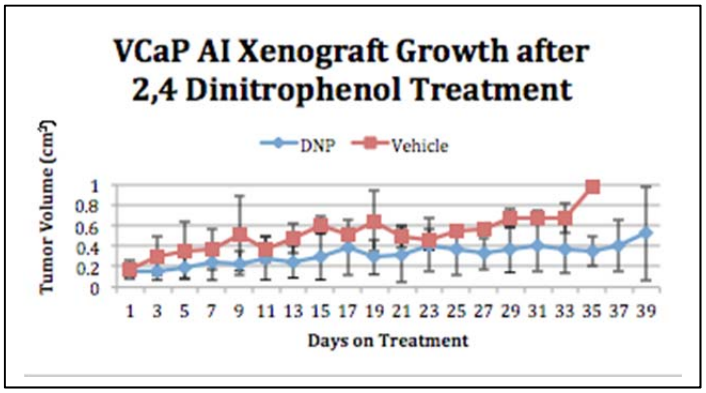

Figure 16. Effects on DNP and androgen suppression on VCaP xenograft growth.

Task Complete.

4e. Determine the impact on hormone naïve prostate cancer xenograft growth of co-targeting

*candidate pathway #3 and AR (Y3Q4) --- **NF***

We carried out studies using the androgen sensitive cell line/xenograft VCaP. We co-targeted the AR pathway with castration and a second Metabolic resistance pathway with Metformin. Castrate CB17 SCID mice were injected with 1 x 10^6 VCaP cells mixed with matrigel/RPMI media in a 50:50 ratio. Treatments were started when the tumor volume was 0.2 cm^3. The treatments were administered by oral gavage fives times a week. Measurements were taken every two days. Metformin dosage was 300 mg/kg/day. There were at least four tumors in each treatment group. An insignificant modest growth suppression effect was observed with metformin treatment (**Figure 17**).

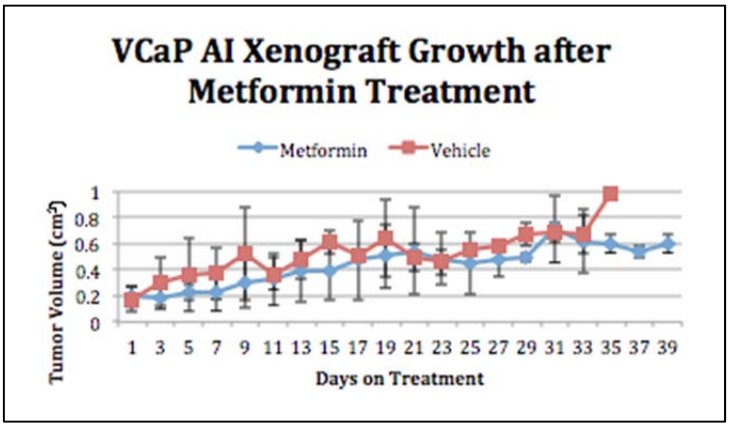

Figure 17. Effects on DNP and androgen suppression on VCaP xenograft growth.

Task Complete.

*Milestone #9: Results demonstrating the impact of co-targeting AR and candidate pathway #1, #2, or #3 on prostate cancer Xenografts --- **NF***

Based on the studies completed in 4c-e showing none to modest effects of targeting the AR pathway with androgen suppression and a secondary metabolic pathway, we opted to attempt to deepen the AR pathway suppression and co-target metabolic effects with metformin. We found that single agent dutasteride suppressed VCaP xenograft growth ($P<0.05$ at 37 weeks) (**Figure 18**) and this effect was further enhanced with the addition of metformin ($P<0.05$ at 20 weeks) (**Figure 19**).

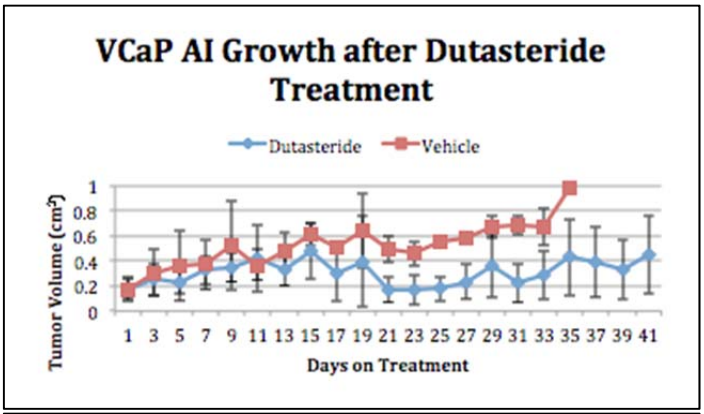

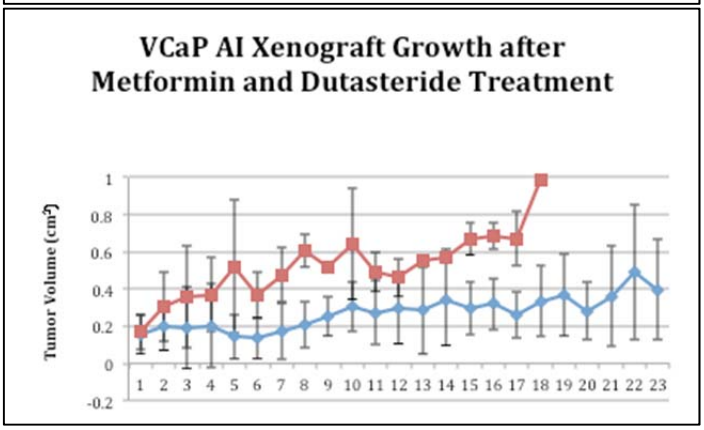

Figure 18 (Top) Effects of Dutasteride and androgen suppression on VCaP xenograft growth.
Figure 19 (Bottom) Effects of Dutasteride, androgen suppression and metformin on VCaP xenograft growth.

Task Complete.

Task 5: Reporting of protocol processes.

5a. Review and summarize pathways specifically associated with ARIPC (Y2Q2)

We completed a series of studies designed to identify molecular alter-

ations that contribute to survival and growth of prostate cancer cells following suppression of the AR pathway leading to AR pathway independent prostate cancer. The molecular profiling studies identified several mechanisms plausibly contributing to ARIPC progression including activation of the SRC pathway, induction of AR splice variants that activate a non-canonical AR signaling program (effectively AR-canonical pathway Independent Prostate Cancer), and augmentation of cellular metabolism. Individually targeting key nodes hypothesized to account for the activation of these pathways did not exert substantial anti-tumor effects including Dasatinib to inhibit SRC, DNP to suppress metabolism/respiratory chain, metformin to suppress metabolism (and AMPK). It is not clear whether each treatment effectively ablated or inhibited the intended signaling pathway, and this will be the focus of future efforts. However, more substantial anti-tumor effects were observed when further targeting the AR pathway (with dutasteride) and metabolism (with metformin). As both of these drugs are approved and widely used clinically, a clinical trial testing the effectiveness of the combination could be implemented without substantial challenges.

Task Complete.

Milestone #10: Abstract submission to AARC annual meeting reporting pathways associated with ARIPC (Y2Q2)

The following abstracts were submitted and presented:

1. Bluemn EG, Annis J, Grandori C, Nelson PS. Exploiting the Genomic Programs Underlying Androgen-Receptor-Null Prostate Cancer. Department of Defense IMPaCT conference. Orlando, FL, March 2011. Poster P6-44.

2. Qu X, Davison J, Bluemn EG, Nelson P, Vessella R, Fang M. Genome-wide methylation analysis in advanced-stage prostate cancer models. AACR-Advances in Prostate Cancer Research Conference, 2012. Orlando, FL, February 2012.

3. Spencer ES, Bluemn EG, Gordon, R, Zhang, X, Johnston, RB, Lucas, J, Nelson, P, Porter, C. Association of decreased expression of protein phosphatase 2A subunit PR55γ (PPP2R2C) with an increased risk of metastases and prostate cancer-specific mortality. ASCO conference. June, 2012.

   Task Complete.

5b. Prepare manuscript reporting identification and validation of pathways specifically associated with ARIPC (Y2Q3)

The following manuscript was submitted for publication in October 2012

> Bluemn EG, Spencer, ES, Mecham, B, Gordon, R, Coleman, I, Lewinshtein, D, Annis, J, Grandori, C, Porter, C, Nelson, PS. PPP2R2C loss promotes castration-resistant prostate cancer growth and is associated with increased prostate cancer-specific mortality. Oncogene. In submission.

Milestone #11: Submit abstract/manuscript reporting identification and validation of pathways associated with ARIPC (Y2Q3)

Task Complete and Milestones Achieved (see 5a and 5b).

5c.Prepare manuscript reporting the impact of inhibiting SRC in castration sensitive and ARIPC prostate cancer xenografts (Y3Q2)

Studies completed and the manuscript is in preparation.

Milestone #12: Submit abstract/manuscript reporting impact of SRC inhibition in castration sensitive and ARIPC xenografts (Y3Q2)

Studies completed and the manuscript is in preparation.

5d.Prepare manuscript reporting the impact of inhibiting oxidative phosphorylation in hormone naïve and ARIPC xenografts (Y3Q2)

Studies completed and the manuscript is in preparation.

Milestone #13: Submit manuscript reporting impact of oxidative phosphorylation inhibition in castration sensitive and ARIPC xenografts (Y3Q2)

Studies completed and the manuscript is in preparation.

5e. Prepare manuscript reporting on the impact of inhibiting candidate pathways #1, #2, and/or #3 in hormone sensitive and ARIPC xenografts (Y3Q4)

Studies are completed and the manuscript is in preparation for submission.

Milestone #14: Submit abstract/manuscript reporting on the impact of inhibiting candidate pathways #1, #2, and/or #3 in hormone sensitive and ARIPC xenografts (Y3Q4)

Studies are completed and the manuscript is in preparation for submission.

Key Research Accomplishments

- We have completed the laser capture microdissection and q/c of attendant RNA/DNA from 196 castration resistant prostate cancers and matched controls.
- We have completed transcript profiling (including AR expression) from 196 prostate cancer metastasis (those with suitable quality RNA) and matched controls.
- We have completed genome analysis (copy number and sequence analysis) for 196 prostate cancer metastasis (those with suitable quality DNA) and matched controls.
- We have completed a high-throughput screen to identify genes and networks involved in maintaining CRPC growth and potentially bypassing AR signaling for facilitating tumor progression. This screen identified components of the PP2A signaling complex as key factors.
- We have completed preclinical trials of 3 key nodes hypothesized to regulate CRPC growth: OxPhos, Src, and AMPK. The Src inhibitor Dasatinib and the OxPhos inhibitor DNP did not delay CRPC growth whereas the SRD5A2 inhibitor dutasteride did inhibit growth.
- We have completed preclinical trials co-targeting the AR pathway with androgen suppression and dutasteride and metabolism/AMPK with metformin and demonstrated a significant suppression of prostate cancer growth.
- We have presented results of these studies at National meetings of prostate cancer research.

Reportable Outcomes

1. Bluemn, EG. Bypassing androgen pathway dependence in advanced prostate cancer. [PhD dissertation]. Seattle, WA: University of Washington; 2012.
2. Spencer ES, Bluemn EG, Gordon, R, Zhang, X, Johnston, RB, Lucas, J, Nelson, P, Porter, C. Association of decreased expression of protein phosphatase 2A subunit PR55γ

(PPP2R2C) with an increased risk of metastases and prostate cancer-specific mortality. ASCO conference. June, 2012.
3. Qu X, Davison J, Bluemn EG, Nelson P, Vessella R, Fang M. Genome-wide methylation analysis in advanced-stage prostate cancer models. AACR-Advances in Prostate Cancer Research Conference, 2012. Orlando, FL, February 2012.
4. Bluemn EG, Nelson PS. The androgen/androgen receptor axis in prostate cancer. Curr Opin Oncol. 2012 May;24(3):251-7.
5. Bluemn EG, Annis J, Grandori C, Nelson PS. Exploiting the Genomic Programs Underlying Androgen-Receptor-Null Prostate Cancer. Department of Defense IMPaCT conference. Orlando, FL, March 2011. Poster P6-44.
6. Cai C, He HH, Chen S, Coleman I, Wang H, Fang Z, Chen S, Nelson PS, Liu XS, Brown M, Balk SP. (2011) Androgen receptor gene expression in prostate cancer is directly suppressed by the androgen receptor through recruitment of lysine-specific demethylase 1. *Cancer Cell*. 2011 Oct 18;20(4):457-71.
7. Chang KH, Li R, Kuri B, Lotan Y, Roehrborn CG, Liu J, Vessella R, Nelson PS, Kapur P, Guo X, Mirzaei H, Auchus RJ, Sharifi N (2013) A Gain-of-Function Mutation in DHT Synthesis in Castration-Resistant Prostate Cancer. *Cell*. 2013 Aug 29;154(5):1074-84
8. Gao L, Schwartzman J, Gibbs A, Lisac R, Kleinschmidt R, Wilmot B, Bottomly D, Coleman I, Nelson P, McWeeney S, Alumkal J. (2013) Androgen receptor promotes ligand-independent prostate cancer progression through c-Myc upregulation. *PLoS One*. 2013 May 21;8(5):e63563
9. Qu X, Randhawa G, Friedman C, Kurland BF, Glaskova L, Coleman I, Mostaghel E, Higano CS, Porter C, Vessella R, Nelson PS, Fang M. (2013) A Three-Marker FISH Panel Detects More Genetic Aberrations of AR, PTEN and TMPRSS2/ERG in Castration-Resistant or Metastatic Prostate Cancers than in Primary Prostate Tumors. *PLoS One*. Sep 30;8(9):e74671
10. Mostaghel EA, Nelson PS, Lange P, Lin DW, Taplin ME, Balk S, Ellis W, Kantoff P, Marck B, Tamae D, Matsumoto AM, True LD, Vessella R, Penning T, Hunter Merrill R, Gulati R, Montgomery B. (2014) Targeted Androgen Pathway Suppression in Localized Prostate Cancer: A Pilot Study. J Clin Oncol. 2014 Jan 20;32(3):229-37 PMID: 24323034
11. Yu Z, Chen S, Sowalsky AG, Voznesensky O, Mostaghel EA, Nelson PS, Cai C, Balk SP (2014) Rapid Induction of Androgen Receptor Splice Variants by Androgen Deprivation in Prostate Cancer. Clin Cancer Res. 2014 Jan 21. PMID: 24449822

Conclusion

We have completed the tasks that comprised the specific aims of our proposal. The data generated from profiling human castration resistant prostate cancer metastasis and shRNA screening studies were used to identify AR-bypass pathways that plausibly contribute to CPRC growth, and specifically, ARIPC progression. Targeting three candidate pathways identified a drug combination, dutasteride and metformin, that when combined with androgen suppression, suppressed the growth of prostate cancer in preclinical models. A clinical trial combining these agents represents the next step in translating these findings to the clinical management of men with prostate cancer.

Appendix.

The following manuscripts detailing experimental methods, results and reportable outcomes are appended to this final report.

1. Cai C, He HH, Chen S, Coleman I, Wang H, Fang Z, Chen S, Nelson PS, Liu XS, Brown M, Balk SP. (2011) Androgen receptor gene expression in prostate cancer is directly suppressed by the androgen receptor through recruitment of lysine-specific demethylase 1. *Cancer Cell*. 2011 Oct 18;20(4):457-71.

2. Chang KH, Li R, Kuri B, Lotan Y, Roehrborn CG, Liu J, Vessella R, Nelson PS, Kapur P, Guo X, Mirzaei H, Auchus RJ, Sharifi N (2013) A Gain-of-Function Mutation in DHT Synthesis in Castration-Resistant Prostate Cancer. *Cell*. 2013 Aug 29;154(5):1074-84

3. Gao L, Schwartzman J, Gibbs A, Lisac R, Kleinschmidt R, Wilmot B, Bottomly D, Coleman I, Nelson P, McWeeney S, Alumkal J. (2013) Androgen receptor promotes ligand-independent prostate cancer progression through c-Myc upregulation. *PLoS One*. 2013 May 21;8(5):e63563

4. Qu X, Randhawa G, Friedman C, Kurland BF, Glaskova L, Coleman I, Mostaghel E, Higano CS, Porter C, Vessella R, Nelson PS, Fang M. (2013) A Three-Marker FISH Panel Detects More Genetic Aberrations of AR, PTEN and TMPRSS2/ERG in Castration-Resistant or Metastatic Prostate Cancers than in Primary Prostate Tumors. *PLoS One*. Sep 30;8(9):e74671

5. Mostaghel EA, Nelson PS, Lange P, Lin DW, Taplin ME, Balk S, Ellis W, Kantoff P, Marck B, Tamae D, Matsumoto AM, True LD, Vessella R, Penning T, Hunter Merrill R, Gulati R, Montgomery B. (2014) Targeted Androgen Pathway Suppression in Localized Prostate Cancer: A Pilot Study. *J Clin Oncol*. 2014 Jan 20;32(3):229-37 PMID: 24323034

6. Yu Z, Chen S, Sowalsky AG, Voznesensky O, Mostaghel EA, Nelson PS, Cai C, Balk SP (2014) Rapid Induction of Androgen Receptor Splice Variants by Androgen Deprivation in Prostate Cancer. *Clin Cancer Res*. 2014 Jan 21. PMID: 24449822

Cancer Cell
Article

Androgen Receptor Gene Expression in Prostate Cancer Is Directly Suppressed by the Androgen Receptor Through Recruitment of Lysine-Specific Demethylase 1

Changmeng Cai,[1] Housheng Hansen He,[2,3] Sen Chen,[1] Ilsa Coleman,[4] Hongyun Wang,[1] Zi Fang,[1] Shaoyong Chen,[1] Peter S. Nelson,[4] X. Shirley Liu,[3] Myles Brown,[2] and Steven P. Balk[1,*]
[1]Hematology-Oncology Division, Department of Medicine, Beth Israel Deaconess Medical Center and Harvard Medical School, Boston, MA 02215, USA
[2]Division of Molecular and Cellular Oncology, Dana-Farber Cancer Institute and Harvard Medical School, Boston, MA 02115, USA
[3]Department of Biostatistics and Computational Biology, Dana-Farber Cancer Institute and Harvard School of Public Health, Boston, MA 02115, USA
[4]Fred Hutchinson Cancer Research Center, University of Washington, Seattle, Washington 91809, USA
*Correspondence: sbalk@bidmc.harvard.edu
DOI 10.1016/j.ccr.2011.09.001

SUMMARY

Androgen receptor (AR) is reactivated in castration-resistant prostate cancer (CRPC) through mechanisms including marked increases in *AR* gene expression. We identify an enhancer in the *AR* second intron contributing to increased *AR* expression at low androgen levels in CRPC. Moreover, at increased androgen levels, the AR binds this site and represses *AR* gene expression through recruitment of lysine-specific demethylase 1 (LSD1) and H3K4me1,2 demethylation. AR similarly represses expression of multiple genes mediating androgen synthesis, DNA synthesis, and proliferation while stimulating genes mediating lipid and protein biosynthesis. Androgen levels in CRPC appear adequate to stimulate AR activity on enhancer elements, but not suppressor elements, resulting in increased expression of AR and AR repressed genes that contribute to cellular proliferation.

INTRODUCTION

The standard treatment for metastatic prostate cancer (PCa) is surgical or medical castration to reduce circulating androgens (androgen deprivation therapy [ADT]) and suppress activity of the androgen receptor (AR), but patients invariably relapse with more aggressive castration-resistant prostate cancer (CRPC). Significantly, early studies showed that AR was highly expressed in CRPC (Ruizeveld de Winter et al., 1994), and further studies in clinical samples and xenograft models have confirmed that AR mRNA is highly expressed and consistently increased in CRPC compared to levels prior to ADT (Taplin et al., 1995; Gregory et al., 2001; Holzbeierlein et al., 2004; Chen et al., 2004; Stanbrough et al., 2006). Multiple androgen regulated-genes, including prostate-specific antigen (*PSA*) and the *TMPRSS2:ERG* fusion gene, are also highly expressed in CRPC, indicating that AR transcriptional activity has been reactivated despite castrate serum androgen levels (Stanbrough et al., 2006; Cai et al., 2009). Mechanisms that may contribute to restoring AR activity in CRPC include AR mutations or alternative splicing, increased intratumoral androgen synthesis, increased coactivator expression, and activation of several kinases that may directly or indirectly sensitize AR to low levels of androgens (Yuan and Balk, 2009). Moreover, studies in xenograft models indicate that even modest increases in AR protein expression may alone render tumors resistant to castration and to available AR antagonists (Chen et al., 2004).

Despite the critical role AR plays in PCa development and progression to CRPC, the mechanisms that regulate its

Significance

This study shows that AR can function through a suppressor element to repress its own expression and the expression of additional genes, including those that mediate androgen synthesis. This negative feedback loop suppresses AR signaling at high androgen levels but allows increased AR and androgen synthesis in CRPC. Moreover, decreased androgen levels in CRPC, although adequate to stimulate AR on enhancer elements, may relieve AR suppression of genes mediating DNA synthesis/proliferation and thereby contribute to tumor growth. Distinct mechanisms of AR action on enhancer versus suppressor elements may make it possible to selectively augment AR transcriptional repressor function and thereby prevent or delay emergence of CRPC.

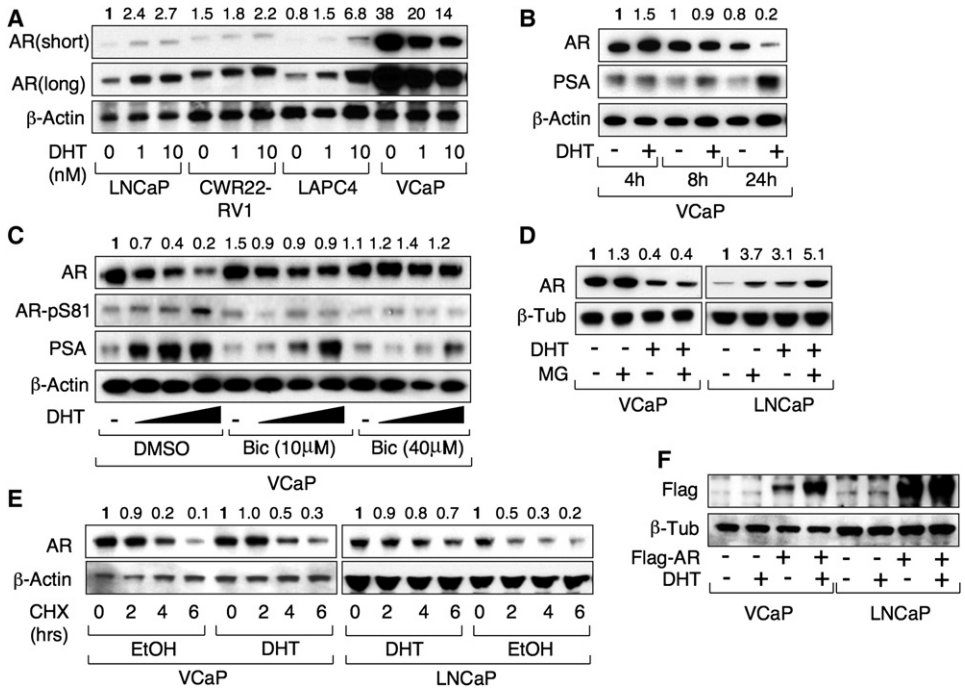

Figure 1. Androgen Decreases AR Protein Expression in VCaP Cells

(A) LNCaP, CWR22Rv1, LAPC4, or VCaP cells were treated with 0, 1, or 10 nM DHT for 24 hr and AR or β-actin were immunoblotted.

(B) VCaP cells were treated with and without DHT for 4, 8, or 24 hr, and AR, PSA, or β-actin were immunoblotted.

(C) VCaP cells were treated with 0, 0.1, 1, or 10 nM DHT and with 0, 10, or 40 μM bicalutamide for 24 hr and immunoblotted for AR, Ser 81 phosphorylated AR, PSA, or β-actin.

(D) VCaP or LNCaP cells were pretreated with and without 10 nM DHT for 24 hr and then treated with MG115/MG132 for 4 hr.

(E) VCaP or LNCaP cells were pretreated with and without DHT for 2 hr and then treated with cycloheximide (10 ng/mL) for 0, 2, 4, or 6 hr.

(F) VCaP or LNCaP cells were transiently transfected with empty vector or 3xFlag-AR. After 24 hr, cells were treated with and without 10 nM DHT for 24 hr (note: the prostate cancer cells were steroid-depleted by culturing in medium with charcoal/dextran stripped serum, CSS, for 3 days before treatments in all experiments). See also Figure S1.

expression and contribute to its increased expression in CRPC are not well understood. AR mRNA levels may be controlled physiologically by a suppressor element in the 5′ UTR of the *AR* gene that regulates transcription (Kumar et al., 1994; Wang et al., 2004, 2008) and by an element in the 3′ UTR that regulates mRNA stability (Yeap et al., 2002). Mechanisms contributing to the increased AR mRNA in CRPC include *AR* gene amplification in about one-third of patients with CRPC (Visakorpi et al., 1995) and increased E2F activity in RB-deficient tumors (Sharma et al., 2010). Previous studies in androgen-sensitive rodent tissues and in LNCaP PCa cells have shown that androgens can negatively regulate *AR* gene transcription, suggesting that AR mRNA may also increase after ADT as a result of relief from this negative regulation (Quarmby et al., 1990; Shan et al., 1990; Krongrad et al., 1991; Blok et al., 1992). However, the androgen-mediated changes in AR mRNA levels in LNCaP cells are modest, and the molecular basis for this negative regulation has not been determined. In contrast to these findings in LNCaP cells, we reported recently that AR mRNA levels in VCaP PCa cells and xenografts were rapidly and substantially increased in response to androgen deprivation, suggesting that relief from AR-mediated negative regulation of *AR* gene expression may make a significant contribution to increasing AR mRNA in CRPC (Cai et al., 2009). This study addresses the molecular basis for this negative regulation of *AR* gene expression by the androgen liganded AR.

RESULTS

Androgen Decreases AR Protein in VCaP Cells

The VCaP PCa cell line was derived from a vertebral metastasis in a patient with CRPC, and it expresses wild-type (WT) AR and AR-regulated genes, such as *PSA* and the *TMPRSS2:ERG* fusion gene (Korenchuk et al., 2001; Loberg et al., 2006; Cai et al., 2009). In the absence of exogenous androgen, AR protein expression in VCaP cells was higher than in other PCa cell lines, including LNCaP, LAPC4, and CWR22Rv1 cells (the latter express a mutant AR with a duplicated exon 3) (Figure 1A). AR protein was increased by 24 hr of DHT treatment in LNCaP, LAPC4, and CWR22Rv1 cells, consistent with previous data showing that androgen binding increases AR protein stability (Kemppainen et al., 1992). In contrast, although AR protein in VCaP was modestly increased after 4 hr of DHT (Figure 1B), it was markedly decreased at 24 hr (Figure 1A) and after 3 days of DHT (see Figure S1, which is available with this article online). This decrease could be blocked by bicalutamide, an AR antagonist, indicating it was dependent on the agonist liganded AR (Figure 1C). Although AR protein was decreased by DHT, serine 81

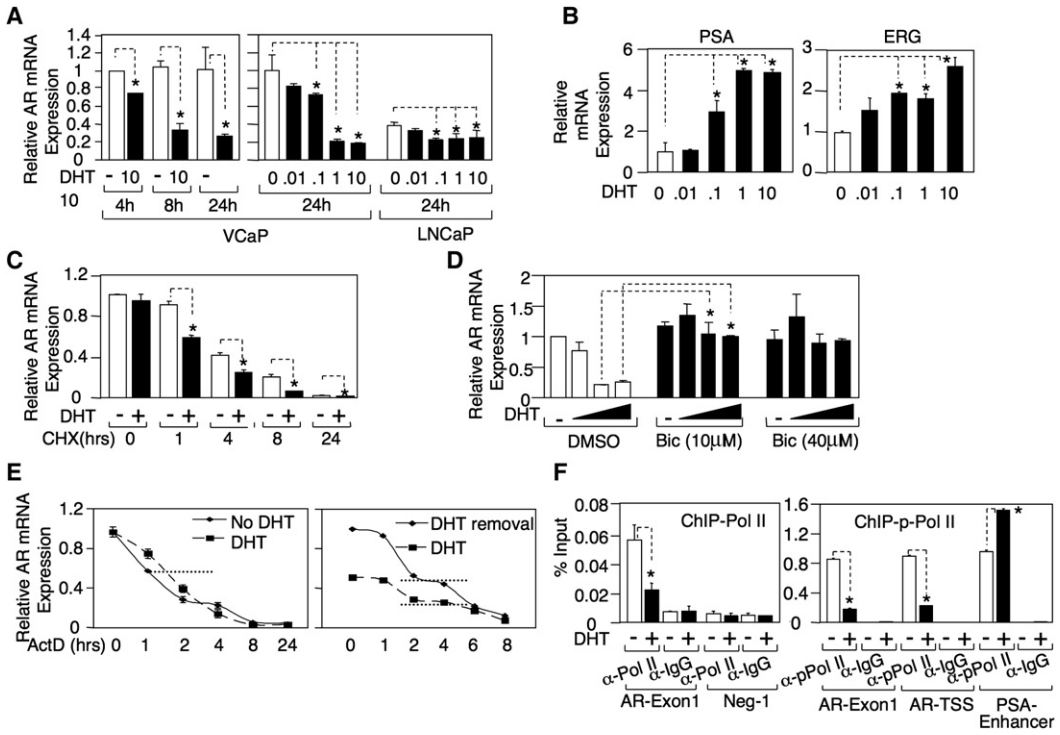

Figure 2. Agonist-Liganded AR Negatively Regulates AR Gene Transcription

(A) VCaP or LNCaP cells were treated with 0, 0.01, 0.1, 1, or 10 nM DHT for 4, 8, or 24 hr and AR mRNA was measured using qRT-PCR.

(B) VCaP cells were DHT stimulated for 24 hr and mRNA for PSA and ERG were measured by qRT-PCR.

(C) VCaP cells were treated with cycloheximide (10 ng/mL) and DHT or vehicle, and AR mRNA was then measured by qRT-PCR after 0, 1, 4, 8, or 24h (mRNA expression was normalized to internal control 18S RNA in all the experiments).

(D) VCaP cells were treated with 0, 0.1, 1, or 10 nM DHT and with 0, 10, or 40 μM bicalutamide for 24 hr and AR mRNA was measured by qRT-PCR.

(E) Left panel: androgen-starved VCaP cells were pretreated with DHT or vehicle for 2 hr followed by addition of actinomycin D (10 μM); right panel: VCaP cells growing in medium with DHT were switched to the same medium with or without DHT for 16 hr, followed by addition of actinomycin D. AR mRNA was measured by qRT-PCR at the indicated times after actinomycin D addition. Levels at time 0 were normalized to 1 under both conditions in the left panel and under the DHT removal condition in the right panel. Dotted lines indicate 50% maximal level.

(F) VCaP cells were treated with or without DHT for 4 hr. The DNA bound to RNA polymerase II or active RNA polymerase II (phospho-Ser5) was immunoprecipitated and measured by qPCR. Error bars in each experiment indicate standard deviation (SD).

phosphorylation (associated with AR transcriptional activity) and PSA expression were markedly increased, indicating that DHT was strongly inducing AR transcriptional activity (Figures 1B and 1C).

AR protein levels in VCaP and LNCaP cells were increased by proteasome inhibitors (MG115 and MG132, MG) in the absence of DHT, but these inhibitors did not prevent the marked decrease in AR protein in response to DHT in VCaP cells, indicating that the molecular basis for this decline was not increased proteasome-mediated AR degradation (Figure 1D). To directly address whether the DHT liganded AR was less stable in VCaP versus LNCaP cells, we pretreated androgen-depleted cells with DHT or vehicle for 2 hr and then added cycloheximide (CHX) to block new protein synthesis. Significantly, AR protein half-life in VCaP cells, similarly to LNCaP cells, was not decreased by DHT, demonstrating that DHT was not directly (through binding to the AR) enhancing AR degradation (Figure 1E). Finally, DHT in VCaP cells markedly increased expression of transiently transfected Flag-tagged AR regulated by a CMV promoter, further indicating that DHT was not enhancing AR protein degradation (Figure 1F). Therefore, we next examined effects on AR mRNA.

Agonist-Liganded AR Negatively Regulates *AR* Gene Transcription

Androgen has been reported to cause a modest decrease in AR mRNA in LNCaP cells (Krongrad et al., 1991), but DHT in VCaP caused a rapid and more dramatic decrease in AR mRNA (Figure 2A). Interestingly, a higher DHT concentration was required to suppress AR mRNA compared to the levels for induction of PSA and ERG mRNA (the latter from the androgen-regulated *TMPRSS2:ERG* fusion gene), which were half-maximal at <0.1 nM DHT (Figure 2B). To determine whether this decrease in AR mRNA required new protein synthesis, including the synthesis of ERG that was recently reported to suppress *AR* gene expression (Yu et al., 2010), we treated androgen-starved cells with cycloheximide and DHT and then measured AR mRNA levels over 24 hr. Significantly, treatment with cycloheximide did not prevent the enhanced decline in AR mRNA, indicating that it was not dependent on the DHT-stimulated synthesis of new proteins (Figure 2C). Bicalutamide blocked the suppression of AR mRNA by DHT (Figure 2D), consistent with the effect being dependent on the agonist-liganded AR. To determine whether DHT was increasing AR mRNA

degradation, we pretreated androgen-starved VCaP cells with DHT for 2 hr and then added actinomycin D to block new mRNA synthesis. Significantly, AR mRNA half-life was not decreased by DHT (Figure 2E, left panel), suggesting that DHT was decreasing *AR* gene transcription. We also assessed AR mRNA half-life in VCaP cells growing in medium with DHT versus cells where DHT was removed for 16 hr before the addition of actinomycin D. Although AR mRNA was decreased in the presence of DHT, there was no evident decrease in AR half-life (Figure 2E, right panel). Finally, we found by chromatin immunoprecipitation (ChIP) that DHT decreased the binding of RNA polymerase II to exon 1 in the *AR* gene (Figure 2F, left panel) and also decreased binding of active RNA polymerase II as shown by anti-phospho-RNA polymerase II ChiP (Figure 2F, right panel). Together these results indicated that the DHT liganded AR in VCaP cells was directly repressing AR gene transcription.

Androgen Stimulates AR Recruitment to a Conserved Site in Intron 2 of the *AR* Gene

Data from a recent ChIP-chip analysis of AR binding sites (ARBSs) in LNCaP cells identified three sites linked to the *AR* gene: ARBS1 in the promoter region (10% FDR), ARBS2 in intron 2 (5% FDR), and ARBS3 in the 3′ downstream region (5% FDR) (Wang et al., 2009) (Figure S2A). To assess these binding sites in VCaP cells, we designed two pairs of primers for each ARBS and utilized ChIP coupled with quantitative real-time PCR to measure AR binding. Only the ARBS2 site (ARBS2-1) showed clear DHT induced AR binding, although basal and androgen-induced AR binding to the well-characterized major ARE upstream of the *PSA* gene (ARE III) were higher (Figure 3A). Because important regulatory elements may be conserved between species, we compared the human ARBS2 region to the corresponding regions in other species. Interestingly, a fragment of ARBS2 (~400 bp) that overlapped ARBS2-1 was highly conserved among species (100% identical between mouse and rat and 88% identical between mouse or rat and human) and contained multiple binding sites for FOXA1, a pioneer transcription factor that interacts with AR and is generally found at steroid-responsive enhancer elements (Figure 3B and Figure S2B). Therefore, we synthesized an additional set of primer pairs spanning this conserved region (ARBS2a, 2b, and 2c) and repeated the AR ChIP assays. AR binding to all three sites was substantially increased by DHT, and this binding was blocked by the AR antagonist bicalutamide (Figure 3C). The DHT-stimulated increase was comparable to the ~5-fold increase on the AREs in the control *PSA* and *TMPRSS2* enhancers, but basal binding to ARBS2 was again lower (Figure 3C). As observed on the *PSA* enhancer, DHT-stimulated AR recruitment to ARBS2 was maximal at early times (2 hr) but still persisted after 24 hr (Figure S2C). As noted for suppression of AR mRNA versus induction of PSA and ERG mRNA (Figure 2), AR binding to ARBS2 required higher DHT concentrations (Figure 3D). Finally, anti-FOXA1 ChIP showed that FOXA1 was associated constitutively with ARBS2 (Figure 3E).

Androgen Stimulates Demethylation of H3K4 Associated with ARBS2

Consistent with ARBS2 functioning as an enhancer, ChIP with an anti-TATA binding protein (TBP) antibody indicated that there was an interaction between this site and *AR* gene promoter (Figure S3A). Significantly, we also detected a basal association between activated RNA polymerase II and ARBS2 that was decreased by DHT, suggesting that the agonist liganded AR may be mediating repression through this site (Figure 4A). Further evidence for an interaction between the AR recruited to ARBS2 and the *AR* gene promoter was obtained by anti-AR ChIP followed by a chromatin conformation capture (3C) assay, which identified a DHT-dependent association between AR, ARBS2, and the *AR* gene promoter (Figure S3B).

The agonist liganded AR generally stimulates transcription through recruitment of coactivator proteins and histone acetyltransferases, but can more weakly mediate recruitment of transcriptional corepressors, such as NCoR or SMRT, and their associated histone deacetylases (HDACs) (Cheng et al., 2002). Therefore, we next used ChIP to determine whether DHT was directly or indirectly stimulating recruitment of an HDAC to AR-binding sites in the *AR* gene. Interestingly, control experiments indicated that HDAC3 (which forms a complex with NCoR and SMRT) was associated with ARE III in the *PSA* enhancer and that this association was decreased by DHT (Figure S3C). There also appeared to be a very weak association of HDAC3 with each of the ChIP-chip identified AR-binding sites (ARBS1, 2, and 3) in the *AR* gene, but these were not increased by DHT (Figure S3C). Moreover, ChIP with antibodies against acetylated H3K9/14 did not detect decreases in histone acetylation at any of the sites in response to DHT (Figure S3D). As a positive control, in the absence of DHT, we detected high levels of histone acetylation in *AR* exon 1 and this decreased in response to DHT, consistent with down-regulation of *AR* gene expression.

Because interaction with the promoter and FOXA1 binding suggested that ARBS2 may function as an enhancer, we next assessed changes in histone marks that are associated with active enhancers (H3K4 mono- and dimethylation) at ARBS1, 2, and 3. Substantial H3K4 methylation was detected at each site, but there were no changes in response to DHT at ARBS1 or ARBS3, or at the ARE III site in the *PSA* enhancer (Figure 4B). The *TMPRSS2* enhancer ARE was similarly unaffected (Figure 4C). In contrast, DHT caused a decrease in both H3K4me1 and H3K4me2 levels at ARBS2-1 (Figure 4B), and this was confirmed using the set of ARBS2 primers (ARBS2a, b, and c) spanning the conserved region (Figure 4C). Taken together, these results suggested that ARBS2 contains an enhancer that is rapidly inactivated by androgen.

VCaP xenografts that relapse after castration have higher levels of AR mRNA and renewed expression of AR-regulated genes, similarly to what is observed in patients who progress to CRPC (Cai et al., 2009). To determine whether the ARBS2 site contributes to the increased *AR* gene expression in these relapsed tumors, we generated a cell line (VCS2) from a relapsed VCaP xenograft tumor. VCS2 cells in steroid-depleted medium had higher levels of AR, PSA, and ERG (from the androgen-regulated *TMPRSS2:ERG* fusion gene) relative to the parental VCaP cells (Figure 4D) and were less dependent on androgens for cell survival (Figure S3E), but AR protein was still markedly decreased by DHT. An analysis of basal (in steroid depleted medium without exogenous DHT) mRNA levels confirmed that AR, PSA, and ERG mRNA were increased in VCS2 cells compared to VCaP and showed that AR mRNA was markedly

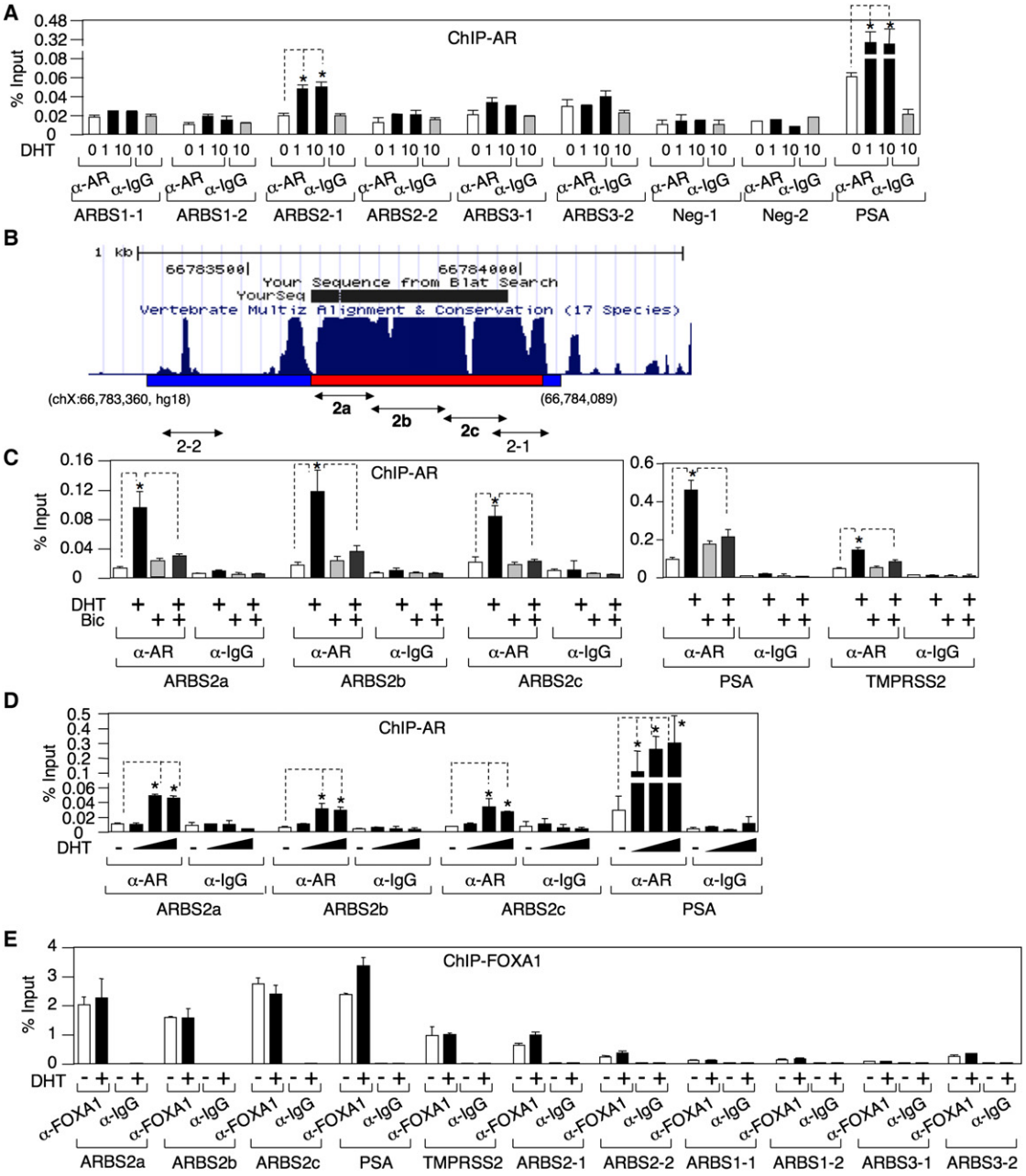

Figure 3. Androgen Stimulates AR Recruitment to a Site in Intron 2 of the AR Gene

(A) VCaP cells in steroid-depleted medium (CSS medium) were treated with 0, 1, or 10 nM DHT for 4 hr and the DNA bound to AR was measured by ChIP followed by qPCR.

(B) The conserved region of ARBS2 (intron2) among 17 vertebrate species was plotted using UCSC Genome Browser.

(C) VCaP cells were pretreated with or without 10 μM bicalutamide for 4 hr followed by treatment with 10 nM DHT for 4 hr. The DNA bound to AR was measured by ChIP followed by qPCR.

(D) VCaP cells were treated for 4 hr with 0, 0.1, 1, or 10 nM DHT. AR binding to ARBS2 or the PSA enhancer ARE were measured by ChIP followed by qPCR.

(E) VCaP cells were treated with or without 10 nM DHT for 4 hr and the DNA bound to FOXA1 was measured by ChIP and qPCR. Error bars in each experiment indicate SD. See also Figure S2 and see Table S1 for raw qPCR data for experiments shown.

decreased in response to DHT (Figure 4E). AR ChIP showed that DHT stimulated recruitment of AR to ARBS2 in the VCS2 cells, with the increased binding compared to VCaP being consistent with higher AR levels in the VCS2 cells (Figure 4F, left panel). Significantly, basal ARBS2 H3K4 methylation was increased in the VCS2 cells compared to VCaP, but was still decreased by DHT (Figure 4F, right panel). Finally, transcription factors shown previously to interact with AR on enhancers, Oct1 and GATA-2 (Wang et al., 2007), were associated with ARBS2 and were increased in VCS2 (Figure 4G). Overall, these findings further

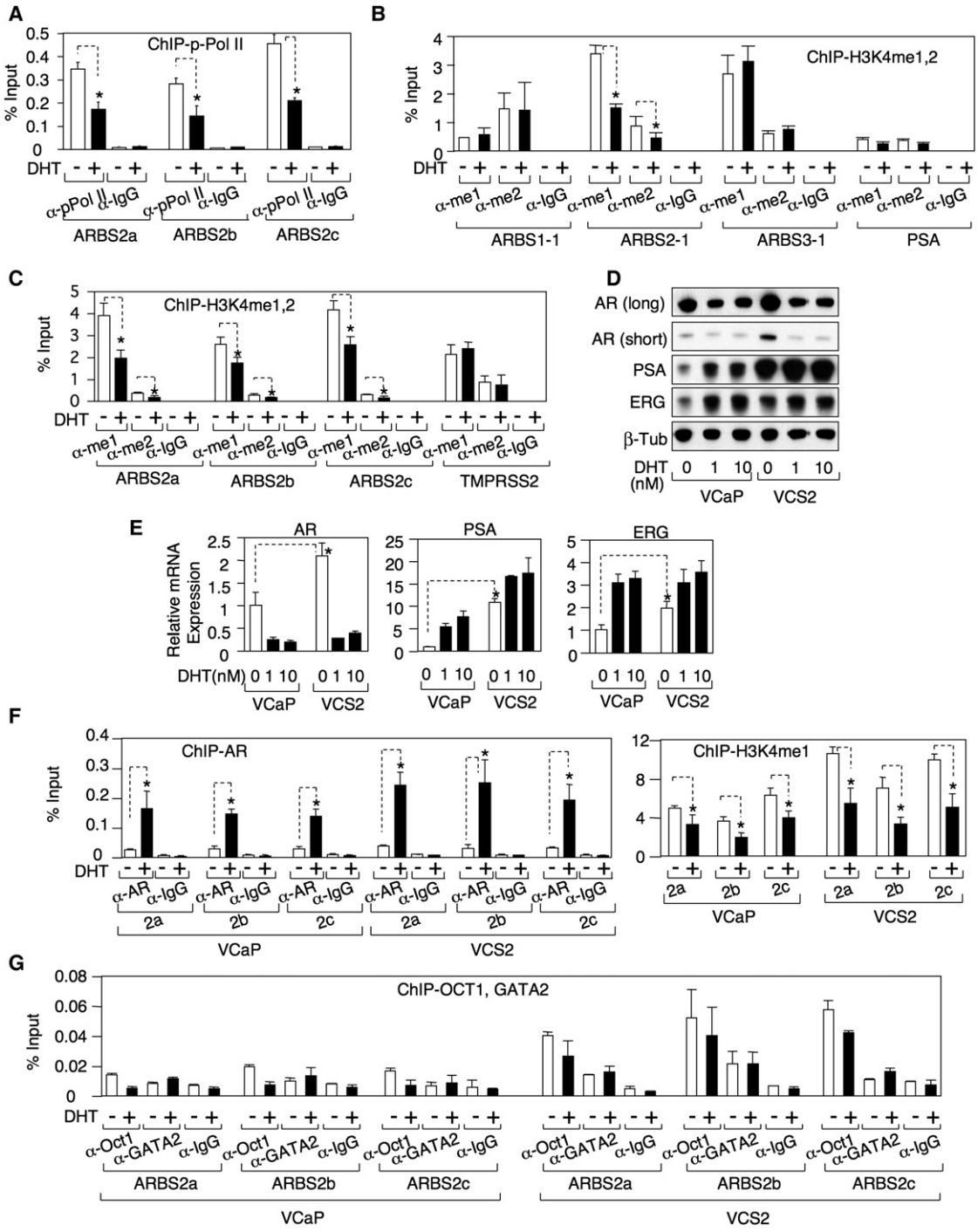

Figure 4. Androgen Stimulates Rapid Demethylation of H3K4 in VCaP and VCaP-Derived VCS2 Cells

(A–C) VCaP cells were treated with or without DHT for 4 hr and the DNA bound to active RNA polymerase II, mono- or di-methylated H3K4 were measured ChIP and qPCR.

(D and E) VCaP or VCS2 cells were treated with 0, 1, or 10 nM DHT for 24 hr and AR, PSA, ERG, and β-tubulin proteins were immunoblotted or mRNA were measured by ChIP followed by qRT-PCR (18S as internal control).

(F and G) VCaP or VCS2 cells were treated with or without DHT for 4 hr and the DNA bound to AR, mono-methylated H3K4, Oct1, or GATA2 were measured by ChIP followed by qPCR. Error bars in each experiment indicate SD. See also Figure S3 and see Table S2 for raw qPCR data for experiments shown.

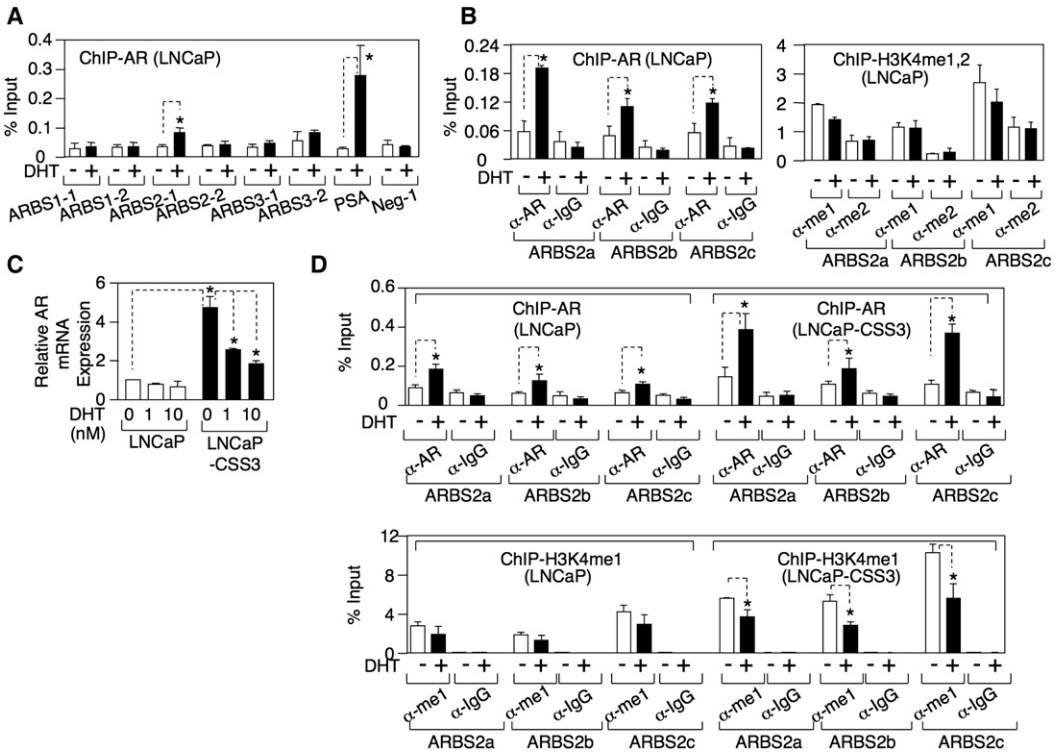

Figure 5. Androgen Deprivation Activates the ARBS2 Site in LNCaP Cells

(A) LNCaP cells were treated with or without 10 nM DHT for 4 hr and the DNA bound to AR was immunoprecipitated and measured by qPCR.

(B) LNCaP cells were treated with or without 10 nM DHT for 4 hr and the DNA bound to AR, mono- or di-methylated H3K4 was immunoprecipitated and measured by qPCR.

(C) LNCaP or LNCaP-CSS3 (adapted to steroid-depleted medium for > 3 w) were treated with 0, 1, or 10 nM DHT for 24 hr and AR mRNA was measured by qRT-PCR (18S as internal control).

(D) LNCaP or LNCaP-CSS3 cells were treated with or without 10 nM DHT for 4 hr and the DNA bound to AR or mono-methylated H3K4 was measured by ChIP and qPCR. Error bars in each experiment indicate SD. See Table S3 for raw qPCR data for experiments shown.

supported the conclusion that ARBS2 contains an enhancer that contributes to increased *AR* gene expression at low androgen levels in CRPC and indicated that this enhancer is repressed by the agonist liganded AR.

Androgen Deprivation Activates the ARBS2 Site in LNCaP Cells

We next examined the LNCaP PCa cell line, which shows only a small decrease in AR mRNA in response to DHT (see Figure 2A). Anti-AR ChIP showed DHT stimulated recruitment of AR to ARBS2-1 (Figure 5A), which was confirmed using the ARBS2a, b, and c primers (Figure 5B, left panel). However, in contrast to VCaP cells, there was less AR binding to ARBS2 and no marked DHT stimulated decreases in H3K4me1 or me2 (Figure 5B, right panel). On the basis of the results above in VCaP versus VCS2 cells, we next examined LNCaP cells that were passaged in vitro in steroid-depleted medium (basal medium with 5% charcoal/dextran stripped serum, CSS). As shown in Figure 5C, after 3 weeks in steroid-depleted medium, the cells expressed higher levels of AR mRNA, which markedly declined in response to DHT. AR ChIP in these LNCaP-CSS3 cells showed increased DHT-stimulated AR recruitment to ARBS2 relative to the parental LNCaP cells (Figure 5D, upper panel). Most significantly, basal H3K4 methylation of ARBS2 was increased in the LNCaP-CSS3 cells, and it declined in response to DHT (Figure 5D, lower panel). These results in LNCaP cells further support the conclusion that ARBS2 contains an androgen-repressed enhancer that contributes to increased *AR* gene expression in response to androgen deprivation.

Lysine-Specific Demethylase 1 (LSD1) Is Recruited to ARBS2 In Vitro and In Vivo by the DHT Liganded AR and Mediates Repression

The decrease in H3K4 mono- and dimethylation over the ARBS2 site indicated that AR was either suppressing the activity of a histone methyltransferase or increasing a histone demethylase. Significantly, lysine-specific demethylase 1 (LSD1) has been shown to interact with AR (Metzger et al., 2005; Wissmann et al., 2007), and we confirmed this interaction by coimmunoprecipitation of endogenous AR and LSD1 (Figure 6A). LSD1 is reported to function as an AR coactivator on the *PSA* gene ARE III enhancer through demethylation of repressive mono- and dimethylated H3K9 (Metzger et al., 2005; Wissmann et al., 2007). However, mono- and dimethylated H3K4 are also substrates for LSD1, and in most contexts LSD1 appears to function as a repressor through H3K4me1 and H3K4me2 demethylation (Shi et al., 2004). Therefore, we next tested the hypothesis that DHT stimulates LSD1 recruitment to ARBS2. An association

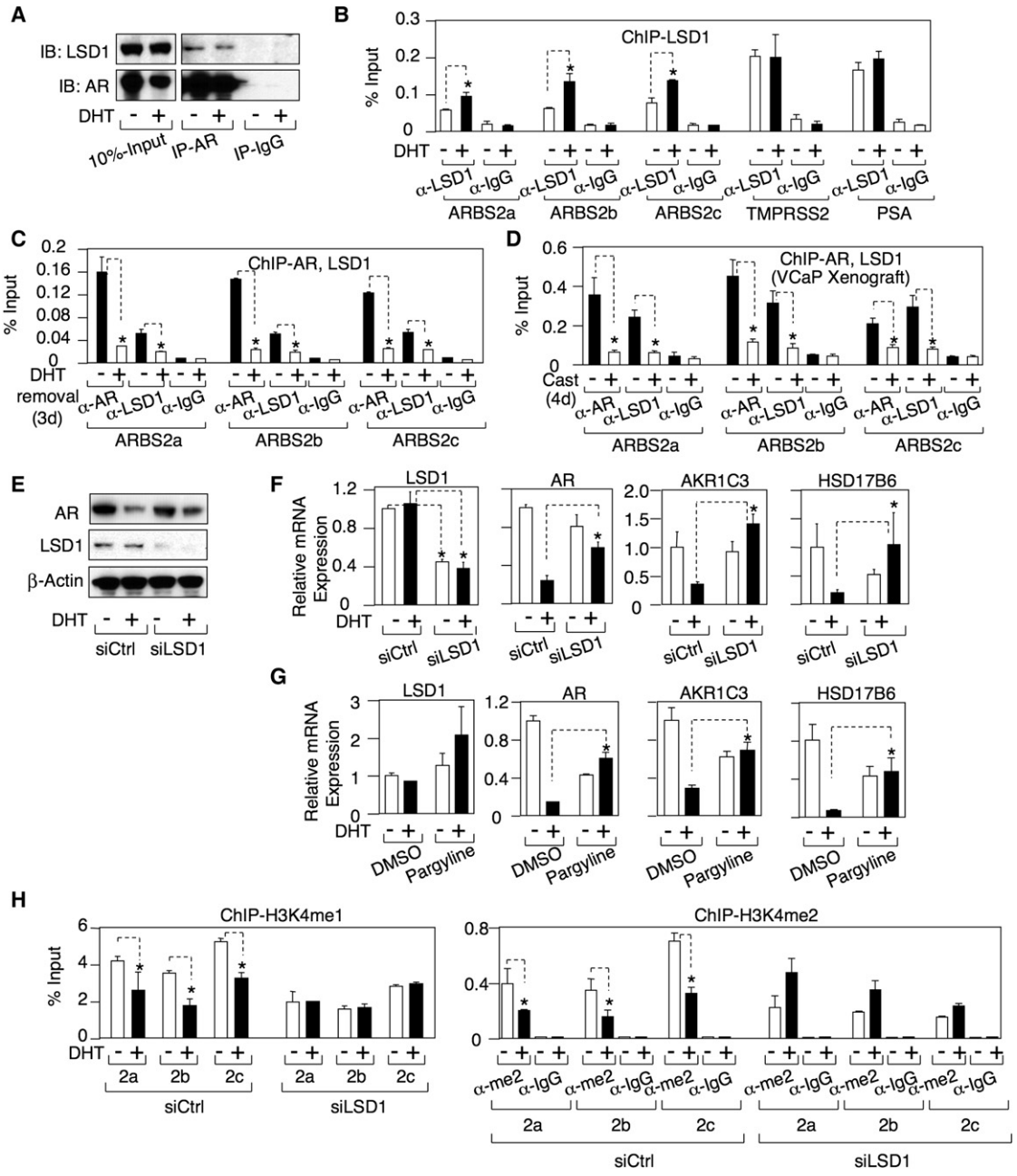

Figure 6. LSD1 Is Recruited to ARBS2 by the DHT Liganded AR In Vitro and In Vivo

(A) VCaP cells were treated with or without 10 nM DHT for 24 hr and protein was then immunoprecipitated using anti-AR antibody or IgG control, followed by immunoblotting for LSD1 and AR.

(B) VCS2 cells were treated with 0 or 10 nM DHT for 4 hr and the DNA bound to LSD1 was measured by ChIP and qPCR.

(C) VCaP cells were grown in steroid-depleted medium supplemented with 10 nM DHT for 3 days and then DHT was removed for 3 days. The DNA bound to AR or LSD1 was measured by ChIP and qPCR.

(D) The tissue of VCaP xenograft tumor (precastrated [−] or 4-day postcastration [+] mice) was formalin fixed, lysed, and sonicated. The DNA bound to AR or LSD1 was immunoprecipitated and measured by qPCR.

(E) VCaP cells were transfected with 20 nM LSD1 siRNA (Dharmacon) for 2 days and then treated with or without DHT for 24 hr. AR, LSD1, and β-actin were immunoblotted.

(F) VCaP cells transfected with LSD1 or control siRNA were stimulated with 10 nM DHT and LSD1, AR, AKR1C3, or HSD17B6 mRNA were measured using qRT-PCR.

(G) VCaP cells were pretreated with pargyline (2 mM) for 8 hr and then treated with or without DHT for 16 hr. LSD1, AR, AKR1C3, or HSD17B6 mRNA were measured using qRT-PCR (normalized to GAPDH as internal control).

(H) VCaP cells were transfected with 20 nM LSD1 siRNA for 2 days and then treated with or without 10 nM DHT for 4 hr. The DNA bound to mono- or di-methylated H3K4 was immunoprecipitated and measured by qPCR. Error bars in each experiment indicate SD. See also Figure S4 and see Table S4 for raw qPCR data for experiments shown.

between LSD1 and ARBS2 was detected by ChIP in VCaP cells (Figure S4A) and in VCS2 cells (Figure 6B), and this interaction was increased by DHT. Consistent with previous reports in LNCaP cells (Metzger et al., 2005; Wissmann et al., 2007), LSD1 was constitutively associated with the ARE III in the *PSA* enhancer and was not clearly increased by DHT (Figure 6B). LSD1 was similarly constitutively associated with the ARE in the *TMPRSS2* enhancer (Figure 6B). Finally, we confirmed that DHT stimulated the recruitment of LSD1 to ARBS2 in LNCaP cells and found that LSD1 recruitment to ARBS2 was increased in the LNCaP-CSS3 cells (Figure S4B).

In the converse experiment, we examined VCaP cells cultured in medium with androgen that were then shifted to steroid-depleted medium for 3 days. As shown in Figure 6C, both AR and LSD1 binding to ARBS2 were decreased in the steroid-depleted cells. We showed previously that AR mRNA levels in VCaP xenografts were markedly increased at 4 days after castration (Cai et al., 2009). To determine whether this increase in AR mRNA in vivo correlated with decreased binding of AR and LSD1 to ARBS2, we used ChIP to examine VCaP xenografts prior to castration and at 4 days after castration. As shown in Figure 6D, both AR and LSD1 were associated with ARBS2 prior to castration, and these associations were markedly decreased 4 days after castration.

LSD1 can potentially function as a coactivator or corepressor by demethylating H3K9 or H3K4, respectively, and we found that DHT also stimulated a decline in H3K9 methylation as well as H3K4 methylation across the ARBS2 site (Figure S4C, left panel). In contrast, DHT did not cause a decrease in H3K4me3, which is associated with both promoters and enhancers but is not a substrate for LSD1 (Figure S4C, right panel). Therefore, as these changes in methylation would be consistent with LSD1 functioning as a coactivator or corepressor, we next utilized siRNA to address directly whether LSD1 was mediating the down-regulation of AR gene expression in response to DHT. Expression of LSD1 protein (Figure 6E) and mRNA (Figure 6F) were substantially decreased by the LSD1 siRNA, and the DHT-stimulated decrease in AR protein was diminished (Figure 6E). An analysis of AR mRNA confirmed that the DHT-stimulated decrease in AR expression was blunted by LSD1 siRNA (Figure 6F).

To determine whether this LSD1-dependent suppression was unique to the *AR* gene, we also examined expression of AKR1C3 and HSD17B6, which are androgen repressed and increased in CRPC. AKR1C3 catalyzes synthesis of testosterone from androstenedione and HSD17B6 oxidizes 5α-androstene-3α, 17β-diol back to DHT (Bauman et al., 2006). Similarly to AR, we reported previously that mRNA expression of AKR1C3 was consistently increased in CRPC (Stanbrough et al., 2006), and both AKR1C3 and HSD17B6 were negatively regulated by androgens in VCaP cells (Cai et al., 2009). As shown in Figure 6F, the DHT-stimulated declines in AKR1C3 and HSD17B6 mRNA were abrogated by the LSD1 siRNA. Similar results were obtained using a chemical inhibitor of LSD1, pargyline (Figure 6G), which also prevented the DHT-stimulated decline in AR protein (Figure S4D). Consistent with previous data showing that LSD1 functions as a coactivator on the *PSA* gene (Metzger et al., 2005; Wissmann et al., 2007), pargyline also blocked the DHT stimulated increase in PSA protein (Figure S4D).

The LSD1 siRNA did not decrease the DHT-stimulated recruitment of AR to ARBS2 (Figure S4E, left panel). However, the DHT-stimulated declines in H3K9 methylation (Figure S4E, right panel) and H3K4 methylation (Figure 6H) across ARBS2 were impaired or abrogated by the LSD1 siRNA. Pargyline similarly impaired DHT-stimulated H3K4me1 demethylation across ARBS2 (Figure S4F). Together, these data indicated that AR was mediating repression through recruitment of LSD1 and H3K4 demethylation. Finally, we used pargyline to assess whether LSD1 was mediating the DHT-stimulated repression of AR gene expression in other PCa cell lines. C4-2 cells were derived from a castration-resistant LNCaP xenograft and CWR22Rv1 cells were from a castration-resistant CWR22 xenograft. In both cells, pargyline abrogated the DHT-stimulated decrease in AR mRNA (Figure S4G). Moreover, consistent with LSD1 functioning as an AR coactivator on androgen-stimulated genes, pargyline suppressed the DHT-stimulated increase in FKBP5.

Previous studies have shown that LSD1 functions as a coactivator for AR on the *PSA* (*KLK3*) and *KLK2* genes because of phosphorylation of H3T6 and H3T11, which suppress LSD1-mediated H3K4 demethylation and enhance H3K9 demethylation, respectively (Metzger et al., 2008; Metzger et al., 2010). Therefore, we next used ChIP to determine whether differences in H3T6 or H3T11 phosphorylation were a basis for the distinct effects of AR and LSD1 on the *AR* gene versus AR-stimulated genes. Significantly, DHT-stimulated H3T6 and H3T11 phosphorylation were lower across ARBS2 and were also lower in the androgen-suppressed *OPRK1* (see Figure 7) and *AKR1C3* genes, compared to AREs in the androgen-stimulated *PSA*, *KLK2*, and *FKBP5* genes (Figure S4G). However, H3T6 and H3T11 phosphoryation were also low in the strongly androgen-stimulated *TMPRSS2* gene. These findings are consistent with the conclusion that phosphorylation of H3T6 and H3T11 contribute to the regulation of LSD1 substrate specificity, but additional mechanisms may also contribute to this regulation.

Expression of Androgen Repressed Genes Is Increased in CRPC Xenografts

Expression microarrays were used to identify genes that were androgen repressed in both VCaP and VCS2 cells in vitro, and to then assess the expression of these genes in vivo in androgen-dependent versus relapsed castration-resistant VCaP xenografts. AR, AKR1C3, and HSD17B6 were again found to be androgen repressed in VCaP (4.2-, 2.8-, and 3.7-fold higher in the absence of androgen, respectively) and were even more highly androgen repressed in VCS2 cells (6.4-, 8.5-, and 4.7-fold, respectively) (Table S5). In contrast, expression of these genes was highly up-regulated in the relapsed VCaP xenografts (5.4-, 2.3-, and 3.5-fold for AR, AKR1C3, and HSD17B6, respectively). These findings, in conjunction with the low intratumoral androgen levels in these castration-resistant tumors (Figure S5A), support a feedback mechanism that negatively regulates AR signaling at high androgen levels and enhances signaling at the lower androgen levels.

To more systematically assess the significance of additional in vitro identified androgen-repressed genes, we next focused on the 411 genes that were repressed by >2-fold in VCS2 and >1.5-fold in VCaP (the lower threshold in VCaP being based on the more robust repression of AR, AKR1C3, and HSD17B6 in

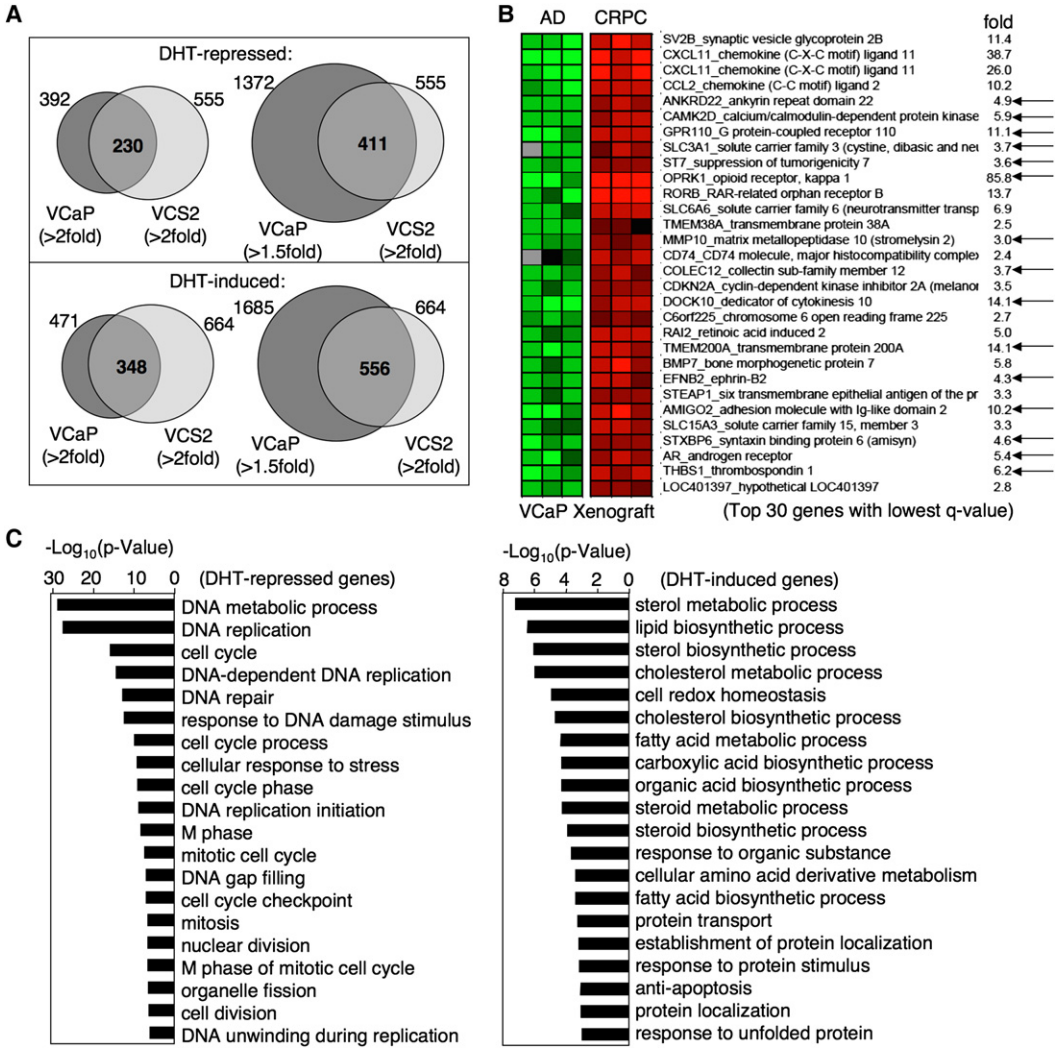

Figure 7. Identification of Androgen-Repressed Genes in VCaP Cells and Xenografts

(A) VCaP or VCS2 cells were treated with or without 10 nM DHT for 24 hr and were analyzed on Affymetrix U133A microarrays. The numbers of DHT-repressed genes or DHT-induced genes in VCaP and VCS2 cells and their overlaps are shown.

(B) VCaP xenografts were established and biopsied at three stages: androgen-dependent tumor (AD), 4 days after castration (CS), and castration-resistant relapsed tumor (CRPC). mRNA were extracted from the biopsies of tumors of AD or CRPC stages and analyzed on Agilient microarrays. The data was analyzed using SAM software (Significance Analysis of Microarrays). The top 30 genes with lowest q-value are shown, with black arrows indicating DHT-repressed genes.

(C) GO term analysis of DHT-repressed genes (left panel) versus androgen-induced genes (right panel). See also Figure S5 and Table S5.

VCS2 cells) (Figure 7A and Table S5). Remarkably, among the top 30 genes with most significantly elevated expression in the castration-resistant VCaP xenografts, 12 were in this group of 411 androgen-repressed genes (Figure 7B). In addition, further genes among this group of 30 that appeared to be androgen-repressed were ANKRD22 (1.64-fold in VCaP and 1.82-fold in VCS2), MMP10 (1.32-fold in VCaP and 4.2-fold in VCS2), and STXBP6 (1.60-fold in VCaP and 1.93-fold in VCS2).

We next took advantage of recent AR ChIP-seq data in VCaP cells (Yu et al., 2010) to assess the frequency of AR-binding sites in androgen-repressed versus androgen-activated genes in VCaP cells. AR-binding sites were found in 20% of AR-activated genes and in 14% of AR-repressed genes, with the background being 11% (fraction of total 31,810 genes that contain AR-binding sites), indicating that there is enrichment for AR-binding sites within the AR-repressed genes (Figure S5B). The lower enrichment versus the AR-activated genes could mean that more genes in the AR-activated group are directly regulated by AR, but could also be in part technical and reflect somewhat weaker binding of AR to AR-repressed genes. To further assess whether suppression of these genes was mediated directly by AR through an LSD1-dependent mechanism, we focused on another androgen-repressed gene (*OPRK1*) that was strongly up-regulated in the VCaP CRPC xenografts. Using real-time RT-PCR, we first confirmed that DHT markedly decreases OPRK1 mRNA in VCaP cells, similarly to the decreases in AR, AKR1C3, and HSD17B6 (Figure S5C). Using AR siRNA we also showed that AR down-regulation could blunt the DHT-mediated

repression of these genes, providing further evidence that the repression was AR mediated (Figure S5C). The AR siRNA also decreased basal, but not DHT stimulated PSA or TMPRSS2 expression, consistent with AR functioning more efficiently on AR-stimulated genes. *OPRK1* has a single AR-binding site in its 3′ UTR based on ChIP-chip and ChIP-seq data in both LNCaP and VCaP cells (Wang et al., 2009; Yu et al., 2010) (Figure S5D). Therefore, we used ChIP with primers covering this site to assess AR and LSD1 binding. Significantly, DHT stimulated AR and LSD1 recruitment to this site and also decreased H3K4 methylation (Figure S5E). Together, these data indicate that AR is directly negatively regulating a set of genes that are up-regulated in the VCaP CRPC xenografts.

To assess the potential functional consequences of failing to suppress androgen-repressed genes after castration, we determined the pathways that were associated with the 411 androgen-repressed genes identified in VCaP and VCS2 cells. Importantly, expression of these genes was most significantly associated with increased DNA replication and cell cycle progression (Figure 7C, left panel), whereas genes that were increased in response to DHT in VCaP and VCS2 cells were associated with synthesis of lipids, proteins, and other metabolic processes distinct from DNA replication (Figure 7C, right panel). Finally, we treated VCaP CRPC xenografts with testosterone to assess effects on AR repressed genes in vivo, and found by RT-PCR that AR, AKR1C3, HSD17B6, and OPRK1 were repressed (Figure S5F). Testosterone also suppressed expression of BCL11A, another strongly AR repressed gene that was increased in castration-resistant VCaP xenografts, but did not clearly suppress PSA or TMPRSS2. Moreover, there was marked regression in the xenografts (Figure S5G). These findings indicated that a partial restoration of androgen levels and AR transcriptional activity in CRPC cells may drive tumor growth by activating cellular metabolism while failing to suppress DNA replication and proliferation.

Increased Expression of Androgen Repressed Genes in Patients with CRPC

To determine whether increased expression of androgen-repressed genes may contribute to CRPC in patients, we used expression data from a set of CRPC bone marrow metastases versus primary prostate cancers that had not received hormonal therapy (Stanbrough et al., 2006; Mendiratta et al., 2009). Consistent with lower androgen levels and reduced AR transcriptional activity in CRPC, only a small fraction of the genes that were androgen induced in VCaP/VCS2 were overexpressed in CRPC (18/556), whereas a much larger fraction were underexpressed (71/556) (Figure 8A). Similarly, very few of the AR repressed genes were underexpressed in CRPC (9/411), whereas many more were overexpressed (53/411) (Table S6). As noted previously, genes that are overexpressed in CRPC are highly associated with proliferation (Stanbrough et al., 2006; Wang et al., 2009) (Figure 8B), whereas genes that are underexpressed are more associated with developmental pathways (Figure S6A). Significantly, the set of 53 androgen-repressed genes that were overexpressed in the CRPC biopsy samples were similarly highly associated with DNA replication and proliferation (Figure 8C).

To further assess the biological importance of these 53 androgen-repressed genes in CRPC, we removed them from the set of 1490 genes that were overexpressed in the CRPC biopsy samples and repeated the Gene Ontology analysis on the remaining 1437 genes. Although these 1437 genes were still associated with cell cycle progression and DNA metabolism, the significance of all these associations was markedly decreased, and DNA replication was no longer among the most highly associated pathways in the absence of these 53 androgen-repressed genes (Figure S6B). Finally, we selected for further analysis a set of eight genes that were androgen repressed in VCaP/VCS2 cells and were also overexpressed in the relapsed VCaP xenografts or the clinical CRPC biopsies. Quantitative real-time RT-PCR confirmed that they were all DHT repressed in VCaP and VCS2 cells, and that this could be prevented with bicalutamide (Figure S6C). Moreover, in all cases the androgen-stimulated down-regulation was decreased or abrogated by treatment with pargyline, indicating that it was mediated by LSD1 (Figure 8D). Together, these findings elucidate a mechanism by which loss of negative regulation by the agonist liganded AR, in association with LSD1, increases the expression of AR and of multiple genes that contribute to increased androgen synthesis, DNA replication, and proliferation in CRPC.

DISCUSSION

Studies in clinical samples and xenograft models indicate that increased *AR* gene expression plays a major role in the progression to CRPC. We observed previously in VCaP cells in vitro and in VCaP xenografts in vivo that AR mRNA levels decline rapidly in response to androgen stimulation and increase rapidly in response to androgen withdrawal (Cai et al., 2009). In this report we have identified a highly conserved site in the second intron of the AR gene that regulates its expression in response to androgen stimulation and withdrawal. RNA polymerase II and FOXA1 are associated with this ARBS2 site, as are OCT1, GATA2, and substantial levels of H3K4 mono- and dimethylation that are further increased in cells adapted to androgen deprivation, consistent with this element functioning as an enhancer that contributes to increased AR gene expression in CRPC. Moreover, we show that the agonist liganded AR decreases *AR* gene expression by functioning as a transcriptional repressor at this site through recruitment of LSD1 and demethylation of H3K4me1,2. The rapid androgen-mediated down-regulation of AKR1C3 and HSD17B6 is similarly LSD1 dependent, indicating that the agonist liganded AR directly mediates a physiological intracellular negative feedback loop to regulate AR activity. Taken together, these findings elucidate a mechanism that contributes to increased *AR* gene expression and restored AR activity in CRPC, and identify a suppressor element and transcriptional repressor function for the agonist liganded AR.

Further analysis of gene expression in androgen-starved versus androgen-stimulated VCaP and VCS2 cells showed that the agonist liganded AR also suppressed the expression of multiple genes mediating DNA synthesis and cell cycle progression, while it increased the expression of genes mediating synthesis of lipids, amino acids, and other metabolic processes. This profile is consistent with AR function in normal prostate epithelium to drive terminal differentiation and synthesis of seminal fluid and provides a molecular basis for the biphasic response to androgen stimulation whereby PCa cells proliferate

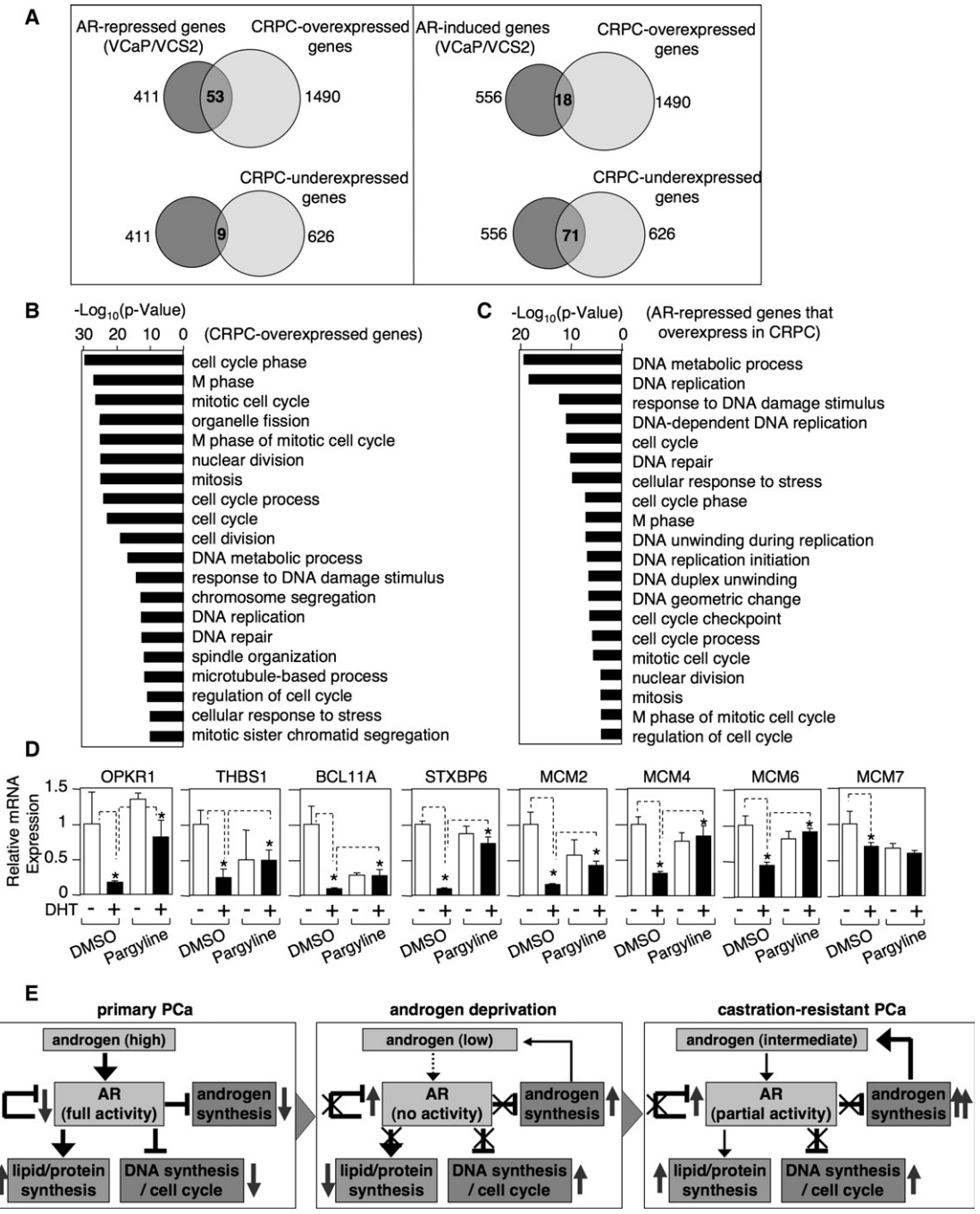

Figure 8. Expression of Androgen-Repressed Genes Is Increased in Human CRPC Samples

(A) Affymetrix microarray expression data showing overlaps between androgen repressed/induced genes and the expression of 1490 genes that were increased and 626 genes that were decreased ($p < 0.001$ and fold-change > 1.5) in 34 CRPC bone marrow metastases compared with 27 primary tumors prior to any hormonal therapy.

(B and C) GO term analysis of the group of 1490 CRPC-overexpressed genes (B) and 53 AR-repressed genes that were overexpressed in CRPC (C).

(D) VCaP cells were pretreated with pargyline (2 mM) for 8 hr and then were treated with or without DHT for 16 hr. OPKR1, THBS1, BCL11A, STXBP6, MCM2, MCM4, MCM6, or MCM7 mRNA were measured using qRT-PCR (normalized to GAPDH as internal control). Error bars in each experiment indicate SD.

(E) Graphical summary showing divergent effects of androgen deprivation on expression of AR-stimulated genes, which are decreased, versus AR-repressed genes (including the *AR* gene), which are increased. In castration-resistant PCa, mechanisms including further increases in intratumoral androgen synthesis result in partial restoration of AR transcriptional activation function on genes mediating lipid and protein biosynthesis, but do not restore AR repressor function on the *AR* gene, or on genes mediating androgen synthesis, DNA synthesis, and cell cycle progression. See also Figure S6 and Table S6.

in response to low levels of androgen but are growth arrested at high concentrations (Xu et al., 2006). Significantly, a set of these androgen-repressed genes associated with increased DNA synthesis and proliferation were overexpressed in vivo in castration-resistant VCaP xenografts and in CRPC patient samples. We suggest that androgen levels in CRPC cells are adequate to stimulate AR activity on enhancer elements of genes mediating certain critical metabolic functions such as lipid synthesis, which are sensitive to lower levels of androgens, but are not adequate to effectively recruit AR and LSD1 to suppressor elements in multiple genes that negatively regulate AR signaling and cellular proliferation. A graphical summary showing divergent effects of AR on expression of AR-stimulated versus AR-repressed genes after androgen deprivation and in CRPC is shown in Figure 8E.

LSD1 was initially identified in corepressor complexes and shown to function by demethylating mono- and dimethylated H3K4 (Shi et al., 2004). However, it was subsequently shown to function as a coactivator through demethylation of repressive mono- and dimethylated H3K9 when associated with AR and possibly other nuclear receptors including estrogen receptor α (Metzger et al., 2005, Garcia-Bassets et al., 2007, Perillo et al., 2008). The results of this study indicate that the association with AR does not determine the coactivator versus corepressor function of LSD1, and that it is instead determined by properties of the element to which it is being recruited. For example, hypoacetylated nucleosomes are more susceptible substrates for LSD1 mediated demethylation (Shi et al., 2005). Moreover, recent data indicate that phosphorylation of H3T11 by an AR-associated kinase (PRK1/PKN1) enhances the demethylation of H3K9me3 by JMJD2C and subsequent demethylation of H3K9me1,2 by LSD1 (Metzger et al., 2008), whereas phosphorylation of H3T6 by a distinct kinase (PKCβ1) can suppress the LSD1-mediated demethylation of H3K4me1,2 (Metzger et al., 2010). Our data indicate that lower H3T6 and H3T11 phosphorylation may contribute to the substrate specificity and corepressor function of LSD1 at AR repressed genes, although LSD1 may be regulated by a distinct mechanism on the TMPRSS2 gene. It will clearly be important to further characterize these and additional AR suppressor elements and determine the extent to which histone modifications or other factors regulate the function of AR and LSD1 on these suppressor versus AR enhancer elements.

It has been well appreciated for many years that AR has both growth-promoting and growth-suppressing activities and that androgen deprivation therapies may directly or indirectly stimulate some pathways that contribute to growth and eventual relapse. Indeed, androgens can suppress the growth of some CRPC-derived cell lines, and high-dose androgens have been explored as a therapy for CRPC (Umekita et al., 1996, Morris et al., 2009). However, the molecular basis for androgen-stimulated growth suppression has not been clear, and there have been no previous studies suggesting that distinct AR transcriptional mechanisms may underlie these functions. Therefore, the results of this study provide a paradigm with implications for both basic molecular mechanisms of steroid action and for AR targeted therapy of prostate cancer. In particular, the distinct mechanisms of AR action on enhancer versus suppressor elements may make it possible to selectively augment AR transcriptional repressor function and thereby prevent or delay the emergence of CRPC.

EXPERIMENTAL PROCEDURES

Cell Culture and Xenografts

LNCaP or C4-2 cells were cultured in RPMI1640 medium with 10% FBS. VCaP cells were cultured in DMEM medium with 10% FBS, and VCS2 cells were cultured in DMEM medium with 8% charcoal/dextran-stripped FBS (CSS) plus 2% FBS. For most immunoblotting, RT-PCR, or ChIP assays, cells were grown to 50%–60% confluence in 5% (CSS) medium for 3 days and then treated with androgens or drugs. VCaP xenografts were established in the flanks of male scid mice by injecting ~2 million cells in 50% Matrigel. When the tumors reached ~1 cm, biopsies were obtained and then the mice were castrated. Additional biopsies were obtained 4 days after castration, and the tumors were harvested at relapse. Frozen sections were examined to confirm that the samples used for RNA and protein extraction contained predominantly nonnecrotic tumor. All animal experiments were approved by the Beth Israel Deaconess Institutional Animal Care and Use Committee and were performed in accordance with institutional and national guidelines.

RT-PCR and Immunoblotting

Quantitative real-time RT-PCR amplification was performed on RNA extracted from tissue samples or cell lines using TRIZOL reagent. RNA (50 ng) was used for each reaction and the result was normalized by coamplification of 18S RNA. Reactions were performed on an ABI Prism 7700 Sequence Detection System using Taqman one-step RT-PCR reagents. Primers and probes are listed in Supplemental Information. PCR data are represented as mean ± STD for repeats. Protein extracts were prepared by boiling for 15 min in 2% SDS. Blots were incubated with anti-PSA (1:3000, polyclonal, BioDesign), anti-AR (1:2000, polyclonal, Upstate), anti-LSD1 (1:1000, Abcam), anti-β-actin (1:5000, monoclonal, Abcom), or anti-β-tubulin (1:2000, Upstate), and then with 1:5000 anti-rabbit or anti-mouse secondary antibodies (Promega).

Coimmunoprecipitation

VCaP cells were harvested in Triton lysis buffer (0.5% Triton X-100, 20 mM Tris-HCl, 150 mM NaCl, 5 mM EDTA, and 2 mM dithiothreitol) with protease inhibitors. The protein was immunoprecipitated using monoclonal anti-AR (AR441 from NeoMarkers) or mouse IgG control and then subjected to immunoblotting.

Chromatin-Immunoprecipitation (ChIP) Assay

Cells were formalin fixed, lysed, and sonicated to break the chromatin into 500–800 bp fragments. Anti-AR (Santa Cruz), anti-FOXA1 (Abcam), anti-OCT1 (Santa Cruz), anti-GATA2 (Santa Cruz), anti-RNA Polymerase II (Santa Cruz), anti-RNA Polymerase II CTD repeat (phospho Ser5), anti-TBP (Santa Cruz), anti-LSD1 (Abcam), anti-HDAC1 (Santa Cruz), anti-HDAC2 (Santa Cruz), anti-HDAC3 (Santa Cruz), anti-H3K4me1 (Abcam), anti-H3K4me2 (Upstate), anti-H3K4me3 (Abcam), anti-H3K9me1 (Abcam), anti-H3K9/14ace (Upstate), anti-H3T6pho (Abcam), anti-H3T11pho (Abcam), or rabbit IgG (Santa Cruz) were used to precipitate chromatin fragments from cell extracts. Quantitative real-time PCR was used to analyze binding to the ARBS-1, −2, and −3; *PSA* enhancer (ARE3); *TMPRSS2* enhancer (−14 k upstream); *OPRK1* enhancer (3′ UTR); or negative-1 (3′ irrelevant region of PSA) or -2 (irrelevant region of chromosome 18). The primers are listed in the Supplemental Information. We used real-time quantitative PCR (SYBR green) to amplify the DNA fragment in the antibody precipitated DNA and the unprecipitated input DNA to calculate ΔC_T values. The R_Q values ($R_Q = 2^{-\Delta CT}$) are presented and reflect the precipitated DNA as a percentage of the input DNA. Results are represented as mean ± STD for replicate samples. Data are representative of at least three experiments. Significant differences are indicated (*) in the experiments. Raw data for the real-time quantitative PCR are provided in Tables S1–S4.

Gene Expression Microarray Assay

VCaP or VCS2 cells treated with ethanol or 10 nM DHT were subjected to microarray assay (Affymetrix) to identify genes whose expression was repressed by DHT in both VCaP and VCS2 cells. Tissue mRNA was extracted and purified

from three sets (precastrated, 4 days after castration, and relapsed) of xenograft tumors (3 mice) and then subjected to microarray assay (Agilent). SAM software was used to perform t test on these three biological repeats (three mice) to determine the score and q-value. The genes whose expression was significantly elevated in relapsed tumors ($q < 0.05$) were picked for the next screening to determine whether they were DHT-repressed in VCaP and VCS2.

ACCESSION NUMBERS

The expression microarray data has been deposited in the Gene Expression Omnibus (GEO) database (www.ncbi.nlm.nih.gov/geo) under accession number GSE31410.

SUPPLEMENTAL INFORMATION

Supplemental Information includes six figures and six tables and may be found with this article online at doi:10.1016/j.ccr.2011.09.001.

ACKNOWLEDGMENTS

We thank J. He for analyzing three AR binding sites among species; and E. A. Mostaghel, B. Marck, and A. M. Matsumoto for measuring intratumoral level of steroids. This work was supported by the National Institutes of Health (grant R01 CA111803 to S.P.B., Prostate SPORE P50 CA090381 to S.P.B. and M.B., a Career Development Award from the Prostate SPORE to C.C., grant R00 CA135592 to S.C., and grants Prostate SPORE P50 CA097186 and RC1 CA146849 to P.S.N.), Department of Defense Prostate Cancer Research Program (grant PC060807 to S.P.B., postdoctoral fellowships to C.C. and H.W., and grant PC093509 to P.S.N.), and a Challenge Grant from the Prostate Cancer Foundation.

Received: August 26, 2010
Revised: January 14, 2011
Accepted: September 1, 2011
Published: October 17, 2011

REFERENCES

Bauman, D.R., Steckelbroeck, S., Williams, M.V., Peehl, D.M., and Penning, T.M. (2006). Identification of the major oxidative 3alpha-hydroxysteroid dehydrogenase in human prostate that converts 5alpha-androstane-3alpha,17beta-diol to 5alpha-dihydrotestosterone: a potential therapeutic target for androgen-dependent disease. Mol. Endocrinol. *20*, 444–458.

Blok, L.J., Themmen, A.P., Peters, A.H., Trapman, J., Baarends, W.M., Hoogerbrugge, J.W., and Grootegoed, J.A. (1992). Transcriptional regulation of androgen receptor gene expression in Sertoli cells and other cell types. Mol. Cell. Endocrinol. *88*, 153–164.

Cai, C., Wang, H., Xu, Y., Chen, S., and Balk, S.P. (2009). Reactivation of androgen receptor-regulated TMPRSS2:ERG gene expression in castration-resistant prostate cancer. Cancer Res. *69*, 6027–6032.

Chen, C.D., Welsbie, D.S., Tran, C., Baek, S.H., Chen, R., Vessella, R., Rosenfeld, M.G., and Sawyers, C.L. (2004). Molecular determinants of resistance to antiandrogen therapy. Nat. Med. *10*, 33–39.

Cheng, S., Brzostek, S., Lee, S.R., Hollenberg, A.N., and Balk, S.P. (2002). Inhibition of the dihydrotestosterone-activated androgen receptor by nuclear receptor corepressor. Mol. Endocrinol. *16*, 1492–1501.

Garcia-Bassets, I., Kwon, Y.S., Telese, F., Prefontaine, G.G., Hutt, K.R., Cheng, C.S., Ju, B.G., Ohgi, K.A., Wang, J., Escoubet-Lozach, L., et al. (2007). Histone methylation-dependent mechanisms impose ligand dependency for gene activation by nuclear receptors. Cell *128*, 505–518.

Gregory, C.W., Johnson, R.T., Jr., Mohler, J.L., French, F.S., and Wilson, E.M. (2001). Androgen receptor stabilization in recurrent prostate cancer is associated with hypersensitivity to low androgen. Cancer Res. *61*, 2892–2898.

Holzbeierlein, J., Lal, P., LaTulippe, E., Smith, A., Satagopan, J., Zhang, L., Ryan, C., Smith, S., Scher, H., Scardino, P., et al. (2004). Gene expression analysis of human prostate carcinoma during hormonal therapy identifies androgen-responsive genes and mechanisms of therapy resistance. Am. J. Pathol. *164*, 217–227.

Kemppainen, J.A., Lane, M.V., Sar, M., and Wilson, E.M. (1992). Androgen receptor phosphorylation, turnover, nuclear transport, and transcriptional activation: specificity for steroids and antihormones. J. Biol. Chem. *267*, 968–974.

Korenchuk, S., Lehr, J.E., McLean, L., Lee, Y.G., Whitney, S., Vessella, R., Lin, D.L., and Pienta, K.J. (2001). VCaP, a cell-based model system of human prostate cancer. In Vivo *15*, 163–168.

Krongrad, A., Wilson, C.M., Wilson, J.D., Allman, D.R., and McPhaul, M.J. (1991). Androgen increases androgen receptor protein while decreasing receptor mRNA in LNCaP cells. Mol. Cell. Endocrinol. *76*, 79–88.

Kumar, M.V., Jones, E.A., Grossmann, M.E., Blexrud, M.D., and Tindall, D.J. (1994). Identification and characterization of a suppressor element in the 5′-flanking region of the mouse androgen receptor gene. Nucleic Acids Res. *22*, 3693–3698.

Loberg, R.D., St John, L.N., Day, L.L., Neeley, C.K., and Pienta, K.J. (2006). Development of the VCaP androgen-independent model of prostate cancer. Urol. Oncol. *24*, 161–168.

Mendiratta, P., Mostaghel, E., Guinney, J., Tewari, A.K., Porrello, A., Barry, W.T., Nelson, P.S., and Febbo, P.G. (2009). Genomic strategy for targeting therapy in castration-resistant prostate cancer. J. Clin. Oncol. *27*, 2022–2029.

Metzger, E., Wissmann, M., Yin, N., Müller, J.M., Schneider, R., Peters, A.H., Günther, T., Buettner, R., and Schüle, R. (2005). LSD1 demethylates repressive histone marks to promote androgen-receptor-dependent transcription. Nature *437*, 436–439.

Metzger, E., Yin, N., Wissmann, M., Kunowska, N., Fischer, K., Friedrichs, N., Patnaik, D., Higgins, J.M., Potier, N., Scheidtmann, K.H., et al. (2008). Phosphorylation of histone H3 at threonine 11 establishes a novel chromatin mark for transcriptional regulation. Nat. Cell Biol. *10*, 53–60.

Metzger, E., Imhof, A., Patel, D., Kahl, P., Hoffmeyer, K., Friedrichs, N., Müller, J.M., Greschik, H., Kirfel, J., Ji, S., et al. (2010). Phosphorylation of histone H3T6 by PKCbeta(I) controls demethylation at histone H3K4. Nature *464*, 792–796.

Morris, M.J., Huang, D., Kelly, W.K., Slovin, S.F., Stephenson, R.D., Eicher, C., Delacruz, A., Curley, T., Schwartz, L.H., and Scher, H.I. (2009). Phase 1 trial of high-dose exogenous testosterone in patients with castration-resistant metastatic prostate cancer. Eur. Urol. *56*, 237–244.

Perillo, B., Ombra, M.N., Bertoni, A., Cuozzo, C., Sacchetti, S., Sasso, A., Chiariotti, L., Malorni, A., Abbondanza, C., and Avvedimento, E.V. (2008). DNA oxidation as triggered by H3K9me2 demethylation drives estrogen-induced gene expression. Science *319*, 202–206.

Quarmby, V.E., Yarbrough, W.G., Lubahn, D.B., French, F.S., and Wilson, E.M. (1990). Autologous down-regulation of androgen receptor messenger ribonucleic acid. Mol. Endocrinol. *4*, 22–28.

Ruizeveld de Winter, J.A., Janssen, P.J., Sleddens, H.M., Verleun-Mooijman, M.C., Trapman, J., Brinkmann, A.O., Santerse, A.B., Schröder, F.H., and van der Kwast, T.H. (1994). Androgen receptor status in localized and locally progressive hormone refractory human prostate cancer. Am. J. Pathol. *144*, 735–746.

Shan, L.X., Rodriguez, M.C., and Jänne, O.A. (1990). Regulation of androgen receptor protein and mRNA concentrations by androgens in rat ventral prostate and seminal vesicles and in human hepatoma cells. Mol. Endocrinol. *4*, 1636–1646.

Sharma, A., Yeow, W.S., Ertel, A., Coleman, I., Clegg, N., Thangavel, C., Morrissey, C., Zhang, X., Comstock, C.E., Witkiewicz, A.K., et al. (2010). The retinoblastoma tumor suppressor controls androgen signaling and human prostate cancer progression. J. Clin. Invest. *120*, 4478–4492.

Shi, Y., Lan, F., Matson, C., Mulligan, P., Whetstine, J.R., Cole, P.A., Casero, R.A., and Shi, Y. (2004). Histone demethylation mediated by the nuclear amine oxidase homolog LSD1. Cell *119*, 941–953.

Shi, Y.J., Matson, C., Lan, F., Iwase, S., Baba, T., and Shi, Y. (2005). Regulation of LSD1 histone demethylase activity by its associated factors. Mol. Cell. *19*, 857–864.

Stanbrough, M., Bubley, G.J., Ross, K., Golub, T.R., Rubin, M.A., Penning, T.M., Febbo, P.G., and Balk, S.P. (2006). Increased expression of genes converting adrenal androgens to testosterone in androgen-independent prostate cancer. Cancer Res. *66*, 2815–2825.

Taplin, M.E., Bubley, G.J., Shuster, T.D., Frantz, M.E., Spooner, A.E., Ogata, G.K., Keer, H.N., and Balk, S.P. (1995). Mutation of the androgen-receptor gene in metastatic androgen-independent prostate cancer. N. Engl. J. Med. *332*, 1393–1398.

Umekita, Y., Hiipakka, R.A., Kokontis, J.M., and Liao, S. (1996). Human prostate tumor growth in athymic mice: inhibition by androgens and stimulation by finasteride. Proc. Natl. Acad. Sci. USA *93*, 11802–11807.

Visakorpi, T., Hyytinen, E., Koivisto, P., Tanner, M., Keinänen, R., Palmberg, C., Palotie, A., Tammela, T., Isola, J., and Kallioniemi, O.P. (1995). In vivo amplification of the androgen receptor gene and progression of human prostate cancer. Nat. Genet. *9*, 401–406.

Wang, L.G., Johnson, E.M., Kinoshita, Y., Babb, J.S., Buckley, M.T., Liebes, L.F., Melamed, J., Liu, X.M., Kurek, R., Ossowski, L., and Ferrari, A.C. (2008). Androgen receptor overexpression in prostate cancer linked to Pur alpha loss from a novel repressor complex. Cancer Res. *68*, 2678–2688.

Wang, L.G., Ossowski, L., and Ferrari, A.C. (2004). Androgen receptor level controlled by a suppressor complex lost in an androgen-independent prostate cancer cell line. Oncogene *23*, 5175–5184.

Wang, Q., Li, W., Liu, X.S., Carroll, J.S., Jänne, O.A., Keeton, E.K., Chinnaiyan, A.M., Pienta, K.J., and Brown, M. (2007). A hierarchical network of transcription factors governs androgen receptor-dependent prostate cancer growth. Mol. Cell *27*, 380–392.

Wang, Q., Li, W., Zhang, Y., Yuan, X., Xu, K., Yu, J., Chen, Z., Beroukhim, R., Wang, H., Lupien, M., et al. (2009). Androgen receptor regulates a distinct transcription program in androgen-independent prostate cancer. Cell *138*, 245–256.

Wissmann, M., Yin, N., Müller, J.M., Greschik, H., Fodor, B.D., Jenuwein, T., Vogler, C., Schneider, R., Günther, T., Buettner, R., et al. (2007). Cooperative demethylation by JMJD2C and LSD1 promotes androgen receptor-dependent gene expression. Nat. Cell Biol. *9*, 347–353.

Xu, Y., Chen, S.Y., Ross, K.N., and Balk, S.P. (2006). Androgens induce prostate cancer cell proliferation through mammalian target of rapamycin activation and post-transcriptional increases in cyclin D proteins. Cancer Res. *66*, 7783–7792.

Yeap, B.B., Voon, D.C., Vivian, J.P., McCulloch, R.K., Thomson, A.M., Giles, K.M., Czyzyk-Krzeska, M.F., Furneaux, H., Wilce, M.C., Wilce, J.A., and Leedman, P.J. (2002). Novel binding of HuR and poly(C)-binding protein to a conserved UC-rich motif within the 3′-untranslated region of the androgen receptor messenger RNA. J. Biol. Chem. *277*, 27183–27192.

Yu, J., Yu, J., Mani, R.S., Cao, Q., Brenner, C.J., Cao, X., Wang, X., Wu, L., Li, J., Hu, M., et al. (2010). An integrated network of androgen receptor, polycomb, and TMPRSS2-ERG gene fusions in prostate cancer progression. Cancer Cell *17*, 443–454.

Yuan, X., and Balk, S.P. (2009). Mechanisms mediating androgen receptor reactivation after castration. Urol. Oncol. *27*, 36–41.

Cell

A Gain-of-Function Mutation in DHT Synthesis in Castration-Resistant Prostate Cancer

Kai-Hsiung Chang,[1,2,3,4] Rui Li,[4] Barbara Kuri,[1,2,3] Yair Lotan,[5] Claus G. Roehrborn,[5] Jiayan Liu,[8] Robert Vessella,[9] Peter S. Nelson,[9,10] Payal Kapur,[6] Xiaofeng Guo,[7] Hamid Mirzaei,[7] Richard J. Auchus,[8] and Nima Sharifi[1,2,3,4,*]

[1]Department of Cancer Biology, Lerner Research Institute
[2]Department of Solid Tumor Oncology, Taussig Cancer Institute
[3]Glickman Urological and Kidney Institute
Cleveland Clinic, Cleveland, OH 44195, USA
[4]Division of Hematology/Oncology, Department of Internal Medicine and Simmons Cancer Center
[5]Department of Urology
[6]Department of Pathology
[7]Department of Biochemistry
UT Southwestern Medical Center, Dallas, TX 75390, USA
[8]Division of Endocrinology and Metabolism, Department of Internal Medicine, University of Michigan Medical School, Ann Arbor, MI 48109, USA
[9]Department of Urology, University of Washington School of Medicine, Seattle, WA 91809, USA
[10]Divisions of Human Biology and Clinical Research, Fred Hutchinson Cancer Research Center, Seattle, WA 91809, USA
*Correspondence: sharifn@ccf.org
http://dx.doi.org/10.1016/j.cell.2013.07.029

SUMMARY

Growth of prostate cancer cells is dependent upon androgen stimulation of the androgen receptor (AR). Dihydrotestosterone (DHT), the most potent androgen, is usually synthesized in the prostate from testosterone secreted by the testis. Following chemical or surgical castration, prostate cancers usually shrink owing to testosterone deprivation. However, tumors often recur, forming castration-resistant prostate cancer (CRPC). Here, we show that CRPC sometimes expresses a gain-of-stability mutation that leads to a gain-of-function in 3β-hydroxysteroid dehydrogenase type 1 (3βHSD1), which catalyzes the initial rate-limiting step in conversion of the adrenal-derived steroid dehydroepiandrosterone to DHT. The mutation (N367T) does not affect catalytic function, but it renders the enzyme resistant to ubiquitination and degradation, leading to profound accumulation. Whereas dehydroepiandrosterone conversion to DHT is usually very limited, expression of 367T accelerates this conversion and provides the DHT necessary to activate the AR. We suggest that 3βHSD1 is a valid target for the treatment of CRPC.

INTRODUCTION

The growth of cancerous prostate cells requires stimulation of the androgen receptor (AR) by androgens, the most potent of which is dihydrotestosterone (DHT). Advanced prostate cancer usually initially regresses with gonadal testosterone (T) deprivation therapy (i.e., medical or surgical castration), but it almost always eventually progresses as castration-resistant prostate cancer (CRPC) (Attard et al., 2009; Penning, 2010; Scher and Sawyers, 2005; Sharifi et al., 2005; Yuan and Balk, 2009). The CRPC phenotype is driven by a gain of function in the androgen receptor (AR) that is usually accompanied by intratumoral DHT concentrations of about 1 nM, an amount sufficient to drive expression of AR-induced genes, including the TMPRSS2-ETS fusion oncogene (Geller et al., 1978; Luu-The et al., 2008; Montgomery et al., 2008; Sharifi, 2013; Titus et al., 2005; Tomlins et al., 2005). The requirement for intratumoral androgen synthesis in driving CRPC progression is most clearly demonstrated by the survival benefit conferred by abiraterone acetate, a drug that blocks androgen synthesis by inhibiting 17α-hydroxylase/17,20-lyase (CYP17A1), and enzalutamide, a potent AR antagonist that blocks DHT access to the AR ligand-binding domain (Barrie et al., 1994; de Bono et al., 2011; Scher et al., 2012; Tran et al., 2009). Intratumoral synthesis of DHT from precursors that are secreted from the adrenal gland occurs through a pathway that circumvents T (Chang et al., 2011). This synthesis requires three enzymes: 3β-hydroxysteroid dehydrogenase (3βHSD; encoded by *HSD3B*), steroid-5α-reductase (SRD5A), and 17β-hydroxysteroid dehydrogenase (17βHSD) isoenzymes (see Figure 1A) (Chang et al., 2011; Knudsen and Penning, 2010). Nonetheless, increased DHT synthesis in CRPC has not yet been ascribed to any mutations in genes encoding components of the steroidogenic machinery. 3βHSD oxidizes 3β-hydroxyl to 3-keto and isomerizes Δ^5 to Δ^4 (see Figure 1A), reactions that together make this step practically irreversible by an enzyme that is required for all possible pathways that lead to the synthesis of DHT (Evaul et al., 2010). *HSD3B1*

encodes for the peripherally expressed isoenzyme (3βHSD1) and has a germline single-nucleotide polymorphism (SNP) at position 1245 of *HSD3B1*, converting A → C, which exchanges an asparagine (N) for a threonine (T) at 3βHSD1 amino acid position 367.

Here, we show that CRPC sometimes expresses the 367T form of 3βHSD1 (3βHSD1(367T)), which increases metabolic flux from dehydroepiandrosterone (DHEA) via the 5α-androstanedione (5α-dione) pathway to DHT by protein resistance to ubiquitination and degradation rather than increased catalytic activity. Selection for 3βHSD1(367T) is evident from somatic mutation in human CRPC tumors, by loss of heterozygosity (LOH) of the wild-type copy in patients with germline heterozygous inheritance, and from the generation and expression of the same somatic mutation occurring in a mouse xenograft model treated with abiraterone acetate.

RESULTS

Cells with 3βHSD1(367T) Have Increased Flux to DHT

Conversion of DHEA by 3βHSD1 to Δ^4-androstenedione (AD) is a proximal step in peripheral tissues for metabolism from adrenal precursors to DHT (Lorence et al., 1990; Simard et al., 2005). Two cell lines derived from patients with CRPC have widely disparate flux from DHEA to AD (Figure 1A), despite comparable expression of transcripts encoding both 3βHSD1 and 3βHSD2 (Figure S1A available online). Under the same conditions, LNCaP cells metabolize >90% of [^{3}H]-DHEA by 3βHSD enzymatic activity to AD after 48 hr, whereas LAPC4 cells metabolize only approximately 10% of [^{3}H]-DHEA. In LAPC4, but not in LNCaP, apparent rate-limiting conversion of DHEA to AD, en route to DHT via the dominant pathway (DHEA → AD → 5α-dione → DHT) (Chang et al., 2011), is further evident by limited accumulation of downstream metabolites and absence of DHEA concentration-dependent increases in AR-regulated PSA and TMPRSS2 (Figure 1B). Sequencing the exons of both *HSD3B* isoenzymes reveals a single nonsynonymous substitution (Figure 1C) at position 1245 of *HSD3B1*, converting A → C, and exchanges an asparagine (N) for a threonine (T) at 3βHSD1 amino acid position 367 in LNCaP, but not in LAPC4. To further test the association between *HSD3B1* sequence and steroid metabolism, other human prostate cell lines were investigated. The presence of wild-type (1245A) and variant (1245C) *HSD3B1* sequences in other prostate cancer and immortalized prostate cell lines is also concordant with "slow" and "fast" flux from DHEA to AD, respectively (Figure S1B). The kinetic properties of recombinant 3βHSD1(367N) and 3βHSD1(367T) proteins, however, do not explain the differences in steroid metabolism between cells expressing each protein (Figure 1D). Western blot was performed to determine if the allele encoding 3βHSD1(367T) is associated with a greater amount of protein in these cells. Both models that encode for 3βHSD1(367T) have increased 3βHSD1 protein compared with the models that have wild-type sequence (Figure 1E).

Androgen Deprivation Selects for *HSD3B1*(1245C)

The *HSD3B1*(1245C); 3βHSD1(367T) allele occurs as a germline SNP variant (rs1047303; 22% allele frequency) (Shimodaira et al., 2010) but might also occur as a somatic mutation in prostate cancer. Although germline homozygous *HSD3B1*(1245C) inheritance cannot be ruled out, the most likely scenarios accounting for the sole presence of the *HSD3B1*(1245C) allele evident in both LNCaP and VCaP, given the low expected frequency of homozygous *HSD3B1*(1245C) inheritance, are either germline heterozygous inheritance followed by loss of heterozygosity (LOH) of the wild-type allele or germline homozygous wild-type inheritance followed by somatic mutation of 1245 A → C. To identify the existence of these possible mechanisms of *HSD3B1*(1245C) selection in human tumors, matching germline and tumor DNA were sequenced from men with CRPC. Genomic DNA was isolated from CRPC and normal tissue from patients treated at the University of Texas Southwestern Medical Center (UTSW) and from the University of Washington (UW) rapid autopsy program (Montgomery et al., 2008). Patient and tumor characteristics are available in Table S1. Of 40 men with CRPC, the germline of 25, 11, and 4 individuals is homozygous wild-type *HSD3B1*(1245A), heterozygous and homozygous variant *HSD3B1*(1245C), respectively. Three of 25 (12%) CRPC tumors with homozygous *HSD3B1*(1245A) inheritance have acquired the *HSD3B1*(1245C) allele (Figure 2A). Expression of *HSD3B1*(1245C) transcript was confirmed in the one available fresh-frozen tumor. It is highly likely that the observation of three identical de novo mutations occurring in 25 patients is due to selection rather than chance alone, with a high degree of statistical significance ($p = 1.47 \times 10^{-13}$), using the binomial method and assuming a mutation rate of 4 per 1,000,000 base pairs (Greenman et al., 2007). Of 11 CRPC tumors with heterozygous inheritance, three (27%) have LOH of the *HSD3B1*(1245A) allele, resulting in the *HSD3B1*(1245C) allele being predominantly detectable (Figure 2B). In these three tumors, LOH of adjacent heterozygous SNPs further confirms loss of this region of chromosome 1. In contrast, none of the 11 cases with heterozygous inheritance exhibited LOH of the *HSD3B1*(1245C) allele (Figure S2A).

Two tumors (UW9 and UW25) with LOH of the *HSD3B1*(1245A) allele had tissue remaining for additional studies. Consistent with the findings in LNCaP and VCaP that only have the *HSD3B1*(1245C) allele, both of these tumors have abundant detectable 3βHSD1 protein (Figure 2C). In contrast, both tumors tested with heterozygous expression and homozygous *HSD3B1*(1245A) expression have little or no detectable 3βHSD1. Messenger RNA (mRNA) quantitation by qRT-PCR demonstrates that the increased 3βHSD1 protein abundance occurring specifically in the tumors with LOH is not attributable to transcript overexpression (Figure S2B). Both tumors with LOH robustly express AR and PSA, suggesting that flux to DHT sustained by 3βHSD1 protein functions to elicit AR signaling (Figure 2C).

Abiraterone inhibits CYP17A1 and weakly inhibits 3βHSD, further decreasing intratumoral androgen concentrations and extending survival in CRPC (de Bono et al., 2011; Li et al., 2012); therefore, conversion to the *HSD3B1*(1245C) allele encoding 3βHSD1(367T) might permit sustained androgen synthesis despite lower availability of precursors. To determine if abiraterone treatment selects for the *HSD3B1*(1245C) allele, genomic DNA from LAPC4 xenograft tumors grown in orchiectomized

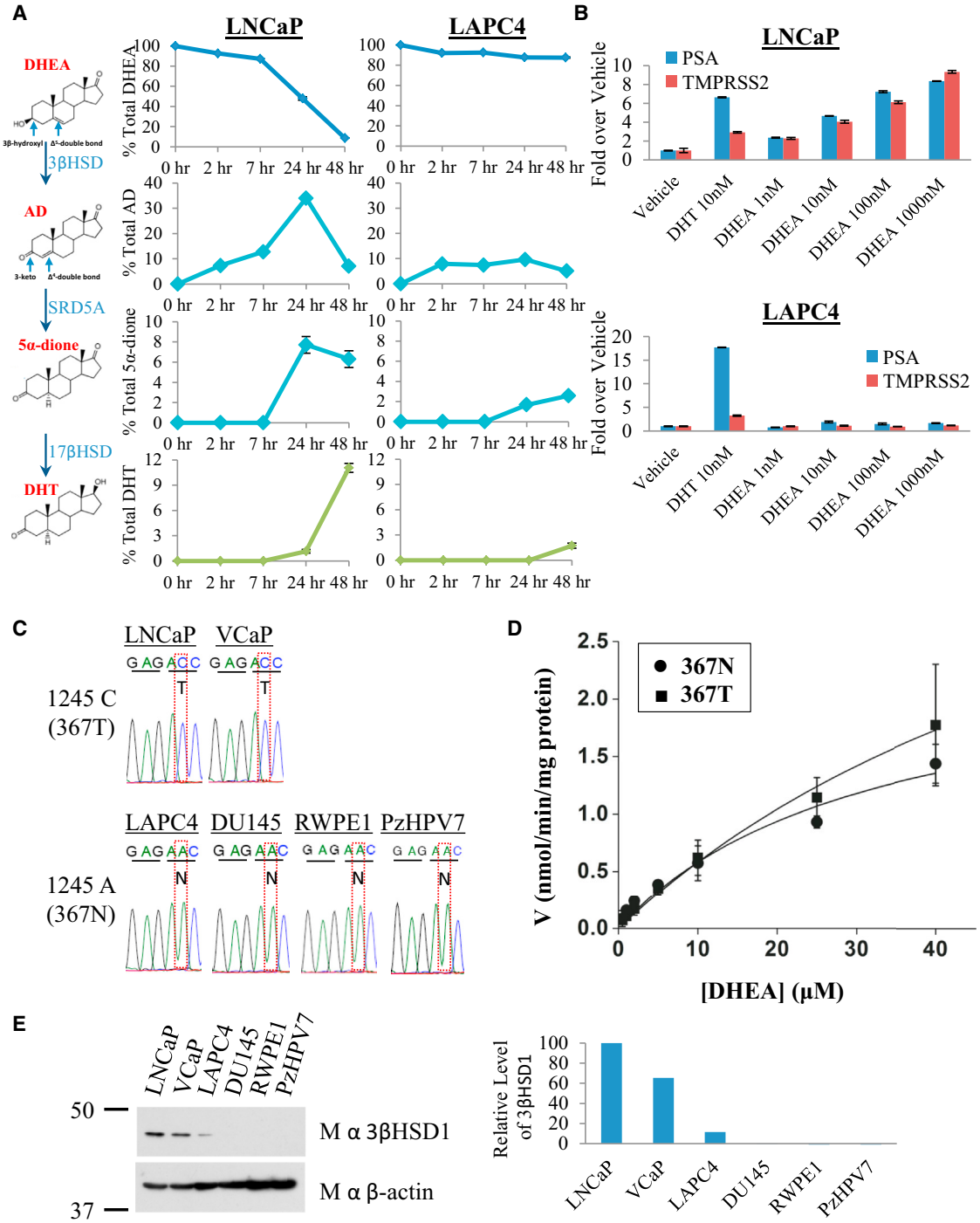

Figure 1. The 3βHSD1(367T) Protein Encoded by Mutant *HSD3B1*(1245C) Increases Flux from DHEA to AD, which Is Otherwise Rate-Limiting, En Route to DHT and Expression of AR-Responsive Genes

(A) Metabolic flux from [^{3}H]-DHEA (100 nM) to AD and downstream to 5α-dione and DHT is robust in LNCaP but limited in LAPC4. The metabolic pathway and steroid structures are shown, indicating sites of modification by 3βHSD1 in converting DHEA to AD. Steroids were quantitated at the indicated time points by high-performance liquid chromatography (HPLC).

(B) DHEA induces PSA and TMPRSS2 expression in a concentration-dependent manner in LNCaP, but not in LAPC4. Expression was assessed by qRT-PCR and normalized to *RPLP0* and vehicle control.

(C) A substitution converting A → C at position 1245 in *HSD3B1* occurs in LNCaP and VCaP, encoding a change from N → T at amino acid 367 in 3βHSD1.

(legend continued on next page)

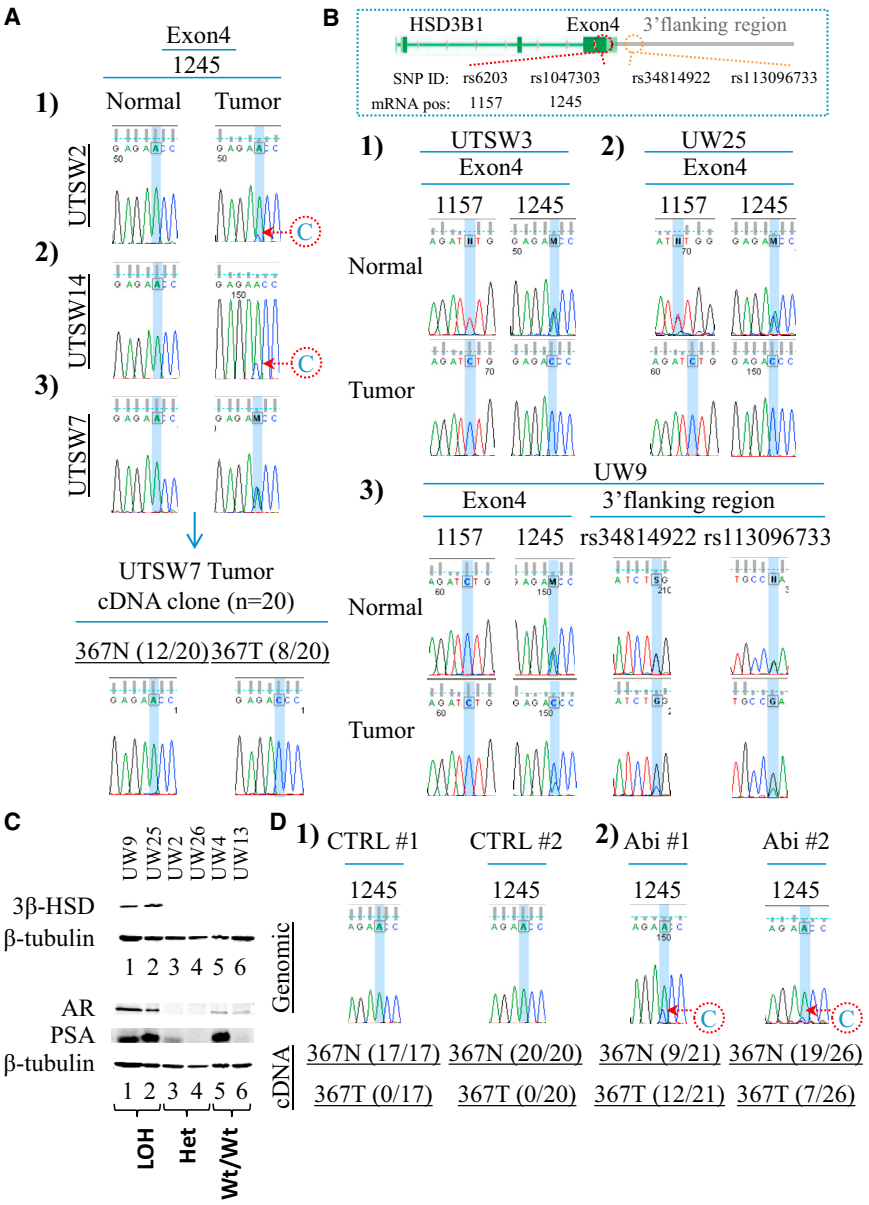

Figure 2. Somatic Selection for *HSD3B1* (1245C) Encoding 3βHSD1(367T) Occurs with Resistance to Androgen Deprivation

(A) Conversion from A → C in *HSD3B1* occurs in three CRPC tumors from patients with homozygous wild-type inheritance. Sequence of cDNA clones from a fresh-frozen tumor (UTSW7) confirms expression of *HSD3B1*(1245C) transcript.

(B) Three CRPC tumors from patients with heterozygous inheritance exhibit LOH of the wild-type *HSD3B1*(1245A) allele. Sequencing informative (heterozygous) adjacent 5′ (rs6203) and 3′ (rs34814922 and rs113096733) SNPs confirms LOH.

(C) 3βHSD1 protein is abundant in tumors with LOH of the *HSD3B1*(1245A) allele, but not in tumors with heterozygous expression or homozygous *HSD3B1*(1245A) expression. Both tumors with LOH tested also express AR and PSA (20 μg protein loaded per lane for each tumor).

(D) Somatic mutation converting A → C in *HSD3B1* occurs in two LAPC4 xenograft tumors treated with abiraterone acetate (Abi) after orchiectomy and expression of *HSD3B1*(1245C) transcript encoding 3βHSD1(367T) is evidenced by sequencing cDNA clones from these tumors. Genomic sequence from two representative control tumors (CTRL#1 and CTRL#2) treated with orchiectomy alone is shown for comparison. All 37 cDNA clones from CTRL#1 and CTRL#2 have *HSD3B1*(1245A) transcript encoding 3βHSD1(367N).

See also Figure S2 and Table S1.

mice treated with abiraterone or vehicle (n = 8 mice per treatment) was isolated and sequenced (Li et al., 2012). The 1245C allele is detectable in 2 of 8 tumors (Abi #1 and Abi #2) in the abiraterone treatment group and no tumors in the vehicle group (Figure 2D). To confirm expression of the somatically acquired mutation in the abiraterone group, complementary DNA (cDNA) clones were generated and sequenced. The mutant *HSD3B1*(1245C) transcript encoding for 3βHSD1(367T) is confirmed in 12 of 21 (57%) cDNA clones sequenced from Abi #1 and 7 of 26 (27%) clones from Abi #2. In contrast, the mutant transcript is not present in any of the 37 cDNA clones obtained from two vehicle-treated LAPC4 xenograft tumors.

Blocking 3βHSD1(367T) Inhibits DHT Synthesis, the AR Response, and CRPC

To determine the role of 3βHSD1(367T) expression in regulating flux from DHEA to DHT and AR stimulation, endogenous expression was silenced in LNCaP using two independent lentiviral short hairpin RNAs (shRNAs) (Figure 3A). Blocking 3βHSD1 expression with both shRNAs inhibits flux from DHEA to AD, resulting in little or no detectable conversion to downstream 5α-dione and DHT (Figure 3B). Silencing expression of mutant 3βHSD1 and blocking flux to DHT impedes the expression of AR-regulated PSA and TMPRSS2 (Figure 3C), leading to inhibition of cell proliferation in vitro (Figure 3D). In vivo, depletion of endogenously expressed mutant 3βHSD1 significantly

(D) Wild-type 3βHSD1(367N) and 3βHSD1(367T) have comparable kinetic properties. Michaelis-Menten plot of DHEA metabolism with 3βHSD1(367N) (circle) and 3βHSD1(367T) (square) enzyme. The K_M for 3βHSD1(367N) and 3βHSD1(367T) protein is 32 and 77 μM, respectively.

(E) Endogenous expression of 3βHSD1(367T) is associated with increased protein quantity. Error bars in (A), (B), and (D) represent the SD from experiments performed in triplicate.

See also Figure S1.

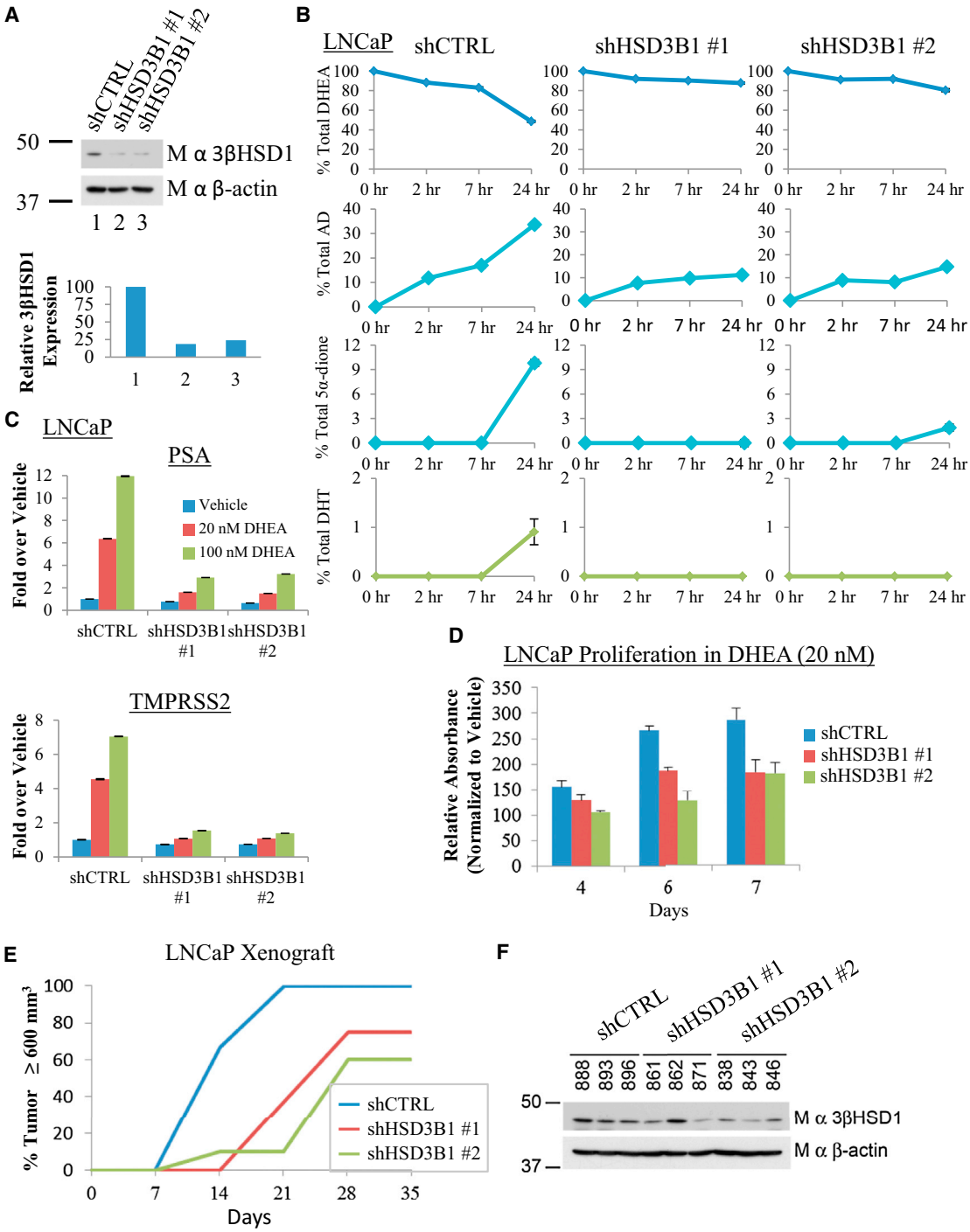

Figure 3. Genetic Silencing of 3βHSD1(367T) Impedes Conversion of DHEA to DHT, Induction of PSA and TMPRSS2 Expression, and CRPC Growth

(A) Stable lentiviral expression of two independent shRNA constructs against *HSD3B1* (shHSD3B1 #1 and shHSD3B1 #2) silences 3βHSD1 protein expression in LNCaP. The 3βHSD1 protein was quantitated and normalized to cells expressing nonsilencing lentiviral vector (shCTRL) and β-actin.

(B) Silencing 3βHSD1(367T) blocks flux from [^{3}H]-DHEA (100 nM) to AD as well as further downstream conversion to 5α-dione and DHT. Cells were treated with [^{3}H]-DHEA in triplicate, and steroids were quantitated with HPLC at the designated time points.

(C) Inhibition of AR-regulated genes. Cells were treated with the indicated concentration of DHEA for 24 hr, and gene expression was assessed by qRT-PCR and normalized to shCTRL-infected cells treated with vehicle and the *RPLP0* housekeeping gene.

(D) Silencing 3βHSD1(367T) inhibits in vitro growth. Cells were grown in the presence of 20 nM DHEA or vehicle, and growth for each cell line was normalized to vehicle for each designated day.

(legend continued on next page)

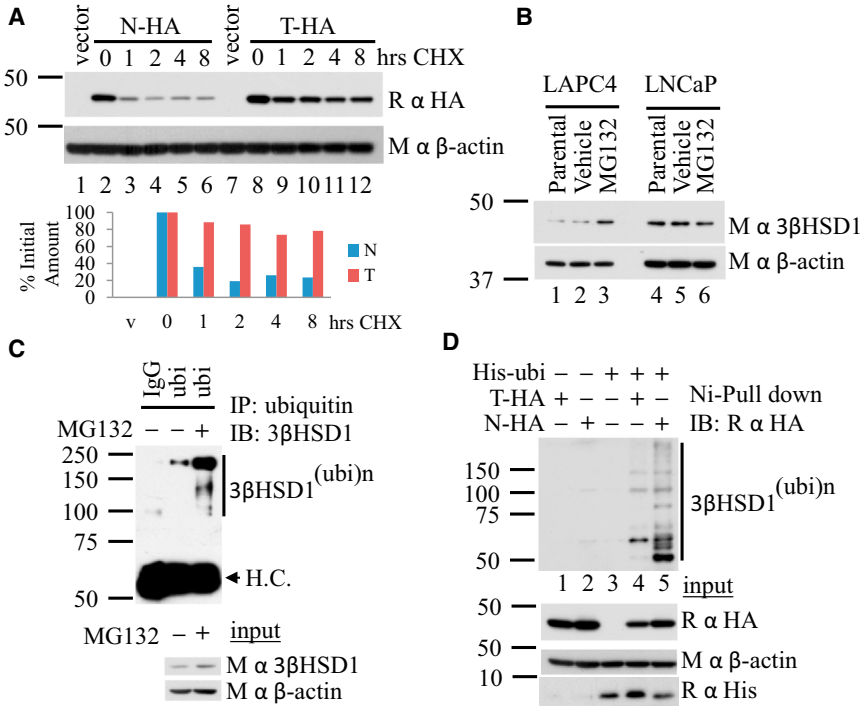

Figure 4. Resistance to Ubiquitination and Proteosome-Mediated Degradation Occurs with 3βHSD1(367T), Resulting in Prolonged Protein Half-Life

(A) 3βHSD1(367T) persists after inhibition of protein translation. LAPC4 cells were transiently transfected with constructs encoding for wild-type (N-HA) and (T-HA) protein and treated with cycloheximide (CHX) for the designated incubation times. Western blot with anti-HA antibody was performed, and the signal was quantitated and normalized to time zero and β-actin.

(B) Treatment with MG132 (10 μM; 8 hr) reverses 3βHSD1(367N) protein loss in LAPC4 and results in no 3βHSD1(367T) protein increase in LNCaP.

(C) Proteosome inhibition with MG132 (10 μM; 8 hr) results in an increase in polyubiquitinated 3βHSD1(367N) protein in LAPC4 as evidenced by immunoprecipitation with an anti-ubiquitin antibody. H.C., heavy chain.

(D) Loss of 3βHSD1(367T) vulnerability to proteosome-mediated degradation is explained by diminished susceptibility to ubiquitination. His-ubiquitin (His-ubi) was expressed with wild-type (N-HA) or (T-HA) protein in 293 cells, followed by pull-down with Ni-agarose beads and anti-HA immunoblot.

See also Figure S3.

hinders CRPC growth in surgically orchiectomized mice (Figure 3E). CRPC tumors that eventually develop from cell lines initially expressing lentiviral shRNA knockdown constructs regain 3βHSD1 protein, probably from selection for cells that have lost the shRNA construct (Figure 3F).

3βHSD1(367T) Is Resistant to Ubiquitination and Degradation

Endogenous expression of 3βHSD1(367T) appears to engender increased protein abundance compared to expression of 3βHSD1(367N) (Figure 1E). To determine if the underlying mechanism is due to an alteration in protein degradation, wild-type (HSD3B1(N)-HA) and (HSD3B1(T)-HA) constructs were generated and transiently expressed, and protein levels were compared following inhibition of translation with cycloheximide (CHX) treatment. The 367 N → T mutation substantially increases protein half-life from 2.1 to 27 hr (Figure 4A). Similar experiments with an alternative prostate cancer cell line (Figure S3A) and with stable expression of lentiviral constructs confirm the longer half-life of 3βHSD1(367T) (Figure S3B). To determine whether increased degradation of wild-type protein is reversible with proteasome inhibition, cells were treated with MG132. Pharmacologic proteasome inhibition increases endogenous wild-type 3βHSD1(367N) in LAPC4 but does not increase 3βHSD1(367T) in LNCaP (Figure 4B), and polyubiquitinated endogenous 3βHSD1(367N) accumulates with MG132 treatment in LAPC4 (Figure 4C). In contrast, polyubiquitinated endogenous 3βHSD1(367T) is not increased in LNCaP with MG132 treatment (Figure S3C). A direct comparison of ubiquitination between HA-tagged wild-type and mutant protein by Ni-agarose pull-down demonstrates that 3βHSD1(367T) is resistant to polyubiquitination (Figure 4D), explaining decreased vulnerability to proteasome-mediated degradation and longer protein half-life.

AMFR Binds 3βHSD1(367N) and Is Required for Ubiquitination

We employed mass spectrometry to determine the lysine residue(s) ubiquitinated on 3βHSD1(367N). Ubiquitination is detectable on both K70 (Figure 5A) and K352 (Figure 5B) of 3βHSD1(367N). The effects of K352R and K70R single mutations and a double mutation on ubiquitination were assessed by Ni-agarose pull-down (Figure 5C). K352 appears to be a more critical site of ubiquitination than does K70, and mutation of both sites decreases ubiquitination greater than does either mutation alone.

Autocrine mobility factor receptor (AMFR, also known as gp78) is a membrane-anchored ubiquitin ligase that functions through

(E) 3βHSD1(367T) depletion blocks CRPC growth in LNCaP xenografts. Mice underwent surgical orchiectomy and DHEA pellet implantation concomitantly when xenograft tumors reached a threshold volume of 100 mm^3. Fifteen mice were initiated in each cohort, 7, 8, and 10 mice in shCTRL, shHSD3B1 #1, and shHSD3B1 #2 groups, respectively, achieved a tumor volume of 100 mm^3 in eugonadal mice, underwent orchiectomy, and were included in the CRPC analysis. The number of days from orchiectomy to tumor volume $\geq$600 mm^3 is shown. In the comparisons of shCTRL versus shHSD3B1 #1 and shHSD3B1 #2, $p = 0.002$ and 0.003, respectively, using a log rank test.

(F) 3βHSD1(367T) protein is regained in CRPC tumors that grow from LNCaP expressing shHSD3B1 #1 and shHSD3B1 #2. Immunoblot for 3βHSD1 and β-actin were performed on protein from the indicated LNCaP CRPC tumors. Error bars in (B), (C), and (D) represent the SD for experiments performed in triplicate.

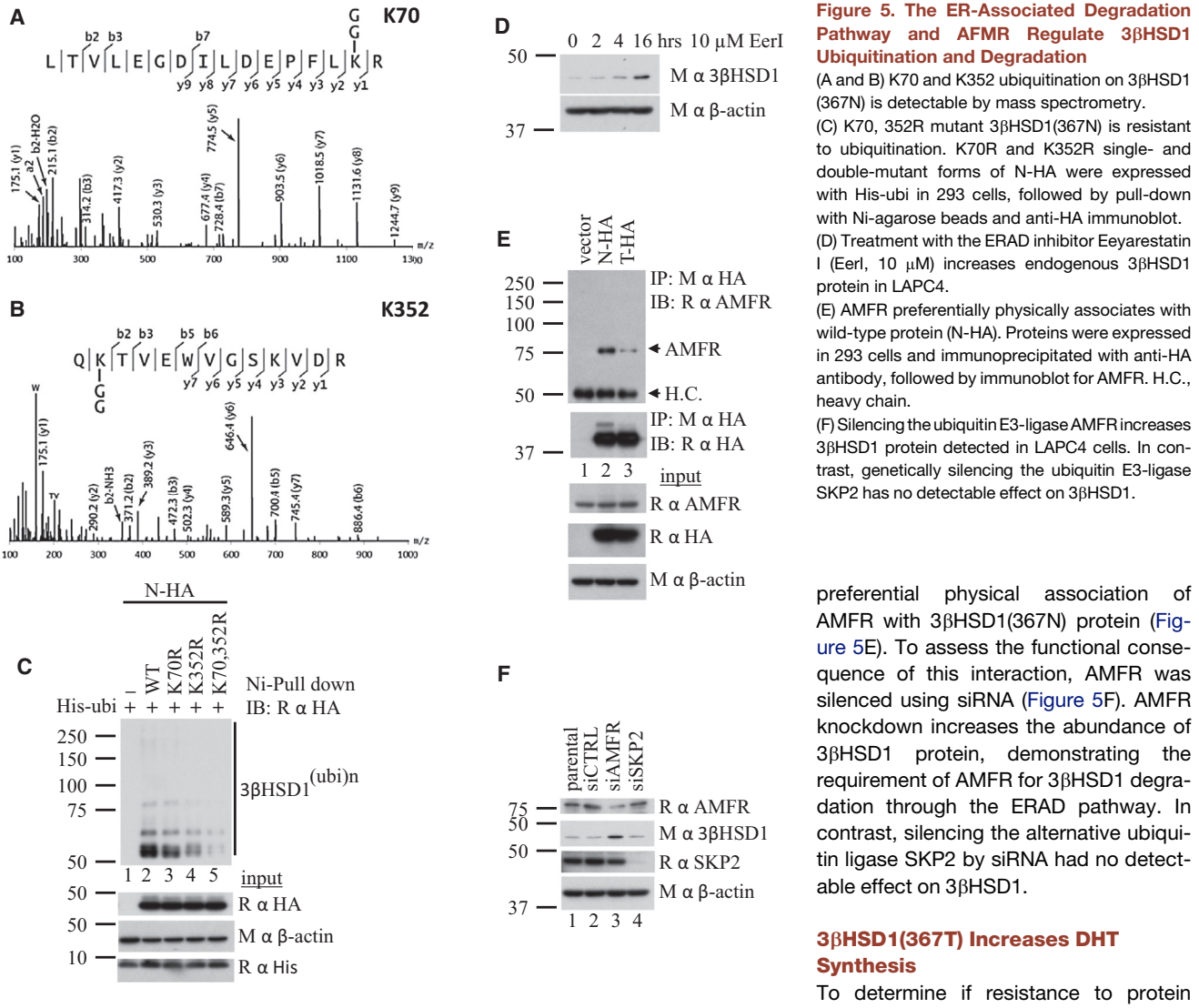

Figure 5. The ER-Associated Degradation Pathway and AFMR Regulate 3βHSD1 Ubiquitination and Degradation

(A and B) K70 and K352 ubiquitination on 3βHSD1 (367N) is detectable by mass spectrometry.

(C) K70, 352R mutant 3βHSD1(367N) is resistant to ubiquitination. K70R and K352R single- and double-mutant forms of N-HA were expressed with His-ubi in 293 cells, followed by pull-down with Ni-agarose beads and anti-HA immunoblot.

(D) Treatment with the ERAD inhibitor Eeyarestatin I (EerI, 10 μM) increases endogenous 3βHSD1 protein in LAPC4.

(E) AMFR preferentially physically associates with wild-type protein (N-HA). Proteins were expressed in 293 cells and immunoprecipitated with anti-HA antibody, followed by immunoblot for AMFR. H.C., heavy chain.

(F) Silencing the ubiquitin E3-ligase AMFR increases 3βHSD1 protein detected in LAPC4 cells. In contrast, genetically silencing the ubiquitin E3-ligase SKP2 has no detectable effect on 3βHSD1.

the endoplasmic reticulum-associated protein degradation (ERAD) pathway (Song et al., 2005). Eeyarestatin I (EerI) is a small molecule that inhibits protein degradation through the ERAD pathway (Wang et al., 2008, 2009). Endogenous 3βHSD1(367N) protein increases in LAPC4 cells with EerI treatment, suggesting that the ERAD pathway is required for 3βHSD1(367N) degradation (Figure 5D). Stable isotope labeling by amino acids in cell culture (SILAC) coupled with high-resolution mass spectrometry was employed to identify candidate ubiquitin ligases in an unbiased manner that preferentially associate with 3βHSD1(367N) (Ong et al., 2002). In this experiment, cells expressing 3βHSD1(367T)-HA and 3βHSD1(367N)-HA were grown in light and heavy media, respectively. AMFR was detected with a normalized protein ratio of 1.67 (derived from peptide ratios varying $\leq$17%) in a mixture of 3βHSD1(367N)-HA and 3βHSD1(367T)-HA immunoprecipitations mixed in a 1:1 ratio, indicating preferential physical association with 3βHSD1(367N) protein. Immunoprecipitation of 3βHSD1(367N)-HA and 3βHSD1(367T)-HA, followed by AMFR immunoblot, confirms a preferential physical association of AMFR with 3βHSD1(367N) protein (Figure 5E). To assess the functional consequence of this interaction, AMFR was silenced using siRNA (Figure 5F). AMFR knockdown increases the abundance of 3βHSD1 protein, demonstrating the requirement of AMFR for 3βHSD1 degradation through the ERAD pathway. In contrast, silencing the alternative ubiquitin ligase SKP2 by siRNA had no detectable effect on 3βHSD1.

3βHSD1(367T) Increases DHT Synthesis

To determine if resistance to protein ubiquitination and degradation ascribed to 3βHSD1(367T) confers increased synthesis of DHT from precursor steroids, we expressed constructs that encode for 3βHSD1(367N), 3βHSD1(367T), or vector alone in LAPC4 cells and assessed metabolic flux from [^{3}H]-DHEA to downstream steroids. LAPC4 cells transiently transfected with the construct encoding for 3βHSD1(367T) exhibit increased flux from DHEA → AD → 5α-dione → DHT (Figure 6A). Equivalent expression of both transcripts was confirmed by qRT-PCR (Figure 6B). Stable lentiviral expression of 3βHSD1(367T) similarly confers increased flux from DHEA → AD → 5α-dione → DHT (Figure 6C), with transcript expression comparable to wild-type transcript expression (Figure 6D). Finally, we determined that the 3βHSD1(367T) phenotype that accelerates flux from DHEA to DHT amplifies the response of androgen-regulated gene expression (Figure 6E) and hastens the time to the development of CRPC xenograft tumors (Figure 6F) in orchiectomized mice supplemented with DHEA to mimic human adrenal physiology. 3βHSD1(367T) tumors express higher levels of PSA transcript compared to 3βHSD1(367N) tumors, suggesting

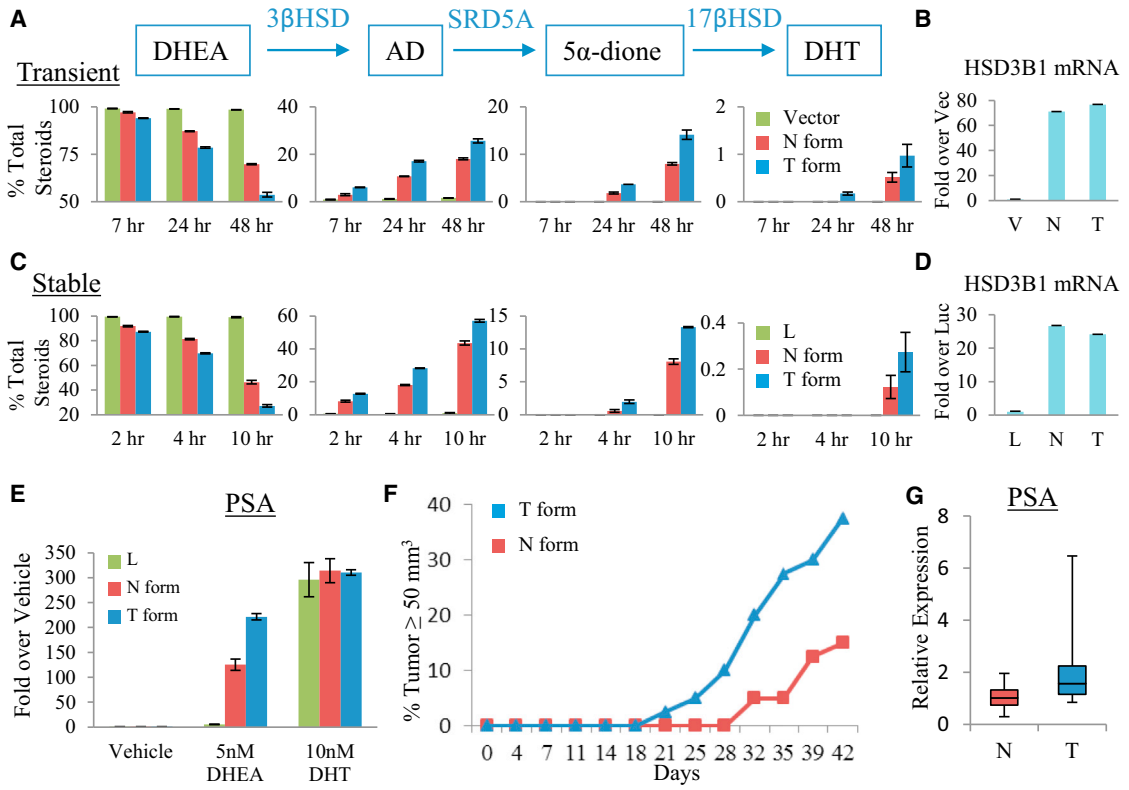

Figure 6. 3βHSD1(367T) Increases Metabolic Flux from DHEA to DHT and Elicits CRPC

(A) Transient expression of 3βHSD1(367T) (T, blue bars) leads to increased conversion from DHEA to AD and downstream steroids compared with 3βHSD1(367N) (N, red bars). LAPC4 cells were transfected with the indicated plasmid, treated with CHX, and cultured with [^{3}H]-DHEA (100 nM); steroids were extracted and measured by HPLC at the designated time points (p value = 0.023 for the difference in DHT synthesis by the N and T forms using Student's t test).

(B) Transient transfection results in equivalent expression of both transcripts by qRT-PCR.

(C) Stable expression demonstrates increased activity of 3βHSD1(367T). Lentiviral constructs expressing luciferase (L), wild-type (N), or (T) were stably expressed (without CHX treatment), and flux from [^{3}H]-DHEA to DHT was assessed, as described previously (p value = 0.015 for the difference in DHT synthesis by the N and T forms using Student's t test).

(D) Expression of both enzyme transcripts by qRT-PCR is comparable.

(E) Increased flux from DHEA to DHT with stable expression of 3βHSD1(367T) leads to amplified expression of PSA in LAPC4. Cells stably expressing the designated constructs were treated with the indicated steroids for 48 hr. PSA expression induced by the DHT-positive control is equivalent among the three cell populations. For (B), (D), and (E), expression is normalized to *RPLP0* and vector, luciferase, or vehicle controls. Error bars represent the SD for experiments performed in triplicate.

(F) Development of CRPC occurs more rapidly in LAPC4 xenografts stably expressing 3βHSD1(367T) as compared with 3βHSD1(367N). Time from subcutaneous injection of cells in each flank to tumor size = 50 mm^3 is shown for each tumor that developed in a mouse flank (n = 40 mouse flanks in each group). p = 0.017 for the comparison using a log rank test.

(G) PSA expression is higher in CRPC tumors expressing 3βHSD1(367T) compared with 3βHSD1(367N) (p value = 0.015 using Student's t test). Expression is normalized to *RPLP0*. Bars represent the upper and lower quartiles of individual tumor values.

the presence of higher sustained DHT concentrations generated in 3βHSD1(367T) tumors (Figure 6G). Together, these findings support a mechanism that favors genetic selection for the allele encoding 3βHSD1(367T) in the setting of androgen depletion.

DISCUSSION

A major mechanism of resistance to frontline gonadal T depletion (or castration) therapy is an acquired metabolic capability, which allows CRPC tumors to sustain sufficient DHT concentrations for AR stimulation and tumor progression. This study identifies a gain-of-function mutation in the steroidogenic machinery that increases flux to DHT. Notably, whether CRPC utilizes the major adrenal pathway, or possibly de novo steroidogenesis from cholesterol, 3β-hydroxyl oxidation to 3-keto and $\Delta^{5\rightarrow4}$ isomerization occurring through 3βHSD enzymatic activity is required for all pathways culminating in T and/or DHT synthesis (Evaul et al., 2010). Adrenal DHEA and DHEA-sulfate are typically present in abundant concentrations in human serum. In the context of intratumoral 3βHSD1(367N) expression, the clinical response to gonadal T depletion probably occurs in part due to the limited contribution of adrenal precursors to intratumoral DHT. Augmented 3βHSD activity occurring

through increased protein abundance with 3βHSD1(367T) would therefore serve to open the floodgates on a proximal and otherwise rate-limiting step for the synthesis of DHT, resulting in the development of CRPC. Notably, in the setting of heterozygous inheritance, 3βHSD1 protein expression is markedly higher in tumors that have lost the wild-type *HSD3B1*(1245A) allele compared to tumors that retain the wild-type sequence (Figure 2C). This finding might occur because expression and colocalization of the wild-type 3βHSD1(367N) protein reinstates mutant 3βHSD1(367T) ubiquitination and subsequent degradation via dimerization or oligomerization. Nonetheless, engineered 3βHSD1(367T) expression engenders increased flux to DHT and development of CRPC despite endogenous 3βHSD1(367N) expression (Figure 6). Therefore, the transition from sole 3βHSD1(367N) expression to mixed expression to dominant 3βHSD1(367T) expression probably represents a stepwise selection for an increased capacity for DHT synthesis.

The population frequency of the *HSD3B1*(1245C) allele is approximately 22% but appears to vary widely by ethnicity (http://genome.ucsc.edu/). Other studies suggest that the *HSD3B1*(1245C) allele may raise aldosterone levels and increase the risk of essential hypertension (Shimodaira et al., 2010). This is probably attributable to increased 3βHSD enzyme activity, which is required for aldosterone synthesis, although aldosterone is generally thought to require 3βHSD2. Interestingly, this phenotype appears to be more severe with homozygous *HSD3B1*(1245C). The observation of extremely high aldosterone with homozygous *HSD3B1*(1245C) is consistent with higher enzymatic activity and stepwise selection for sole 3βHSD1(367T) expression that occurs in CRPC. *HSD3B1*(1245C) has no consistent effect on risk of localized prostate cancer (Chang et al., 2002; Cunningham et al., 2007; Thomas et al., 2008).

Although abiraterone potently inhibits androgen synthesis, clinical studies of urinary androgen metabolites in patients with CRPC treated with this drug have demonstrated that the block is incomplete and that the synthesis of residual androgen precursors persists (Attard et al., 2012). This finding raises the possibility that tumor mechanisms that augment androgen synthesis from limited precursor steroids by increasing flux to DHT might contribute to abiraterone resistance (Chang and Sharifi, 2012). Our data demonstrating the selection and expression of 3βHSD1(367T) in a xenograft model of abiraterone resistance suggest a genetic mechanism for clinical resistance to abiraterone and that pharmacologic inhibition of 3βHSD1 might be a viable therapeutic strategy to overcome this resistance against tumors expressing the mutant enzyme. Despite the potent activity of the AR antagonist enzalutamide, its affinity for the ligand-binding domain of AR is lower than the affinity of DHT (Tran et al., 2009). Increased metabolic flux from steroid precursors to DHT by 3βHSD1(367T) may therefore conceivably tip the scales in the favor of DHT and lead to enzalutamide resistance as well. The contribution of 3βHSD1(367T) in clinical resistance to abiraterone and enzalutamide, however, remain to be determined.

The past decade has brought to the fore the development of molecularly targeted therapies that are matched to specific disease-driving enzyme mutations present in a given patient. These advances come mainly in the form of tyrosine kinase inhibitors that target gain-of-function mutations in these signaling enzymes. These include the examples of EGF receptor inhibitors matched with tumors harboring mutant EGF receptor in non-small-cell lung cancer and BRAF inhibitors for melanomas that are driven by *BRAF* mutations (Chapman et al., 2011; Kobayashi et al., 2005; Lynch et al., 2004). In contrast, no examples of drug targeting based on enzyme mutations exist in the standard of care for metastatic CRPC. Although our demonstration is in a gain of function in a metabolic enzyme, rather than a signaling enzyme, we believe the underlying principle is the same, and our findings expose the opportunity for matching a mutant disease-driving enzyme biomarker with its cognate pharmacologic inhibitor.

EXPERIMENTAL PROCEDURES

Steroid Metabolism Experiments

Steroid metabolism experiments were performed 12 hr after seeding cells by treatment with 1 ml serum-free medium containing [^{3}H]-labeled DHEA (100 nM, 300,000–600,000 cpm; PerkinElmer). Aliquots of medium were collected for up to 48 hr and treated with β-glucuronidase (1,000 units; Sigma-Aldrich) at 65°C for 4 hr. Deconjugated steroids were extracted, evaporated under nitrogen stream, dissolved in 50% methanol, and injected on a Breeze 1525 system equipped with model 717 plus autoinjector (Waters), and steroid metabolites were separated on a Luna 150 × 3 mm, 3.0 μM C_{18} reverse-phase column (Phenomenex). The column effluent was mixed with Liquiscint scintillation cocktail (National Diagnostics) and analyzed by a β-RAM model 3 in-line radioactivity detector (IN/US Systems). Steroid metabolism experiments with transient enzyme expression were performed with pCMV5-HSD3B1 (367N and 367T) constructs 24 hr after transfection and 12 hr after treatment with 25 μM cycloheximide (CHX). Steroid metabolism experiments with stable enzyme expression were performed after lentiviral infection with pLVX-Tight-Puro vector. Human tissues were obtained using Institutional Review Board-approved protocols at UT Southwestern and the University of Washington rapid autopsy program. Lentiviral constructs were made from miR30-styled shRNA sequences and cloned into the pGIPZ vector, and infected cells expressing the constructs were selected with 2 μg/ml puromycin. Gene expression was performed by qRT-PCR using the iTaq SYBR Green Supermix with the ROX kit (Bio-Rad) in an ABI-7500 Real-Time PCR machine (Applied Biosystems). Protein half-life was determined after transient transfection with pCMX-HSD3B1-HA (367N and 367T) plasmids, followed in 24 hr with 25 μM CHX in serum-free medium containing 100 nM DHEA. Cells stably expressing HA-tagged *HSD3B1* (367N and 367T) in pLVX-Tight-Puro were used to determine protein half-life 24 hr after induction of protein expression with 2 ng/ml doxycycline and treatment with CHX.

For details on all other experiments, including cell line and human tissue analyses, xenograft studies, gene expression studies, mass spectrometry, and other biochemical experiments, please refer to the Extended Experimental Procedures.

SUPPLEMENTAL INFORMATION

Supplemental Information includes Extended Experimental Procedures, three figures, and one table and can be found with this article online at http://dx.doi.org/10.1016/j.cell.2013.07.029.

ACKNOWLEDGMENTS

We thank Ralph Deberardinis, Mike Brown, Kevin Courtney, George DeMartino, and Eugene Frenkel for helpful comments, Russell DeBose-Boyd for the anti-AFMR antibody, J.T. Hsieh for the anti-SKP2 antibody, Cheng-Ming Chiang for the anti-His antibody and Actinomycin D, David Trudgian for

assistance with protein mass spectrometry, and An Jia and Chul Ahn for assistance with statistical analysis. This publication has been funded in part by a Howard Hughes Medical Institute Physician-Scientist Early Career Award (to N.S.), by the Prostate Cancer Foundation (to N.S., R.V., and P.S.N.), by an American Cancer Society Research Scholar Award (12-038-01-CCE [to N.S.]), by a grant from the U.S. Army Medical Research and Materiel Command (PC080193) (to N.S.), and additional grants from the National Cancer Institute (1R01CA168899 and 1R01CA172382-01 [to N.S.]). The acquisition of metastatic tumors through the UW Rapid Autopsy Program was funded in part by grants (PO1-CA85859 [to R.V. and P.S.N.], PC093509 [to P.S.N.], P01-CA163227 [P.S.N.], and P50CA097186 [R.V. and P.S.N.]).

Received: May 10, 2013
Revised: June 28, 2013
Accepted: July 22, 2013
Published: August 29, 2013

REFERENCES

Attard, G., Cooper, C.S., and de Bono, J.S. (2009). Steroid hormone receptors in prostate cancer: a hard habit to break? Cancer Cell *16*, 458–462.

Attard, G., Reid, A.H., Auchus, R.J., Hughes, B.A., Cassidy, A.M., Thompson, E., Oommen, N.B., Folkerd, E., Dowsett, M., Arlt, W., and de Bono, J.S. (2012). Clinical and biochemical consequences of CYP17A1 inhibition with abiraterone given with and without exogenous glucocorticoids in castrate men with advanced prostate cancer. J. Clin. Endocrinol. Metab. *97*, 507–516.

Barrie, S.E., Potter, G.A., Goddard, P.M., Haynes, B.P., Dowsett, M., and Jarman, M. (1994). Pharmacology of novel steroidal inhibitors of cytochrome P450(17) alpha (17 alpha-hydroxylase/C17-20 lyase). J. Steroid Biochem. Mol. Biol. *50*, 267–273.

Chang, K.H., and Sharifi, N. (2012). Prostate cancer-from steroid transformations to clinical translation. Nat. Rev. Urol. *9*, 721–724.

Chang, B.L., Zheng, S.L., Hawkins, G.A., Isaacs, S.D., Wiley, K.E., Turner, A., Carpten, J.D., Bleecker, E.R., Walsh, P.C., Trent, J.M., et al. (2002). Joint effect of HSD3B1 and HSD3B2 genes is associated with hereditary and sporadic prostate cancer susceptibility. Cancer Res. *62*, 1784–1789.

Chang, K.H., Li, R., Papari-Zareei, M., Watumull, L., Zhao, Y.D., Auchus, R.J., and Sharifi, N. (2011). Dihydrotestosterone synthesis bypasses testosterone to drive castration-resistant prostate cancer. Proc. Natl. Acad. Sci. USA *108*, 13728–13733.

Chapman, P.B., Hauschild, A., Robert, C., Haanen, J.B., Ascierto, P., Larkin, J., Dummer, R., Garbe, C., Testori, A., Maio, M., et al.; BRIM-3 Study Group. (2011). Improved survival with vemurafenib in melanoma with BRAF V600E mutation. N. Engl. J. Med. *364*, 2507–2516.

Cunningham, J.M., Hebbring, S.J., McDonnell, S.K., Cicek, M.S., Christensen, G.B., Wang, L., Jacobsen, S.J., Cerhan, J.R., Blute, M.L., Schaid, D.J., and Thibodeau, S.N. (2007). Evaluation of genetic variations in the androgen and estrogen metabolic pathways as risk factors for sporadic and familial prostate cancer. Cancer Epidemiol. Biomarkers Prev. *16*, 969–978.

de Bono, J.S., Logothetis, C.J., Molina, A., Fizazi, K., North, S., Chu, L., Chi, K.N., Jones, R.J., Goodman, O.B., Jr., Saad, F., et al.; COU-AA-301 Investigators. (2011). Abiraterone and increased survival in metastatic prostate cancer. N. Engl. J. Med. *364*, 1995–2005.

Evaul, K., Li, R., Papari-Zareei, M., Auchus, R.J., and Sharifi, N. (2010). 3β-hydroxysteroid dehydrogenase is a possible pharmacological target in the treatment of castration-resistant prostate cancer. Endocrinology *151*, 3514–3520.

Geller, J., Albert, J., Loza, D., Geller, S., Stoeltzing, W., and de la Vega, D. (1978). DHT concentrations in human prostate cancer tissue. J. Clin. Endocrinol. Metab. *46*, 440–444.

Greenman, C., Stephens, P., Smith, R., Dalgliesh, G.L., Hunter, C., Bignell, G., Davies, H., Teague, J., Butler, A., Stevens, C., et al. (2007). Patterns of somatic mutation in human cancer genomes. Nature *446*, 153–158.

Knudsen, K.E., and Penning, T.M. (2010). Partners in crime: deregulation of AR activity and androgen synthesis in prostate cancer. Trends Endocrinol. Metab. *21*, 315–324.

Kobayashi, S., Boggon, T.J., Dayaram, T., Jänne, P.A., Kocher, O., Meyerson, M., Johnson, B.E., Eck, M.J., Tenen, D.G., and Halmos, B. (2005). EGFR mutation and resistance of non-small-cell lung cancer to gefitinib. N. Engl. J. Med. *352*, 786–792.

Li, R., Evaul, K., Sharma, K.K., Chang, K.-H., Yoshimoto, J., Liu, J., Auchus, R.J., and Sharifi, N. (2012). Abiraterone inhibits 3β-hydroxysteroid dehydrogenase: a rationale for increasing drug exposure in castration-resistant prostate cancer. Clin. Cancer Res. *18*, 3571–3579.

Lorence, M.C., Murry, B.A., Trant, J.M., and Mason, J.I. (1990). Human 3 beta-hydroxysteroid dehydrogenase/delta 5— —4isomerase from placenta: expression in nonsteroidogenic cells of a protein that catalyzes the dehydrogenation/isomerization of C21 and C19 steroids. Endocrinology *126*, 2493–2498.

Luu-The, V., Bélanger, A., and Labrie, F. (2008). Androgen biosynthetic pathways in the human prostate. Best Pract. Res. Clin. Endocrinol. Metab. *22*, 207–221.

Lynch, T.J., Bell, D.W., Sordella, R., Gurubhagavatula, S., Okimoto, R.A., Brannigan, B.W., Harris, P.L., Haserlat, S.M., Supko, J.G., Haluska, F.G., et al. (2004). Activating mutations in the epidermal growth factor receptor underlying responsiveness of non-small-cell lung cancer to gefitinib. N. Engl. J. Med. *350*, 2129–2139.

Montgomery, R.B., Mostaghel, E.A., Vessella, R., Hess, D.L., Kalhorn, T.F., Higano, C.S., True, L.D., and Nelson, P.S. (2008). Maintenance of intratumoral androgens in metastatic prostate cancer: a mechanism for castration-resistant tumor growth. Cancer Res. *68*, 4447–4454.

Ong, S.E., Blagoev, B., Kratchmarova, I., Kristensen, D.B., Steen, H., Pandey, A., and Mann, M. (2002). Stable isotope labeling by amino acids in cell culture, SILAC, as a simple and accurate approach to expression proteomics. Mol. Cell. Proteomics *1*, 376–386.

Penning, T.M. (2010). New frontiers in androgen biosynthesis and metabolism. Curr. Opin. Endocrinol. Diabetes Obes. *17*, 233–239.

Scher, H.I., and Sawyers, C.L. (2005). Biology of progressive, castration-resistant prostate cancer: directed therapies targeting the androgen-receptor signaling axis. J. Clin. Oncol. *23*, 8253–8261.

Scher, H.I., Fizazi, K., Saad, F., Taplin, M.E., Sternberg, C.N., Miller, K., de Wit, R., Mulders, P., Chi, K.N., Shore, N.D., et al.; AFFIRM Investigators. (2012). Increased survival with enzalutamide in prostate cancer after chemotherapy. N. Engl. J. Med. *367*, 1187–1197.

Sharifi, N. (2013). Minireview: Androgen metabolism in castration-resistant prostate cancer. Mol. Endocrinol. *27*, 708–714.

Sharifi, N., Gulley, J.L., and Dahut, W.L. (2005). Androgen deprivation therapy for prostate cancer. JAMA *294*, 238–244.

Shimodaira, M., Nakayama, T., Sato, N., Aoi, N., Sato, M., Izumi, Y., Soma, M., and Matsumoto, K. (2010). Association of HSD3B1 and HSD3B2 gene polymorphisms with essential hypertension, aldosterone level, and left ventricular structure. Eur. J. Endocrinol. *163*, 671–680.

Simard, J., Ricketts, M.L., Gingras, S., Soucy, P., Feltus, F.A., and Melner, M.H. (2005). Molecular biology of the 3beta-hydroxysteroid dehydrogenase/delta5-delta4 isomerase gene family. Endocr. Rev. *26*, 525–582.

Song, B.L., Sever, N., and DeBose-Boyd, R.A. (2005). Gp78, a membrane-anchored ubiquitin ligase, associates with Insig-1 and couples sterol-regulated ubiquitination to degradation of HMG CoA reductase. Mol. Cell *19*, 829–840.

Thomas, G., Jacobs, K.B., Yeager, M., Kraft, P., Wacholder, S., Orr, N., Yu, K., Chatterjee, N., Welch, R., Hutchinson, A., et al. (2008). Multiple loci identified in a genome-wide association study of prostate cancer. Nat. Genet. *40*, 310–315.

Titus, M.A., Schell, M.J., Lih, F.B., Tomer, K.B., and Mohler, J.L. (2005). Testosterone and dihydrotestosterone tissue levels in recurrent prostate cancer. Clin. Cancer Res. *11*, 4653–4657.

Tomlins, S.A., Rhodes, D.R., Perner, S., Dhanasekaran, S.M., Mehra, R., Sun, X.W., Varambally, S., Cao, X., Tchinda, J., Kuefer, R., et al. (2005). Recurrent

fusion of TMPRSS2 and ETS transcription factor genes in prostate cancer. Science *310*, 644–648.

Tran, C., Ouk, S., Clegg, N.J., Chen, Y., Watson, P.A., Arora, V., Wongvipat, J., Smith-Jones, P.M., Yoo, D., Kwon, A., et al. (2009). Development of a second-generation antiandrogen for treatment of advanced prostate cancer. Science *324*, 787–790.

Wang, Q., Li, L., and Ye, Y. (2008). Inhibition of p97-dependent protein degradation by Eeyarestatin I. J. Biol. Chem. *283*, 7445–7454.

Wang, Q., Mora-Jensen, H., Weniger, M.A., Perez-Galan, P., Wolford, C., Hai, T., Ron, D., Chen, W., Trenkle, W., Wiestner, A., and Ye, Y. (2009). ERAD inhibitors integrate ER stress with an epigenetic mechanism to activate BH3-only protein NOXA in cancer cells. Proc. Natl. Acad. Sci. USA *106*, 2200–2205.

Yuan, X., and Balk, S.P. (2009). Mechanisms mediating androgen receptor reactivation after castration. Urol. Oncol. *27*, 36–41.

OPEN ACCESS Freely available online

PLOS ONE

Androgen Receptor Promotes Ligand-Independent Prostate Cancer Progression through c-Myc Upregulation

Lina Gao[1], Jacob Schwartzman[1], Angela Gibbs[1], Robert Lisac[1], Richard Kleinschmidt[1], Beth Wilmot[2,3], Daniel Bottomly[2,3], Ilsa Coleman[4], Peter Nelson[4], Shannon McWeeney[2,3], Joshi Alumkal[1]*

1 Division of Hematology/Oncology, Knight Cancer Institute, Oregon Health and Science University, Portland, Oregon, United States of America, **2** Oregon Clinical and Translational Research Institute, Portland, Oregon, United States of America, **3** Department of Medical Informatics and Clinical Epidemiology; Division of Bioinformatics and Computational Biology; Oregon Health and Science University, Portland, Oregon, United States of America, **4** Fred Hutchinson Cancer Research Center, University of Washington, Seattle, Washington, United States of America

Abstract

The androgen receptor (AR) is the principal therapeutic target in prostate cancer. For the past 70 years, androgen deprivation therapy (ADT) has been the major therapeutic focus. However, some patients do not benefit, and those tumors that do initially respond to ADT eventually progress. One recently described mechanism of such an effect is growth and survival-promoting effects of the AR that are exerted independently of the AR ligands, testosterone and dihydrotestosterone. However, specific ligand-independent AR target genes that account for this effect were not well characterized. We show here that *c-Myc,* which is a key mediator of ligand-independent prostate cancer growth, is a key ligand-independent AR target gene. Using microarray analysis, we found that *c-Myc* and AR expression levels strongly correlated with each other in tumors from patients with castration-resistant prostate cancer (CRPC) progressing despite ADT. We confirmed that AR directly regulates *c-Myc* transcription in a ligand-independent manner, that *AR* and *c-Myc* suppression reduces ligand-independent prostate cancer cell growth, and that ectopic expression of c-Myc attenuates the anti-growth effects of AR suppression. Importantly, treatment with the bromodomain inhibitor JQ1 suppressed c-Myc function and suppressed ligand-independent prostate cancer cell survival. Our results define a new link between two critical proteins in prostate cancer – AR and c-Myc – and demonstrate the potential of AR and c-Myc-directed therapies to improve prostate cancer control.

Citation: Gao L, Schwartzman J, Gibbs A, Lisac R, Kleinschmidt R, et al. (2013) Androgen Receptor Promotes Ligand-Independent Prostate Cancer Progression through c-Myc Upregulation. PLoS ONE 8(5): e63563. doi:10.1371/journal.pone.0063563

Editor: Natasha Kyprianou, University of Kentucky College of Medicine, United States of America

Received October 30, 2012; **Accepted** April 2, 2013; **Published** May 21, 2013

Funding: This publication was made possible with support from the Oregon Clinical and Translational Research Institute, grant number KL2 RR024141 from the National Center for Research Resources and the National Center for Advancing Translational Sciences of the National Institutes of Health (JA). This work was also supported by the Pacific Northwest Prostate Cancer SPORE/National Cancer Institute (P50CA097186) (JA, PN, IC), the Department of Defense (PC093509) (PSN), a Flight Attendant Medical Research Institute Young Clinical Scientist Award (JA), a Wayne D. Kuni & Joan E. Kuni Foundation Kuni Scholar Award (JA), and a Prostate Cancer Foundation Young Investigator Award (JA). With special thanks to Platt Electric, Bruce Burns, and The Burns Family Fund of the Oregon Community Foundation for their philanthropic support of this work. The funders had no role in study design, data collection and analysis, decision to publish, or preparation of the manuscript.

Competing Interests: The authors have declared that no competing interests exist.

* E-mail: alumkalj@ohsu.edu

Introduction

Prostate cancer is the most common cancer in men in the United States with 241,740 new cases anticipated this year [1]. Despite screening and early treatment, prostate cancer commonly recurs, and 28,170 men are predicted to die from prostate cancer this year [1]. Nearly all of these prostate cancer deaths are attributable to metastatic, castration-resistant prostate cancer (CRPC) that has progressed despite androgen deprivation therapy (ADT) – the most common treatment for patients with recurrent or advanced prostate cancer.

ADT works by lowering levels of the potent AR ligands testosterone and dihydrotestosterone (DHT) or interfering with binding of androgen ligands to the androgen receptor (AR) protein, the principal therapeutic target in prostate cancer [2]. Despite ADT, including novel and more potent treatments, all prostate cancers eventually progress [3,4]. At progression, the AR is ubiquitously expressed [5,6].

There are several possible explanations for AR-dependent mechanisms of progression despite the suppression or interference with androgen ligands. These include intratumoral androgen synthesis, the generation of constitutively active AR transcript variants, AR gene amplification, activating AR mutations, or activation of the AR by growth factors [7–16]. It is also now clear that the AR protein can promote the activation of AR ligand-independent pathways distinct from AR's canonical ligand-activated pathways in CRPC [17]. However, critical downstream AR target genes of this type that account for AR dependent, ligand-independent prostate cancer cell survival have not been fully clarified. The study of such AR target genes and mechanisms by which AR regulates their expression will improve our understanding of castration-resistance and lead to the identification of key AR dependent proteins whose activity may control growth and survival of CRPC cells. Such targets and pathways would naturally become high priorities for drug development.

To understand genes that might account for that effect, we focused on *c-Myc*. This is because: 1) *c-Myc* overexpression promotes prostate cancer development [18]; 2) *c-Myc* is upregulated in androgen ligand-dependent prostate cancer and further upregulated in CRPC [19,20]; and 3) prior reports have demonstrated that c-Myc, like AR, contributes to ligand-independent prostate cancer cell growth [21]. Our review of prior data that localized AR binding sites throughout the genome by chromatin immunoprecipitation (ChIP) showed that the AR localizes to an enhancer element of the *c-Myc* gene [17]. However, it was unclear if *c-Myc* was a direct AR target gene and whether androgen ligands were necessary for AR regulation of *c-Myc* expression.

We determined that *c-Myc* upregulation in human CRPC tumors correlates with *AR* upregulation, and we confirmed that *c-Myc* is a direct AR target gene using chromatin immunoprecipitation (ChIP) assays. *c-Myc* suppression achieves the same overall effects as *AR* suppression, and *c-Myc* overexpression attenuates the anti-growth effects of *AR* suppression. While AR promotes *c-Myc* expression, treatment with androgen ligands did not increase *c-Myc* expression. Thus, AR promotes the expression of *c-Myc* in a ligand-independent manner, and *c-Myc* is a key AR target gene.

Finally, we treated prostate cancer cells with the BET bromodomain inhibitor JQ1 that suppresses c-Myc expression [22,23]. Treatment with JQ1 achieved the same overall effect as *c-Myc* RNAi and reduced prostate cancer cell survival in androgen ligand-depleted conditions.

Our studies clarify that *c-Myc* is a key androgen ligand-independent AR target gene that contributes to androgen ligand-independent but AR-dependent prostate cancer cell survival. Our results also demonstrate the potential of AR-directed therapies or c-Myc-directed therapies in prostate cancer as adjuncts to ADT.

Results

AR and *c-Myc* are Concordantly Expressed in Metastatic CRPC

Both AR and c-Myc are critical survival pathways in prostate cancer, and expression levels of both *AR* and *c-Myc* are commonly increased in human CRPC tumors progressing despite ADT [24,25]. However, it was unknown whether overexpression of *AR* and *c-Myc* was linked with the other in human CRPC tumors. Therefore, we determined the expression levels of *AR* and *c-Myc* using gene expression microarrays in 140 human CRPC tumors versus 15 normal prostate samples. Next, we examined the association of *AR* upregulation and *c-Myc* upregulation in the human CRPC tumors. *AR* mRNA levels in CRPC samples were strongly associated with *c-Myc* mRNA levels (Pearson correlation = 0.3698, 95% Confidence Interval: 0.2172–0.5048, two-tailed p-value$<$0.0001) (Figure 1A). We also calculated the odds ratio for *c-Myc* and *AR* upregulation in these CRPC specimens. There was a statistically significant association with *AR* upregulation and *c-Myc* upregulation (OR = 3.528, 95% Confidence Interval: 1.347 to 9.240, p-value: 0.0108 by Fisher's Exact Test) (Figure 1B).

AR Suppression Reduces the Growth of AR Ligand-dependent and AR Ligand–independent Castration-resistant Prostate Cancer Cells

We suppressed expression of the *AR* with RNAi in prostate cancer cells grown in charcoal-stripped, androgen ligand-depleted serum. *AR* RNAi reduced cell growth of both androgen ligand-dependent LNCaP cells and their CRPC derivatives called LNCaP-abl (Figure 2A). Of note, both of these cells only express the full-length AR transcript. *AR* suppression with RNAi in the 22RV1 CRPC cell line that expresses both full-length AR and an AR transcript variant achieved the same effect (Figure 2A). In all cell lines, AR suppression reduced cell growth without inducing apoptosis (data not shown), suggesting a defect in proliferation. Thus, despite androgen ligand depletion, *AR* suppression further reduces prostate cancer cell growth.

c-Myc Suppression Recapitulates the Effect of AR Suppression, and c-Myc Overexpression Attenuates the Anti-tumor Activity of AR Suppression

To determine if c-Myc also influenced prostate cancer cell growth independent of androgen ligands, we suppressed *c-Myc* using RNAi. Like *AR* downregulation, *c-Myc* down-regulation suppressed ligand-independent growth of LNCaP, abl, and 22RV1 cells (Figure 2B). Further, we simultaneously suppressed *AR* and *c-Myc* with RNAi. Co-suppression of both proteins did not reduce cell growth more than suppression of either *AR* or *c-Myc* by itself (Figure S1).

We also demonstrated that *c-Myc* overexpression conferred ligand-independent growth to ligand-dependent LNCaP cells propagated long-term in castrate conditions, which is concordant with a prior report (Figure S2) [21]. Next, we suppressed *AR* with RNAi in LNCaP cells overexpressing empty vector or *c-Myc* and quantified cell growth. *c-Myc* overexpression was protective against the growth suppressive effects of *AR* RNAi (Figure 2C). This demonstrates that *c-Myc* at least partially contributes to AR's effects on promoting ligand-independent prostate cancer cell survival.

AR but not Androgens Promote c-Myc Expression

The *c-Myc* oncogene is commonly upregulated in prostate cancer, and *c-Myc* upregulation promotes ligand-independent prostate cancer cell survival [21]. However, the dependency of *c-Myc* expression on AR had not been established. Accordingly, we examined previously published ChIP microarray data that localized AR throughout the genome of androgen ligand-dependent LNCaP cells and their Abl CRPC derivatives [17]. AR was reported to be bound to an enhancer element of the *c-Myc* gene in both of these cell lines. Therefore, we next used ChIP to confirm these results.

First, we grew cells in charcoal-stripped, androgen ligand-depleted serum and determined the effect of treatment with the androgen ligand R1881 on AR occupancy and histone acetylation, a mark of active transcription, at the *c-Myc* enhancer element using ChIP. We also measured the effects of R1881 treatment at the well-described, ligand-activated gene *KLK3*. AR and high levels of histone acetylation were present at the *c-Myc* enhancer even when cells were grown in ligand-depleted serum (Figure 3A). Further, the addition of R1881 to culture did not enhance AR occupancy or histone acetylation at *c-Myc* (Figure 3A). This contrasts with the effect of R1881 at the *KLK3* gene enhancer- increased enrichment of AR and histone acetylation (Figure 3A).

We next determined the effect of R1881 treatment on expression of *c-Myc* or *KLK3*. R1881 treatment increased *KLK3* expression (Figure 3B). However, R1881 treatment did not increase *c-Myc* expression. Figure 3B,C).

Next, we treated prostate cancer cells with MDV3100, a potent, new androgen antagonist [26]. MDV3100 treatment suppressed expression of *KLK3* but did not affect expression of *c-Myc*. (Figure S3). These results further support the notion that androgen ligands do not promote expression of *c-Myc*.

A.

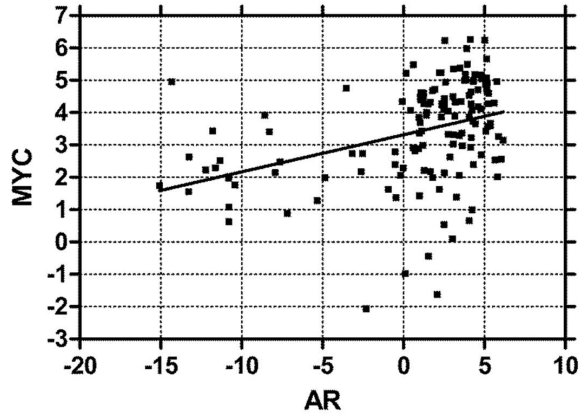

Pearson r	0.3698
95% confidence interval	0.2172 to 0.5048
P value (two-tailed)	P<0.0001

B.

		c-Myc upregulation	
		No	Yes
AR upregulation	No	16	46
	Yes	7	71

Odds ratio 3.528
95% confidence interval 1.347 to 9.240
Fisher's exact test P value 0.0108

Figure 1. *AR* and *c-Myc* levels are positively correlated in CRPC specimens. A) Z-scores (to normal prostate specimens) of *AR* versus *c-Myc* mRNA expression across 140 human CRPC metastases. The Pearson correlation coefficient, linear regression, and F test for significantly non-zero slope were performed for each pair of genes. B) Fisher's exact test and odds ratio on the contingency table analyzing the co-occurrence of tumors with *AR* or *c-Myc* z-scores greater than 2.
doi:10.1371/journal.pone.0063563.g001

To determine if the AR was capable of regulating *c-Myc* in a ligand-independent manner, we used RNAi to suppress the expression of *AR* and measured *c-Myc* expression. RNAi-mediated suppression of *AR* reduced c-Myc mRNA and protein expression (Figure 4A, B). We performed ChIP assays and confirmed that *AR* RNAi reduced AR and histone acetylation from the *c-Myc* enhancer (Figure 4C). This was most significant in the 22RV1 cell line, although strong trends were also seen in LNCaP and Abl cells. Thus, *c-Myc* is a direct AR target gene, and *AR* RNAi suppresses *c-Myc* expression at least in part through depletion of AR and histone acetylation from the *c-Myc* enhancer. We also overexpressed AR in the M12 prostate cancer cell line that does not normally express AR. AR overexpression increased c-Myc mRNA and protein expression (Figure S4). This further supports the notion that AR activates *c-Myc* expression in a ligand-independent manner.

AR Suppression Recapitulates the Effect of c-Myc Suppression

We next determined whether RNAi-mediated suppression of *AR* recapitulated the effect of RNAi-mediated suppression of *c-Myc* on expression of well-described *c-Myc* target genes (Figure 5) [27,28]. Both *c-Myc* RNAi and *AR RNAi* reduced expression of the *c-Myc*-activated gene *E2F1*; conversely, *c-Myc* and *AR* RNAi both increased expression of the *c-Myc*-repressed gene *CDKN1A* (Figure 5). Recent reports demonstrate that mitotic genes, including *KIF11*, *AURKB*, and *TPX2*, are key c-Myc target genes [29–31]. *AR* RNAi recapitulated the effect of c-*Myc* RNAi and also reduced expression of these genes (Figure 5). This demonstrates that AR suppression disrupts c-Myc function and expression of well-established c-Myc target genes.

The BET Bromodomain Inhibitor JQ1 Suppresses c-Myc Function and Reduces AR Ligand-independent Prostate Cancer Cell Survival

Our results demonstrate that *c-Myc* is an important AR target gene but that *c-Myc*'s expression is not activated by androgenic ligands. Currently, therapies to suppress AR expression are not yet available. However, recent work demonstrates that a BET bromodomain inhibitor called JQ1 suppresses c-Myc expression and c-Myc function because *c-Myc* is a bromodomain target gene [22,23]. Therefore, we treated prostate cancer cells with JQ1. JQ1 treatment reduced mRNA and protein levels of c-Myc (Figure 6A,B) and suppressed c-Myc function as measured by c-Myc target gene expression (Figure 6B). Finally, like *c-Myc* RNAi, JQ1 treatment with nanomolar concentrations reduced ligand-independent prostate cancer cell survival (Figure 6C).

Discussion

It is well-appreciated that the AR is a critical driver of prostate cancer cell survival and that AR accounts for progression to fatal CRPC despite treatment with ADT [24]. In many cases androgens persist intracellularly within CRPC tumors despite castrate serum levels of androgens [24,32]. However, androgen ligand-independent but AR-dependent mechanisms that also promote survival of CRPC cells have been reported. These include activation of the AR by IL-6, AR gene amplification, and AR transcript variants that lack the androgen ligand binding domain [7–9,15]. All of these mechanisms may contribute to prostate cancer progression despite ADT since none are directly targeted by ADT.

Recently, it was demonstrated that the AR protein promotes the expression of a gene program distinct from its canonical androgen ligand-directed targets in CRPC cells [17]. One such example is the AR target gene *UBE2C* that promotes ligand-independent prostate cancer proliferation [17]. Which of the other AR-induced gene products is critical for ligand-independent prostate cancer cell

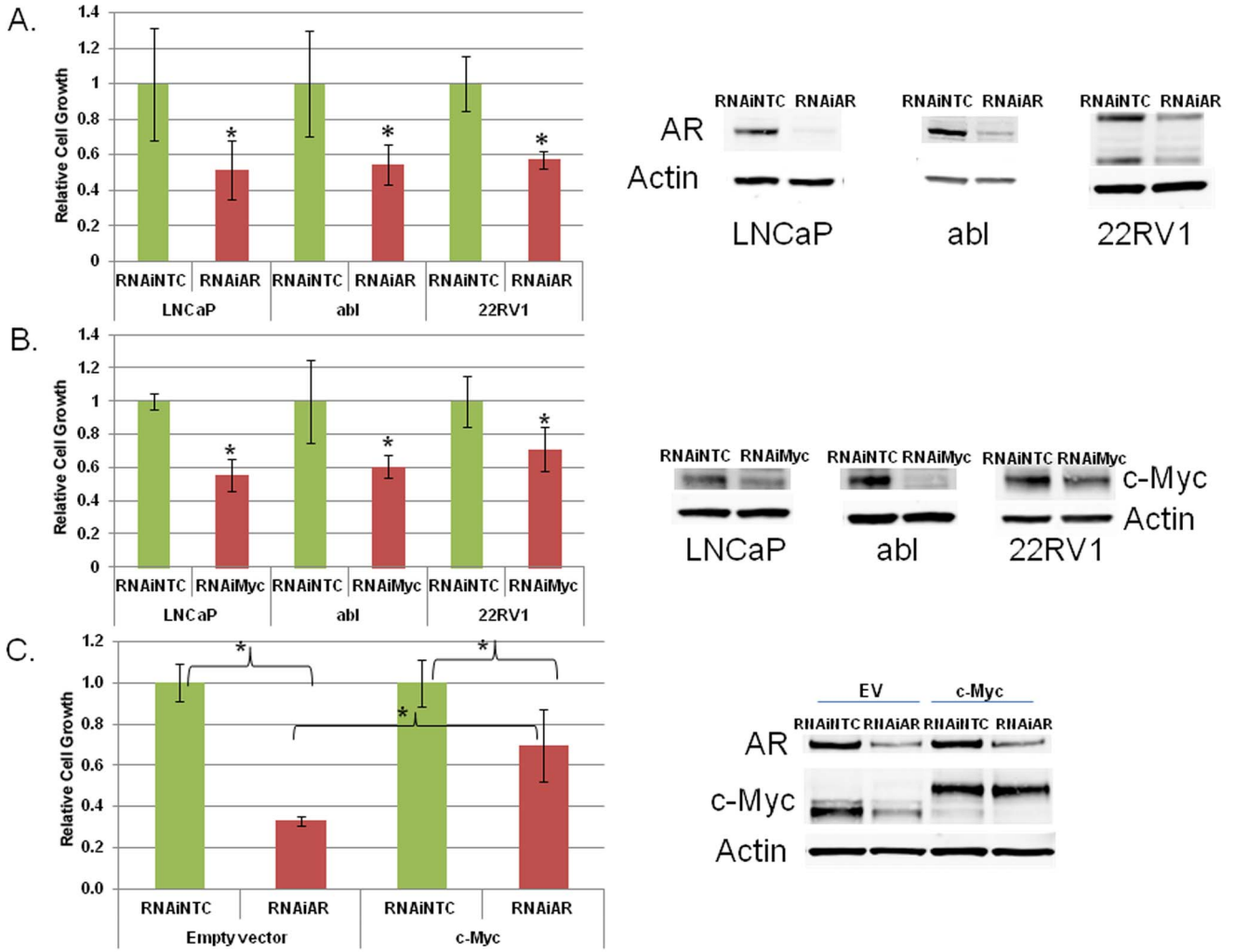

Figure 2. AR and c-Myc promote ligand-independent prostate cancer cell growth. A) LNCaP, abl and 22RV1 cells were transfected with 50 nM of non-targeted control (NTC) or *AR* RNAi oligonucleotides. Cells were switched to charcoal-stripped serum on the day of transfection. Cell growth was determined 5 days later for LNCaP and 6 days later for abl and CRPC 22RV1 with the trypan blue exclusion method. B) Immunoblot for AR expression. The lower bands in the AR immunoblot in 22RV1 cells reflect the presence of an AR transcript variant [7]. B) LNCaP, abl and 22RV1 cells were transfected with 50 nM of NTC or *c-Myc* RNAi oligonucleotides. Cells were switched to charcoal-stripped serum on the day of transfection. Cell growth was determined 5 days later for LNCaP cells and 6 days later for abl and 22RV1 with the trypan blue exclusion method. Immunoblot for c-Myc protein expression. C) LNCaP cells with stable overexpression of empty vector (EV) or c-Myc were generated. These cells were transfected with 50 nM of non-targeted control (NTC) or AR siRNA oligonucleotides. Cell growth was determined 6 days later with the trypan blue exclusion method. Immunoblot for AR and c-Myc protein expression. The higher bands on the c-Myc immunoblot in the c-Myc-overexpressing cells represent the ectopically-expressed c-Myc. *denotes $p<0.05$ compared to NTC.
doi:10.1371/journal.pone.0063563.g002

survival has been unclear. Our work demonstrates that the *c-Myc* oncogene is such a ligand-independent AR target gene.

c-Myc is commonly upregulated in prostate cancer, and *c-Myc* overexpression transforms normal prostatic epithelial cells in genetically engineered mouse models of prostate cancer and confers ligand-independent prostate cancer cell survival, but the dependency of *c-Myc* expression on the AR was unclear [18,20,21,33]. We show here that *AR* and *c-Myc* are commonly upregulated in CRPC, and we confirmed that *AR* and *c-Myc* upregulation strongly correlated with each other in a large series of metastatic CRPC patient tumors (Figure 1).

We confirmed that *AR* suppression leads to loss of c-Myc expression in prostate cancer cell lines expressing full-length AR (LNCaP and Abl) and in another CRPC cell line 22RV1 that expresses both full-length AR and an AR transcript variant. Although we cannot exclude a role for the AR transcript variant in also promoting *c-Myc* expression, our results with AR RNAi in LNCaP and Abl and our results with AR overexpression in M12 cells demonstrate that full-length AR is capable of activating *c-Myc* expression (Figure 4, Figure S4).

Like *AR* RNAi, *c-Myc* RNAi reduced prostate cancer cell survival in androgen ligand-depleted conditions while co-suppression of *AR* and *c-Myc* was not more effective than suppression of either protein alone (Figure 2, Figure S1). *c-Myc* overexpression confers ligand-independent survival to prostate cancer cells (Figure S2), which matches a prior report [21]. We also showed that *c-Myc* overexpression attenuated the anti-tumor activity of *AR* suppression with RNAi (Figure 2C). Thus, c-Myc contributes to AR's effects on promoting ligand-independent prostate cancer cell survival.

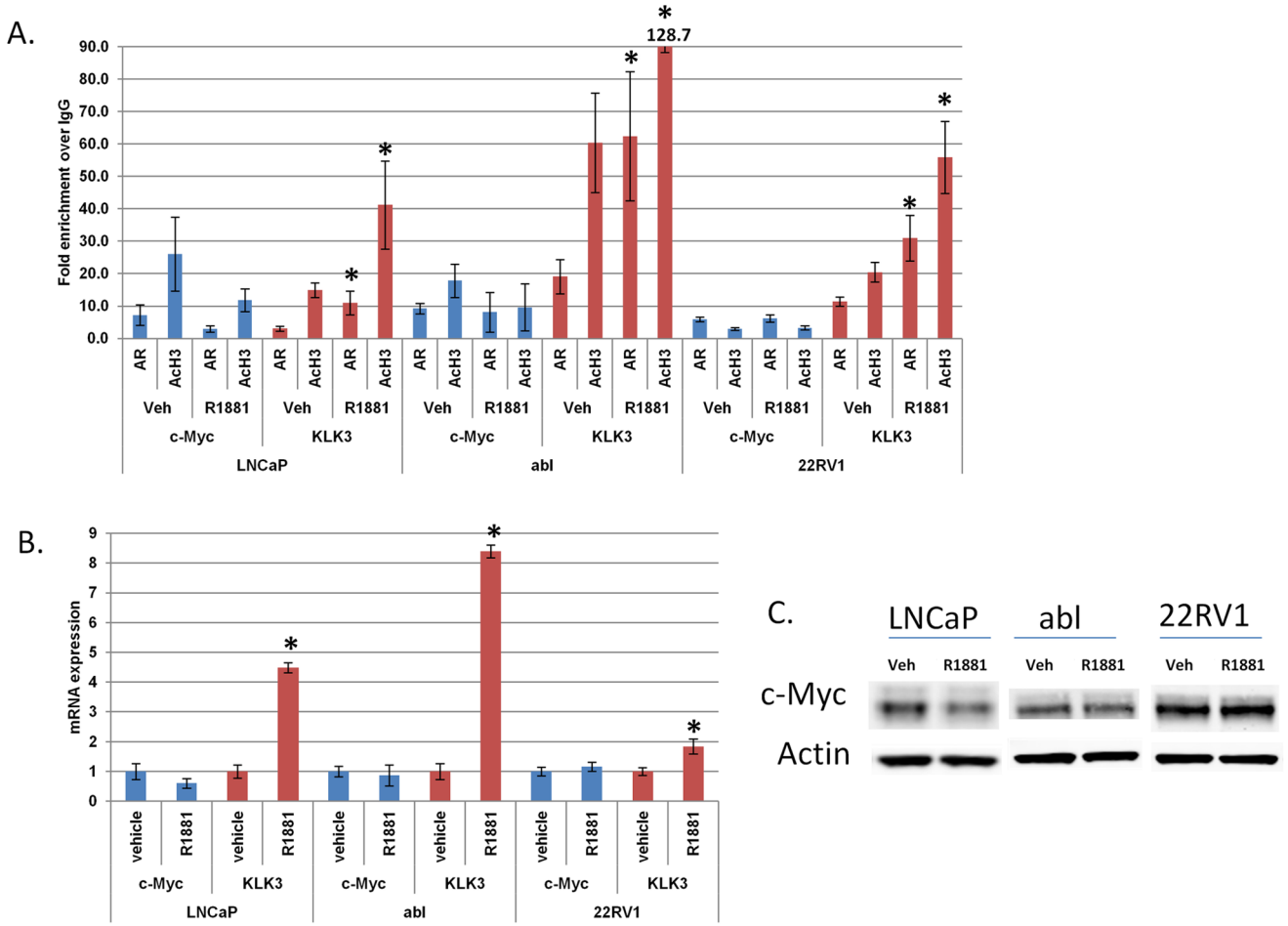

Figure 3. *c-Myc* expression is not activated by androgen ligands. LNCaP, abl, and 22RV1 cells were grown in charcoal-stripped serum for 72 hours and then treated with 10 nM R1881 (or ethanol vehicle) for 4 hours. A) Chromatin immunoprecipitation was performed to determine the enrichment of AR and histone H3 acetylation (AcH3) at the *c-Myc* and *KLK3* enhancer elements. B) QRT-PCR was performed to determine the mRNA levels of *KLK3* and *c-Myc* relative to actin. C) Immunoblotting was performed to determine the protein levels of AR, c-Myc, and actin. *denotes $p<0.05$ compared to vehicle.
doi:10.1371/journal.pone.0063563.g003

Despite the fact that AR promotes expression of *c-Myc*, treatment with androgen ligand did not increase *c-Myc* expression (Figure 3). Additionally, treatment with androgen ligands did not enhance AR occupancy at the *c-Myc* enhancer (Figure 3). This contrasts with the effects of androgen stimulation on expression of the *KLK3* gene, a well-described androgen-activated gene, and AR occupancy at the *KLK3* enhancer (Figure 3). To further confirm that AR promotes expression of *c-Myc* in a ligand-independent manner, we treated prostate cancer cells with the new, potent androgen antagonist MDV3100 [26]. Treatment with MDV3100 in a recent randomized, placebo-controlled phase III clinical trial improved overall survival of patients with CRPC [34]. However, in some patients there is no tumor response, and at progression the AR remains in the nucleus [3,6,34]. While MDV3100 treatment reduced expression of *KLK3*, MDV3100 treatment had no effect on *c-Myc* expression (Figure S3). These data further support the notion that AR promotes *c-Myc* expression in a ligand-independent manner. *c-Myc* is a critical factor in ligand-independent prostate cancer progression (Figure 2, Figure S2) [21]. Therefore, in the future, it will be important to measure *c-Myc* expression and function in CRPC patient tumors progressing despite more complete androgen interference with drugs such as MDV3100.

Because of the importance of *c-Myc* as a downstream contributor to AR's effects on ligand-independent prostate cancer cell survival, we treated prostate cancer cells with the BET bromodomain inhibitor JQ1, a drug known to suppress expression of bromodomain target genes; foremost among which was *c-Myc* [22,23]. In prior studies, JQ1 treatment in vitro and in vivo suppressed c-Myc expression and function and suppressed tumor growth without appreciable toxicity [22,23].

We confirmed that JQ1 treatment of prostate cancer cells using nanomolar concentrations achieved the same overall effects as RNAi-mediated suppression of *c-Myc* – c-Myc mRNA and protein depletion, suppression of c-Myc function, and suppression of ligand-independent prostate cancer cell survival (Figure 6). In light of the involvement of *c-Myc* in critical physiological processes, targeting the c-Myc protein generally in multiple cell types through long-term administration could be undesirable [35,36]. Clinical trials will be necessary to determine the safety of bromodomain inhibition. However, the results to date, including our own, suggest that this is a promising anti-tumor strategy for the treatment of CRPC (Figure 6) [22,23].

Finally, that the AR controls expression of its target genes such as *c-Myc* in a tissue specific manner suggests that the ideal agent for

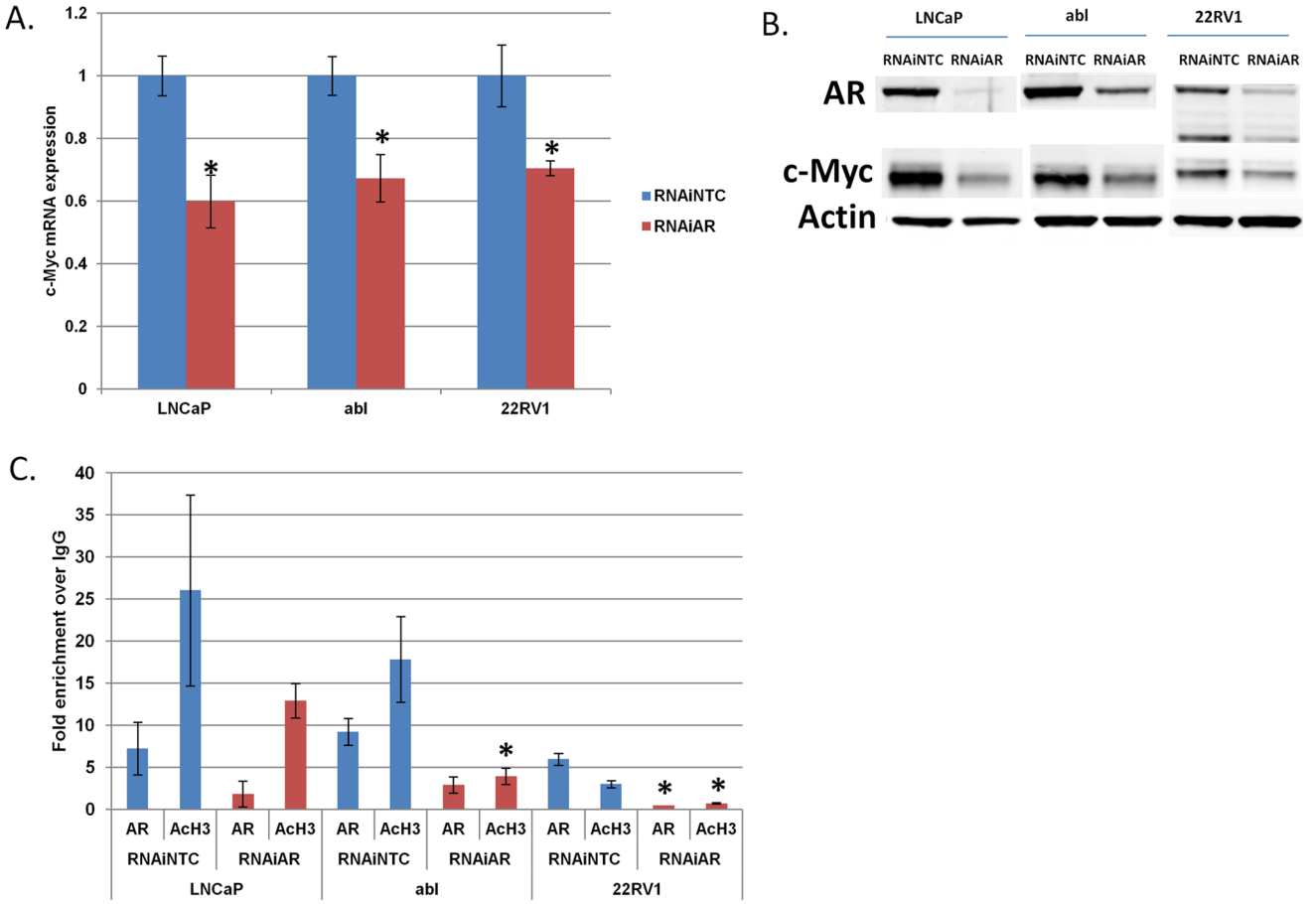

Figure 4. AR promotes ligand-independent expression of *c-Myc*. LNCaP, abl and 22RV1 cells were transfected with 50 nM of non-targeted control (NTC) or AR RNAi oligonucleotides. Cells were then grown in charcoal-stripped serum for 96 hours. At the end of the treatment, cells were harvested to extract mRNA and protein. A) QRT-PCR was performed to determine the levels of *c-Myc* relative to *actin*. B) Immunoblotting was performed to determine the levels of AR, c-Myc and actin. C) Parallel treatments were performed and cells were cross-linked and processed for ChIP to determine AR and histone H3 acetylation (AcH3) enrichment at the *c-Myc* enhancer. *denotes $p<0.05$ compared to NTC.
doi:10.1371/journal.pone.0063563.g004

suppression of *c-Myc* expression in prostate cancer cells specifically would target AR, itself. Indeed, our studies clarify that androgen ligand-independent but AR-dependent *c-Myc* gene upregulation is a mechanism by which the AR protein promotes ligand-independent survival of prostate cancer cells. Our studies support the worthiness of efforts to suppress AR's ligand-independent function and expression of important ligand-independent AR target genes such as *c-Myc* (Figure 7). Drugs capable of suppressing AR expression are only now beginning to enter testing. These drugs include selective AR degraders and AR anti-sense oligonucleotides [37–40]. We await the results of these clinical studies to determine the safety, specificity, and efficacy of these agents in men with advanced prostate cancer.

Methods

Cell Culture

LNCaP and 22RV1 cells were purchased from American Type Culture Collection (ATCC) and grown in 10% charcoal-stripped fetal bovine serum for all experiments. Abl cells, a CRPC derivative of LNCaP, were a kind gift from Zoran Culig, PhD and were grown in RPMI with 10% charcoal-stripped fetal bovine serum. M12 prostate cancer cells expressing empty vector or AR were a kind gift from Stephen R. Plymate, PhD, and grown as described previously [9].

For RNAi experiments, LNCaP and abl cells were transfected with RNAi oligonucleotides (*AR*: 5′-GACCUACCGAGGAG-CUUUCUU-3′, and *c-Myc*: 5′-GAGCUAAAACGGAG-CUUUUdTdT-3′) by using DharmaFECT 3 (Dharmacon) transfection reagent for a final concentration of 50 nM [41]. 22RV1 cells were transfected with siRNA oligonucleotides by using Lipofectamine2000 (Life Technologies) transfection reagent for a final concentration of 50 nM. Cells were harvested at indicated time points post-transfection.

R1881 (Sigma) was resuspended in 100% ethanol. MDV3100 was purchased (Selleckchem) and resuspended in DMSO. JQ1 was purchased from Sigma and resuspended in DMSO. Cell growth was determined at the end of treatment with the trypan blue exclusion method (Life Technologies) following manufacturers' instructions. All cell culture experiments were performed with biological triplicate samples and confirmed in repeat experiments.

LNCaP cells with stable overexpression of c-Myc or empty vector were generated by transfecting LNCaP cells with pCDNA-DEST40-*c-Myc* (kindly provided by Rosalie Sears, PhD) or pCMV6-AN-His (Origene) and selecting with G418.

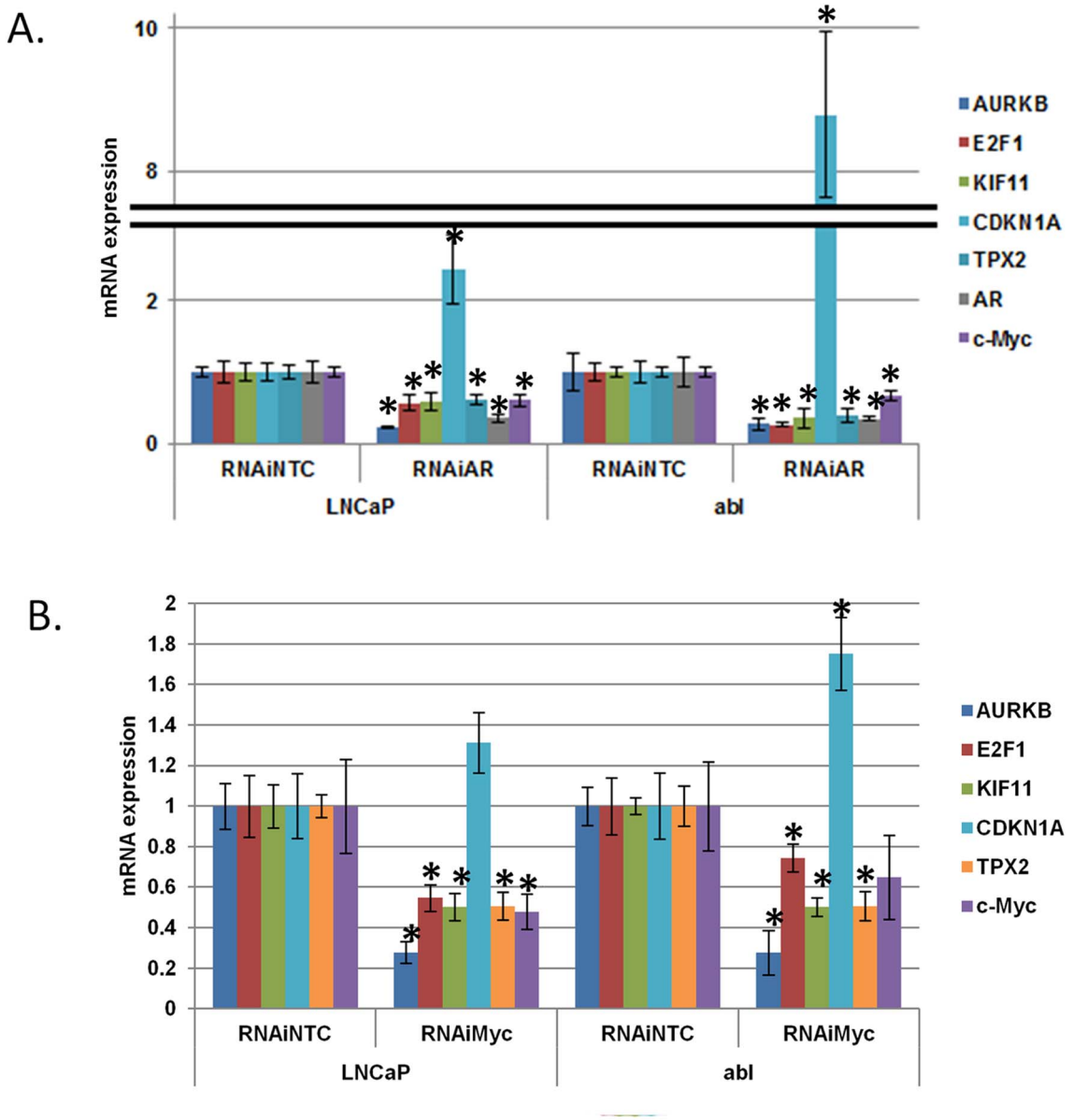

Figure 5. *AR* suppression recapitulates the effect of *c-Myc* suppression on *c-Myc* target gene expression. LNCaP and abl cells were transfected with 50 nM of non-targeted control (NTC) and either A) *AR* or B) *c-Myc* RNAi oligonucleotides. Cells were switched to charcoal-stripped serum on the day of transfection and harvested 96 hours later. QRT-PCR was performed to determine the levels of the indicated *c-Myc* target genes relative to *actin*. *denotes $p<0.05$ compared to NTC.
doi:10.1371/journal.pone.0063563.g005

Colony-formation Assay

200,000 LNCaP cells with stable overexpression of empty vector (EV) or *c-Myc* were plated in 10 cm dishes. RPMI with 10% charcoal-stripped fetal bovine serum supplemented with 300 ug/ml G418 and 10 ug/ml bicalutamide treatment was added to the cells every other day for 14 days. Next, the cells were fixed with 4% formaldehyde and stained with syto60 (Invitrogen). Images were taken with Licor Odyssey imaging system.

Immunoblotting

Immunoblotting experiments were performed as described previously [42]. Final images were obtained with Licor Odyssey imaging system. Primary antibodies used were: AR (N-20, Santa Cruz); actin (Sigma) and c-Myc (Epitomics). Secondary antibodies were purchased from Licor.

QRT-PCR

RNA was extracted from cell pellets stored in RNAlater reagent (Life Technologies) using a MagMAX Total RNA Isolation kit (Life Technologies) or Trizol (Invitrogen) according to the manufacturer's instructions. RNA concentration was determined using a NanoDrop ND-1000 spectrophotometer (NanoDrop). 250 ng–1 ug RNA (normalized for each experiment) was reverse-transcribed using a High-Capacity cDNA Reverse Transcription kit (Life Technologies) with random primers. Realtime (QRT)-PCR was performed using a 7500 Fast thermocycler (Life Technologies) with the following cycling program: 50°C for

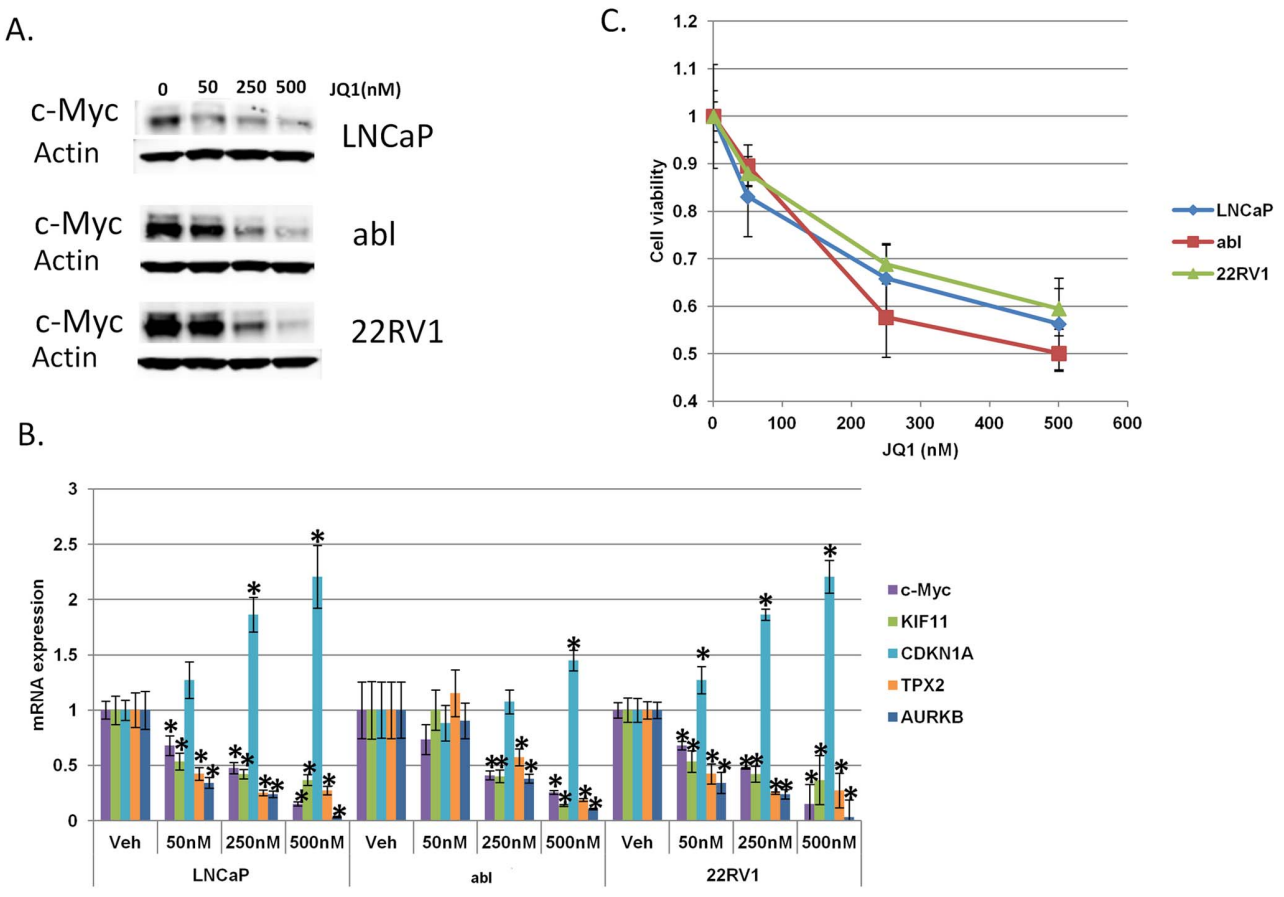

Figure 6. JQ1 treatment suppresses c-Myc expression and function and reduces ligand-independent prostate cancer cell survival. LNCaP, abl, and 22RV1 cells were grown in charcoal-stripped serum and treated with vehicle, 50 nM, 250 nM or 500 nM JQ1 every 24 hours for 72 hours. A) Immunoblotting was performed to determine the protein levels of c-Myc. B) QRT-PCR was performed to determine the mRNA level of *c-Myc* and c-Myc targets genes *KIF11*, *CDKN1A*, *TPX2*, and *AURKB* relative to *actin*. *denotes $p<0.05$ compared to vehicle. C) Cell viability was determined at the end of treatment with the trypan blue exclusion method. $p<0.01$ for the 250 nM and 500 nM doses vs. vehicle in all three cell lines.
doi:10.1371/journal.pone.0063563.g006

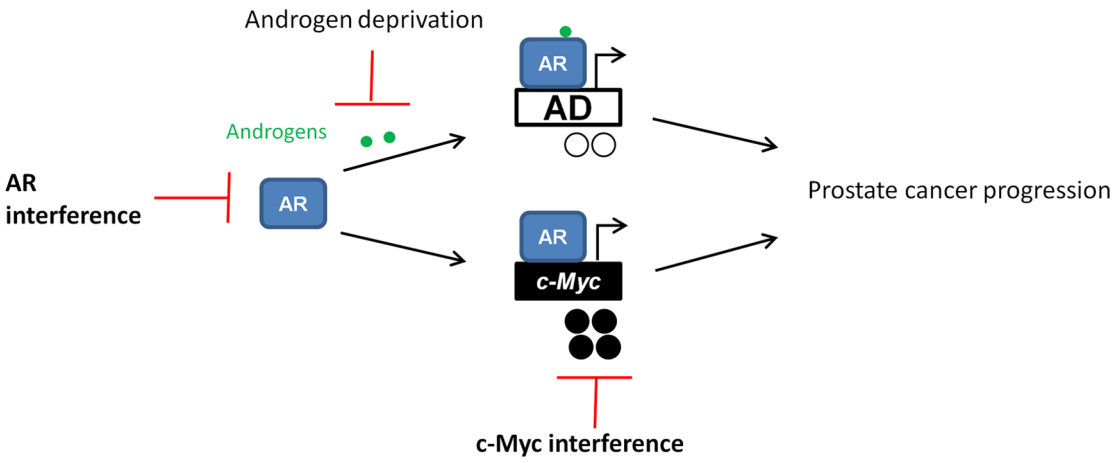

Figure 7. AR and c-Myc are critical drivers of ligand-independent mechanisms of prostate cancer progression. Currently, androgen deprivation therapies that interfere with androgen ligand activation of the AR are primarily used to treat this disease. These therapies suppress AR's androgen ligand-dependent function and suppress expression of androgen ligand-dependent (AD) AR target genes. However, despite these treatments prostate cancer progression is inevitable. The AR also promotes the expression of androgen ligand-independent pathways such as *c-Myc*. The *c-Myc* gene is commonly upregulated in prostate cancer and contributes to androgen ligand-independent prostate cancer progression. This model strongly suggests that AR or c-Myc-directed therapies would complement current androgen deprivation strategies.
doi:10.1371/journal.pone.0063563.g007

2 min, 95°C for 10 min, 40 cycles of 95°C for 15 sec dissociation, 60°C for 1 min annealing/extension/read. 10 μL singleplex RTPCR reactions contained 1X Taqman universal standard mastermix, 1X Taqman hydrolysis probe, and 10 ng RNA-equivalent cDNA template. Human beta-actin (#4326315E) was used as an endogenous control. Primer information is included in Table S1. QRT-PCR for each biological replicate sample was performed with technical triplicates and analyzed with 7500 Software v2.0.5 and DataAssist Software v3.0 (Life Technologies).

Chromatin Immunoprecipitation (ChIP)

5 μg of anti-AR antibody (N-20, Santa Cruz), anti-acetylated histone H3 (AcH3) antibody (Millipore) or normal rabbit (IgG) antibody (Millipore) were added to sheared, formaldehyde cross-linked chromatin derived from 1 to 2×10^6 cells to immunoprecipitate DNA overnight at 4°C. 1% of chromatin was removed prior to immunoprecipitation as input. Immune complexes were collected with protein A magnetic beads (Dynabeads, Life Technologies). After extensive washing, immune complexes were released, cross-links were reversed, and DNA was purified with mini-elute PCR purification kit (Qiagen) and eluted with 60 μl EB. Realtime QPCR was performed as described above using 1X SYBR GreenER mastermix (Life Technologies), 750 ng of each primer, and 2 μl of the immunoprecipitated DNA or 2 μl of the 1% input in a 20 μL reaction. Immunoprecipitated DNA was calculated as "fold enrichment over IgG" with ddCt method. Primer information is included in Table S1.

Statistical Analysis

Data are expressed as standard deviation of the mean. All PCR results and cell count results represent one single experiment performed in triplicate. p-values were calculated from one single experiment with two-tailed unpaired student's T-test in Excel (Microsoft) or Study Results 1.0 software. Each experiment was confirmed in two to three separate experiments.

AR ChIP-microarray Data Mining

The AR ChIP-microarray data was downloaded from http://research4.dfci.harvard.edu/brownlab/datasets/index.php?dir=Wang_AR_Data/for both abl and LNCaP cells. We filtered the data requiring that each peak have a FDR <5% and be within 50 Kb of either the 5′ or 3′ end of a RefSeq gene. Using these criteria, we found overlapping peaks with proximity to the *c-Myc* locus at chr8:128844491–128845592 (~21.6 Kb from *c-Myc*) in abl cells and chr8:128844572–128845592 (~21.7 Kb from *c-Myc*) in LNCaP cells.

AR and *c-Myc* Expression in Human Castration-Resistant Prostate Cancer Tumors

Agilent 44 K whole human genome expression oligonucleotide microarrays (Agilent Technologies, Inc.) were used to profile 140 human castration-resistant prostate cancer soft tissue metastases from 55 patients. Tissue samples were collected from autopsies performed at the University of Washington Medical Center under the rapid autopsy program with Institutional Review Board approval as described previously [43]. The tumor samples were laser-capture microdissected, and total RNA was isolated and amplified as described previously [44]. Probe labeling and hybridization were performed following the Agilent suggested protocols, and fluorescent array images were collected using the Agilent DNA microarray scanner G2565BA. Expression ratios were normalized using the R software Bioconductor snm package and combined with expression profiles from 15 normal prostate specimens to create z-scores, which represent the number of standard deviations away from the mean of expression in the normal prostate group [45,46]. GraphPad Prism v4.03 software was used to analyze the correlation of expression and strength of association between genes. A Pearson correlation coefficient, linear regression, and F test for significantly non-zero slope were performed for each pair of genes as well as a Fisher's exact test and odds ratio on the contingency table analyzing the co-occurrence of tumors with *AR* or *c-Myc* z-scores greater than 2.

Supporting Information

Figure S1 Co-suppression of *AR* and *c-Myc* does not lead to greater anti-tumor activity than suppression of either protein by itself. A) LNCaP cells were transfected with 50 nM of NTC, *AR*, *c-Myc*, or both *AR* and *c-Myc* RNAi oligonucleotides. Cells were switched to charcoal-stripped serum on the day of transfection. Cell growth was determined 5 days later with the trypan blue exclusion method. *denotes $p<0.01$ compared to NTC. B) Immunoblotting was performed to determine the levels of AR, c-Myc, and actin.
(TIF)

Figure S2 *c-Myc* over expression promotes ligand-independent prostate cancer growth. A) The same number of LNCaP cells with stable overexpression of empty vector or c-Myc were grown in 10% charcoal-stripped fetal bovine serum. Cell number was determined 1, 4, and 7 days after plating with the trypan blue exclusion method. Cell growth was calculated compared to day 1. $p<0.01$ for both time points. B) The same number of LNCaP cells with stable overexpression of empty vector or c-Myc was plated. Cells were grown in charcoal-stripped serum supplemented with bicalutamide for 14 days. Colony formation was determined.
(TIF)

Figure S3 MDV3100 treatment does not reduce *c-Myc* expression. LNCaP, abl, and 22RV1 cells were grown in androgen-replete serum and treated with 10 μM MDV3100 or vehicle for 24 hours. QRT-PCR was performed to determine the mRNA levels of *KLK3* and *c-Myc* relative to *actin*. *denotes $p<0.001$ compared to vehicle.
(TIF)

Figure S4 AR overexpression promotes *c-Myc* upregulation. AR or empty vector was stably overexpressed in M12 prostate cancer cells that do not express endogenous AR [9]. RNA and protein were harvested. A) QRT-PCR was performed to determine the level of *c-Myc* relative to *actin*. B) Immunoblotting was performed to determine the levels of AR, c-Myc and actin. *denotes $p<0.003$ compared to empty vector.
(TIF)

Table S1 Primers used for ChIP-PCR and QRTPCR.
(DOCX)

Author Contributions

Conceived and designed the experiments: LG JA. Performed the experiments: LG JS AG RL RK BW DB IC JA. Analyzed the data: LG BW DB IC PN SM JA. Contributed reagents/materials/analysis tools: PN SM JA. Wrote the paper: LG DB IC PN SM JA.

References

1. Siegel R, Naishadham D, Jemal A (2012) Cancer statistics, 2012. CA Cancer J Clin 62: 10–29.
2. Taplin ME (2007) Drug insight: role of the androgen receptor in the development and progression of prostate cancer. Nat Clin Pract Oncol 4: 236–244.
3. Scher HI, Beer TM, Higano C, Anand A, Taplin M-E, et al. (2010) Antitumour Activity of MDV3100 in a Phase 1–2 Study of Castration-Resistant Prostate Cancer. Lancet 375: 1437–1446.
4. de Bono JS, Logothetis CJ, Molina A, Fizazi K, North S, et al. (2011) Abiraterone and increased survival in metastatic prostate cancer. N Engl J Med 364: 1995–2005.
5. Efstathiou E, Titus M, Tsavachidou D, Tzelepi V, Wen S, et al. (2012) Effects of abiraterone acetate on androgen signaling in castrate-resistant prostate cancer in bone. J Clin Oncol 30: 637–643.
6. Efstathiou E, Titus MA, Tsavachidou D, Hoang A, Karlou M, Wen S, et al. (2011) MDV3100 effects on androgen receptor (AR) signaling and bone marrow testosterone concentration modulation: A preliminary report. J Clin Oncol 29: abstr 4501.
7. Guo Z, Yang X, Sun F, Jiang R, Linn DE, et al. (2009) A novel androgen receptor splice variant is up-regulated during prostate cancer progression and promotes androgen depletion-resistant growth. Cancer Res 69: 2305–2313.
8. Hu R, Dunn TA, Wei S, Isharwal S, Veltri RW, et al. (2009) Ligand-independent androgen receptor variants derived from splicing of cryptic exons signify hormone-refractory prostate cancer. Cancer Res 69: 16–22.
9. Sun S, Sprenger CC, Vessella RL, Haugk K, Soriano K, et al. (2010) Castration resistance in human prostate cancer is conferred by a frequently occurring androgen receptor splice variant. J Clin Invest 120: 2715–2730.
10. Carver BS, Chapinski C, Wongvipat J, Hieronymus H, Chen Y, et al. (2011) Reciprocal feedback regulation of PI3K and androgen receptor signaling in PTEN-deficient prostate cancer. Cancer Cell 19: 575–586.
11. Mulholland DJ, Tran LM, Li Y, Cai H, Morim A, et al. (2011) Cell autonomous role of PTEN in regulating castration-resistant prostate cancer growth. Cancer Cell 19: 792–804.
12. Gottlieb B, Beitel LK, Nadarajah A, Paliouras M, Trifiro M (2012) The androgen receptor gene mutations database: 2012 update. Hum Mutat 33: 887–894.
13. Linja MJ, Savinainen KJ, Saramaki OR, Tammela TL, Vessella RL, et al. (2001) Amplification and overexpression of androgen receptor gene in hormone-refractory prostate cancer. Cancer Res 61: 3550–3555.
14. Visakorpi T, Hyytinen E, Koivisto P, Tanner M, Keinanen R, et al. (1995) In vivo amplification of the androgen receptor gene and progression of human prostate cancer. Nat Genet 9: 401–406.
15. Ueda T, Bruchovsky N, Sadar MD (2002) Activation of the androgen receptor N-terminal domain by interleukin-6 via MAPK and STAT3 signal transduction pathways. J Biol Chem 277: 7076–7085.
16. Chang KH, Li R, Papari-Zareei M, Watumull L, Zhao YD, et al. (2011) Dihydrotestosterone synthesis bypasses testosterone to drive castration-resistant prostate cancer. Proc Natl Acad Sci U S A 108: 13728–13733.
17. Wang Q, Li W, Zhang Y, Yuan X, Xu K, et al. (2009) Androgen receptor regulates a distinct transcription program in androgen-independent prostate cancer. Cell 138: 245–256.
18. Ellwood-Yen K, Graeber TG, Wongvipat J, Iruela-Arispe ML, Zhang J, et al. (2003) Myc-driven murine prostate cancer shares molecular features with human prostate tumors. Cancer Cell 4: 223–238.
19. Hawksworth D, Ravindranath L, Chen Y, Furusato B, Sesterhenn IA, et al. (2010) Overexpression of C-MYC oncogene in prostate cancer predicts biochemical recurrence. Prostate Cancer Prostatic Dis 13: 311–315.
20. Jenkins RB, Qian J, Lieber MM, Bostwick DG (1997) Detection of c-myc oncogene amplification and chromosomal anomalies in metastatic prostatic carcinoma by fluorescence in situ hybridization. Cancer Res 57: 524–531.
21. Bernard D, Pourtier-Manzanedo A, Gil J, Beach DH (2003) Myc confers androgen-independent prostate cancer cell growth. J Clin Invest 112: 1724–1731.
22. Delmore JE, Issa GC, Lemieux ME, Rahl PB, Shi J, et al. (2011) BET bromodomain inhibition as a therapeutic strategy to target c-Myc. Cell 146: 904–917.
23. Mertz JA, Conery AR, Bryant BM, Sandy P, Balasubramanian S, et al. (2011) Targeting MYC dependence in cancer by inhibiting BET bromodomains. Proc Natl Acad Sci U S A 108: 16669–16674.
24. Chen CD, Welsbie DS, Tran C, Baek SH, Chen R, et al. (2004) Molecular determinants of resistance to antiandrogen therapy. Nat Med 10: 33–39.
25. Tomlins SA, Mehra R, Rhodes DR, Cao X, Wang L, et al. (2007) Integrative molecular concept modeling of prostate cancer progression. Nat Genet 39: 41–51.
26. Tran C, Ouk S, Clegg NJ, Chen Y, Watson PA, et al. (2009) Development of a second-generation antiandrogen for treatment of advanced prostate cancer. Science 324: 787–790.
27. Claassen GF, Hann SR (2000) A role for transcriptional repression of p21CIP1 by c-Myc in overcoming transforming growth factor beta -induced cell-cycle arrest. Proc Natl Acad Sci U S A 97: 9498–9503.
28. Fernandez PC, Frank SR, Wang L, Schroeder M, Liu S, et al. (2003) Genomic targets of the human c-Myc protein. Genes Dev 17: 1115–1129.
29. Kessler JD, Kahle KT, Sun T, Meerbrey KL, Schlabach MR, et al. (2012) A SUMOylation-dependent transcriptional subprogram is required for Myc-driven tumorigenesis. Science 335: 348–353.
30. den Hollander J, Rimpi S, Doherty JR, Rudelius M, Buck A, et al. (2010) Aurora kinases A and B are up-regulated by Myc and are essential for maintenance of the malignant state. Blood 116: 1498–1505.
31. Lal A, Navarro F, Maher CA, Maliszewski LE, Yan N, et al. (2009) miR-24 Inhibits cell proliferation by targeting E2F2, MYC, and other cell-cycle genes via binding to "seedless" 3'UTR microRNA recognition elements. Mol Cell 35: 610–625.
32. Montgomery RB, Mostaghel EA, Vessella R, Hess DL, Kalhorn TF, et al. (2008) Maintenance of intratumoral androgens in metastatic prostate cancer: a mechanism for castration-resistant tumor growth. Cancer Res 68: 4447–4454.
33. Hawksworth D, Ravindranath L, Chen Y, Furusato B, Sesterhenn IA, et al. (2010) Overexpression of C-MYC oncogene in prostate cancer predicts biochemical recurrence. Prostate Cancer Prostatic Dis 13: 311–315.
34. Scher HI, Fizazi K, Saad F, Taplin ME, Sternberg CN, et al. (2012) Increased Survival with Enzalutamide in Prostate Cancer after Chemotherapy. N Engl J Med.
35. Muncan V, Sansom OJ, Tertoolen L, Phesse TJ, Begthel H, et al. (2006) Rapid loss of intestinal crypts upon conditional deletion of the Wnt/Tcf-4 target gene c-Myc. Mol Cell Biol 26: 8418–8426.
36. Soucek L, Whitfield J, Martins CP, Finch AJ, Murphy DJ, et al. (2008) Modelling Myc inhibition as a cancer therapy. Nature 455: 679–683.
37. Snoek R, Cheng H, Margiotti K, Wafa LA, Wong CA, et al. (2009) In vivo knockdown of the androgen receptor results in growth inhibition and regression of well-established, castration-resistant prostate tumors. Clin Cancer Res 15: 39–47.
38. Zhang Y, Castaneda S, Dumble M, Wang M, Mileski M, et al. (2011) Reduced expression of the androgen receptor by third generation of antisense shows antitumor activity in models of prostate cancer. Mol Cancer Ther 10: 2309–2319.
39. Bradbury RH, Hales NJ, Rabow AA, Walker GE, Acton DG, et al. (2011) Small-molecule androgen receptor downregulators as an approach to treatment of advanced prostate cancer. Bioorg Med Chem Lett 21: 5442–5445.
40. Loddick S, Bradbury R, Broadbent N, Campbell H, Gaughan L, et al. (2012) Preclinical profile of AZD3514: A small molecule-targeting androgen receptor function with a novel mechanism of action and the potential to treat castration-resistant prostate cancer. Cancer Res 72: abstr 3848.
41. Haag P, Bektic J, Bartsch G, Klocker H, Eder IE (2005) Androgen receptor down regulation by small interference RNA induces cell growth inhibition in androgen sensitive as well as in androgen independent prostate cancer cells. J Steroid Biochem Mol Biol 96: 251–258.
42. Gibbs A, Schwartzman J, Deng V, Alumkal J (2009) Sulforaphane destabilizes the androgen receptor in prostate cancer cells by inactivating histone deacetylase 6. Proc Natl Acad Sci U S A 106: 16663–16668.
43. Morrissey C, True LD, Roudier MP, Coleman IM, Hawley S, et al. (2008) Differential expression of angiogenesis associated genes in prostate cancer bone, liver and lymph node metastases. Clin Exp Metastasis 25: 377–388.
44. True L, Coleman I, Hawley S, Huang CY, Gifford D, et al. (2006) A molecular correlate to the Gleason grading system for prostate adenocarcinoma. Proc Natl Acad Sci U S A 103: 10991–10996.
45. Mecham BH, Nelson PS, Storey JD (2010) Supervised normalization of microarrays. Bioinformatics 26: 1308–1315.
46. Page ST, Lin DW, Mostaghel EA, Marck BT, Wright JL, et al. (2011) Dihydrotestosterone administration does not increase intraprostatic androgen concentrations or alter prostate androgen action in healthy men: a randomized-controlled trial. J Clin Endocrinol Metab 96: 430–437.

OPEN ACCESS Freely available online

PLOS ONE

A Three-Marker FISH Panel Detects More Genetic Aberrations of *AR*, *PTEN* and *TMPRSS2/ERG* in Castration-Resistant or Metastatic Prostate Cancers than in Primary Prostate Tumors

Xiaoyu Qu[1], Grace Randhawa[2], Cynthia Friedman[2], Brenda F. Kurland[1], Lena Glaskova[2], Ilsa Coleman[1], Elahe Mostaghel[1,3], Celestia S. Higano[1,2,3], Christopher Porter[4], Robert Vessella[3,5], Peter S. Nelson[1,3], Min Fang[1,2,3]*

1 Fred Hutchinson Cancer Research Center, Seattle, Washington, United States of America, **2** Seattle Cancer Care Alliance, Seattle, Washington, United States of America, **3** University of Washington, Seattle, Washington, United States of America, **4** Virginia Mason Medical Center, Seattle, Washington, United States of America, **5** Puget Sound VA Health Care System, Seattle, Washington, United States of America

Abstract

TMPRSS2/ERG rearrangement, *PTEN* gene deletion, and androgen receptor (*AR*) gene amplification have been observed in various stages of human prostate cancer. We hypothesized that using these markers as a combined panel would allow better differentiation between low-risk and high-risk prostate cancer. We analyzed 110 primary prostate cancer samples, 70 metastatic tumor samples from 11 patients, and 27 xenograft tissues derived from 22 advanced prostate cancer patients using fluorescence in situ hybridization (FISH) analysis with probes targeting the *TMPRSS2/ERG*, *PTEN*, and *AR* gene loci. Heterogeneity of the aberrations detected was evaluated. Genetic patterns were also correlated with transcript levels. Among samples with complete data available, the three-marker FISH panel detected chromosomal abnormalities in 53% of primary prostate cancers and 87% of metastatic (Met) or castration-resistant (CRPC) tumors. The number of markers with abnormal FISH result had a different distribution between the two groups ($P<0.001$). At the patient level, Met/CRPC tumors are 4.5 times more likely to show abnormalities than primary cancer patients ($P<0.05$). Heterogeneity among Met/CRPC tumors is mostly inter-patient. Intra-patient heterogeneity is primarily due to differences between the primary prostate tumor and the metastases while multiple metastatic sites show consistent abnormalities. Intra-tumor variability is most prominent with the *AR* copy number in primary tumors. *AR* copy number correlated well with the *AR* mRNA expression (rho = 0.52, $P<0.001$). Especially among *TMPRSS2:ERG* fusion-positive CRPC tumors, *AR* mRNA and *ERG* mRNA levels are strongly correlated (rho = 0.64, $P<0.001$). Overall, the three-marker FISH panel may represent a useful tool for risk stratification of prostate cancer patients.

Citation: Qu X, Randhawa G, Friedman C, Kurland BF, Glaskova L, et al. (2013) A Three-Marker FISH Panel Detects More Genetic Aberrations of *AR*, *PTEN* and *TMPRSS2/ERG* in Castration-Resistant or Metastatic Prostate Cancers than in Primary Prostate Tumors. PLoS ONE 8(9): e74671. doi:10.1371/journal.pone.0074671

Editor: Dean G. Tang, The University of Texas M.D Anderson Cancer Center, United States of America

Received May 3, 2013; **Accepted** August 4, 2013; **Published** September 30, 2013

Funding: This study was supported by PNW SPORE P50 CA097186, P50CA138293, P01CA085859, PC093372, and PC093509 awarded by the National Cancer Institute. The xenograft generation and clinical specimen collection was supported by Richard M. Lucas Foundation. The funders had no role in study design, data collection and analysis, decision to publish, or preparation of the manuscript.

Competing Interests: The authors have declared that no competing interests exist.

* E-mail: mfang@fhcrc.org

Introduction

The discovery of recurrent *ETS* gene rearrangements in prostate cancers has led to studies evaluating the functional role of *ETS* genes in the pathogenesis of this disease and as diagnostic and prognostic biomarkers. The most common type of *ETS* rearrangement, the fusion of androgen-regulated *TMPRSS2* with the oncogenic *ERG* is detected in approximately half of prostate tumors but none of benign glands [1]. However, studies assessing the prognostic significance of *TMPRSS2:ERG* fusion have yielded inconsistent results [2–5]. Additional genetic factors are likely to work in concert with the fusion during cancer progression. Recent studies have shown that genetic aberrations are not only common in prostate cancer but also interact with each other through related pathways, thereby contributing to the progression to invasive diseases. *TMPRSS2* is regulated by androgens, and the androgen receptor (AR) is often amplified in patients treated with androgen deprivation therapy [6,7]. *PTEN* deletion, another common aberration in prostate cancer, was correlated with the expression of downstream p-Akt and associated with cancer-specific mortality [8,9]. *ETS* gene rearrangements were shown to cooperate with *PTEN* deletion and impact prostate cancer prognosis [10,11]. Crosstalk between PI3K and AR signaling pathways was recently suggested as a mechanism for the development of castration resistant prostate cancer (CRPC) [12,13]. *PTEN* deletion was shown to suppress androgen-responsive gene expression by modulating *AR* transcription factor activity. Also, *PTEN* and *AR* expression has been shown to inversely correlate in prostate cancer [14].

A critical clinical question concerns identifying characteristics of newly diagnosed prostate cancers that will distinguish aggressive from indolent behavior. The molecular heterogeneity of prostate cancers suggests that individual biomarkers may not be sufficient, and that multiple genetic markers may better associate with outcome. In the present study, we used a three-marker fluorescence in situ hybridization (FISH) panel to detect *TMPRSS2* and/or *ERG* rearrangements, *AR* gene amplification, and *PTEN* deletion in both primary and CRPC prostate cancer samples and compared the prevalence, concurrence, and interaction of these three markers. With the reference of mRNA expression data generated from matching tumor samples from the same patient, we also demonstrated how FISH findings correlated with changes in gene expression. Intra- and inter-patient tumor heterogeneity was also analyzed.

Materials and Methods

Sample Acquisition

Ethics Statement. The study was approved by the Institutional Review Boards (IRB) of the Fred Hutchinson Cancer Research Center and the University of Washington Medical Center. IRB waived the need for written consent for this study because only de-identified materials were used, which were from the University of Washington Urology tissue bank.

Patient samples. De-identified archived untreated primary prostate cancer samples (n = 110) were obtained from the University of Washington (UW) and Virginia Mason Hospital in Seattle. A total of 83 primary tumors generated analyzable data for at least one FISH marker in the panel, including 69 patients with *TMPRSS2/ERG* FISH data, 65 patients with *AR* FISH data and 42 patients with *PTEN* FISH data. Metastatic tumor samples (n = 70) were collected at UW from autopsies performed within 2 to 4 hours of death of 11 CRPC patients under the rapid autopsy program [15]. Tumors were obtained from various organ sites, frozen immediately and stored at −80°C. All tissues were sectioned for H&E staining and, for verification of histology, reviewed by a pathologist. FISH analysis was focused on cancer areas. A total of 67 tumors yielded analyzable data for at least one FISH marker in the panel, including 56 tumors from 10 patients with *TMPRSS2/ERG* FISH data, 65 tumors from 11 patients with *AR* FISH data, and 62 tumors from 11 patients with *PTEN* FISH data.

Prostate cancer xenografts. Prostate cancer xenografts (LuCaP lines) were originally isolated from various organs of advanced patients [16]. FISH analyses were successful on 27 LuCaP lines, representing 22 patients, one of which was also among the metastatic patients described above. These included 27 tumors from 22 patients with *TMPRSS2/ERG* FISH data, 26 tumors from 21 patients with *AR* FISH data, and 25 tumors from 21 patients with *PTEN* FISH data. Together, combining metastatic patient tumors and xenografts derived from advanced-stage prostate cancer patients, the current study evaluated a total of 94 tumors from 32 patients.

Fluorescent In Situ Hybridization (FISH)

TMPRSS2/ERG rearrangement was assessed using our novel 4-color FISH assay as described separately [17]. "*TMPRSS2:ERG*" refers to the presence of fusion of the two genes. "*TMPRSS2/ERG* rearrangement" refers to various subtypes of rearrangement of either or both genes as specified in the Results section. FISH analysis of *AR* gene amplification was performed using the SpectrumOrange AR (Xq12) probe combined with the SpectrumGreen labeled ChrX centromere (Xp11.1-q11.1) CEP X probe as the control (Abbott Molecular, IL). *PTEN* gene deletion was examined using the *PTEN*/CEP10 dual-color FISH Probe set (Abbott Molecular, IL), including the SpectrumOrange labeled PTEN (10q23) probe and the SpectrumGreen labeled Chr10 centromere (10p11.1–10q11.1) CEP 10 probe.

For each sample, a range of 25 to 50 intact and non-overlapping interphase nuclei were enumerated manually using a 100×oil immersion lens on a Zeiss Z1 microscope (Carl Zeiss Canada Ltd, Canada). *AR* gain and *PTEN* deletion were assessed by counting the number of gene signal and the corresponding centromere signal per nucleus. *AR* gain was defined as an average copy number of *AR* per nuclei equal or higher than 2. True *AR* gene amplification was defined as the ratio of the total number of *AR* signals divided by the total number of the X-chromosome centromere equal or greater than 2. Samples with *PTEN* heterozygous deletion had a ratio of the total number of *PTEN* signals divided by the total number of CEP10 signals equal or below 0.75. A *PTEN*/CEP10 ratio equal or below 0.2 is considered homozygous *PTEN* deletion. For patient-level analyses of CRPC patients with multiple tumors, expression by a given marker was considered abnormal if the aberration was seen in at least one tumor.

Expression Array

Agilent 44 K whole human genome expression oligonucleotide microarrays (Agilent Technologies, Inc., Santa Clara, CA) were used to profile prostate cancer xenografts and human castration-resistant soft tissue metastases of prostate. Freshly frozen xenografts were processed to extract total RNA which was amplified one round; patient samples were laser-capture microdissected and amplified two rounds as described previously [18]. Probe labeling and hybridization was performed following the Agilent suggested protocols and fluorescent array images were collected using the Agilent DNA microarray scanner G2565BA. Agilent Feature Extraction software was used to grid, extract, and normalize data. Expression ratios were $\log_2$ scaled and mean-centered across each gene.

Statistical Analysis

To complement the comparisons of archived primary tumor with a separate cohort of patients with metastatic disease, we examined within-patient heterogeneity of *AR* and *PTEN* for patients with metastatic disease, hypothesizing that prostate tumors could differ from contemporaneous metastatic lesions. Linear mixed models with random patient effects were fitted to non-prostate tumors, and a 95% confidence interval calculated for subject-specific [19] predictions of average expression. If a subject's prostate tumor copy number status fell outside the confidence interval, it would be interpreted as evidence of potential differences between the copy number status of primary and metastatic lesions. A linear mixed effects model and the %ICC9 SAS macro was used to calculate intraclass correlation coefficients and their confidence intervals [20]. Logistic regression and generalized estimating equations (GEE) were used to compare rates of abnormality for primary and metastatic samples, controlling for tissue source (rapid autopsy vs xenograft) and within-patient correlation for tumor-level analysis. Heterogeneity of intratumoral variance for different tumor sites was also explored using linear mixed models. Additional statistical inference included Spearman correlation coefficients, and the Wilcoxon rank sum test to compare distributions of the number of markers with abnormal expression. *P*-values were two-sided; statistical analyses were conducted using SAS/STAT software, version 9.3 (SAS Institute, Inc., Cary, NC).

Results

The Prevalence of Genetic Aberrations Detected by the Three-marker FISH Panel in Localized Primary and Metastatic or Castration Resistant (Met/CRPC) Patients

The three-marker FISH panel (Figure 1) used in our study detected frequent genetic aberrations in prostate cancer, and these were significantly more common in Met/CRPC tumors than in untreated primary tumors (Figure 2A).

Of the 34 primary tumors in which all 3 markers could be assessed, 16 (47%) exhibited no aberrations involving *AR*, *PTEN* or *TMPRSS2/ERG*; 11 (32%) were abnormal by one marker only. Six patients' tumors (18%) were detected abnormal by two markers, including 3 with *TMPRSS2*:*ERG* fusion and homozygous *PTEN* deletion, 2 with *TMPRSS2*:*ERG* fusion and heterozygous *PTEN* deletion, and 1 with non-fusion alternative rearrangement along with heterozygous *PTEN* deletion. None of the patients were abnormal by all three markers because there was no detectable *AR* abnormality when the cutoff for *AR* gain was set to $>=2.0$ *AR* per nucleus, an arbitrarily determined stringent cutoff. Two patients would be classified as mild *AR* gain if using *AR* copy number per nuclei $>=1.5$ as the cutoff value, established as mean+3SD based on enumeration results on normal prostate epithelial cells from 18 different samples.

Of the 30 Met/CRPC patients/xenografts with FISH results from all three markers, 4 (13%) had no abnormal marker values. Five (17%) were shown as abnormal by one marker only; 13 (43%) were detected as abnormal by two markers, including 8 (27%) shown as abnormal by *TMPRSS2/ERG* and *AR* FISH and 5 (17%) by *TMPRSS2/ERG* and *PTEN*. Eight patients (27%) were abnormal by all three tests.

We further evaluated subtypes of genetic aberrations detected by each marker in the Met/CRPC cohort (Figure 2 B–D). Rearrangements of *TMPRSS2* and/or *ERG* were detected in 14 patients (47%), including 5 (17%) with the typical single *TMPRSS2*:*ERG* fusion, 5 (17%) with dual or complex *TMPRSS2*:*ERG* fusion, and 4 (13%) with alternative rearrangements without fusion. Copy number increase (CNI) of chromosome 21 was observed in 10 patients (33%) using the *TMPRSS2/ERG* FISH probes. *AR* gain in one or more lesions was observed in 18 patients (60%), including 6 (20%) that resulted from gain of the X-chromosome and 12 (40%) with true *AR* gene amplification ($AR/X >= 2$). Deletion of *PTEN* was detected in 15 patients (50%), including 5 with homozygous deletion.

A Wilcoxon rank sum test suggested that the Met/CRPC cohort ($n = 30$) generally had more alterations detected by FISH than the cohort of primary cancers ($N = 34$) ($W = 1287$, $P<0.001$). *AR* gain, including moderate gain ($W = 1334$, $P<0.001$), and the combination of *TMPRSS2/ERG* and *PTEN* alterations ($W = 1181$, $P = 0.005$) were also significantly more common in the Met/CRPC tumors.

The investigation of individual markers reflected unique trends of changes of each genetic abnormality during the progression of prostate cancer. About 80% of Met/CRPC samples were identified by *TMPRSS2/ERG* FISH as abnormal, compared to 48% in primary samples, and the difference was statistically significant (Table 1; Figure 2B) ($P = 0.03$). This difference appeared to be due to the CNI aberration rather than the *TMPRSS2:ERG* fusion itself; the percentage of patients with fusion or alternative rearrangement remains similar, but the percentage of patients with dual fusion as opposed to single fusion is clearly greater in the Met/CRPC category than in the primary tumor group (Figure 2B). Examining individual tumors (adjusting for within-person correlation and xenograft status), the odds of a Met/CRPC tumor exhibiting an abnormality was 4.5 times greater than odds for a primary tumor ($P = 0.05$). While nearly all primary cancer patients showed normal *AR* status, over 70% of Met/CRPC patients demonstrated various degrees of *AR* gene copy number gain (Table 1; Figure 2C). PTEN FISH showed increased heterozygous *PTEN* deletion and homozygous *PTEN* deletion in Met/CRPC compared with primary patients (Table 1; Figure 2D) ($P = 0.07$ at the tumor level, $P = 0.003$ at the patient level). Of note, for patient-level assessments there was a hierarchy, so if one lesion was heterozygous and the other homozygous, the patient level was considered homozygous.

Data of the entire panel across different individuals showed that prostate cancer patients with *PTEN* deletion also tended to exhibit abnormal results in *TMPRSS2/ERG* FISH (Figure 2E). Among the 34 primary cancer patients with data available from all three markers, 6 of the 8 individuals with *PTEN* deletion (75%) also showed an abnormal *TMPRSS2/ERG* FISH result (Figure 2E). Among the 30 Met/CRPC patients with data available from with either both or all three markers, 13 of the 14 individuals with *PTEN* deletion (93%) also showed abnormalities in *TMPRSS2/ERG* FISH analysis. In Met/CRPC patients, abnormal *TMPRSS2/ERG* FISH results were also more prevalent among patients demonstrating gain of *AR*, and vice versa (Figure 2E). Sixteen out of 17 patients (94%) with *AR* gain showed *TMPRSS2/ERG* abnormalities. Sixteen of 24 patients (67%) with *TMPRSS2/ERG* abnormalities also demonstrated *AR* gain. Detailed FISH results on all metastatic samples from each CRPC patient are summarized in Table 2. Results of xenograft samples are listed in Table 3.

Intra- and Inter-patient Comparison of Genomic Aberrations and Heterogeneity in Castration Resistant Prostate Cancer

The 3-marker FISH analyses yielded two observations from patients with metastatic prostate cancer: (1) within the same patient, aberrations in metastatic tumors were generally consistent across tumors; (2) several primary prostate tumors of CRPC patients exhibited a profile distinct from distant metastatic sites. FISH analyses for *AR* copy number (Figure 3A) and *PTEN*/CEP10 ratio (Figure 3B) showed discordant results between the primary tumors and metastatic lesions. In particular, for patient #9, the prostate tumor showed *AR* copy number increase, whereas the metastatic lesions all had average $AR<2$. For patient #11, the primary prostate tumors showed normal *AR* results while metastatic lesions showed *AR* gain. Similarly, the prostate lesion in patients #3 demonstrated heterozygous *PTEN* deletion when all metastatic lesions had normal *PTEN*. In contrast, for patient #11, the metastatic lesions showed homozygous *PTEN* deletion while the prostate lesion did not. In other cases (#8 and #10), prostate tumors did not differ from metastatic lesions in abnormal *vs* normal marker signals, but were outside of the 95% confidence interval for the subject-specific average based on linear mixed models fit to metastatic lesions.

In general, more than 75% of the variability was between-patient, with relatively little within-patient variation: the intraclass correlation coefficient was 0.76 (95% CI 0.54–0.90) for average *AR* and 0.82 (95% CI 0.62–0.92) for *PTEN*/CEP10. However, when the entire panel was evaluated for each individual, 4 (#3, #5, #9 and #11) out of 8 patients (50%) with data available from all three markers in the local prostate tumors showed different profiles between the primary and metastatic tumors. Further comparison using data of individual markers showed different levels of deviation of the primary from metastatic tumors. Of the 8 patients with available *TMPRSS2/ERG* FISH results on prostate site

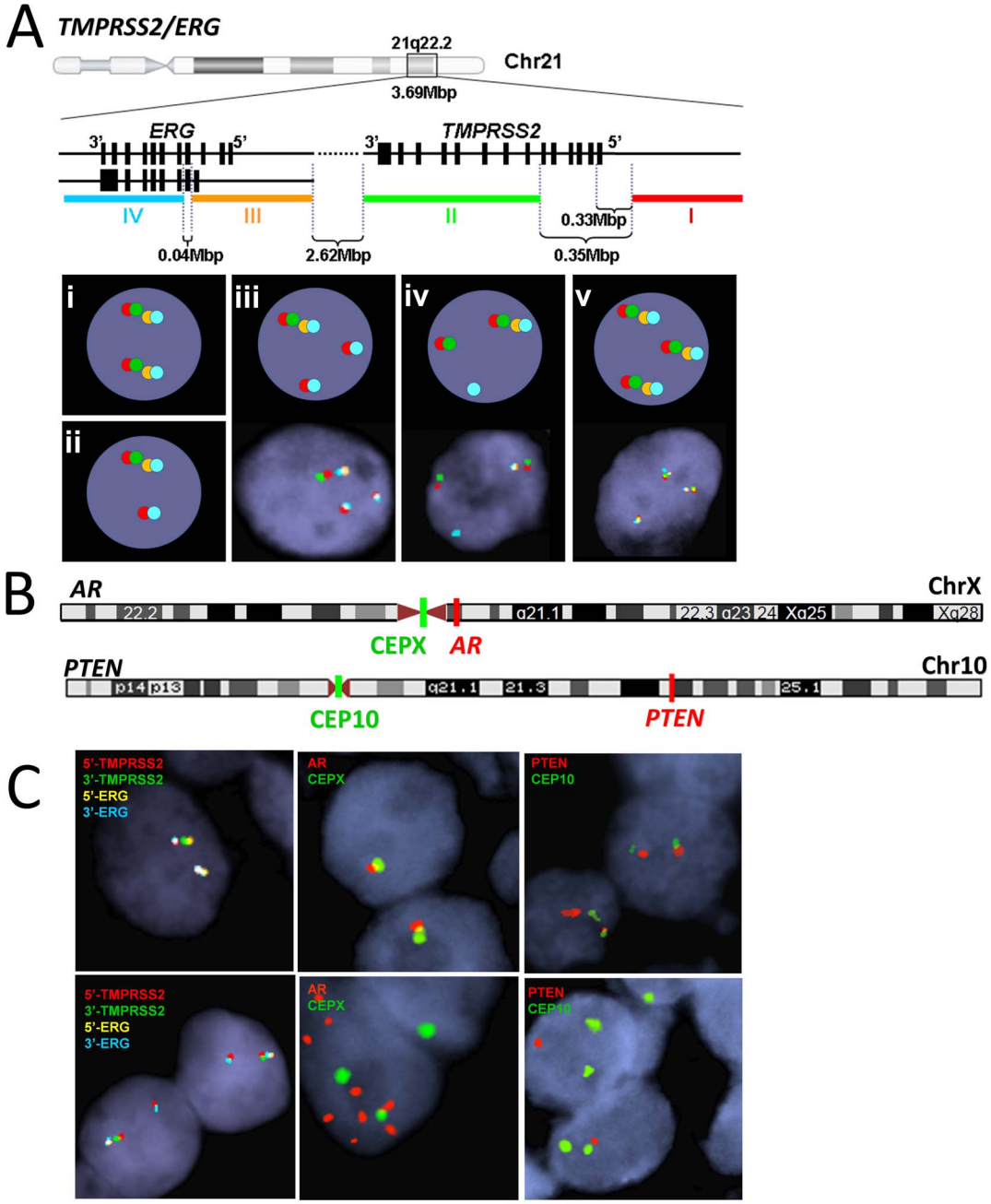

Figure 1. The three-marker FISH panel including *TMPRSS2*/*ERG* rearrangements, *AR* gene amplification, and *PTEN* gene deletion. (A) Illustration of the 4-color FISH technique for the detection of rearrangements of *TMPRSS2* and/or *ERG*. FISH probes target 5′-*TMPRSS2* (red, probe I), 3′-*TMPRSS2* (green, probe II), 5′-*ERG* (gold, probe III), and 3′-*ERG* (blue, probe IV) simultaneously, detecting various signal patterns including normal (i), single fusion(ii), dual/complex fusion(iii), alternative rearrangement without fusion (iv), and copy number increase(CNI) without rearrangements. Captured FISH images of (i) and (ii) are shown in the left panel of 1C; images of (iii) – (v) are shown below the corresponding illustration. (B) FISH probes used to detect *AR* gene amplification and *PTEN* gene deletion *AR* gene amplification was analyzed using probes targeting *AR* (orange) and the X-chromosome centromere (green, CEPX). *PTEN* gene deletion was detected using probes targeting *PTEN* (orange) and the chromosome 10 centromere (green, CEP10). (C) Representative interphase FISH images. Top left, normal *TMPRSS2* and *ERG* signal pattern demonstrating two sets of the four probes per nucleus; Bottom left, *TMPRSS2*: *ERG* fusion shown as juxtaposed red and blue signals concurrent with missing or separation of the interstitial green and gold signals; Top middle, normal *AR* signal pattern demonstrating one orange *AR* and one green X signal per nucleus; Bottom middle, *AR* gene amplification presenting more than twice the number of *AR* signals than the CEPX signals; Top right, normal *PTEN* signal pattern demonstrating 2 orange *PTEN* and 2 green CEP10 signals per nucleus; Bottom right, *PTEN* deletion showing none or 1 copy of *PTEN* signals per nucleus.
doi:10.1371/journal.pone.0074671.g001

tumors, 3 (37.5%) had results in the prostate different from those in other metastatic sites (Table 2). Interestingly, patient #5 demonstrated dual deletion fusion among metastatic sites, while only single deletion fusion was detected in a tumor from the prostate of the same patient. In the analyses of *AR*, 3 (#3, #9, and #11) out of 10 patients (30%) showed results in the prostate that

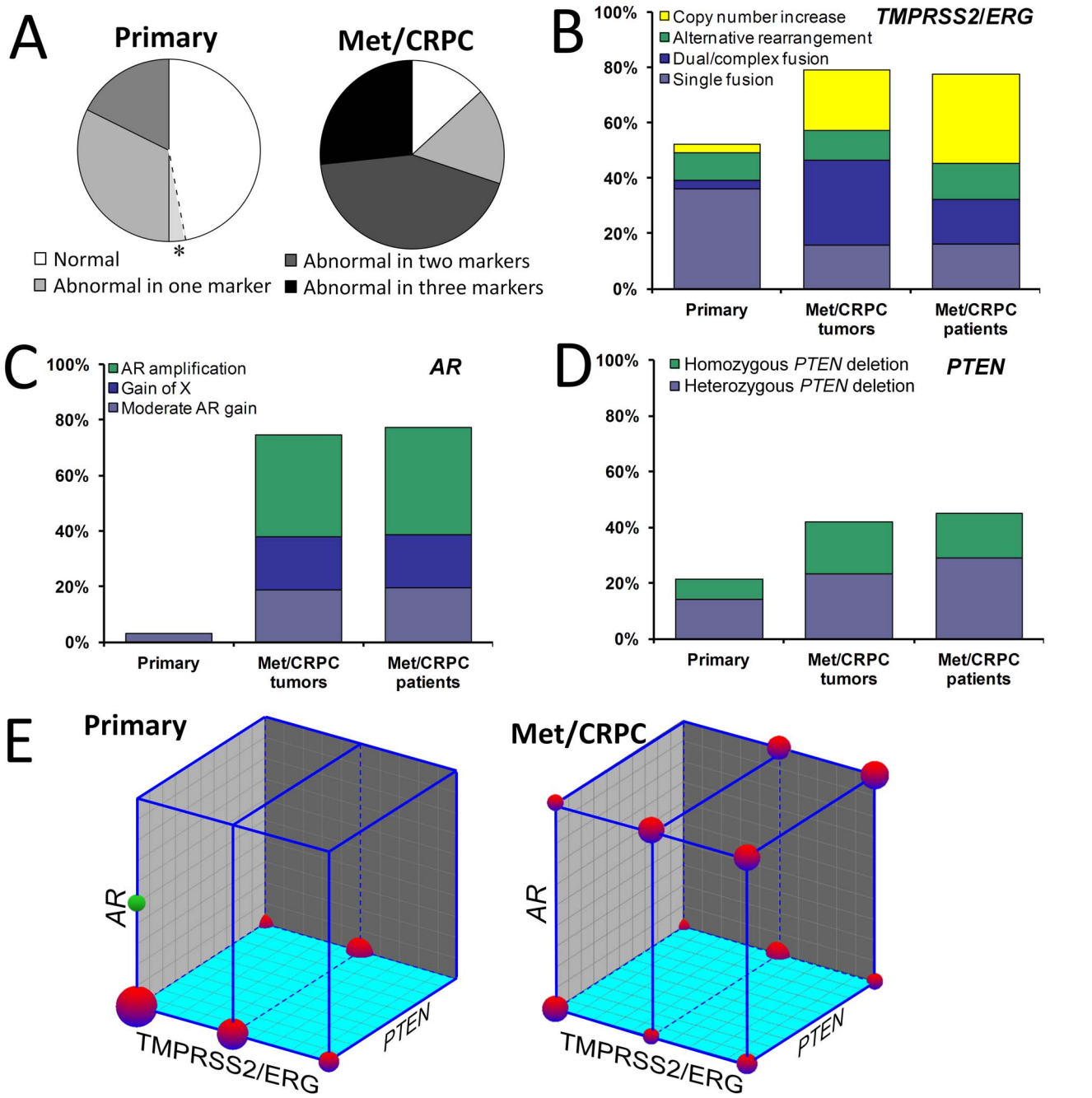

Figure 2. The prevalence of genetic aberrations detected by the panel. A patient with multiple tumors was considered abnormal by a given marker if the aberration was seen in at least one tumor. (A) Pie charts demonstrate the percentage of individuals with no (white), one (light grey), two (dark grey), and three (black) abnormalities detected by the panel among the primary prostate cancer (n = 34) and the metastatic or castration resistant prostate cancer (Met/CRPC) cohort (n = 30), respectively. Among primary patients, an asterisk was used to highlight moderate AR gain (average *AR* per nucleus >= 1.5 but <2). (B-D) Prevalence of each subtype of abnormalities detected by individual FISH marker among the primary patients (one tumor per patient, n = 34), Met/CRPC tumors (n = 81), and Met/CRPC patients/xenografts (n = 30), respectively. *TMPRSS2/ERG* abnormalities are categorized as single fusion (light blue), dual/complex fusion (dark blue), alternative rearrangements (green), and copy number increase (CNI) of the normal gene alleles (yellow). *AR* FISH detected moderate *AR* gain (light blue), gain of X (dark blue) and *AR* gene amplification (green). *PTEN* FISH abnormalities includes heterozygous (light blue) and homozygous (green) *PTEN* deletions. (E) The co-occurrence of abnormalities in the three markers shown as 3D sphere plots for the primary cancer cohort (left) and the Met/CRPC cohort (right). *TMPRSS2/ERG*, *PTEN*, and *AR* results are presented on X, Y, and Z axes, respectively. The value presented on each axis ranges from 0 to 1. "0" denotes normal for a given marker. For *TMPRSS2/ERG*, "0.5" indicates rearrangements, including fusion and alternative rearrangements; "1" means CNI of the normal alleles without any rearrangement. For *PTEN* FISH, both heterozygous and homozygous deletions are presented as "1". For *AR* FISH, "1" indicates *AR* copy number gain (>= 2.0). Patients with the same combination of abnormalities are clustered into a sphere, the volume of which is proportional to the percentage of patients in the respective cohort. Only patients with available data from all three markers are included. The green sphere in the primary patient plot denotes moderate *AR* gain (>1.5 but <2.0).
doi:10.1371/journal.pone.0074671.g002

Table 1. Prevalence of abnormalities detected by each FISH marker among the primary and the metastatic or castration-resistant prostate cancer (Met/CRPC) patients.

	Primary		Met/CRPC		Met/CRPC		*P*value	
	# of patients	%	# of tumors	%	# of patients	%	Tumors[6]	Patients[7]
TMPRSS2/ERG	69		82		31		0.05	0.03
Single fusion	25	36%	13	16%	5	16%		
Dual/complex fusion	2	3%	25	30%	5	16%		
Alternative rearrangement without fusion	4	6%	9	11%	4	13%		
Copy number increase	2	3%	18	22%	10	32%		
Normal	36	52%	17	21%	7	23%		
AR	65		90		31		<0.001	<0.001
Moderate *AR* gain[1]	2	3%	17	19%	6	19%		
Gain of X[2]	0	0%	17	19%	6	19%		
AR amplification[3]	0	0%	33	37%	12	39%		
Normal	63	97%	23	26%	7	23%		
PTEN	42		86		31		0.07	0.003
Heterozygous *PTEN* deletion[4]	6	14%	20	23%	9	29%		
Homozygous *PTEN* deletion[5]	3	7%	16	19%	5	16%		
Normal	33	79%	50	58%	17	55%		

[1]Average *AR* per nucleus ≥1.5 but <2.
[2]Average *AR* per nucleus ≥2 but average AR/X ratio<2.
[3]Average *AR*/X ratio≥2.
[4]Average *PTEN*/CEP10 ratio≤0.75 but >0.2.
[5]Average *PTEN*/CEP10 ratio≤0.2.
[6]Wald tests of abnormal vs. normal for primary vs. CRPC, generalized estimating equations (GEE) with independence autocorrelation, adjusting for rapid autopsy vs xenograft sample for CRPC. Likelihood ratio test for AR (without adjustment for autocorrelation), since no primary samples had abnormal AR.
[7]Wald tests of abnormal vs. normal for primary vs. CRPC, logistic regression adjusting for rapid autopsy vs xenograft sample for CRPC. Likelihood ratio test for AR, since no primary samples had abnormal AR.
doi:10.1371/journal.pone.0074671.t001

deviated from extra-prostatic tumors. The assessment of *PTEN* deletion showed that 2 (#3 and #11) out of 9 patients (22.2%) demonstrated different *PTEN* FISH results between prostate site and metastatic tumors. In patient #11, all extra-prostatic metastasis showed homozygous *PTEN* deletion, while prostate tumors showed normal *PTEN* results. Similarly, the panel data for xenografts also indicated that xenograft lines derived from the same patient tend to show the same genomic abnormality (Table 3).

Intra-tumoral Assessments of Genomic Heterogeneity in Metastatic Patients

We next sought to evaluate variation in genomic alterations detected by the FISH panel in individual cells comprising a primary or metastatic tumor. We found substantial intratumor variation in *AR* copy number for prostate site tumors. Linear mixed models predicted *AR* copy number at the cell level by tumor type, with random patient effects. Table 4 shows estimates for the number of *AR* per cell, and for the covariance parameter estimates that show how within-tumor variation and measurement error differ between tumor types. Prostate site tumors had the highest estimated within-person *AR* standard deviation (1.43 *AR* per cell). Several prostate tumors and lymph node metastasis had some unusually high counts that may have contributed to the estimate. For the *PTEN/CEP10* ratio, the covariance estimates were also found to be heterogeneous by tumor type ($\chi^2_6 = 20$, p = 0.003), but within-patient prostate *PTEN*/CEP10 intratumoral heterogeneity was not different from that of metastasis ($\chi^2_1 = 0.7$, p = 0.40). Table 4 suggests that the tissue-based heterogeneity differences were due to low within-patient variation in the peritoneal and adrenal lesions. These effects may be confounded with patient effects, since few patients had adrenal or peritoneal lesions. By a likelihood ratio test, statistical models with separate covariate estimates for each tumor type fit the data better than a model that did not distinguish between tumors ($\chi^2_6 = 412$, $P<0.001$), and a model that distinguished between prostate tissue and other lesions ($\chi^2_5 = 332$, $P<0.001$).

Correlation of Genomic Alterations and Gene Expression in Castration Resistant Prostate Cancer

In order to investigate the functional relationship of genetic aberrations detected by our panel, we correlated our FISH findings with gene expression data from 91 matching Met/CRPC samples, including 65 patient tumors and 26 xenografts (Table S1).

We first compared *AR* copy number, determined by FISH, with the *AR* transcript abundance, determined by cDNA microarray, from the same tumor sample. We observed a wide range of *AR* expression in Met/CRPC tumors (Figure 4A). The average number of *AR* per nucleus and the level of relative *AR* mRNA were positively correlated with rho = 0.52 ($P<0.001$) (Figure 4A). When normalized to the median *AR* mRNA expression level of all tumors with both *AR* FISH and mRNA expression data (n = 88),

Table 2. FISH data of individual castration resistant metastatic patient tumors.

Patient	Tissue	*TMPRSS2/ERG*	Average *AR* per nucleus	*AR*/*X*	*PTEN*/*CEP10*
8	Liver	Normal	5.50	3.27	1.19
8	LN1	Normal	1.12	1.00	1.04
8	LN2	Normal	4.94	2.74	1.20
8	LN3	Normal	5.70	3.35	1.16
8	Lung	Normal	4.38	2.74	1.12
8	Prostate	Normal	2.52	1.42	1.00
1	Liver	Normal	NA	NA	0.50
1	LN1	Normal	1.00	1.00	0.52
1	LN2	Normal	1.03	1.00	0.49
1	Prostate	Copy number increase	1.00	1.00	0.50
4	Liver	Single fusion	1.19	1.00	0.00
4	LN1	Single fusion	1.05	0.98	0.00
4	Lung1	Single fusion	1.00	1.00	0.00
4	Lung2	NA	1.11	1.00	NA
4	Spleen	Single fusion	1.04	1.00	0.00
4	Prostate	NA	1.08	1.00	NA
5	LN1	Dual/complex fusion	20.37	7.10	0.04
5	LN2	Dual/complex fusion	20.76	6.18	0.05
5	LN3	Dual/complex fusion	37.48	10.18	0.00
5	LN4	Dual/complex fusion	18.16	6.78	0.08
5	LN5	Dual/complex fusion	14.48	6.58	0.10
5	Prostate	Single fusion	102.64	54.60	0.03
2	LN1	Dual/complex fusion	1.10	1.00	1.00
2	LN2	Dual/complex fusion	1.66	0.99	0.80
2	LN3	Dual/complex fusion	1.92	1.02	0.97
2	Lung1	Dual/complex fusion	1.22	1.00	0.96
2	Lung2	Dual/complex fusion	2.00	1.00	0.98
2	Prostate	Dual/complex fusion	1.75	1.00	0.95
9	Adrenal1	Dual/complex fusion	1.62	1.09	1.02
9	Adrenal2	Dual/complex fusion	1.62	1.09	1.02
9	Liver	Dual/complex fusion	1.50	0.99	0.96
9	LN1	Dual/complex fusion	1.86	1.06	0.96
9	LN2	Dual/complex fusion	1.50	0.96	1.00
9	LN3	Dual/complex fusion	1.28	0.98	1.02
9	LN4	Dual/complex fusion	1.26	1.02	0.90
9	Lung1	Dual/complex fusion	NA	NA	0.94
9	Lung2	Dual/complex fusion	1.48	1.04	1.04
9	Spleen	Dual/complex fusion	1.64	1.01	0.86
9	Prostate	Dual/complex fusion	14.22	6.35	0.95
7	LN1	Alternative rearrangement	8.20	3.20	0.73
7	LN2	Alternative rearrangement	16.48	9.81	0.80
7	LN3	Alternative rearrangement	17.32	8.33	0.82
7	LN4	Alternative rearrangement	37.64	12.38	0.50
7	Prostate	Alternative rearrangement	10.20	5.31	0.76
11	LN1	Copy number increase	6.88	3.91	0.03
11	LN2	NA	7.38	4.15	0.05
11	LN3	Copy number increase	7.44	4.33	0.06
11	Lung	NA	5.56	3.39	0.01
11	Prostate	Alternative rearrangement	1.00	1.00	0.94
11	Prostate	Alternative rearrangement	1.10	1.04	1.02
3	Liver	Copy number increase	2.58	1.16	0.94
3	LN1	Copy number increase	2.80	1.32	0.76
3	LN2	Copy number increase	2.88	1.29	0.82
3	Lung	Copy number increase	2.74	1.28	1.00
3	Prostate 1	Normal	4.04	3.61	0.64
3	Prostate 2	Normal	1.32	1.06	NA
6	LN1	Copy number increase	2.56	1.00	NA
6	LN2	Copy number increase	2.44	1.00	0.57
6	LN3	Copy number increase	2.55	1.00	NA
6	Peritoneal	Copy number increase	2.21	0.99	0.45
10	Liver	NA	2.88	1.73	0.51
10	LN1	NA	5.62	3.39	0.44
10	LN2	NA	5.35	3.54	0.51
10	LN3	NA	6.36	3.46	0.50
10	LN4	NA	9.78	5.62	0.50
10	Lung	NA	6.18	3.19	0.47
10	Prostate	NA	9.12	5.36	0.68

Only samples successfully hybridized with at least one marker were presented in the table, including 56 tumors with *TMPRSS2/ERG* FISH, 65 tumors with *AR* FISH, and 62 tumors with *PTEN* FISH results.

doi:10.1371/journal.pone.0074671.t002

samples with *AR* gain (n = 48), including gain of X (n = 17) and *AR* amplification (n = 31) expressed *AR* mRNA at 2.5±0.3-fold (Mean±S.E.) higher than the median, while tumors without *AR* gain (n = 40) had *AR* mRNA level as 0.7±0.2-fold comparing to the median (W = 1106, $P<0.001$). When tumors with *AR* gain were further divided into groups of gain of X (n = 17) vs *AR* gene amplification (n = 31), our data showed that *AR* mRNA was expressed at a similar level between the two (W = 361, $P = 0.24$).

We then assessed the effect of *TMPRSS2*:*ERG* fusion on *ERG* mRNA levels and evaluated whether *ERG* expression also associated with the *AR* abundance in Met/CRPC tumors (n = 80, Figure 4B). Fusion-negative tumors (n = 42) expressed

Table 3. FISH data of individual xenograft tumors.

Xenografts	Tissue	*TMPRSS2/ERG*	Average *AR* per nucleus	*AR/X*	*PTEN/CEP10*
LuCaP81	LN	Normal	1.00	1.00	0.91
LuCaP78	Peritoneal	Normal	1.04	1.00	1.00
LuCaP136	Acites fluid(cells)	Normal	1.04	1.00	0.00
LuCaP153†	NA	Normal	1.50	1.00	1.63
LuCaP147	Liver	Normal	1.96	1.96	1.00
LuCaP49	Omental fat met	Single fusion	1.10	0.97	0.54
LuCaP86.2	Bladder	Single fusion	1.97	1.00	0.93
LuCaP23.12	Liver	Single fusion	2.20	1.04	0.89
LuCaP23.1CR	LuCaP23.1	Single fusion	2.28	1.00	NA
LuCaP23.1	LN	Single fusion	2.48	1.00	0.95
LuCaP35	LN	Single fusion	6.44	2.98	0.91
LuCaP35CR	LuCaP35	Single fusion	34.76	12.78	0.96
LuCaP145.1*	Liver	Single fusion	1.60	1.00	1.15
LuCaP145.2*	LN	Dual/complex fusion	1.79	0.99	0.87
LuCaP93	Prostate	Dual/complex fusion	1.50	0.99	0.00
LuCaP92	Peritoneal	Dual/complex fusion	2.00	1.00	0.90
LuCaP58	LN	Alternative rearrangement	1.52	1.00	0.37
LuCaP96**	Prostate	Alternative rearrangement	1.52	1.03	0.60
LuCaP96CR	LuCaP96	Alternative rearrangement	5.72	3.33	0.79
LuCaP73	Prostate	Copy number increase	1.48	1.00	1.03
LuCaP115	LN	Copy number increase	1.72	1.08	1.02
LuCaP70	Liver	Copy number increase	2.08	1.00	1.00
LuCaP141	Prostate	Copy number increase	2.64	1.00	0.98
LuCaP146	NA	Copy number increase	6.80	3.90	1.16
LuCaP69†	NA	Copy number increase	16.70	7.50	0.53
LuCaP105	Rib	Copy number increase	119.16	70.93	0.61

†Xenograft discontinued.
*Xenograft derived from patient #9 in Table 2.
**Xenograft derived from a patient with localized prostate cancer.
Only samples successfully hybridized with at least one marker were presented in the table, including 23 with *TMPRSS2/ERG* FISH, 26 with *AR* FISH, and 25 xenografts with *PTEN* FISH results.
doi:10.1371/journal.pone.0074671.t003

ERG mRNA at 0.7±0.1 relative to the probe median, while fusion-positive tumors (n = 38) expressed significantly higher *ERG* mRNA at 910.8±3.2 fold relative to probe median (W = 2073, $P<0.001$). Copy number increase (CNI) of *ERG* (or of both *TMPRSS2* and *ERG* without fusion) did not associate with higher *ERG* mRNA expression.

As *ERG* expression in the context of a *TMPRSS2:ERG* fusion is regulated by AR activity, we evaluated the effect of *AR* on *ERG* expression in Met/CRPC tumors with and without *TMPRSS2:ERG* fusion. While both the fusion-positive and fusion-negative samples showed a significant correlation between *AR* mRNA and *ERG* mRNA expression, this correlation appeared stronger in fusion-positive samples (rho = 0.64, $P<0.001$, n = 38) than in fusion-negative samples (rho = 0.36, $P = 0.02$, n = 42). This correlation was further confirmed by a dichotomized comparison of *ERG* expression levels for the 38 fusion-positive samples between low- and high- *AR* mRNA expression groups using the median probe intensity as a divider. The low *AR* expressing tumors (n = 20) expressed *ERG* at 3.6±1.1 fold relative to the probe median, while the high *AR* expressing tumors (n = 18) expressed *ERG* at 21.2±5.8 fold of probe median ($P<0.01$).

Discussion

A Three Marker FISH Panel Detects High Rates of Recurrent Genomic Aberrations in Localized and Metastatic Prostate Cancers

Because of the controversial prognostic utility of *TMPRSS2:ERG* fusion in prostate cancer, we employed the strategy of a three-marker FISH panel to detect well documented prostate cancer DNA aberrations, including *TMPRSS2/ERG* rearrangements, *AR* copy number gain, and *PTEN* deletion. This panel clearly detected a significant number of genetic abnormalities in prostate carcinomas, 53% in primary tumors and 87% in Met/CRPCs. At the individual tumor level, the odds of a Met/CRPC tumor being abnormal were 4.5 times greater than that for a primary tumor. Collectively, if aberrations in these genomic loci associate with aggressive tumor behavior, then this three-marker FISH panel may be a useful tool in distinguishing high-risk patients from low-risk ones at diagnosis or in repeat assessments using active surveillance strategies. In addition, this approach may be particularly useful in characterization of circulating and disseminated tumor cells (CTC/DTC) as using fewer cells for analysis

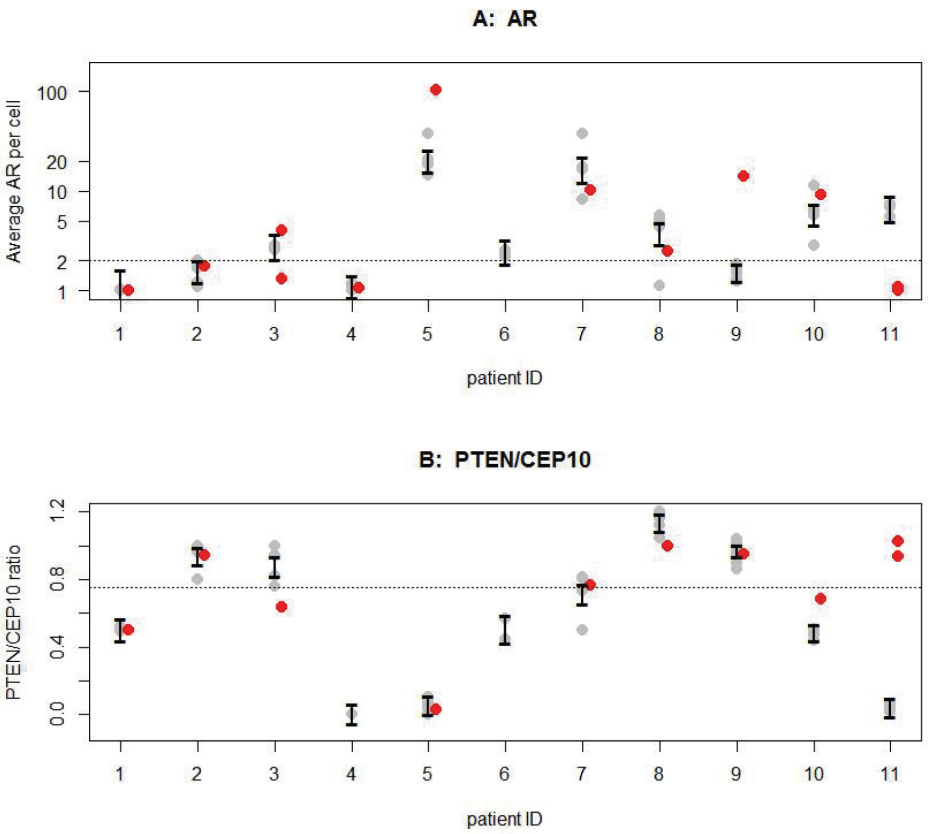

Figure 3. Within-patient heterogeneity of *AR* and *PTEN*/CEP10 for rapid autopsy patients (n = 11). Each tumor's FISH result is represented by a plotting character (grey for metastatic lesions, red for prostate) with multiple lesions in the same patient at the same X coordinate. Confidence intervals for subject-specific average copy number values are shown in black. Thresholds for abnormal signals are marked as horizontal dashed lines on each plot. (A) Average number of *AR* per nucleus. (B) Average *PTEN*/*CEP10* ratio.
doi:10.1371/journal.pone.0074671.g003

Table 4. Summary of intratumoral heterogeneity.

		AR (N = 2591 cells in 11 patients) patients			*PTEN*/*CEP10* (N = 722 cells in 11 patients)		
	N[1]	Average *AR* per cell[2]	Predicted AR per cell (95% confidence interval)	Predicted within-patient standard deviation	Average *PTEN*/*CEP10*[1]	Predicted *PTEN*/*CEP10* (95% confidence interval)	Predicted within-patient standard deviation
Prostate	12	2.1	3.0 (2.6–3.3)	1.43	0.9	0.8 (0.7–0.9)	0.43
Adrenal	2	1.6	1.5 (1.4–1.6)	1.04	1.0	1.0 (0.9–1.1)	0.21
Liver	6	2.6	2.3 (2.1–2.5)	1.12	0.7	0.7 (0.6–0.8)	0.44
Lymph Node	34	5.3	3.5 (3.3–3.7)	1.29	0.5	0.7 (0.6–0.7)	0.47
Lung	10	2.0	2.1 (2.0–2.3)	1.13	1.0	0.7 (0.6–0.8)	0.46
Peritoneal	1	2.2	2.0 (1.7–2.3)	1.06	0.4	0.4 (0.2–0.6)	0.29
Spleen	2	1.3	1.3 (1.2–1.3)	1.02	0.4	0.5 (0.3–0.7)	0.54

[1]Number of tumors in sample.
[2]Median for analyzed tissue.
Predicted values and covariance parameter estimates are from linear mixed models predicting copy number by tumor type, with random patient effects and separate covariance parameter estimates (within-patient heterogeneity and measurement error) for each tumor type.
doi:10.1371/journal.pone.0074671.t004

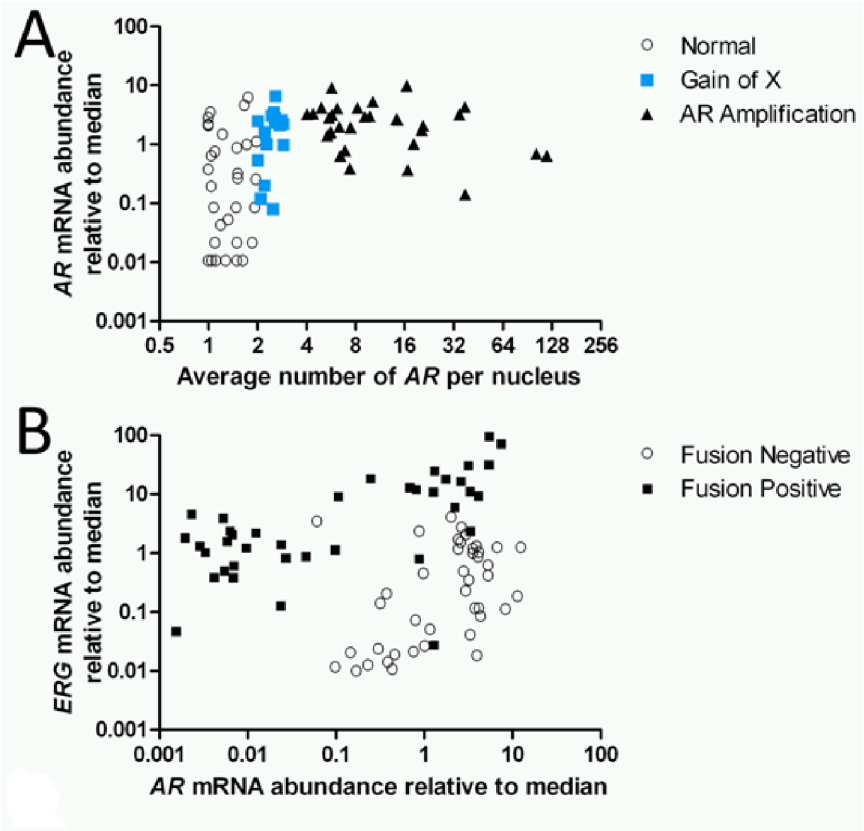

Figure 4. The correlation between changes in gene expression and aberrations detected by the panel. (A) Scatter plot demonstrates the correlation between FISH and expression data of *AR* (n = 88). The X-axis denotes the average number of *AR* signals per nuclei. The Y-axis denotes the *AR* mRNA level detected in the expression array relative to the median. Black open circles denote samples with an average of less than 2 *AR* per nuclei. Blue squares denote samples with copy number gain of *AR* due to gain of X. Black triangles denote samples with *AR* gene amplification. (B) Scatter plot demonstrates the effect of *TMRPSS2*:*ERG* fusion and *AR* expression on the abundance of *ERG* transcript (n = 80). The X- and Y-axis denotes relative mRNA abundance of *AR* and *ERG* compared to the median, respectively. Open circles and filled squares represent tumors without and with *TMPRSS2*:*ERG* fusion, respectively.
doi:10.1371/journal.pone.0074671.g004

and getting data on three specific markers would be a significant advantage. The utility of these three markers is further supported by findings from a recent study using whole exome and transcriptome sequencing technologies [21]. Grasso et al. identified that *AR* and *PTEN* had the highest level of copy number gains and losses, respectively, in prostate cancer, especially CRPC. Their integrated genomic approach also demonstrated the interplay of these genomic alterations with *TMPRSS2*/*ERG* rearrangements. For each individual marker, our study detected similar abnormality rates as reported in the literature. For rearrangements of *TMPRSS2* and/or *ERG*, previous findings showed *ERG* rearrangements in 30–50% of localized prostate cancers [1,2,4,5,22] and 40–50% of metastatic diseases [4,23–25]. With our novel 4-color FISH technique, capable of detecting rearrangements of *TMPRSS2* and/or *ERG* simultaneously in a single hybridization, we found the similar prevalence for *TMPRSS2*:*ERG* fusion, as well as non-fusion alternative rearrangements in 10–12% patients in both groups. However, dual/complex *TMPRSS2*:*ERG* fusion, which has been shown to associate with poor survival, occurs with a substantially greater frequency in Met/CRPC patients (17%) than in primary cancer patients (3%). Similarly, copy number increase (CNI) of *TMPRSS2* and *ERG* without fusion was more frequent in Met/CRPC patients (33%) than in primary cancer patients (3%), suggesting increased genetic instability as the disease progresses, which was also observed in our studies of disseminated tumor cells obtained from prostate cancer patients [23,26].

To date, multiple studies have demonstrated the occurrence of *PTEN* loss ranging from less than 20% to nearly 70% in early stage prostate cancer [8,11,27,28]. The variation could be attributed to multiple factors such as differences in patient populations, cohort sizes, and the cutoffs used to determine the *PTEN* deletion. Setting the cutoffs (based on the percentage of abnormal nuclei among all nuclei scored) as 10% for homozygous and 40% for heterozygous deletion, Reid and colleagues identified 17% of untreated primary prostate cancers exhibiting heterozygous or homozygous deletion of *PTEN* [11]. Setting the cutoffs as 30% for homozygous and 20% for heterozygous deletion, Yoshimoto et al. identified the presence of heterozygous and homozygous *PTEN* deletion in 39% and 5% prostate cancer patients, respectively [8]. We observed *PTEN* deletion in 21% of primary cancer patients and 47% of the CRPC patients based on the average ratio of *PTEN*/CEP 10 signals. Similar to previous findings [29], our study found that *PTEN* deletion tumors also tended to harbor *TMPRSS2*/*ERG* abnormalities (Figure 2E).

Our findings on *AR* gene amplification are unique and particularly interesting. *AR* amplification is generally considered to be only associated with CRPC tumors, induced by hormonal deprivation therapy or treatment with AR antagonists. Previous FISH studies rarely detected *AR* gene amplification in clinically

localized prostate tumors before hormonal therapy, but gain of the X-chromosome has been reported in 30–50% patients when a cutoff for gain was set at 9.8% of all cells examined [30,31], which implied that an average of >= 1.1 copies of the X-chromosome per nucleus were considered abnormal. In recurrent prostate cancer, *AR* amplification was common, with the reported frequency varying between 20% and 60% [6,7,32,33]. In these studies, *AR* gene amplification was defined in a slightly different manner. For example, among the studies that used *AR*/X ratio to define the amplification, the cutoffs vary from 1.5 [32,33], 2.0 [6], to 3.0 [7]. In the present study, we separated the subtype of true *AR* gene amplification, defined as *AR*/X ratio >= 2.0, from general *AR* gain, defined as having an average *AR* per nucleus of >= 2.0. We found *AR* gain in 58% of Met/CRPC patients, including 39% presenting as true *AR* gene amplification and 19% demonstrating *AR* gain due to simultaneous gain of the X-chromosome, with an average number of X-chromosomes per nuclei exceeding 2.0 (Table 1). There was, however, no difference in the *AR* mRNA expression between the groups of X-gain vs *AR* gene amplification; *AR* copy numbers correlated well with *AR* mRNA levels (Figure 3A). We also observed by SNP-array CGH analysis that the multiple X centromere signals observed by FISH sometimes represent only focal gain or amplification of the genomic region around the centromere of the X-chromosome including *AR* rather than gain of the entire X-chromosome (Schoenborn, unpublished data not shown). These data argue for using the absolute *AR* copy number alone to define *AR* gain/amplification in FISH studies regardless of the *AR*/X ratio. Consequently, using the cutoff of 2.0 for *AR* gain would mean that a tumor would be considered abnormal for *AR* gain when *AR* copy number is at least doubled (from one copy in normal male cells to two copies in cancer cells) in 100% of the cells, which might be too stringent a criterion and explains why *AR* gain was never reported previously in primary prostate cancer. Our experimental cutoff based on signal patterns seen in a series of normal controls was 1.48. Therefore, we used the 1.50 cutoff for moderate *AR* gain in Table 1, which translates to that *AR* gain in 50% of the cells would be considered abnormal. With this cutoff, we observed 6% of primary patients and 77% of Met/CRPC patients with *AR* gain. This should be a better definition for *AR* gain and may allow identification of primary prostate cancer patients with high risk for disease progression. Supporting evidence came from LuCaP 96 (Table 3), a xenograft line derived from a localized primary prostate cancer which showed moderate *AR* gain (1.52 *AR* per nucleus). Its castration-resistant derivative line LuCaP 96CR showed clear *AR* amplification (5.72 *AR* per nucleus). The original patient indeed had aggressive disease and died from prostate cancer. The caveat, however, is that the xenograft data may not faithfully represent the original tumor genomics due to potential selection pressures over time on the xenograft specimens.

FISH Detected Genetic Abnormalities Strongly Correlate with Changes at the Expression Level and Suggest Functional Interactions between *AR*, *PTEN* and *TMPRSS2/ERG*

Chaux *et al.* identified a strong association between ERG protein staining using immunohistochemistry and the *TMPRSS2*:*ERG* fusion status defined by FISH [34]. Similarly, our study showed that *ERG* mRNA expression was significantly correlated with the presence of *TMPRSS2*:*ERG* fusion. We also demonstrated a strong positive correlation between *AR* copy number gain and increased level of *AR* mRNA expression, supporting previous studies which showed higher levels of AR protein expression in prostate tumors with *AR* gene amplification than tumors without *AR* amplification [33]. Unlike this study that did not find an effect of X-chromosome gain on *AR* mRNA, we found higher *AR* mRNA levels in tumors with simple gain of X-chromosome, the amplitude of which could not be differentiated from tumors with true *AR* gene amplification. The similarity in *AR* mRNA levels in these two groups may in part be due to the nature of transcriptome array analyses, where the quantification of very high levels of *AR* mRNA reaches a plateau.

Related to the functional interactions of these genetic aberrations, previous studies demonstrated the cooperative relations between *PTEN* deletion and *TMPRSS2/ERG* rearrangements in animal models [29,35]. Clinical studies demonstrated significant correlations between *PTEN* gene deletion and deregulation of p-AKT as well as AR protein expression in advanced localized prostate cancer [9]. Two recent studies suggested cross-talk between androgen signaling pathway and the PI3K signaling in a reciprocal fashion [12,13]. At the genomic level, studies using large clinical cohorts demonstrated both presence and absence of enrichment between *TMPRSS2*:*ERG* fusion and *PTEN* gene deletion in prostate cancer [9,11]. Our study also confirmed enrichment of *TMPRSS2/ERG* abnormalities in tumors with either *PTEN* deletion or *AR* gain (Figure 2E). *AR* gain, but not *PTEN* deletion, was enriched in Met/CRPC tumors with *TMPRSS2/ERG* abnormalities. However, it is not obvious from our study that *PTEN* and *AR* expression were inversely correlated in prostate cancer, as previously reported [14].

More importantly, we demonstrated that *AR* and *ERG* expression levels strongly correlated with each other, especially in *TMPRSS2:ERG* fusion-positive tumors (Figure 4B). We propose the model that moderate *AR* gain in a *TMPRSS2:ERG* fusion-positive primary prostate cancer might synergistically enhance the expression of *ERG*, which gives growth advantage to those cells with moderate *AR* gain. *ERG* expression beyond a certain threshold would convey castration resistance to the tumor cells, which in turn increases the *AR* copy number and expression to compensate for androgen deprivation, contributing to disease progression and metastasis. Future work is needed to further study the hypothesis and the prognostic utility of the three-marker FISH panel.

Heterogeneity of Genetic Aberrations Detected by the Three-marker FISH Panel

The genetic heterogeneity assessment among CRPC patients showed that the major variability were between-patient. Within a given CRPC patient, aberrations in metastatic tumors were generally consistent across tumors, which are congruent with the general notion that metastatic cancer cells originated from the primary cancer cells and, therefore, likely maintain the same genetic lesion. However, some primary tumors may differ from metastatic lesions (Figure 3). This observation supported previous findings which demonstrated that primary prostate cancer is multiclonal, but most prostate cancer metastases are likely monoclonal in origin [23,36]. Also, primary tumors in the CRPC patient population have been exposed to aggressive therapy, which over time could result in genomic alterations inconsistent with the original primary tumor. In addition, intra-tumor variation was evident by both the *AR* and *PTEN* markers, which showed greater heterogeneity from tumors at the prostate site than distant metastases. This does not negate the significant intra-patient protein expression observed in our previously reported studies [37]. These findings support the multifocal and possibly multiclonal nature of advanced stage prostate cancer, especially at the prostate microenvironment [38].

In summary, we evaluated both primary cancer patients and Met/CRPC patients for the presence of *TMPRSS2/ERG* rearrangements, *AR* gene copy number gain, and *PTEN* deletion using a three-marker FISH panel. Our panel detected highly recurrent genetic abnormalities that showed distinct distribution between primary prostate cancer patients and Met/CRPC patients. Since these abnormalities occurred more frequently in Met/CRPCs, which represent more aggressive disease, when present in localized primary prostate cancer, would convey aggressive characteristics to these localized tumors. Therefore, our results support the prognostic potential of the three-marker FISH panel for risk stratification. FISH findings strongly correlated with the transcriptome levels and provided further insight in the interaction of these three gene related functional pathways. Tumor heterogeneity analysis demonstrated more inter-patient variability than intra-patient, and that the intra-patient tumor heterogeneity was mainly due to the deviation of the prostate site tumor from metastases. Future studies will focus on applying this panel to retrospective or prospective studies on untreated primary cancer patients and on CTC/DTC to test its ability to stratify patients and predict clinical outcome.

Supporting Information

Table S1 Shows the mRNA expression results of *AR* and *ERG* of all Met/CRPC tumor samples used in this study.
(DOCX)

Acknowledgments

Our special deep thanks to Barbara Trask, Ph.D. for her tremendous support for this study. We also thank Eva Corey, Ph.D., Colm Morrisey, Ph.D., and Larry True, M.D., for their roles in the rapid autopsy and xenograft generation program.

Author Contributions

Conceived and designed the experiments: XQ MF. Performed the experiments: XQ GR CF LG IC MF. Analyzed the data: XQ GR CF BFK EM CSH CP RV PSN MF. Contributed reagents/materials/analysis tools: EM CSH CP RV PSN MF. Wrote the paper: XQ MF BFK IC EM RV PSN. Critical review of the manuscript: GR CF LG CSH CP.

References

1. Tomlins SA, Rhodes DR, Perner S, Dhanasekaran SM, Mehra R, et al. (2005) Recurrent fusion of TMPRSS2 and ETS transcription factor genes in prostate cancer. Science 310: 644–648.
2. Attard G, Clark J, Ambroisine L, Fisher G, Kovacs G, et al. (2008) Duplication of the fusion of TMPRSS2 to ERG sequences identifies fatal human prostate cancer. Oncogene 27: 253–263.
3. Clark JP, Cooper CS (2009) ETS gene fusions in prostate cancer. Nat Rev Urol 6: 429–439.
4. Gopalan A, Leversha MA, Satagopan JM, Zhou Q, Al-Ahmadie HA, et al. (2009) TMPRSS2-ERG gene fusion is not associated with outcome in patients treated by prostatectomy. Cancer Res 69: 1400–1406.
5. Esgueva R, Perner S, C JL, Scheble V, Stephan C, et al. (2010) Prevalence of TMPRSS2-ERG and SLC45A3-ERG gene fusions in a large prostatectomy cohort. Mod Pathol 23: 539–546.
6. Visakorpi T, Hyytinen E, Koivisto P, Tanner M, Keinanen R, et al. (1995) In vivo amplification of the androgen receptor gene and progression of human prostate cancer. Nat Genet 9: 401–406.
7. Bubendorf L, Kononen J, Koivisto P, Schraml P, Moch H, et al. (1999) Survey of gene amplifications during prostate cancer progression by high-throughout fluorescence in situ hybridization on tissue microarrays. Cancer Res 59: 803–806.
8. Yoshimoto M, Cunha IW, Coudry RA, Fonseca FP, Torres CH, et al. (2007) FISH analysis of 107 prostate cancers shows that PTEN genomic deletion is associated with poor clinical outcome. Br J Cancer 97: 678–685.
9. Sircar K, Yoshimoto M, Monzon FA, Koumakpayi IH, Katz RL, et al. (2009) PTEN genomic deletion is associated with p-Akt and AR signalling in poorer outcome, hormone refractory prostate cancer. J Pathol 218: 505–513.
10. Yoshimoto M, Joshua AM, Cunha IW, Coudry RA, Fonseca FP, et al. (2008) Absence of TMPRSS2:ERG fusions and PTEN losses in prostate cancer is associated with a favorable outcome. Mod Pathol 21: 1451–1460.
11. Reid AH, Attard G, Ambroisine L, Fisher G, Kovacs G, et al. (2010) Molecular characterisation of ERG, ETV1 and PTEN gene loci identifies patients at low and high risk of death from prostate cancer. Br J Cancer 102: 678–684.
12. Carver BS, Chapinski C, Wongvipat J, Hieronymus H, Chen Y, et al. (2011) Reciprocal feedback regulation of PI3K and androgen receptor signaling in PTEN-deficient prostate cancer. Cancer Cell 19: 575–586.
13. Mulholland DJ, Tran LM, Li Y, Cai H, Morim A, et al. (2011) Cell autonomous role of PTEN in regulating castration-resistant prostate cancer growth. Cancer Cell 19: 792–804.
14. Wang Y, Romigh T, He X, Tan MH, Orloff MS, et al. (2011) Differential regulation of PTEN expression by androgen receptor in prostate and breast cancers. Oncogene 30: 4327–4338.
15. Morrissey C, True LD, Roudier MP, Coleman IM, Hawley S, et al. (2008) Differential expression of angiogenesis associated genes in prostate cancer bone, liver and lymph node metastases. Clin Exp Metastasis 25: 377–388.
16. Corey EV, R. (2007) Xenograft Models of Human Prostate Cancer. In: Chung LWK IW, amd Simons JW, editor. Contemporary Cancer Research: Prostate Cancer: Biology, Genetics, and the New Therapeutics. Totowa: Humana Press. pp. 3–31.
17. Qu X, Randhawa G, Friedman C, O'Hara-Larrivee S, Kroeger K, et al. (2013) A novel four-color fluorescence in situ hybridization assay for the detection of TMPRSS2 and ERG rearrangements in prostate cancer. Cancer Genet 206: 1–11.
18. Sharma A, Yeow WS, Ertel A, Coleman I, Clegg N, et al. (2010) The retinoblastoma tumor suppressor controls androgen signaling and human prostate cancer progression. J Clin Invest 120: 4478–4492.
19. Zeger SL, Liang KY, Albert PS (1988) Models for longitudinal data: a generalized estimating equation approach. Biometrics 44: 1049–1060.
20. Hankinson SE, Manson JE, Spiegelman D, Willett WC, Longcope C, et al. (1995) Reproducibility of plasma hormone levels in postmenopausal women over a 2–3-year period. Cancer Epidemiol Biomarkers Prev 4: 649–654.
21. Grasso CS, Wu YM, Robinson DR, Cao X, Dhanasekaran SM, et al. (2012) The mutational landscape of lethal castration-resistant prostate cancer. Nature 487: 239–243.
22. FitzGerald LM, Agalliu I, Johnson K, Miller MA, Kwon EM, et al. (2008) Association of TMPRSS2-ERG gene fusion with clinical characteristics and outcomes: results from a population-based study of prostate cancer. BMC Cancer 8: 230.
23. Holcomb IN, Young JM, Coleman IM, Salari K, Grove DI, et al. (2009) Comparative analyses of chromosome alterations in soft-tissue metastases within and across patients with castration-resistant prostate cancer. Cancer Res 69: 7793–7802.
24. Mehra R, Tomlins SA, Yu J, Cao X, Wang L, et al. (2008) Characterization of TMPRSS2-ETS gene aberrations in androgen-independent metastatic prostate cancer. Cancer Res 68: 3584–3590.
25. Perner S, Demichelis F, Beroukhim R, Schmidt FH, Mosquera JM, et al. (2006) TMPRSS2:ERG fusion-associated deletions provide insight into the heterogeneity of prostate cancer. Cancer Res 66: 8337–8341.
26. Holcomb IN, Grove DI, Kinnunen M, Friedman CL, Gallaher IS, et al. (2008) Genomic alterations indicate tumor origin and varied metastatic potential of disseminated cells from prostate cancer patients. Cancer Res 68: 5599–5608.
27. Verhagen PC, van Duijn PW, Hermans KG, Looijenga LH, van Gurp RJ, et al. (2006) The PTEN gene in locally progressive prostate cancer is preferentially inactivated by bi-allelic gene deletion. J Pathol 208: 699–707.
28. Yoshimoto M, Cutz JC, Nuin PA, Joshua AM, Bayani J, et al. (2006) Interphase FISH analysis of PTEN in histologic sections shows genomic deletions in 68% of primary prostate cancer and 23% of high-grade prostatic intra-epithelial neoplasias. Cancer Genet Cytogenet 169: 128–137.
29. King JC, Xu J, Wongvipat J, Hieronymus H, Carver BS, et al. (2009) Cooperativity of TMPRSS2-ERG with PI3-kinase pathway activation in prostate oncogenesis. Nat Genet 41: 524–526.
30. Gallucci M, Merola R, Leonardo C, De Carli P, Farsetti A, et al. (2009) Genetic profile identification in clinically localized prostate carcinoma. Urol Oncol 27: 502–508.
31. Gallucci M, Merola R, Farsetti A, Orlandi G, Sentinelli S, et al. (2006) Cytogenetic profiles as additional markers to pathological features in clinically localized prostate carcinoma. Cancer Lett 237: 76–82.
32. Brown RS, Edwards J, Dogan A, Payne H, Harland SJ, et al. (2002) Amplification of the androgen receptor gene in bone metastases from hormone-refractory prostate cancer. J Pathol 198: 237–244.
33. Ford OH, (2003) Androgen receptor gene amplification and protein expression in recurrent prostate cancer. J Urol 170: 1817–1821.
34. Chaux A, Albadine R, Toubaji A, Hicks J, Meeker A, et al. (2011) Immunohistochemistry for ERG expression as a surrogate for TMPRSS2-ERG fusion detection in prostatic adenocarcinomas. Am J Surg Pathol 35: 1014–1020.

35. Carver BS, Tran J, Gopalan A, Chen Z, Shaikh S, et al. (2009) Aberrant ERG expression cooperates with loss of PTEN to promote cancer progression in the prostate. Nat Genet 41: 619–624.
36. Liu W, Laitinen S, Khan S, Vihinen M, Kowalski J, et al. (2009) Copy number analysis indicates monoclonal origin of lethal metastatic prostate cancer. Nat Med 15: 559–565.
37. Roudier MP, True LD, Higano CS, Vesselle H, Ellis W, et al. (2003) Phenotypic heterogeneity of end-stage prostate carcinoma metastatic to bone. Hum Pathol 34: 646–653.
38. Lindberg J, Klevebring D, Liu W, Neiman M, Xu J, et al. (2012) Exome Sequencing of Prostate Cancer Supports the Hypothesis of Independent Tumour Origins. Eur Urol.

VOLUME 32 · NUMBER 3 · JANUARY 20 2014

JOURNAL OF CLINICAL ONCOLOGY

ORIGINAL REPORT

Targeted Androgen Pathway Suppression in Localized Prostate Cancer: A Pilot Study

Elahe A. Mostaghel, Peter S. Nelson, Paul Lange, Daniel W. Lin, Mary Ellen Taplin, Steven Balk, William Ellis, Philip Kantoff, Brett Marck, Daniel Tamae, Alvin M. Matsumoto, Lawrence D. True, Robert Vessella, Trevor Penning, Rachel Hunter Merrill, Roman Gulati, and Bruce Montgomery

Author affiliations appear at the end of this article.

Published online ahead of print at www.jco.org on December 9, 2013.

Supported by the Prostate Cancer Foundation (Career Development Award to E.A.M. and Synergy Award to R.B.M. and P.S.N.); Damon Runyon Cancer Research Foundation (Damon Runyon-Genentech Clinical Investigator Award CI-40-08 to E.A.M.); National Institutes of Health (Pacific Northwest Prostate Cancer SPORE Grants No. P50 CA97186; P01CA085859), Department of Defense Prostate Cancer Research Program Clinical Consortium (the University of Washington: Grant No. W81XWH-07-1-0097; Dana-Farber Cancer Institute: Grant No. W81XWH-06-1-0261) and Congressionally Directed Medical Research Program Award PC093509. GlaxoSmithKline provided dutasteride and research support. AstraZeneca provided goserelin and bicalutamide.

Terms in blue are defined in the glossary, found at the end of this article and online at www.jco.org.

Presented at the 48th Annual Meeting of the American Society for Clinical Oncology, Chicago, IL, June 1-5, 2012.

Authors' disclosures of potential conflicts of interest and author contributions are found at the end of this article.

Clinical trial information: NCT00298155.

Corresponding author: Bruce Montgomery, MD, Department of Medicine, Division of Oncology, University of Washington, 1959 NE Pacific, Box 356158, Seattle, WA 91895; e-mail: rbmontgo@uw.edu.

0732-183X/14/3203w-229w/$20.00

DOI: 10.1200/JCO.2012.48.6431

ABSTRACT

Purpose
Ligand-mediated activation of the androgen receptor (AR) is critical for prostate cancer (PCa) survival and proliferation. The failure to completely ablate tissue androgens may limit suppression of PCa growth. We evaluated combinations of CYP17A and 5-α-reductase inhibitors for reducing prostate androgen levels, AR signaling, and PCa volumes.

Patients and Methods
Thirty-five men with intermediate/high-risk clinically localized PCa were randomly assigned to goserelin combined with dutasteride (ZD), bicalutamide and dutasteride (ZBD), or bicalutamide, dutasteride, and ketoconazole (ZBDK) for 3 months before prostatectomy. Controls included patients receiving combined androgen blockade with luteinizing hormone-releasing hormone agonist and bicalutamide. The primary outcome measure was tissue dihydrotestosterone (DHT) concentration.

Results
Prostate DHT levels were substantially lower in all experimental arms (0.02 to 0.04 ng/g *v* 0.92 ng/g in controls; $P < .001$). The ZBDK group demonstrated the greatest percentage decline in serum testosterone, androsterone, and dehydroepiandrosterone sulfate ($P < .05$ for all). Staining for AR and the androgen-regulated genes prostate-specific antigen and TMPRSS2 was strongly suppressed in benign glands and moderately in malignant glands ($P < .05$ for all). Two patients had pathologic complete response, and nine had ≤ 0.2 cm^3 of residual tumor (defined as a near-complete response), with the largest numbers of complete and near-complete responses in the ZBDK group.

Conclusion
Addition of androgen synthesis inhibitors lowers prostate androgens below that achieved with standard therapy, but significant AR signaling remains. Tissue-based analysis of steroids and AR signaling is critical to informing the search for optimal local and systemic control of high-risk prostate cancer.

J Clin Oncol 32:229-237. © 2013 by American Society of Clinical Oncology

INTRODUCTION

Therapeutic approaches that reduce circulating testosterone are the most effective treatments available for metastatic prostate cancer. Strategies designed to impede androgen receptor (AR) signaling have also shown beneficial effects in preventing or treating localized prostate cancers.[1,2] However, the efficacy of androgen deprivation therapy (ADT) is limited by the inability to consistently reduce tissue androgens to below levels that activate AR signaling. Despite reduction of serum testosterone and dihydrotestosterone (DHT) levels to lower limits of assay quantification, prostate androgens in patients who have undergone castration remain at 25% to 35% of levels in untreated patients.[3-5] Consistent with these high residual androgen levels, persistent expression of AR-regulated genes is noted in prostate epithelium after ADT.[5,6] The inability to completely ablate androgens and AR signaling is reflected in the low number of complete clinical responses observed in studies of neoadjuvant ADT, with pathologic complete responses reported in only 4% of men treated with 3 to 8 months of ADT before prostatectomy.[7,8] These observations suggest the AR program continues to function as a key survival factor and that efforts culminating in AR program extinction may produce more substantial response rates.

This study was designed to determine whether combinations of agents targeting testicular, adrenal, and prostate androgen production would suppress prostate androgens and AR signaling more effectively than testicular androgen suppression alone, and, secondarily, whether this would enhance pathologic responses. We used the luteinizing hormone-releasing hormone (LHRH) agonist goserelin to reduce serum testosterone; the 5-α-reductase (SRD5A) inhibitor dutasteride to inhibit conversion of testosterone to the more potent androgen DHT, the CYP11A1/CYP17A1 inhibitor ketoconazole to block production of adrenal androgen precursors, and the AR antagonist bicalutamide to further inhibit AR signaling by remaining androgenic ligands. We used a neoadjuvant strategy to directly assess the efficacy of these agents on their targeted pathways and to permit quantitative measures of tissue androgens and residual tumor volumes.

PATIENTS AND METHODS

Patient Population

This was a randomized, unblinded, parallel-group study. All procedures were approved by institutional review boards of University of Washington, Veterans Affairs Puget Sound, and Dana-Farber Cancer Institute, and all subjects signed written informed consent. Eligible men had localized prostate cancer (T1c-T3, N0/NX,) with Gleason score ≥ 7. Patients with a risk of nodal involvement more than 10% were required to have negative bone scan and computed tomography of the abdomen/pelvis. Prior therapy for prostate cancer, including drugs affecting androgen or ketoconazole metabolism, history of thrombosis, unstable angina, or heart failure were exclusionary. Men were required to have a serum testosterone ≥ 280 ng/dL and normal blood counts, creatinine, and transaminases.

Study Procedures

Patients were randomly assigned to 3 months of neoadjuvant therapy with (1) goserelin (Zoladex; AstraZeneca, London, United Kingdom) 10.8 mg with high-dose dutasteride (Avodart, GlaxoSmithKline, London, United Kingdom) 3.5 mg per day (ZD; n = 12); (2) goserelin, bicalutamide (Casodex; AstraZeneca) 50 mg per day, and dutasteride (ZBD; n = 12); or (3) goserelin, bicalutamide, dutasteride, and ketoconazole 200 mg three times per day (with prednisone 5 mg per day; ZBDK; n = 13). Otherwise eligible men who presented to clinic already receiving combined androgen blockade with an LHRH agonist and bicalutamide underwent prostatectomy with tissue acquisition at 3 months as controls (ZB, n = 8). A group of untreated patients who met enrollment criteria were included for comparison (n = 11). All patients underwent open retropubic prostatectomy.

Tissue Acquisition and Determination of Tumor Volume

Transverse 2- to 4-mm-thick sections of the prostate were made from apex to base and divided into quadrants. Alternating cross-sections were submitted for formalin fixation or snap frozen. Hematoxylin and eosin–stained slides were used for pathologic staging (International Society of Urological Pathology guidelines)[9] and determination of tumor volume by tissue morphometry.

Androgen Measurements

Serum and tissue androgen levels were determined by mass spectrometry in a blinded manner, using a modification of methods we have previously described.[10] Benign prostate tissue was macro-dissected from snap-frozen prostatectomy tissue (owing to limitations and variability in the amount of residual tumor tissue present in the frozen tissue available for analysis). The lower limit of quantitation in serum was 0.49 pg/sample for testosterone, DHT, and androstenedione (AED) and 3.9 pg/sample for dehydroepiandrosterone (DHEA) and in tissue was 0.49 pg/sample for testosterone and 0.98 pg/sample for DHT, AED, and DHEA. Intra-assay coefficients of variation generated using human serum for high-, mid-, and low-range samples were 5.4%, 4.8%, and 5.2% for testosterone; 6.4%, 6.2%, and 17.2% for DHT; 4.6%, 4.2%, and 3.0% for AED; and 2.9%, 3.7%, and 5.5% for DHEA. Serum levels of DHEA sulfate (DHEA-S) were measured as free DHEA after sulfatase treatment. Free DHEA and androsterone were measured using a Girard testosterone derivatization strategy in conjunction with a stable isotope dilution liquid chromatography electrospray ionization selected reaction monitoring mass spectrometry method that we have recently established (Tamae et al, manuscript submitted for publication).

Immunohistochemistry

A prostate tissue microarray comprising six benign and cancer containing cores (0.6 mm) was created using fixed blocks obtained at prostatectomy. Serial sections were stained using an autostainer (Dako North America, Carpinteria, CA) with primary antibodies against AR (BioGenex antibody F39.4.1, 1:500; BioGenex, Fremont, CA); prostate-specific antigen (PSA) (Dako antibody A562, 1:50), and TMPRSS2 (previously described[11]). Immunostaining was assessed in a blinded manner using a compositional method for the percentage of cells at each intensity level (no stain, weak stain, intense stain). The mean percentage with high-intensity immunohistochemistry (IHC) expression was separately tabulated in benign and cancer glands for each subject. Data are displayed as stacked bar graphs representing the mean percentage staining at each intensity level in benign or malignant prostate epithelium for each treatment group.

Statistical Analyses

Linear regression models were used to compare prostate and serum androgens in each protocol treatment arm (ZD, ZBD, and ZBDK) to the standard treatment arm (ZB). Measurements were log-transformed to satisfy normality assumptions, Dunnett's adjustment was used to correct for multiplicity,[12] and a sandwich estimator of the covariance matrix was used to account for variance across treatment groups.[13] For IHC analyses, the mean percentage high staining in tissues from the control arm receiving combined blockade (ZB) and the grouped study arms (ZD, ZBD, and ZBDK) were compared with the mean percentage high-intensity staining in untreated tissues using Welch's *t* tests. Significant differences in intense staining for AR, PSA, and TMPRSS2 in benign or cancer tissue were not observed among the three study arms (ZD, ZBD, and ZBDK), except for lower percent intense PSA staining in benign tissue from the ZBD cohort compared with ZD and ZBDK, so data from these cohorts were grouped together.

Differences in serum androgens, tissue androgens, tumor volume, and prostate IHC score stratified by PSA nadir were evaluated by Welch's *t* tests. The PSA nadir was dichotomized at 0.2 based on previous reports demonstrating lower tumor volume and relapse rates in patients treated with ADT combined with surgery.[7,14,15] The dependence of time to PSA relapse on change in serum and tissue androgens, PSA nadir, tumor volume, and treatment group was evaluated using Cox proportional hazards models. The proportional hazards assumption was tested with the cox.zph function in the R survival package.

RESULTS

Patient Characteristics

This study enrolled 35 patients with intermediate to high-risk prostate adenocarcinoma (Fig 1; Table 1). Although patients were randomly assigned to the three treatment arms, they were not stratified, and a higher proportion of patients with intermediate-risk prostate cancer were treated in the ZBDK cohort, compromising conclusions about clinical efficacy. All patients had PSA decline, and there was no evidence of disease progression during treatment.

Prostate Tissue Androgen Levels

The primary end point was whether addition of SRD5A and CYP17A inhibition would suppress tissue DHT levels below that achieved with combined androgen blockade using an LHRH agonist

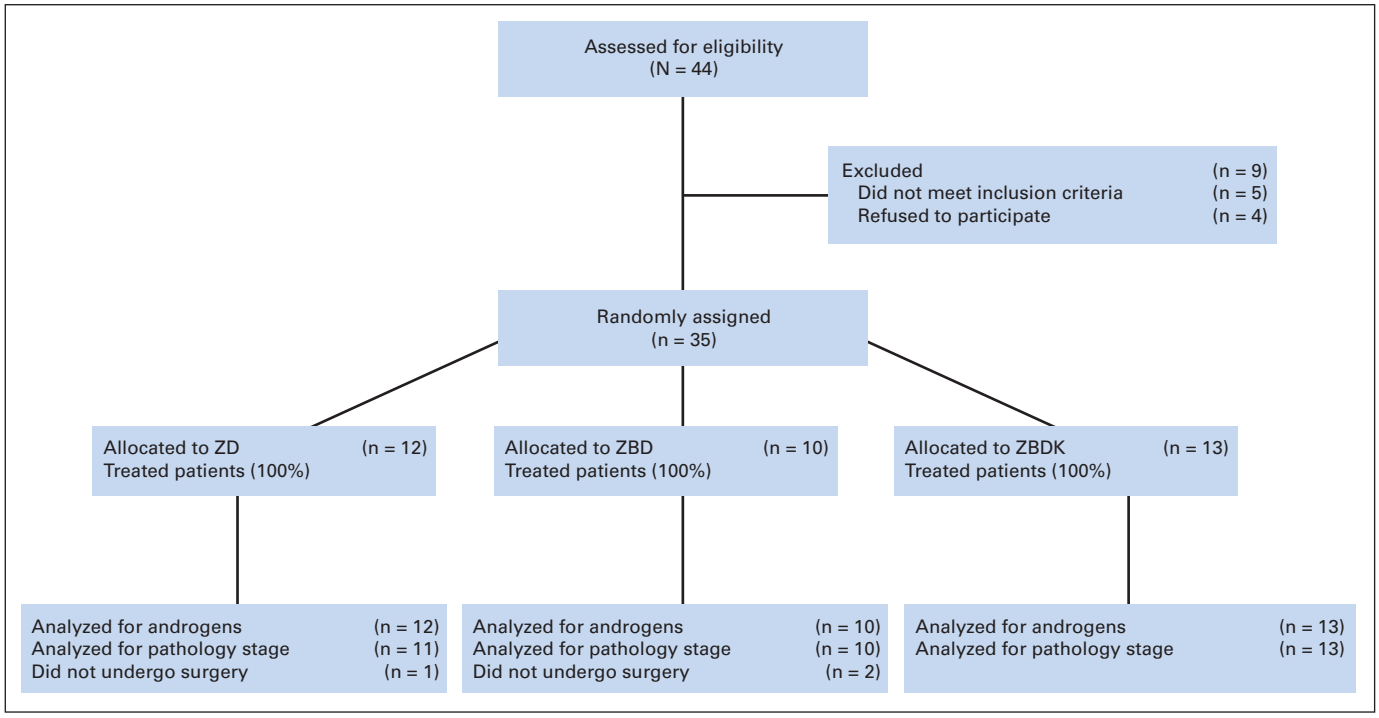

Fig 1. CONSORT diagram. ZBD, goserelin, bicalutamide, and dutasteride; ZBDK, goserelin, bicalutamide, dutasteride, and ketoconazole; ZD, goserelin and dutasteride.

and bicalutamide (ZB group). All experimental cohorts achieved the study end point, with DHT levels of ~0.03 to 0.06 ng/g (0.11 to 0.19 nmol/L) in the ZD, ZBD, and ZBDK groups compared with 0.92 ng/g (3.2 nmol/L) in the control ZB group ($P < .05$ for all; Fig 2A and Table 2).

Consistent with the effect of SRD5A inhibition, prostate tissue testosterone levels in all dutasteride-containing cohorts (0.24 to 0.33 ng/g; 0.8 to 1.1 nmol/L) were higher than those in men treated with combined blockade alone (0.07 ng/g; 0.25 nmol/L, Fig 2B and Table 2), even in the cohort (ZBDK) receiving the CYP17A inhibitor ketoconazole. Levels were numerically but not statistically higher than those in untreated patients (0.26 ng/g) and were an order of magnitude lower than those previously reported in eugonadal men treated with 3.5 mg of dutasteride.[16] Similar to the changes observed for testosterone, AED levels were significantly higher in tissues from dutasteride-treated ZD and ZBD patients (1.94 to 2.58 ng/g *v* 0.70 ng/g in ZB, Fig 2C and Table 2). The increase in AED in the ketoconazole containing arm (1.61 ng/g) trended toward significance ($P = .104$), suggesting that CYP17A inhibition attenuated AED synthesis. Tissue DHEA levels in the dutasteride containing arms were not statistically different from each other (Fig 2D, Table 2). The ZBD and ZBDK groups did show a trend toward a statistically significant decrease in prostate DHEA levels when compared with the standard combined blockade arm (ZB).

Table 1. Baseline Clinical Characteristics of Control and Study Patients

Characteristic	Untreated Patients (n = 11)	Control Patients (ZB, n = 8)*	Study Patients		
			ZD (n = 12)	ZBD (n = 10)†	ZBDK (n = 13)
Median age, years (range, 41-82 years)	59	61	62	66	60
Clinical staging and Gleason score					
cT1c	6	1	3	2	5
cT2a/b	4	5	5	6	7
cT2c/T3	1	1	4	2	1
7/8-10	8/1	1/5	6/6	9/3	12/1
PSA characteristics					
Median PSA	4.7	6.8	11.9	5.8	7.9
< 10/10-20/> 20	10/10	4/12	4/4/4	8/1/1	10/1/2

Abbreviations: PSA, prostate-specific antigen; ZB, goserelin and bicalutamide; ZBD, goserelin, bicalutamide, and dutasteride; ZBDK, goserelin, bicalutamide, dutasteride, and ketoconazole; ZD, goserelin and dutasteride.
*Two patients in this group underwent end-of-study biopsy instead of prostatectomy (one withdrew, one had radiation therapy).
†One patient in this group underwent end-of-study biopsy instead of prostatectomy (because of diagnosis of lung cancer).

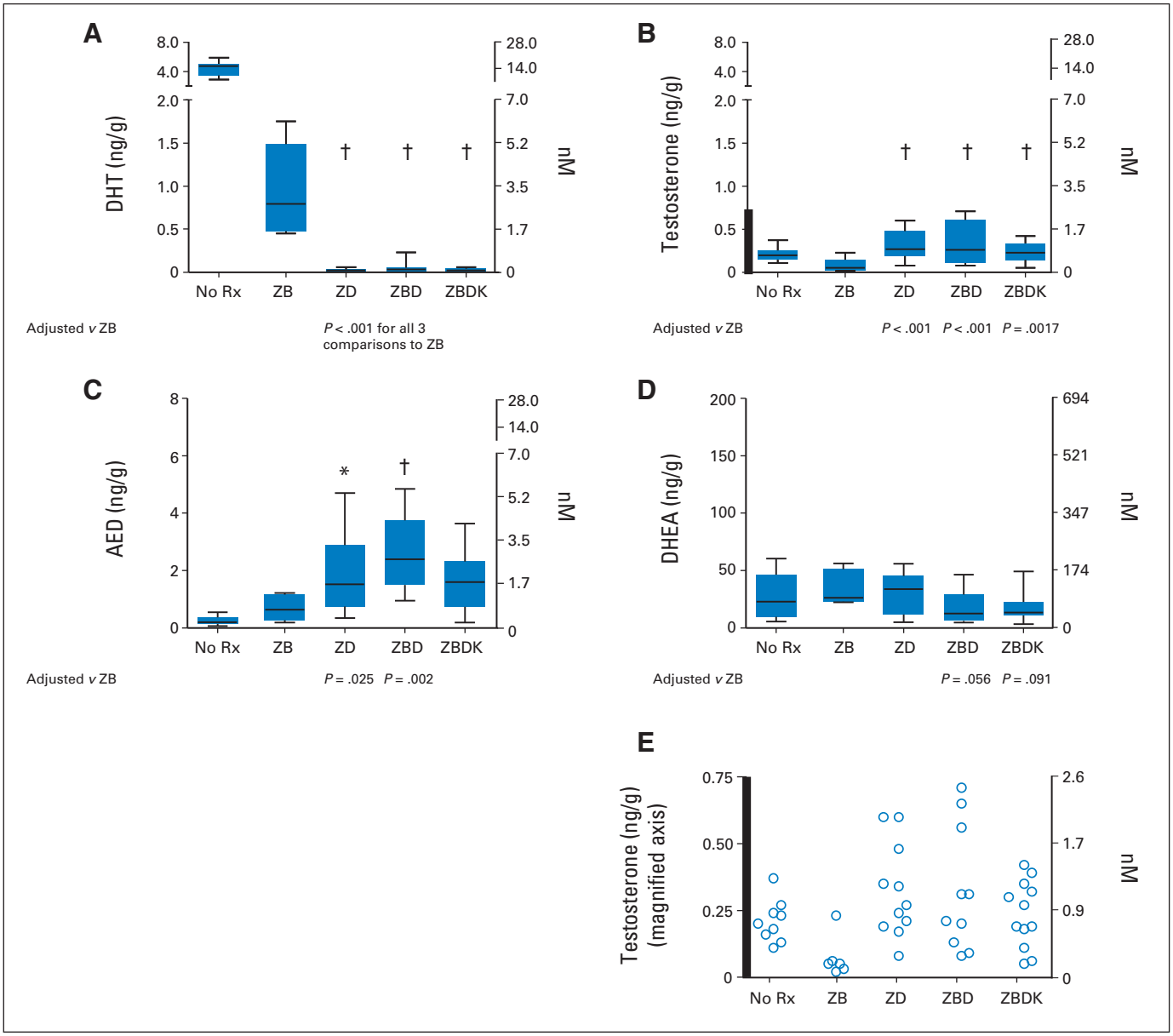

Fig 2. Prostate androgen levels after 3 months of multitargeted neoadjuvant androgen suppression. Tissue androgens from prostatectomy specimens after no treatment (No Rx), or 3 months of combined androgen blockade with a luteinizing hormone-releasing hormone agonist (goserelin) and bicalutamide (ZB); goserelin combined with the SRD5A inhibitor, dutasteride (ZD); goserelin combined with bicalutamide and dutasteride (ZBD); and all three of these agents combined with the CYP17A inhibitor, ketoconazole (ZBDK). Levels of (A) dehydrotestosterone (DHT), (B) testosterone, (C) androstenedione (AED), and (D) dehydroepiandrosterone (DHEA) were measured by mass spectroscopy. The difference in tissue androgen levels between each treatment cohort and the control (ZB) group was evaluated by linear regression. Statistically significant *P* values ($P < .05$) or those trending toward significance ($P < .10$) are presented in italics below the relevant treatment group. Absolute values of the mean and standard deviations are presented in Table 2. (E) Residual prostate testosterone levels are shown on an expanded *x*-axis (corresponding to the region denoted with a dark vertical bar in panel B). (*) $P < .05$. (†) $P < .005$.

To better approximate residual androgen activity in the prostate, we evaluated an androgen index designed to reflect the combined ligand activity of testosterone and DHT. Although both testosterone and DHT are high-affinity ligands for the AR, DHT has three- to five-fold higher potency relative to testosterone.[17] Therefore, we estimated the androgen index as the sum of (5 × DHT) + (1 × testosterone concentration) for each cohort (Table 2). Notably, the combined activity of residual testosterone and DHT levels in the prostate remain at concentrations capable of activating the AR, which has been reported to occur in vitro at DHT concentrations as low as 10 to 14 mol/L in the setting of prolonged androgen deprivation.[18]

Serum Androgen Levels

All treatment arms achieved castrate (< 50 ng/dL) levels of serum testosterone (range, 9.4 to 27.2 ng/dL; Appendix Table A1, online only). We evaluated the paired data from the pre and post-treatment samples in each cohort and computed percentage change as a more accurate indicator of treatment effect. The magnitude of decline in serum DHT levels was significantly higher in patients treated with

Table 2. Post-Treatment (RP) Prostate Tissue Androgen Levels

Treatment Category	DHT (ng/g)			Testosterone (ng/g)			AED (ng/g)		DHEA (ng/g)		Androgen Index* (nM)
	Mean	SD	nM	Mean	SD	nM	Mean	SD	Mean	SD	
No treatment	4.38	0.99	15.2	0.26	0.17	0.73	0.26	0.17	28.2	21.8	76
ZB	0.92	0.49	3.20	0.07	0.08	0.25	0.70	0.41	33.5	14.2	16.3
ZD	0.03	0.01	0.12	0.32	0.17	1.11	1.94	1.38	30.8	17.2	1.7
P (adjusted *v* ZB)		< .001			< .001		.025		NS		
ZBD	0.06	0.06	0.19	0.33	0.23	1.13	2.58	1.27	17.5	13.9	2.1
P (adjusted *v* ZB)		< .001			< .001		.002		.056		
ZBDK	0.03	0.02	0.11	0.24	0.13	0.82	1.61	1.04	19.0	15.1	1.4
P (adjusted *v* ZB)		< .001			.0017		.104		.091		

Abbreviations: AED, androstenedione; DHEA, dehydroepiandrosterone; DHT, dihydrotestosterone; NS, not significant; RP, radical prostatectomy; SD, standard deviation; ZB, goserelin and bicalutamide; ZBD, goserelin, bicalutamide, and dutasteride; ZBDK, goserelin, bicalutamide, dutasteride, and ketoconazole; ZD, goserelin and dutasteride.
*Androgen index is calculated as the sum of (5 × dihydrotestosterone concentration) + (1 × testosterone concentration).

dutasteride as compared with the percentage change from baseline in the control group (ZD, −88%; $P = .003$; ZBD, −86%; $P = .007$; ZBDK, −83%; $P = .049$; *v* ZB, −68%; Fig 3A, Appendix Table A1). Notably, the decreases in circulating testosterone, DHEA-S, and androsterone (a metabolite downstream of DHEA and AED) in the ZBDK cohort were greater than the declines observed in these androgens in the control arm, suggesting an effect of ketoconazole (−97% *v* −92%, $P = .055$ for testosterone; −67% *v* −12% for DHEA-S, $P = .007$; and −81% *v* −2%, $P < .001$ for androsterone; Figures 3B, 3C, and 3D).

Prostate Androgen Receptor Program Activity

To determine the effect of multitargeted AR pathway suppression on AR signaling, we evaluated prostate epithelial expression of AR and the androgen-regulated gene product, PSA, and TMPRSS2 by IHC (Fig 4). Consistent differences in expression among the three study arms were not observed (not shown); therefore, results from these cohorts were grouped and compared with tissues from untreated men and those receiving standard combined blockade (ZB).

Compared with untreated tissues, intense nuclear AR expression in benign prostate epithelium was markedly lower in the ZB

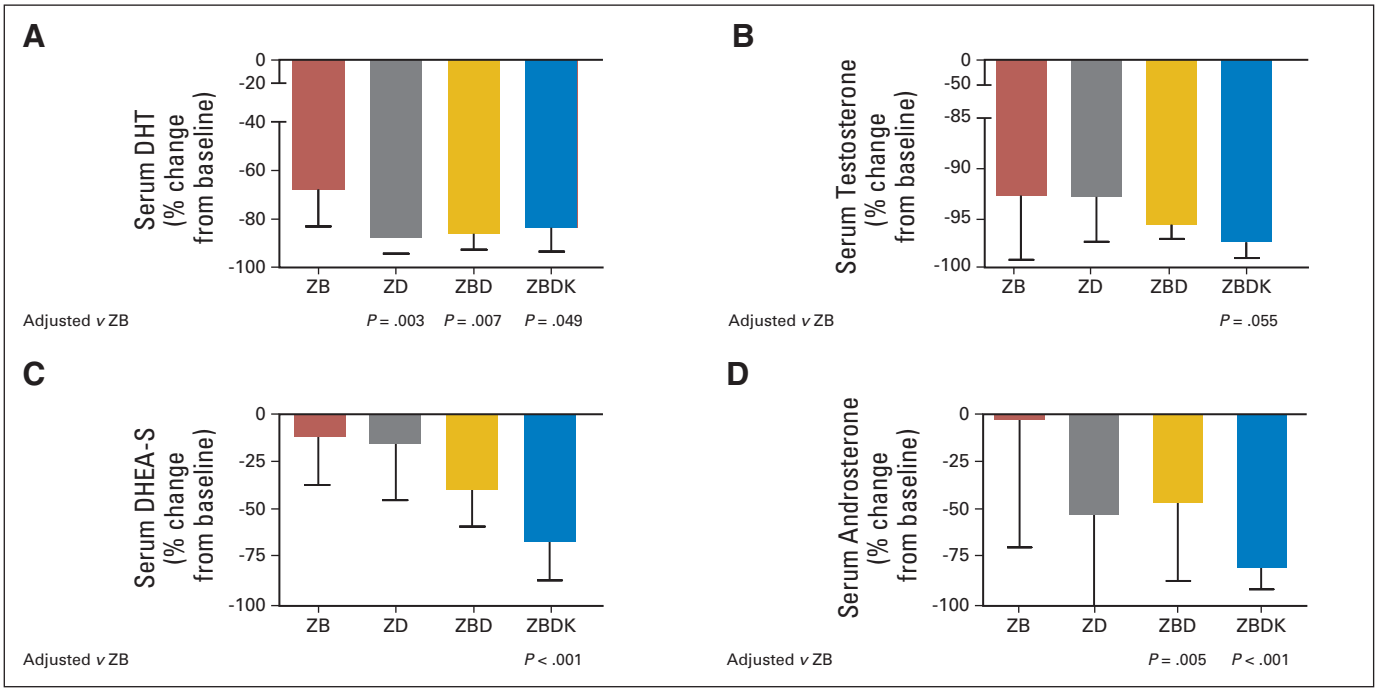

Fig 3. Change in serum androgen levels after 3 months of multitargeted neoadjuvant androgen suppression. The percentage change in androgen levels from baseline are depicted for each treatment group after 3 months of combined androgen blockade with goserelin and bicalutamide (ZB), goserelin and dutasteride (ZD), goserelin with bicalutamide and dutasteride (ZBD), and all three agents combined with ketoconazole (ZBDK). Levels of (A) dehydrotestosterone (DHT), (B) testosterone, (C) dehydroepiandrosterone sulfate (DHEA-S), and (D) androsterone were measured by mass spectroscopy in serum samples obtained before starting treatment and on the morning of prostatectomy. Differences between each treatment cohort and the control (ZB) group were evaluated by linear regression. Statistically significant *P* values ($P < .05$) or those trending toward significance ($P < .10$) are presented in italics below the relevant treatment group. No comparisons for DHEA or androstenedione were significant (data not shown).

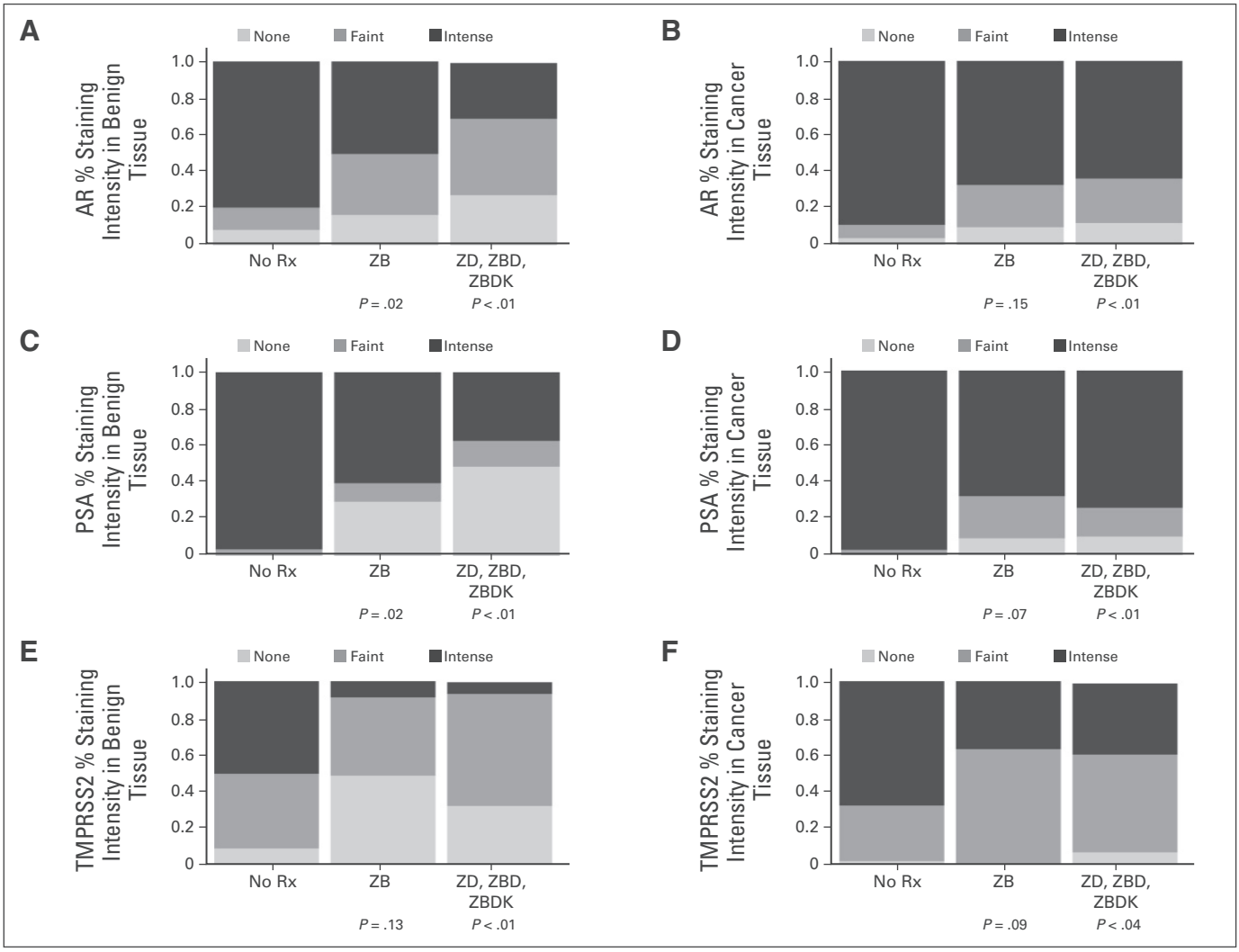

Fig 4. Immunohistochemical expression of androgen receptor (AR) and androgen-regulated genes after 3 months of multitargeted neoadjuvant androgen suppression. A tissue microarray comprising cores of benign and cancer tissue from each patient was analyzed for (A, B) nuclear expression of AR, and (C, D) cytoplasmic expression of prostate-specific antigen (PSA) and (E, F) TMPRSS2. Immunostaining was scored separately in benign (A, C, E) and cancer glands (B, D, F) using a compositional method based on the percentage of cells at each intensity level (0 for none, 1 for faint, and 2 for intense). The stacked bar graphs represent the proportion of cores in each treatment group that stain at the indicated intensity level (light gray, none; medium gray, faint; dark gray, intense). Differences between the indicated cohort and the untreated tissues were evaluated by unpaired *t* tests with Welch's correction. Statistically significant *P* values ($P < .05$) are presented in italics below the relevant treatment group. Rx, treatment; ZB, goserelin and bicalutamide; ZBD, goserelin, bicalutamide, and dutasteride; ZBDK, goserelin, bicalutamide, dutasteride, and ketoconazole; ZD, goserelin and dutasteride.

and combined (ZD, ZBD, and ZBDK) study cohorts (Fig 4A; Appendix Table A2, online only). A trend for lower AR expression in the combined dutasteride cohorts compared with the ZB group was observed, but was not statistically significant. Although suppressed compared with untreated tissue, intense nuclear AR staining remained in the neoplastic epithelium of treated cohorts and was essentially identical in the ZB and the combined dutasteride arms (89% in untreated tissue compared with 62% [ZB, $P = .15$] and 64% [ZD/ZBD/ZBDK, $P = .01$]). The less significant *P* value for the ZB group likely reflects lower power as a result of fewer patients in the ZB subset compared with the grouped ZD/ZBD/ZBDK treatment arm.

Compared with untreated tissues, cytoplasmic expression of the AR-regulated gene products PSA and TMPRSS2 was substantially lower in benign prostate epithelium of both control ZB and combined dutasteride cohorts (Figs 4B and 4C; Appendix Table A2). Paralleling the changes in nuclear AR expression, PSA and TMPRSS2 staining in neoplastic glands was higher than in benign glands and expression was similar in both the ZB and ZD/ZBD/ZBDK groups.

PSA Nadir and Pathologic Outcomes

The median tumor volume at prostatectomy was lower in the ZBDK cohort, although the difference did not reach statistical significance (Fig 5A; Appendix Table A3, online only). The heterogeneity between cohorts and small numbers of patients compromise the ability to draw conclusions regarding clinical efficacy. There was one pathologic complete response in each of the ZBD and ZBDK cohorts, and nine (26%) of 34 patients in the combined study cohorts had small-volume residual disease, defined as tumor volume 0.2 cm^3 or less.[19] In prior studies, achieving a nadir PSA below 0.2 ng/mL in

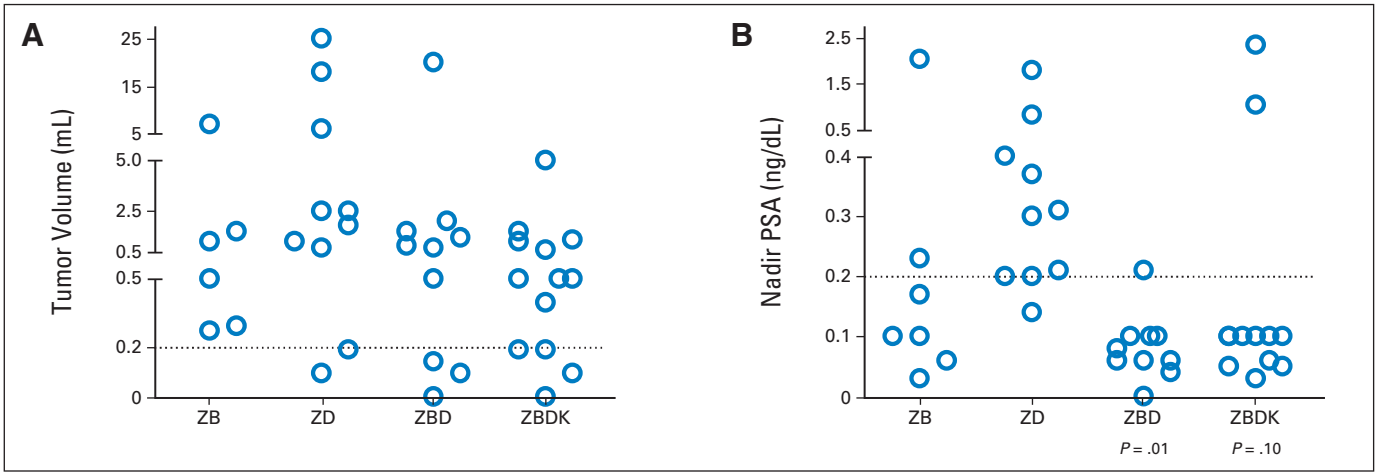

Fig 5. Distribution of tumor volume and prostate-specific antigen (PSA) nadir by treatment group. Tumor volume at (A) prostatectomy and (B) nadir PSA are depicted for each treatment group after 3 months of combined androgen blockade with goserelin and bicalutamide (ZB), goserelin and dutasteride (ZD), goserelin with bicalutamide and dutasteride (ZBD), and all three agents combined with ketoconazole (ZBDK). Dotted lines represent near complete response less than 0.2 cm^3 (A) and nadir PSA less than 0.2 ng/dL (B). *P* values for differences in treatment groups were assessed by two-sample tests of proportions.

response to androgen suppression was associated with improved clinical stage and tumor volume at prostatectomy and better survival in patients with relapsed disease[7,14,15] and is presumed to be related to nadir PSA reflecting greater tumor sensitivity to ADT. Fewer patients in the ZD group had nadir PSA less than 0.2 compared with the ZBD and ZBDK groups, (four of 10 *v* 10 of 10 and 10 of 12, respectively, $P = .01$ and $P = .10$; Fig 5B).

Notably, dichotomizing patients based on nadir PSA less than or ≥ 0.2 ng/mL demonstrated trends toward significantly lower serum testosterone, DHEA, and AED in patients with nadir PSA less than 0.2 ng/mL (Appendix Fig A1A, online only). The expression of AR, PSA, and TMPRSS2 in benign prostate epithelium was significantly lower in patients with PSA nadir less than 0.2 ng/mL; in contrast, expression of AR, PSA, and TMPRSS2 in cancer cells was identical regardless of serum PSA nadir (Appendix Figs A1B and A1C). These data demonstrate that although changes in serum PSA clearly associate with androgen-mediated effects in the prostate, these do not indicate cancer-associated suppression of androgen-mediated gene expression.

DISCUSSION

This study was designed to determine whether intraprostatic concentrations of testosterone and DHT could be suppressed below the levels achieved through standard ADT and whether improved suppression of androgens and AR signaling would enhance pathologic responses. We designed the study in 2006 to evaluate combinations of clinically available drugs that targeted distinct points of androgen metabolism or action. Compared with the group treated with goserelin and bicalutamide, the addition of dutasteride or dutasteride and ketoconazole resulted in substantially lower prostate DHT concentrations, more frequent PSA nadirs of less than 0.2, and more frequent pathologic complete (5.7%) and near-complete responses (20%). The heterogeneity of the treatment groups makes any conclusions regarding clinical response rate hypothesis generating, rather than definitive. The surrogacy of pathologic complete response or small-volume residual disease after neoadjuvant therapy has been clearly demonstrated in locally advanced breast cancer.[20-22] However, although the response rates observed in this study are promising and exceed rates reported in previous neoadjuvant trials of hormone suppression, longer follow-up in larger cohorts will be necessary before we can establish clinical relevance in prostate cancer.

Despite substantially reducing prostate DHT in the cohorts receiving dutasteride or ketoconazole, the combined activity of residual testosterone and DHT levels in the prostate remain at concentrations capable of activating the AR based on previous measurements studies using in vitro assays.[18] Although the absolute prostate or serum androgen levels were not lower in the ZBDK arm compared with the ZD or ZBD arms, the ZBDK group did show a statistically significant difference in the percentage decline of circulating testosterone, DHEA-S, and androsterone levels (particularly for DHEA-S) compared with the declines observed in the standard blockade arm (ZB). DHEA-S is the primary serum reservoir of DHEA, suggesting that in the absence of a CYP17A inhibitor, a significant depot of serum androgen precursors remain. Despite this evidence of activity with the addition of a CYP17A inhibitor, more substantial suppression of upstream precursors will be critical to minimizing tissue androgen levels and overall AR activation. In this context, the agents tested in this study should not be considered part of standard clinical practice.

Consistent with the mechanism of SRD5A inhibition, prostate tissue testosterone levels in all three dutasteride-containing cohorts were statistically higher than in men treated with combined blockade alone, even in the cohort receiving the CYP17A inhibitor ketoconazole. Similarly, AED levels were also significantly higher in tissues from dutasteride-treated patients. As AED is directly interconverted with testosterone, this may reflect metabolism of elevated testosterone to AED by HSD17B2. Alternatively, this could also be explained if AKR1C3 (mediating conversion of AED to testosterone) is rate-limiting, especially because AED is higher than testosterone. These data emphasize that androgen suppression strategies using SRD5A inhibition will require concomitant suppression of upstream androgen synthesis.

Notably, although the expression of AR, PSA, and TMPRSS2 was reduced in benign prostate epithelium and was significantly lower in

patients with PSA nadir less than 0.2 ng/m, the expression of these genes was readily detectable in cancer cells and showed no association with serum PSA nadir. These data suggest that changes in serum PSA clearly represent androgen-mediated effects. However, these most likely reflect the impact of suppressing androgen-mediated PSA secretion from benign prostate tissue and do not necessarily indicate cancer-associated suppression of androgen-mediated gene expression, PSA secretion, or tumor regression.

Important questions for future studies concern the variability in responses. Why a subset of patients had complete or near-complete tumor eradication, whereas substantial residual tumor volumes were found in others, remains to be determined. These tumors may survive androgen inhibition through mechanisms that include increased expression of AR or AR splice variants, the activity of androgen synthetic enzymes such as CYP17A or SRD5A, or through alternative signal transduction pathways.[23-30]

The AR fulfills an important criteria defining a lineage-survival oncogene—a master cell-type regulator on which neoplastic cells derived from prostate epithelium are dependent.[31] This study provides a template for evaluating the mechanisms underlying the efficacy of AR pathway-directed therapeutics. Through direct tissue assessments, our results indicate that treatment failure is likely still occurring via ineffective and incomplete AR pathway suppression. The neoadjuvant approach provides opportunities to rigorously test the hypothesis that extinguishing AR signaling—either through further ligand reduction and/or more effective direct AR targeting—will produce high rates of pathologic complete responses. Combining effective androgen synthesis inhibitors such as abiraterone with more potent AR antagonists such as enzalutamide is a reasonable strategy for assessing whether highly active antiandrogen therapy is an effective treatment strategy.[32]

AUTHORS' DISCLOSURES OF POTENTIAL CONFLICTS OF INTEREST

Although all authors completed the disclosure declaration, the following author(s) and/or an author's immediate family member(s) indicated a financial or other interest that is relevant to the subject matter under consideration in this article. Certain relationships marked with a "U" are those for which no compensation was received; those relationships marked with a "C" were compensated. For a detailed description of the disclosure categories, or for more information about ASCO's conflict of interest policy, please refer to the Author Disclosure Declaration and the Disclosures of Potential Conflicts of Interest section in Information for Contributors.
Employment or Leadership Position: Trevor Penning, Penzyme (U) **Consultant or Advisory Role:** Trevor Penning, Tokai Pharmaceuticals (C), Sage Pharmaceuticals (C) **Stock Ownership:** None **Honoraria:** Elahe A. Mostaghel, Janssen Pharmaceuticals **Research Funding:** Peter S. Nelson, GlaxoSmithKline; Lawrence D. True, GlaxoSmithKline; Bruce Montgomery, GlaxoSmithKline **Expert Testimony:** None **Patents:** None **Other Remuneration:** None

AUTHOR CONTRIBUTIONS

Conception and design: Elahe A. Mostaghel, Peter S. Nelson, Paul Lange, Bruce Montgomery
Financial support: Elahe A. Mostaghel, Peter S. Nelson, Bruce Montgomery
Provision of study materials or patients: All authors
Collection and assembly of data: All authors
Data analysis and interpretation: Elahe A. Mostaghel, Peter S. Nelson, Daniel W. Lin, Mary Ellen Taplin, Steven Balk, Philip Kantoff, Daniel Tamae, Alvin M. Matsumoto, Lawrence D. True, Trevor Penning, Rachel Hunter Merrilll, Roman Gulati, Bruce Montgomery
Manuscript writing: All authors
Final approval of manuscript: All authors

REFERENCES

1. Thompson IM, Goodman PJ, Tangen CM, et al: The influence of finasteride on the development of prostate cancer. N Engl J Med 349:215-224, 2003

2. Andriole GL, Bostwick DG, Brawley OW, et al: Effect of dutasteride on the risk of prostate cancer. N Engl J Med 362:1192-1202, 2010

3. Forti G, Salerno R, Moneti G, et al: Three-month treatment with a long-acting gonadotropin-releasing hormone agonist of patients with benign prostatic hyperplasia: Effects on tissue androgen concentration, 5 alpha-reductase activity and androgen receptor content. J Clin Endocrinol Metab 68:461-468, 1989

4. Titus MA, Gregory CW, Ford OH 3rd, et al: Steroid 5alpha-reductase isozymes I and II in recurrent prostate cancer. Clin Cancer Res 11:4365-4371, 2005

5. Page ST, Lin DW, Mostaghel EA, et al: Persistent intraprostatic androgen concentrations after medical castration in healthy men. J Clin Endocrinol Metab 91:3850-3856, 2006

6. Mostaghel EA, Page ST, Lin DW, et al: Intraprostatic androgens and androgen-regulated gene expression persist after testosterone suppression: Therapeutic implications for castration-resistant prostate cancer. Cancer Res 67:5033-5041, 2007

7. Gleave ME, La Bianca SE, Goldenberg SL, et al: Long-term neoadjuvant hormone therapy prior to radical prostatectomy: Evaluation of risk for biochemical recurrence at 5-year follow-up. Urology 56:289-294, 2000

8. Soloway MS, Pareek K, Sharifi R, et al: Neoadjuvant androgen ablation before radical prostatectomy in cT2bNxMo prostate cancer: 5-year results. J Urol 167:112-116, 2002

9. van der Kwast TH, Amin MB, Billis A, et al: International Society of Urological Pathology (ISUP) Consensus Conference on Handling and Staging of Radical Prostatectomy Specimens: Working group 2—T2 substaging and prostate cancer volume. Mod Pathol 24:16-25, 2011

10. Kalhorn TF, Page ST, Howald WN, et al: Analysis of testosterone and dihydrotestosterone from biological fluids as the oxime derivatives using high-performance liquid chromatography/tandem mass spectrometry. Rapid Commun Mass Spectrom 21:3200-3206, 2007

11. Lucas JM, True L, Hawley S, et al: The androgen-regulated type II serine protease TMPRSS2 is differentially expressed and mislocalized in prostate adenocarcinoma. J Pathol 215:118-125, 2008

12. Hothorn T, Bretz F, Westfall P: Simultaneous inference in general parametric models. Biom J 50:346-363, 2008

13. Hothorn T, Zeileis A: Generalized maximally selected statistics. Biometrics 64:1263-1269, 2008

14. Gleave ME, Goldenberg SL, Jones EC, et al: Biochemical and pathological effects of 8 months of neoadjuvant androgen withdrawal therapy before radical prostatectomy in patients with clinically confined prostate cancer. J Urol 155:213-219, 1996

15. Stewart AJ, Scher HI, Chen MH, et al: Prostate-specific antigen nadir and cancer-specific mortality following hormonal therapy for prostate-specific antigen failure. J Clin Oncol 23:6556-6560, 2005

16. Mostaghel EA, Geng L, Holcomb I, et al: Variability in the androgen response of prostate epithelium to 5alpha-reductase inhibition: Implications for prostate cancer chemoprevention. Cancer Res 70:1286-1295, 2010

17. Grino PB, Griffin JE, Wilson JD: Testosterone at high concentrations interacts with the human androgen receptor similarly to dihydrotestosterone. Endocrinology 126:1165-1172, 1990

18. Gregory CW, Johnson RT Jr, Mohler JL, et al: Androgen receptor stabilization in recurrent prostate cancer is associated with hypersensitivity to low androgen. Cancer Res 61:2892-2898, 2001

19. Carter HB, Sauvageot J, Walsh PC, et al: Prospective evaluation of men with stage T1C adenocarcinoma of the prostate. J Urol 157:2206-2209, 1997

20. Symmans WF, Peintinger F, Hatzis C, et al: Measurement of residual breast cancer burden to predict survival after neoadjuvant chemotherapy. J Clin Oncol 25:4414-4422, 2007

21. Grossman HB, Natale RB, Tangen CM, et al: Neoadjuvant chemotherapy plus cystectomy compared with cystectomy alone for locally advanced bladder cancer. N Engl J Med 349:859-866, 2003

22. Rödel C, Martus P, Papadoupolos T, et al: Prognostic significance of tumor regression after preoperative chemoradiotherapy for rectal cancer. J Clin Oncol 23:8688-8696, 2005

23. Mostaghel EA, Marck BT, Plymate SR, et al: Resistance to CYP17A1 inhibition with abiraterone in castration-resistant prostate cancer: Induction of steroidogenesis and androgen receptor splice variants. Clin Cancer Res 17:5913-5925, 2011

24. Hu R, Lu C, Mostaghel EA, et al: Distinct transcriptional programs mediated by the ligand-dependent full-length androgen receptor and its splice variants in castration-resistant prostate cancer. Cancer Res 72:3457-3462, 2012

25. Guo Z, Yang X, Sun F, et al: A novel androgen receptor splice variant is up-regulated during prostate cancer progression and promotes androgen depletion-resistant growth. Cancer Res 69: 2305-2313, 2009

26. Thomas LN, Douglas RC, Lazier CB, et al: Levels of 5alpha-reductase type 1 and type 2 are increased in localized high grade compared to low grade prostate cancer. J Urol 179:147-151, 2008

27. Montgomery RB, Mostaghel EA, Vessella R, et al: Maintenance of intratumoral androgens in metastatic prostate cancer: A mechanism for castration-resistant tumor growth. Cancer Res 68:4447-4454, 2008

28. Cai C, Chen S, Ng P, et al: Intratumoral de novo steroid synthesis activates androgen receptor in castration-resistant prostate cancer and is upregulated by treatment with CYP17A1 inhibitors. Cancer Res 71:6503-6513, 2011

29. Carver BS, Chapinski C, Wongvipat J, et al: Reciprocal feedback regulation of PI3K and androgen receptor signaling in PTEN-deficient prostate cancer. Cancer Cell 19:575-586, 2011

30. Mulholland DJ, Tran LM, Li Y, et al: Cell autonomous role of PTEN in regulating castration-resistant prostate cancer growth. Cancer Cell 19: 792-804, 2011

31. Garraway LA, Sellers WR: Lineage dependency and lineage-survival oncogenes in human cancer. Nat Rev Cancer 6:593-602, 2006

32. Nelson PS: Molecular states underlying androgen receptor activation: A framework for therapeutics targeting androgen signaling in prostate cancer. J Clin Oncol 30:644-646, 2012

Affiliations

Elahe A. Mostaghel, Rachel Hunter Merrill, and Roman Gulati, Fred Hutchinson Cancer Research Center; Elahe A. Mostaghel, Peter S. Nelson, Paul Lange, Daniel W. Lin, William Ellis, Robert Vessella, and Bruce Montgomery, University of Washington; Brett Marck, Alvin M. Matsumoto, and Lawrence D. True, Veterans Affairs Puget Sound Health Care System, Seattle, WA; Mary Ellen Taplin and Philip Kantoff, Dana-Farber Cancer Institute, Harvard Medical School; Steven Balk, Beth Israel Deaconess Medical Center, Boston, MA; and Daniel Tamae and Trevor Penning, University of Pennsylvania, Philadelphia, PA.

GLOSSARY TERMS

androgen receptor: A DNA-binding and hormone-activated transcription factor important to the development and progression of prostate cancer. Its primary ligand is dihydrotestosterone. In later-stage (castration-resistant) prostate cancer, oncogenic alterations such as androgen receptor overexpression allow the androgen receptor to continue signaling despite undetectable, or castrate, levels of serum testosterone.

PSA (prostate-specific antigen): A protein produced by cells of the prostate gland, the blood level of PSA is used as a tumor marker for men who may be suspected of having prostate cancer. Most physicians consider 0 to 4.0 ng/mL as the normal range. Levels of 4 to 10 and 10 to 20 ng/mL are considered slightly and moderately elevated, respectively. PSA levels have to be complemented with other tests to make a firm diagnosis of prostate cancer.

Acknowledgment

We thank Jing Xia for additional statistical assistance.

Appendix

Table A1. Absolute Values and Mean Percentage Change in Post-Treatment Serum Androgen Levels

Treatment Category	DHT (ng/dL)		Testosterone (ng/dL)		AED (ng/dL)		DHEA (ng/dL)		DHEA-S (pg/dL)		Androsterone (ng/dL)	
	Mean	SD	Mean	SD	Mean	SD	Mean	SD	Mean	SD	Mean	SD
No treatment	34.1	13.8	368	112	85.1	27.8	368	155	132.6	112.5	16.4	12.6
ZB, post-treatment	6.9	3.1	17.9	10.4	93.7	68.9	428	255	68.6	40.1	9.5	9.1
% change versus baseline	–68	12	–92	5	16	41	16	22	–12	3	–2	42
ZD, post-treatment	4.2	3.4	27.2	24.4	106	81.3	446	284	191.8	50.8	6.8	6.8
% change versus baseline	–88	8	–93	5	3	76	0	57	–16	19	–48	59
P (adjusted *v* ZB)	.0027		NS		NS		NS		NS		NS	
ZBD, post-treatment	3.6	2.0	13.4	4.3	66.8	33.7	272	205	53.3	55.7	7.6	7.1
% change versus baseline	–86	9	–95	2	–2	77	5	82	–40	23	–46	53
P (adjusted *v* ZB)	.0067		NS		NS		NS		NS		.005	
ZBDK, post-treatment	5.7	4.9	9.4	6.2	93.8	91.6	315	256	40.6	44.3	2.9	2.3
% change versus baseline	–83	15	–97	0.03	29	1.28	–7	77	–67	31	–81	15
P (adjusted *v* ZB)	.0492		.055		NS		NS		< .001		< .001	

Abbreviations: AED, androstenedione; DHEA, dehydroepiandrosterone; DHEA-S, DHEA sulfate; DHT, dihydrotestosterone; NS, not significant; SD, standard deviation; ZB, goserelin and bicalutamide; ZBD, goserelin, bicalutamide, and dutasteride; ZBDK, goserelin, bicalutamide, dutasteride, and ketoconazole; ZD, goserelin and dutasteride.

Table A2. Percentage of Tissue With High-Intensity IHC Expression of AR and Androgen-Regulated Genes in Benign and Malignant Prostate Epithelial Glands

Variable	Benign Prostate Epithelium			Malignant Prostate Epithelium		
	No Treatment (%)	ZB (%)	ZD, ZBD, ZBDK (%)	No Treatment (%)	ZB (%)	ZD, ZBD, ZBDK (%)
AR*	81	47	32	89	62	64
P v no Rx†		.02	< .01		.15	< .01
PSA*	99	49	42	97	65	74
P v no Rx†		.02	< .01		.14	< .01
TMPRSS2*	50	17	6	68	34	39
P v no Rx†		.13	< .01		.09	.04

Abbreviations: AR, androgen receptor; IHC, immunohistochemistry; PSA, prostate-specific antigen; Rx, treatment; ZB, goserelin and bicalutamide; ZBD, goserelin, bicalutamide, and dutasteride; ZBDK, goserelin, bicalutamide, dutasteride, and ketoconazole; ZD, goserelin and dutasteride.

*AR, nuclear; PSA and TMPRSS2, cytoplasmic.

†*P* from Welch's two sample *t* tests.

14 American Society of Clinical Oncology

Table A3. Post-Treatment PSA Nadir and Pathologic Stage at Prostatectomy in Control and Study Patients

Characteristic	Untreated Patients (n = 11)	Control Patients, ZB (n = 8)*	Study Patients		
			ZD (n = 12)	ZBD (n = 10)†	ZBDK (n = 13)
Nadir PSA ≤ 0.2	NA				
No.		5/7	4/10	10/10	10/12
%		85	40	100	83
Pathologic staging					
pT2	10	3	5	6	10
pT3 a/b	1	1/1	1/3	2/1	1/1
Tumor volume, n		6/6	10/11	10/12	13/13
Mean	1.9	1.8	5.8	2.7	0.9
Median	1.6	0.8	2.2	0.8	0.5
Pathologic response					
Complete (CR)	0	0	0	1	1
Near CR (≤ 0.2 cm^3)	0	0	2	2	3

Abbreviations: CR, complete response; PSA, prostate-specific antigen; ZB, goserelin and bicalutamide; ZBD, goserelin, bicalutamide, and dutasteride; ZBDK, goserelin, bicalutamide, dutasteride, and ketoconazole; ZD, goserelin and dutasteride.

*Two patients in this group underwent end-of-study biopsy instead of prostatectomy (one withdrew, one had radiation treatment).

†One patient in this group underwent end-of-study biopsy instead of prostatectomy (because of diagnosis of lung cancer).

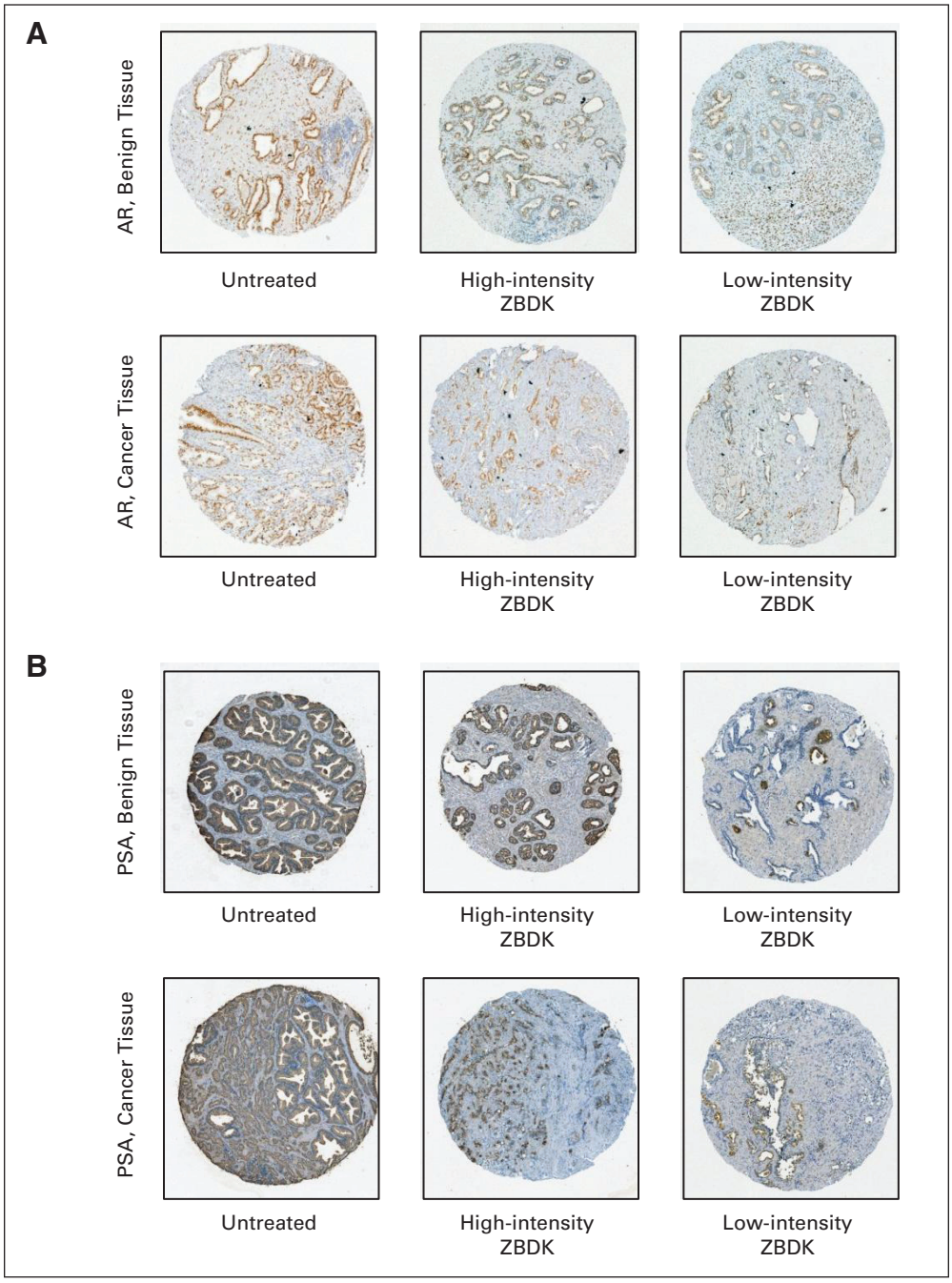

Fig A1. Prostatic expression of androgen receptor (AR) and prostate-specific antigen (PSA) after 3 months of multitargeted neoadjuvant androgen suppression. A tissue microarray comprising six cores of benign and cancer tissue from each patient was analyzed (A) for nuclear expression of AR and (B) for cytoplasmic expression of PSA in benign and malignant prostate epithelium. Representative examples of high- and low-intensity staining from different patients in the untreated and multitargeted treatment arms are shown for both benign and cancer cores. ZBDK, goserelin, bicalutamide, dutasteride, and ketoconazole .

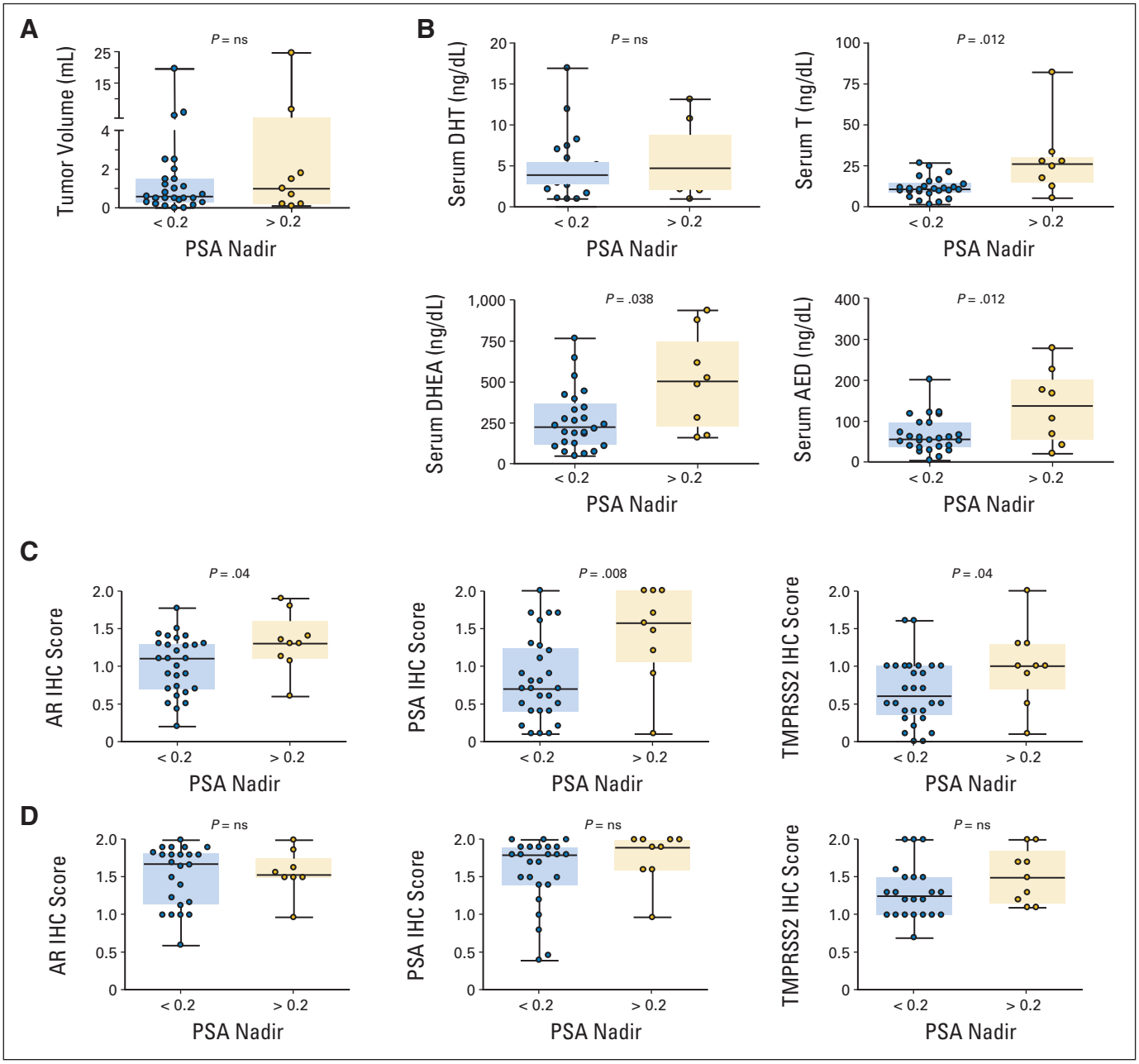

Fig A2. Association of prostate-specific antigen (PSA) nadir with tumor volume, serum androgens, and prostatic immunohistochemistry (IHC). Nadir PSA values were used to dichotomize all study patients into those with PSA nadir less than or more than 0.2 ng/dL to evaluate differences in (A) tumor volume, (B) serum androgen levels, and prostate IHC expression of androgen receptor (AR), PSA, and TMPRSS2 in (C) benign and (D) cancer tissue. Differences were evaluated by linear regression. Statistically significant *P* values ($P < .05$) or those trending toward significance ($P < .10$) are presented in italics below the relevant treatment group. AED, androstenedione; DHEA, dehydroepiandrosterone; DHT, dihydrotestosterone.

Published OnlineFirst January 21, 2014; DOI: 10.1158/1078-0432.CCR-13-1863

Clinical Cancer Research

Rapid Induction of Androgen Receptor Splice Variants by Androgen Deprivation in Prostate Cancer

Ziyang Yu, Sen Chen, Adam G. Sowalsky, et al.

Clin Cancer Res 2014;20:1590-1600. Published OnlineFirst January 21, 2014.

Published OnlineFirst January 21, 2014; DOI: 10.1158/1078-0432.CCR-13-1863

Cancer Therapy: Preclinical

Clinical Cancer Research

Rapid Induction of Androgen Receptor Splice Variants by Androgen Deprivation in Prostate Cancer

Ziyang Yu[1], Sen Chen[1], Adam G. Sowalsky[1], Olga S. Voznesensky[1], Elahe A. Mostaghel[2], Peter S. Nelson[2], Changmeng Cai[1], and Steven P. Balk[1]

Abstract

Purpose: Mechanisms mediating androgen receptor (AR) reactivation in prostate cancer that progresses after castration (castration-resistant prostate cancer; CRPC) and subsequent treatment with abiraterone (CYP17A1 inhibitor that further suppresses androgen synthesis) remain unclear.

Experimental Design: Prostate cancer xenografts were examined to identify mechanism of progression after castration and abiraterone.

Results: AR reactivation in abiraterone-resistant VCaP xenografts was not associated with restoration of intratumoral androgens or alterations in AR coregulators. In contrast, mRNA encoding full-length AR (AR-FL) and a constitutively active splice variant (AR-V7) were increased compared with xenografts before castration, with an increase in AR-V7 relative to AR-FL. This shift toward AR-V7 was due to a feedback mechanism whereby the androgen-liganded AR stimulates expression of proteins that suppress generation of AR-V7 relative to AR-FL transcripts. However, despite the increases in AR-V7 mRNA, it remained a minor transcript (<1%) relative to AR-FL in resistant VCaP xenografts and CRPC clinical samples. AR-V7 protein expression was similarly low relative to AR-FL in castration-resistant VCaP xenografts and androgen-deprived VCaP cells, but the weak basal AR activity in these latter cells was further repressed by AR-V7 siRNA.

Conclusions: AR-V7 at these low levels is not adequate to restore AR activity, but its rapid induction after androgen deprivation allows tumors to retain basal AR activity that may be needed for survival until more potent mechanisms emerge to activate AR. Agents targeting AR splice variants may be most effective when used very early in conjunction with therapies targeting the AR ligand-binding domain. *Clin Cancer Res; 20(6); 1590–600. ©2014 AACR.*

Introduction

Blockade of testicular androgen production by surgical or medical castration (androgen deprivation therapy) is a standard treatment for metastatic prostate cancer, but tumors invariably relapse and progress into a stage termed castration-resistant prostate cancer (CRPC). One mechanism driving these resistant tumors is intratumoral synthesis of androgens (testosterone and dihydrotestosterone, DHT) from precursor steroids produced by the adrenal glands or *de novo* from cholesterol (1–6). Synthesis of these precursor steroids is dependent on the enzyme CYP17A1, and a specific inhibitor of this enzyme (abiraterone) was recently approved for treatment of CRPC, but most men who initially respond will relapse within 1 to 2 years (6–9). These relapses are generally associated with increases in serum prostate-specific antigen (PSA), suggesting that androgen receptor (AR) activity has again been restored. However, the mechanisms mediating this AR activity and the role of AR in resistance to CYP17A1 inhibitor therapy remain unclear (1, 10, 11).

The human VCaP prostate cancer cell xenograft expresses the androgen-regulated TMPRSS2:ERG fusion gene and has been used as a model for progression to CRPC after castration (12, 13). We recently reported that castration-resistant VCaP xenografts initially respond to abiraterone, but relapse within 1 to 2 months (2). Consistent with findings in patients, these abiraterone-relapsed xenografts expressed high levels of several AR-regulated genes, indicating restoration of AR transcriptional activity. These relapsed tumors also had increased expression of CYP17A1 mRNA, suggesting restoration of androgen synthesis as a possible resistance mechanism (2). Recent findings in other xenograft models have similarly suggested that androgen synthesis may mediate resistance in some cases (10), and have identified expression of alternatively spliced AR isoforms as another potential resistance mechanism (10, 14–20). In this study, we assess the contribution of intratumoral

Authors' Affiliations: [1]Hematology-Oncology Division, Department of Medicine, Beth Israel Deaconess Medical Center and Harvard Medical School, Boston, Massachusetts; and [2]Fred Hutchinson Cancer Research Center, University of Washington, Seattle, Washington

Note: Supplementary data for this article are available at Clinical Cancer Research Online (http://clincancerres.aacrjournals.org/).

Corresponding Authors: Steven P. Balk, Beth Israel Deaconess Medical Center, 330 Brookline Avenue, Boston, MA 02215. Phone: 617-735-2065; Fax: 617-735-2050; E-mail: sbalk@bidmc.harvard.edu; and Changmeng Cai, E-mail: ccai1@bidmc.harvard.edu

doi: 10.1158/1078-0432.CCR-13-1863

Published OnlineFirst January 21, 2014; DOI: 10.1158/1078-0432.CCR-13-1863

Translational Relevance

Previous studies have indicated that restoration of androgen receptor (AR) transcriptional activity in prostate cancer that relapses after castration (castration-resistant prostate cancer) or after subsequent therapy with abiraterone, a CYP17A1 inhibitor that further suppresses androgen synthesis, may be mediated by abiraterone-resistant intratumoral androgen synthesis or by constitutively active AR splice variants lacking the ligand-binding domain (LBD). We show that AR reactivation in abiraterone-resistant VCaP xenografts is not associated with restoration of intratumoral androgens. Moreover, we find that increases in the major AR splice variant (AR-V7) occur rapidly through a feedback mechanism and can mediate low-basal AR activity immediately after androgen deprivation, but cannot mediate the high-level AR activity in relapsed tumors. These results indicate that agents targeting AR splice variants may be most effective when used very early in conjunction with therapies targeting the AR LBD before the emergence of additional resistance mechanisms.

androgen synthesis versus alternative mechanisms, including expression of alternatively spliced AR isoforms, in progression to abiraterone resistance.

Materials and Methods

siRNA and transfection analysis

The siRNAs specific for full-length AR (AR-FL; siExon 7, siEX7) and for AR-V7 (siCryptic Exon 3; siCE3) were described previously (17). The siRNA targeting AR exon 1 (siEX1) was described previously (21). Transfection of siRNA was performed using Lipofectamine RNAiMax (Invitrogen) in OptiMEM according to the manufacturer's protocol. The final siRNA concentration was 20 nmol/L. A scrambled nontargeting control siRNA (Qiagen) was used as a negative control. Sixteen hours later, transfection medium was replaced with medium containing 5% charcoal-dextran stripped serum. Another 24 hours later, transfected cells were stimulated with DHT at 10 nmol/L or vehicle (ethanol) for 16 hours.

Immunoblot and steroid analyses

Whole-cell lysates were prepared using lysis buffer containing 2% SDS and subjected to immunoblotting. The antibodies against human AR (N20 and C19) were obtained from Santa Cruz Biotechnology. The antibodies against AR-V7 were from Precision Antibody. Antibodies against β-actin (AC-15) and β-tubulin were from Millipore. The results from a minimum of three experiments were subjected to densitometry and normalized to β-actin or β-tubulin loading control and the mean values relative to control empty vector cells (set to 1.0) are given. AR immunoblot analyses were further quantified by comparison with blots containing serial dilutions of AR protein. Steroid extractions from xenografts and mass spectrometry were performed as described previously (5).

RNA sequencing

Total cellular RNA was extracted and purified from tissues using the RNeasy Mini Kit (Qiagen). One microgram of RNA was treated with DNase in-solution (Qiagen) and purified with the RNeasy MinElute Cleanup Kit (Qiagen). DNA-free RNA was then depleted of ribosomal RNA using the Ribo-Zero rRNA Removal Kit (Epicentre). The remaining fraction of RNA was prepared into an indexed, strand-specific library using the Script-Seq v2 RNA-Seq Library Preparation Kit (Epicentre), pooled, and then clustered and sequenced on a Hi-Seq 2000 (Illumina) with 100-base paired-end reads (100 × 100) and seven indexing cycles. Demultiplexed FASTQ files were aligned to the human genome and genetic features were quantified with the RNA sequencing (RNA-seq) Unified Mapper (http://www.ncbi.nlm.nih.gov/pmc/articles/PMC3167048/). Data were visualized using the Integrative Genome Viewer (22). Data were submitted (SRP019503).

Reverse transcriptase PCR analysis

RNA was isolated using the RNeasy Mini Kit (Invitrogen). Superscript III reverse transcriptase (Invitrogen) was used for reverse transcription with 500 ng RNA in the presence of 100 ng of random primers (Invitrogen). For conventional PCR, the primers for *AR-V7* were described previously (17). Glyceraldehyde-3-phosphate dehydrogenase (*GAPDH*) primers were as follows: Forward: 5′-tcaccatcttccaggag-3′, Reverse: 5′-gcttcaccaccttcttg-3′. For quantitative reverse transcriptase PCR (qRT-PCR), the *AR-V7* TaqMan primers and probe were as follows: Forward: 5′-cggaaatgttatgaagcaggatga-3′, reverse: 5′-ctggtcattttgagatgcttgcaat-3′, probe: 5′-FAM-ggagaaaaattccgggt-3′. The specific TaqMan primer probe sets for *AR-FL*, *PSA*, *FKBP5*, *TMPRSS2-ERG*, *PLZF*, and *GAPDH* were as described previously (2, 21). *KLK2* and *NKX3.1* primer and probe sets were purchased from Applied Biosystems. qRT-PCR was performed in an ABI7900 thermal cycler.

Results

Expression of AR-stimulated genes in abiraterone-resistant VCaP xenografts

We previously reported a castration-resistant VCaP xenograft model that responds initially to abiraterone and then relapses after approximately 6 weeks of abiraterone treatment (2, 12). It should be noted that the abiraterone response in these castration-resistant xenografts primarily reflects blockade of *de novo* androgen synthesis by intratumoral CYP17A1, as the murine adrenal gland does not synthesize the substantial levels of androgen precursors that are produced in humans and are hence a major target of CYP17A1 inhibitors in men with CRPC. AR activity, based on expression of a small panel of AR-regulated genes, was initially markedly repressed by abiraterone and seemed to be restored in these abiraterone-resistant xenografts. To more comprehensively assess AR activity in these xenografts,

Published OnlineFirst January 21, 2014; DOI: 10.1158/1078-0432.CCR-13-1863

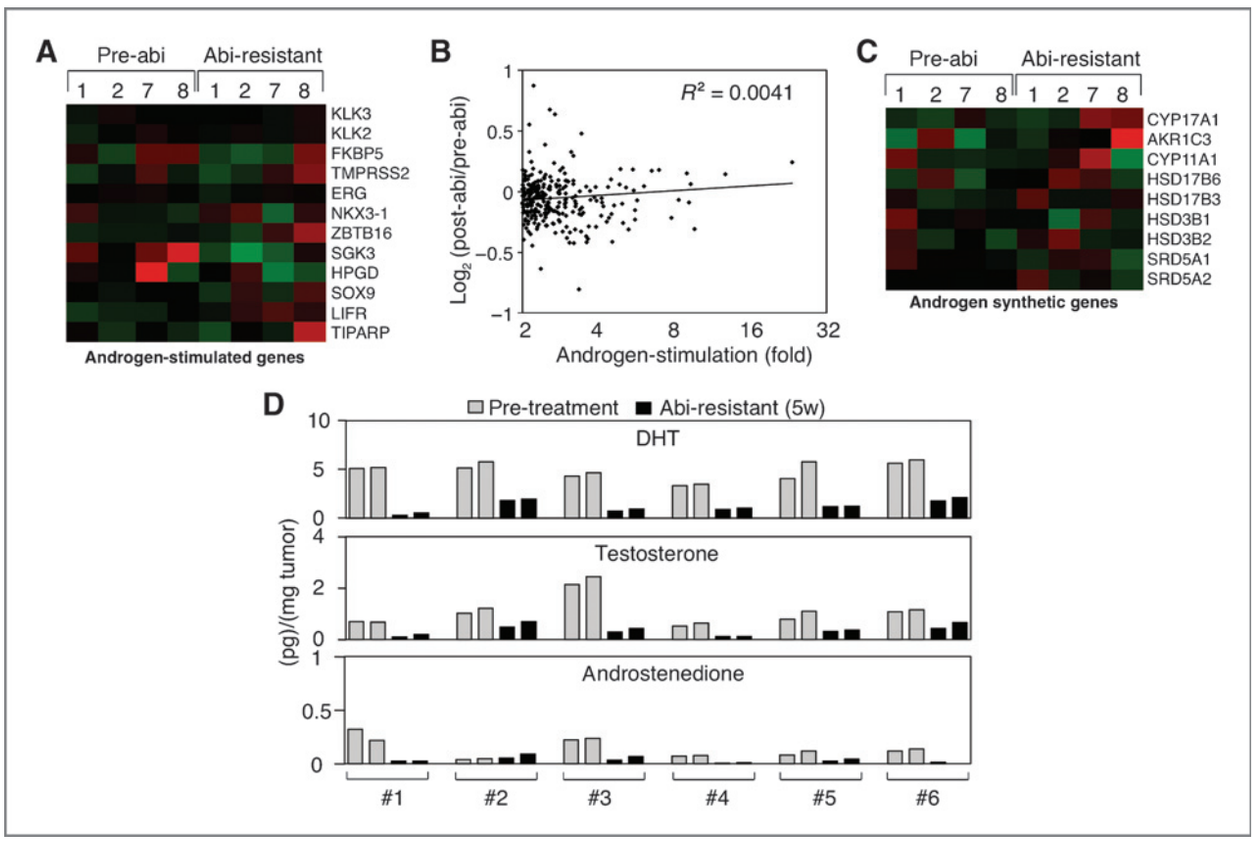

Figure 1. Expression of AR-stimulated genes and androgen synthesis in abiraterone-resistant VCaP xenografts. A, mice bearing recurrent VCaP xenografts were treated with abiraterone until relapse (0.5 mg/mL in drinking water for 4–6 weeks). RNA extracted from four sets of tumor samples pre- (pre-abi) or posttreatment (Abi-resistant) was analyzed by microarray (Affymetrix HuGene 1.0 ST). Expression of 12 androgen-stimulated genes is shown as heatmap (red, high expression; green, low expression). B, the $\log_2$ ratio for expression of androgen-stimulated genes (>2-fold) in abiraterone-relapsed versus pretreatment xenograft is plotted versus their fold androgen induction. R^2 is presented as an indication of the correlation between androgen induction and change induced by abiraterone treatment, and showed no trend toward lower expression in the relapsed tumors. C, expression of nine genes involved in androgen synthesis is shown as heatmap. D, DHT, testosterone, and androstenedione levels in six sets of abiraterone-relapsed VCaP xenograft tumor samples versus pretreatment levels in tumor biopsies were measured using mass spectrometry. Each sample was measured in duplicate.

we used Affymetrix oligonucleotide microarrays to compare expression of AR-regulated genes in biopsies from CRPC xenografts before starting abiraterone and at relapse. This analysis showed that expression of multiple well-recognized AR-stimulated genes, including ERG from the TMPRSS2:ERG fusion gene and the recently reported AR and ERG-dependent oncogene SOX9 (23), was not significantly higher in the tumors before therapy than at relapse, supporting the conclusion that AR transcriptional activity was restored (Fig. 1A).

To more systematically identify alterations in the spectrum of AR-regulated genes, we also examined expression of all genes shown previously to be induced at least 2-fold by androgen in VCaP cells (21). Figure 1B shows a plot of their fold induction by DHT in VCaP cells versus the ratio of their expression in the xenografts before abiraterone and at relapse. These results show that expression of androgen-stimulated genes, whether they are weakly or strongly androgen induced, was broadly restored in the abiraterone-relapsed tumors, with no significant trend toward lower expression in the relapsed tumors.

Androgen synthesis in abiraterone-resistant VCaP xenografts

Consistent with our previous report, expression of CYP17A1 and AKR1C3 were increased in three of the four abiraterone-relapsed xenografts, and there were variable changes in other androgen synthetic enzymes (Fig. 1C). To determine whether restoration of intratumoral androgen synthesis may be mediating relapses, we performed mass spectrometry to examine intratumoral androgens in biopsies from these xenografts before starting abiraterone and at relapse. Significantly, we could readily detect DHT, testosterone, and androstenedione in the relapsed tumors. However, in all cases their levels were markedly lower than those in biopsies from the matched tumors before starting abiraterone treatment (Fig. 1D). These findings are consistent with recent clinical studies showing sustained suppression of testosterone in both blood and bone marrow in patients relapsing after abiraterone treatment (24). Therefore, although AR activity may still be dependent on residual androgen synthesis, it seemed that additional mechanisms must also be driving AR activity at low androgen levels.

Published OnlineFirst January 21, 2014; DOI: 10.1158/1078-0432.CCR-13-1863

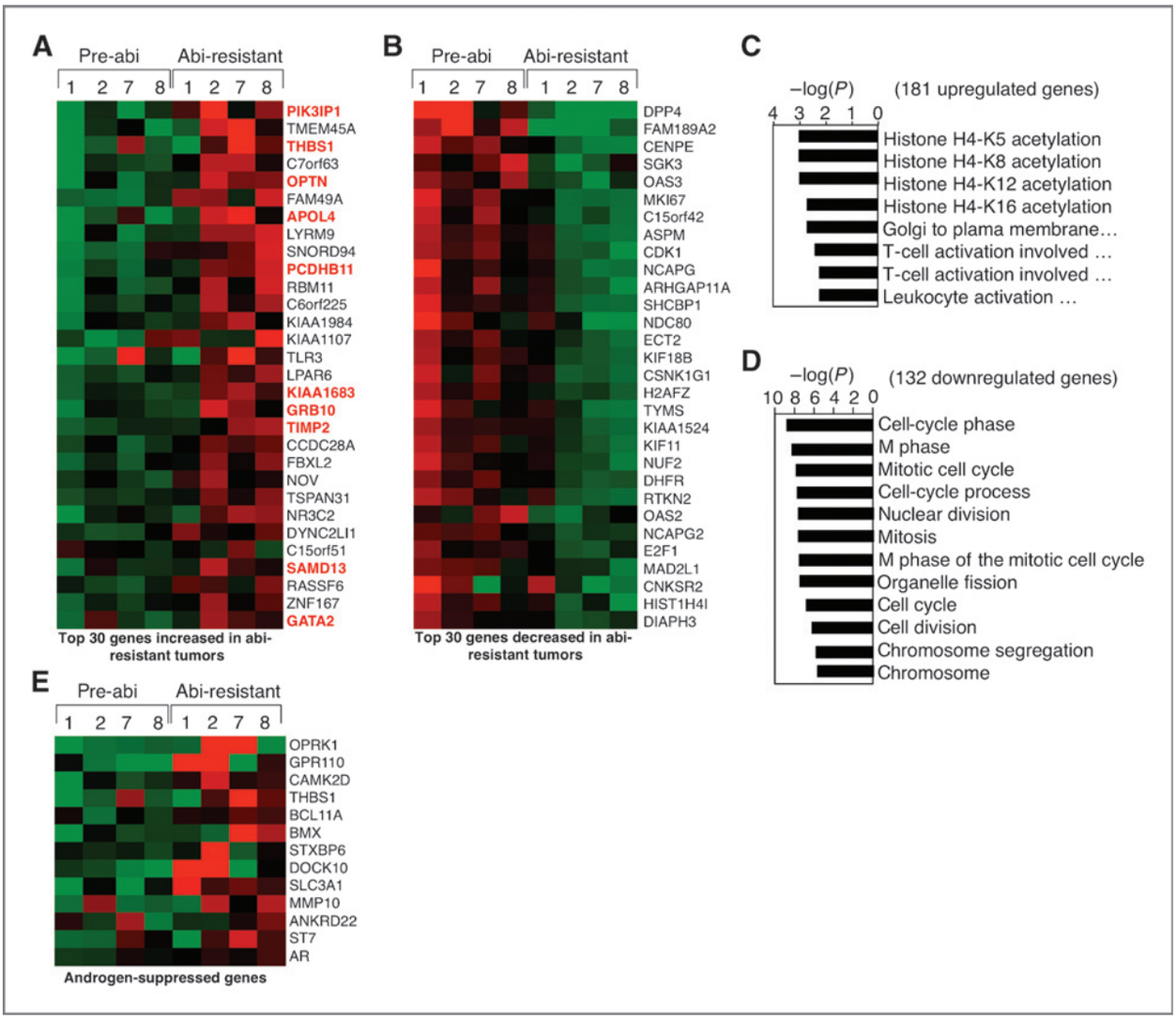

Figure 2. Genes and pathways altered in abiraterone-relapsed xenografts. A and B, heatmap presentations of expression of top 30 most consistently upregulated genes (A) or downregulated genes (B) in abiraterone-resistant tumors. Genes shown in bold and red in (A) were shown previously to be repressed by DHT in VCaP cells. C and D, gene ontology analysis on 181 upregulated genes (C) or 132 downregulated genes (D; $P < 0.05$). E, expression of 13 androgen-suppressed genes shown as heatmap.

Genes and pathways altered in abiraterone-relapsed xenografts

We next did an unbiased analysis and identified all genes with significant ($P < 0.05$) changes in expression in the abiraterone-resistant xenografts versus the matched pretreatment xenografts. A total of 181 genes were upregulated in abiraterone-resistant tumors and 132 genes were downregulated (Fig. 2A and B, and Supplementary Table S1). Amongst the 30 most upregulated and downregulated genes, only GATA2 has been shown to associate with AR and may contribute to enhancing AR activity, and we did not observe consistent increases in any established AR coactivator proteins or decreases in AR corepressors (Fig. 2A and B). Gene ontology analysis using the Database for Annotation, Visualization and Integrated Discovery system showed only weak enrichment for genes associated with histone acetylation amongst the genes that were upregulated in the abiraterone-resistant xenografts (Fig. 2C). In contrast, the downregulated genes were most strongly associated with mitosis (Fig. 2D). This latter finding indicated that although the relapsed tumors were growing, the abiraterone was still slowing their proliferative rate relative to the CRPC tumors before starting abiraterone.

We reported previously that AR functions directly as a transcriptional repressor on a subset of genes, including the *AR* gene itself and multiple genes involved in nucleotide and DNA synthesis (21). Interestingly, 10 of the 30 most upregulated genes in the abiraterone-resistant xenografts were genes we found previously to be AR repressed in VCaP or VCaP-derived CRPC cells (Fig. 2A, in bold and colored

Published OnlineFirst January 21, 2014; DOI: 10.1158/1078-0432.CCR-13-1863

red). Microarray analyses also showed increases in many additional AR-repressed genes in the abiraterone-resistant xenografts (Fig. 2E). Taken together, these findings indicate that the transcriptional activation functions of AR were largely restored in these abiraterone-resistant xenografts, but that its function as a transcriptional repressor (which requires somewhat higher androgen levels) was diminished. As the predominant functions of AR-repressed genes are related to nucleotide and DNA synthesis (21), their increased expression may be contributing to proliferation in the abiraterone-relapsed xenografts.

Structural alterations in AR in abiraterone-resistant xenografts

VCaP cells have an amplified AR that is wild-type (25), and Sanger sequencing of AR from the abiraterone-relapsed xenografts did not reveal any AR mutations (not shown). To identify mutations that may be present in a subset of resistant cells or in only one of the amplified *AR* genes, and therefore present in a minority of AR transcripts, we also performed RNA-seq on three abiraterone-resistant xenografts. However, this analysis only identified AR mutations at low frequencies that were not shared amongst the xenografts and were of unclear functional significance (Supplementary Table S3; RNA-seq data are available in the NCBI Sequence Real Archive: SRP019503).

Previous studies have shown that AR can undergo alternative splicing from exon 3 in the DNA-binding domain (LBD) to cryptic exons in intron 3 or to exon 8 (14–20). These AR isoforms lack the carboxyl-terminal (C-terminal) LBD and can have ligand-independent constitutive activity that may mediate resistance to androgen deprivation therapy and to AR antagonists that target the LBD. Using RT-PCR with primer sets specific for AR-V1 to V7 and V12 in the VCaP xenografts, the only variant we could consistently detect was AR-V7 (not shown). Consistent with this result, using paired-end RNA-seq in three abiraterone-resistant VCaP xenografts, the only AR variant we detected was AR-V7. Relative to transcripts containing exon 3 spliced to exon 4, the abundance of transcripts containing exon 3 spliced to the V7 cryptic exon was 1.0% (1/99), 0.9% (48/5,323), and 0.2% (5/2,223).

As shown in Fig. 3A, AR-V7 was readily detectable and consistently increased in the abiraterone-resistant xenografts relative to levels in biopsies from the matched CRPC xenografts before starting abiraterone. AR-FL was also increased, but the increase in AR-V7 expression seemed to be greater. This was confirmed by qRT-PCR for AR-V7 versus AR-FL in the pre- and postabiraterone-treated tumors (Fig. 3B). We further assessed expression of AR-V7 and AR-FL in a series of previously described VCaP xenografts that were biopsied before castration (androgen dependent), at 4 days postcastration, or at relapse after castration (12). AR-V7 expression was increased at 4 days, was further increased in the relapsed castration-resistant xenografts, and these fold increases in AR-V7 were greater than those of AR-FL (Fig. 3C). As summarized in Fig. 3D, the mean increase of AR-V7 expression was 53-fold during the development of castration resistance, whereas AR-FL was increased to a lesser extent (10-fold). Similarly, AR-V7 was increased approximately 3-fold in abiraterone-resistant xenografts relative to levels in castration-resistant xenografts before abiraterone, whereas AR-FL was less increased (1.4-fold).

Androgen preferentially suppresses expression of AR-V7 versus AR-FL

We reported previously that *AR* gene transcription is rapidly repressed by the androgen-liganded AR through AR binding to a site in intron 2 of the *AR* gene (21). Therefore, we next addressed whether the increase in AR-V7 may reflect this feedback mechanism, versus selection for subpopulations of cells expressing higher AR-V7. Consistent with our previous results, VCaP cells cultured in steroid-depleted medium expressed high levels of AR-FL mRNA that were substantially decreased after 24 hours treatment with DHT (Fig. 4A, right). AR-FL mRNA was similarly decreased by DHT in VCS2 cells, which were derived from a castration-resistant VCaP xenograft (2). Significantly, DHT treatment caused an even greater decrease in the levels of AR-V7 in both the VCaP and VCS2 cells (∼20- and ∼80-fold in VCaP and VCS2 cells, respectively; Fig. 4A, left). AR-V7 is also expressed in high passage LNCaP cells (LN-HP) and in the LNCaP-derived C4-2 line. Although its levels are lower than in VCaP, DHT in both of these lines similarly decreased AR-V7 expression to a greater extent than AR-FL (Fig. 4B).

Examining a DHT dose response in VCaP cells, we found that AR-V7 was decreased by approximately 80% at 0.1 nmol/L DHT versus approximately 60% for AR-FL, and that AR-V7 was further markedly decreased by >95% at 1 to 10 nmol/L DHT versus approximately 80% for AR-FL (Fig. 4C). To confirm that the effects of DHT were mediated by the AR-FL, we used an siRNA targeting exon 7 (siEX7; which is not present in AR-V7) to selectively deplete the AR-FL. As expected, the siEX7 markedly decreased AR-FL, but not AR-V7 (Fig. 4D). Moreover, depletion of the AR-FL by siEX7 prevented the DHT-mediated decrease in AR-V7. To determine whether DHT may be preferentially enhancing degradation of the AR-V7 transcript, we assessed AR-V7 and AR-FL mRNA levels after treatment with actinomycin D to block new mRNA synthesis. Consistent with our previous results (21), DHT did not increase degradation of AR-FL mRNA (Fig. 4E, bottom). Significantly, DHT similarly did not increase degradation of the AR-V7 transcript, which instead seemed to be somewhat more stable in the presence of DHT (Fig. 4E, top). These results indicate that increased mRNA degradation does not account for the relative decrease in AR-V7 versus AR-FL in response to DHT.

Interestingly, examination of AR-FL versus AR-V7 transcripts over a 24-hour time-course showed that both declined similarly in response to DHT for approximately 8 hours, and that there was further loss primarily of AR-V7 between 8 to 24 hours (Fig. 4F; DHT+DMSO). Treatment with DHT and cycloheximide (CHX), which blocks new protein synthesis, abrogated the decline in AR-V7 at 24 hours (Fig. 4F; DHT+CHX), indicating that an androgen-stimulated increased in the synthesis of one or more proteins

Published OnlineFirst January 21, 2014; DOI: 10.1158/1078-0432.CCR-13-1863

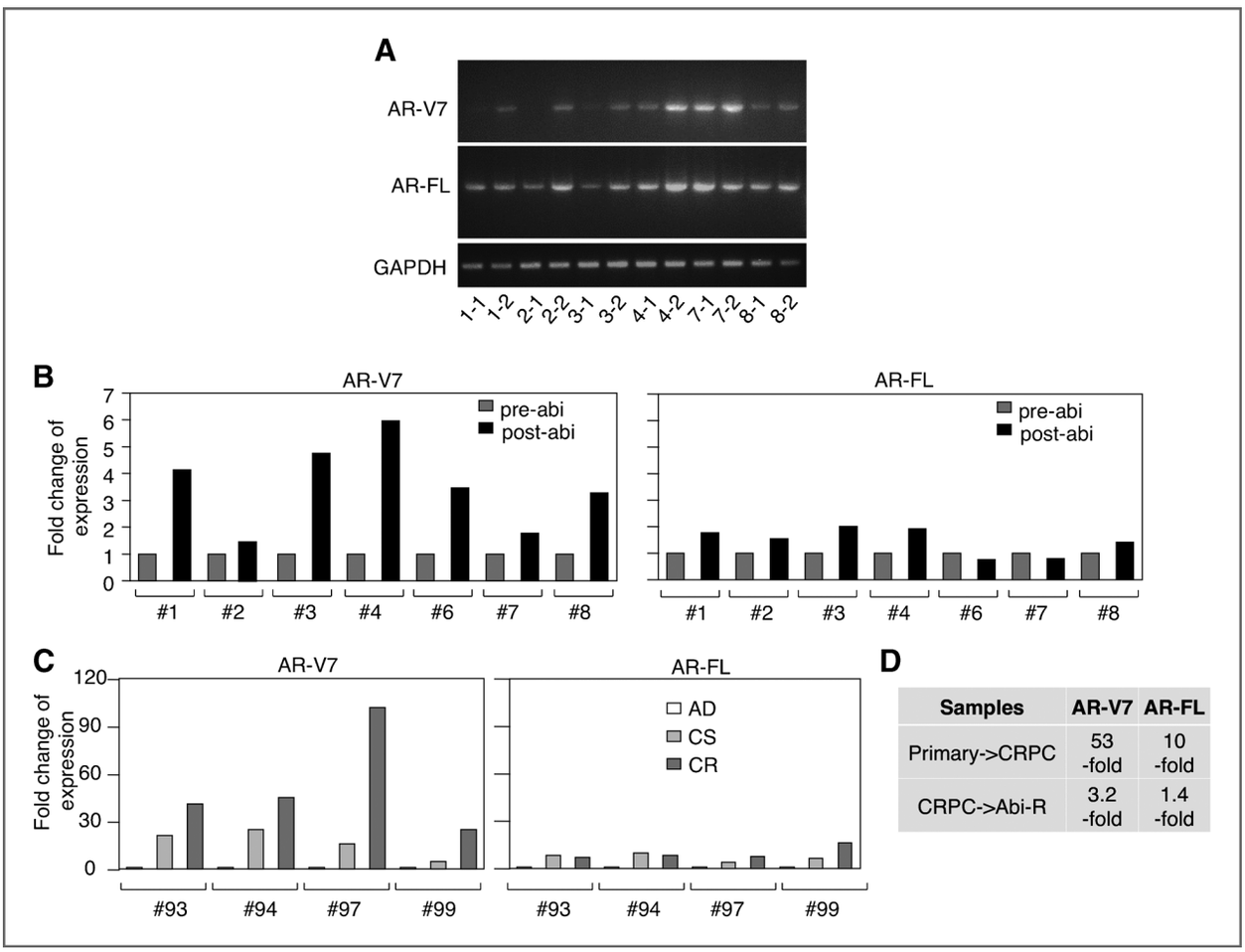

Figure 3. Structural alterations in AR in abiraterone-resistant xenografts. A and B, expression of AR-V7 transcripts versus AR-FL in a series of VCaP xenografts (1–4, 7, 8) were examined using semiquantitative RT-PCR (−1, preabiraterone; −2, postabiraterone; (A) or real-time RT-PCR (B). C, VCaP xenografts were established and biopsied at three stages: androgen-dependent tumor (AD), 4d postcastration (CS), and castration-resistant relapsed tumor (CR). Expression of AR-V7 and AR-FL was examined in four sets of these tumor samples. D, fold-change in expression of AR-V7 and AR-FL in different stages of xenograft tumors are summarized.

mediates the preferential decline in AR-V7 versus AR-FL mRNAs. These may be splicing factors, but also may be proteins that enhance RNA II polymerase elongation and thereby prevent stalling and premature chain termination in intron 3. In any case, our overall conclusion from these data is that the increased expression of AR-V7 in the castration-resistant and abiraterone-resistant xenografts reflects a feedback mechanism that rapidly increases AR-V7 relative to AR-FL at low androgen levels, rather than selective pressure for subsets of cells expressing higher AR-V7.

AR-V7 contribution to AR activity after androgen deprivation

AR-V7 has been detected in prostate cancer cell lines as well as in clinical samples, and higher AR-V7 staining has been associated with progression to CRPC (16–19, 26–28). Functional analyses based on ectopic expression demonstrated that AR-V7 is constitutively active and can induce CRPC growth (16, 29). However, the contribution of endogenous AR-V7, which seems to be expressed at low levels relative to AR-FL, to AR activity remains to be clarified. As noted above, despite the marked increases in AR-V7 mRNA in the castration-resistant VCaP xenografts, and further increases in the abiraterone-resistant xenografts, RNA-seq indicated that AR-V7 mRNA in the abiraterone-resistant xenografts was still only a small fraction (<1%) of total AR mRNA. However, as AR-V7 protein could be higher than suggested by the mRNA levels, we next assessed AR-V7 protein. Immunoblotting of proteins extracted from biopsies of androgen-dependent VCaP xenografts and the matched castration-resistant VCaP xenografts showed only a very minor band migrating at the predicted position of AR-V7, consistent with the low mRNA levels (Fig. 5A). Quantitative analysis of the AR-V7 and AR-FL bands indicated that AR-V7 protein was expressed at approximately 1.0% to 1.5% of the AR-FL levels in castration-resistant xenografts, which was at least 10-fold higher than the AR-V7 to AR-FL ratio in the androgen-dependent xenografts.

Published OnlineFirst January 21, 2014; DOI: 10.1158/1078-0432.CCR-13-1863

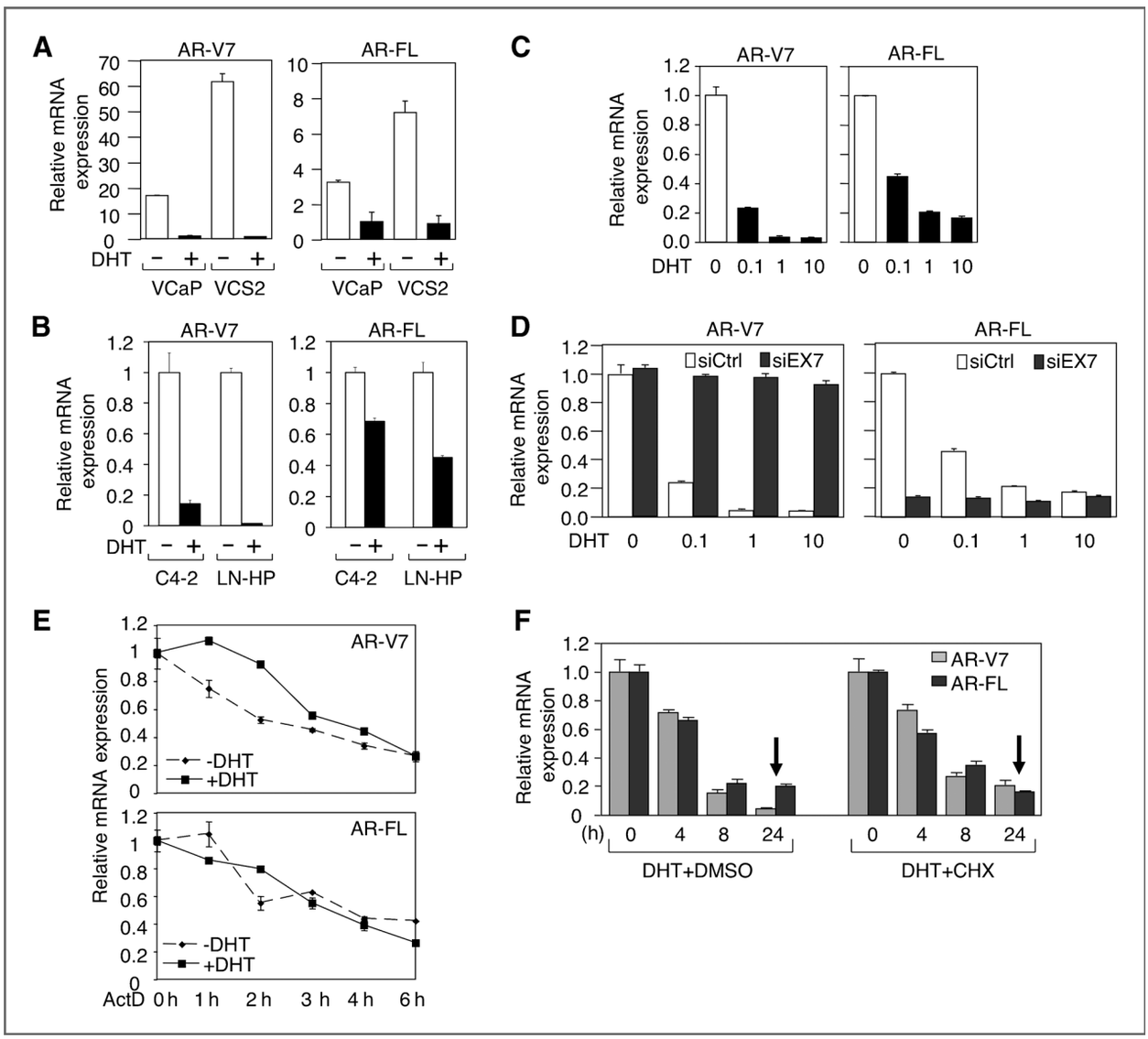

Figure 4. Androgen preferentially suppresses expression of AR-V7 versus AR-FL. A, VCaP or VCS2 cells were treated with 10 nmol/L DHT or vehicle (ethanol) for 24 hours and mRNA for AR-V7 or AR-FL were measured using qRT-PCR (GAPDH as internal normalization control). B, C4-2 and high-passage LNCaP (LN-HP) cells were androgen deprived for 3 or 10 days, respectively, before being treated with 10 nmol/L DHT for overnight. RNA samples were subjected to qRT-PCR for AR-V7 and AR-FL. C, VCaP cells were treated with increasing doses of DHT (0–10 nmol/L) for 24 hours. RNA samples were subjected to qRT-PCR for AR-V7 and AR-FL expression, and the levels shown are normalized to the levels in the absence of added DHT. D, VCaP cells were transfected with siRNA against exon 7 of AR-FL (siEX7) for 48 hours and then treated with 0 to 10 nmol/L DHT for 24 hours. RNA samples were subjected to qRT-PCR. E and F, VCaP cells were pretreated with/out DHT for 2 hours followed by addition of actinomycin D (10 μmol/L) for 0 to 6 hours (E) or cycloheximide (10 μg/mL) for 0 to 24 hours (F). Note: all cells were androgen starved by culturing in steroid-depleted medium before treatments.

Immunoblotting of VCaP cells cultured *in vitro* in androgen-depleted medium similarly showed low levels of a protein that migrated at the predicted position of AR-V7 (Fig. 5B). Consistent with this protein being AR-V7, it was not detected by an antibody directed against the AR C-terminus, and its expression was markedly decreased by treatment with DHT (Fig. 5B). To confirm VCaP expression of AR-V7 protein, VCaP cells in androgen-depleted medium were treated with siCE3. This markedly decreased the faster migrating AR band without decreasing AR-FL (Fig. 5B). In contrast, both the AR-FL and AR-V7 bands were decreased by siEX1. Finally, immunoblotting with an AR-V7–specific antibody further supported the conclusion that the lower AR band was AR-V7 (Fig. 5B, AR-V7). The AR-V7 and AR-FL bands were quantified and AR-V7 versus AR-FL ratio was approximately 1.6% in the negative control siRNA (siCtrl), and was markedly decreased by addition of DHT (siCtrl+DHT). Overall these results indicate that AR-V7 protein, although increased after androgen deprivation, is still expressed at

Published OnlineFirst January 21, 2014; DOI: 10.1158/1078-0432.CCR-13-1863

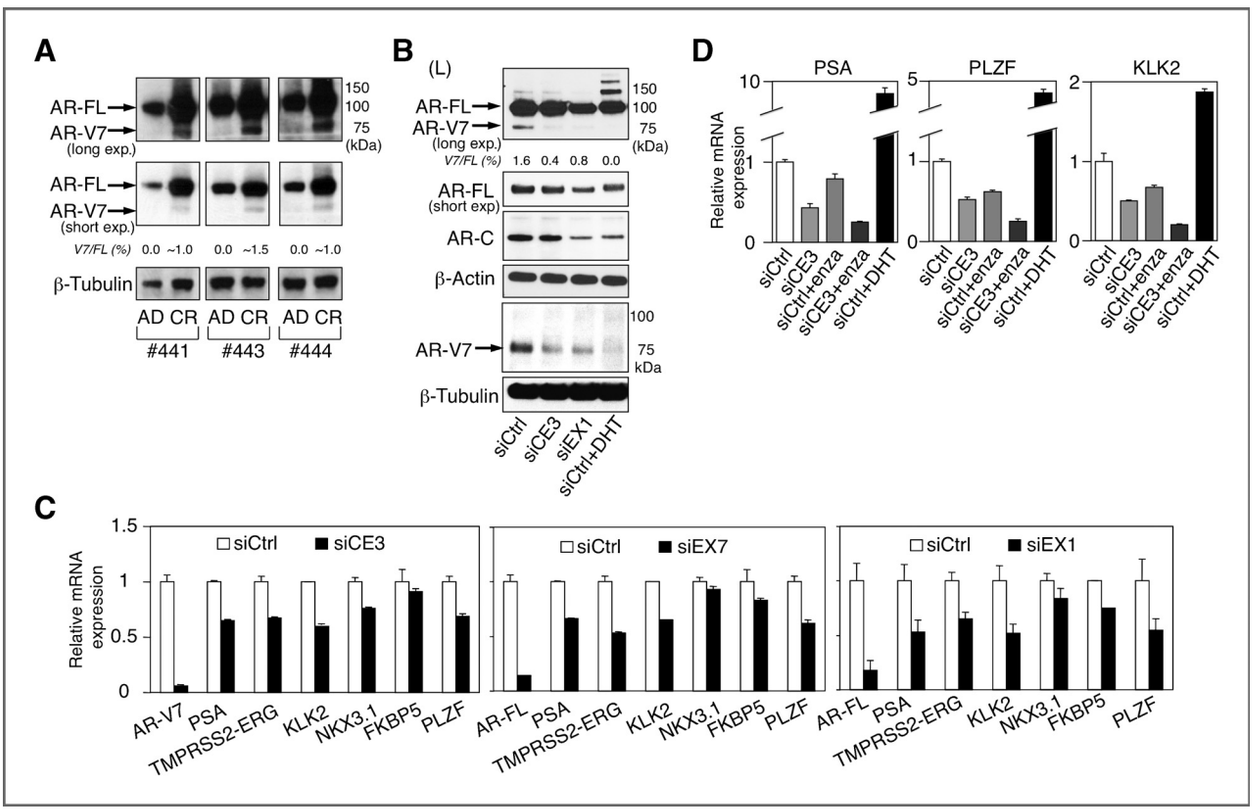

Figure 5. AR-V7 contributes for AR activity in hormone depleted conditions. A, AR protein in androgen-dependent (AD) or castration-resistant (CR) VCaP xenograft tumors was immunoblotted, with β-tubulin as loading control. The AR-V7 and AR-FL bands were quantified using NIH ImageJ software in comparison with band intensity on blots with serial dilutions of AR, and values were further normalized to β-tubulin. Ratios of AR-V7 versus AR-FL expression are presented. B, VCaP cells were transfected with siRNA against nontarget control (siCtrl), siCE3, or siEX1 followed with treatment of DHT or vehicle for 24 hours, and lysates were then immunoblotted with AR N- or C-terminal antibodies or an AR-V7–specific antibody. β-actin and β-tubulin were used as loading control. The AR-V7 and AR-FL bands were quantified as in A and presented as ratios of AR-V7 versus AR-FL. C, effects of siCE3, siEX7 (siRNA against exon 7), and siEX1 (of both AR-FL and AR-V7) on a panel of androgen-stimulated genes in androgen-starved VCaP cells. D, androgen-deprived VCaP cells were transfected with siCtrl or siCE3 for 24 hours and then treated with enzalutamide (enza, 10 μmol/L) or vehicle (DMSO) for overnight. SiCtrl-transfected VCaP cells treated with DHT were included as a positive control for AR activation. RNA samples were subjected to qRT-PCR for *PSA*, *PLZF*, *KLK2*, and *GAPDH* (as internal control).

low levels compared with AR-FL, and that this is consistent with the low levels of AR-V7 mRNA.

Culturing VCaP cells in steroid-depleted medium markedly reduces their AR transcriptional activity compared with androgen-stimulated VCaP cells, but they still retain basal AR activity that can be further reduced by blocking *de novo* androgen synthesis with abiraterone or other agents (2). To assess whether AR-V7 contributes to this basal AR transcriptional activity, we transfected VCaP cells in steroid depleted with siRNA targeting AR-V7 (siCE3). Compared with the control siRNA (siCtrl), depletion of AR-V7 decreased mRNA for a series of AR-regulated genes by approximately 30% (Fig. 5C, left). An siRNA targeting AR-FL (siEX7) decreased these AR-regulated genes to a similar degree (Fig. 5C, middle). Expression of these genes was not substantially further decreased by transfecting the cells with an siEX1 to knockdown both AR-FL and AR-V7, which may reflect an inability to adequately downregulate AR in a subset of the cells (Fig. 5C, right). In contrast, when we used enzalutamide to block activation of the AR-FL by residual androgens, we found that expression of AR-regulated genes could be further reduced by knockdown of AR-V7 (Fig. 5D). Taken together these findings indicate that the rapid induction of AR-V7 protein, although still expressed at low levels, can contribute to maintaining a low basal level of AR transcriptional activity immediately after androgen deprivation therapy. However, these findings further indicate that AR-V7 expressed at these levels is not a major contributor to the high-level AR activity observed in castration-resistant or abiraterone-relapsed tumors.

AR-V7 mRNA expression in CRPC clinical samples

We previously analyzed RNA from a series of CRPC bone marrow metastases and showed that AR-regulated genes were highly expressed, although their levels were not fully restored to those in primary prostate cancers before castration (6). To determine the potential contribution of AR-V7 to this AR activity, we used qRT-PCR to assess expression of AR-V7 and AR-FL in these clinical samples relative to VCaP cells. Significantly, AR-V7 mRNA in some clinical samples

Published OnlineFirst January 21, 2014; DOI: 10.1158/1078-0432.CCR-13-1863

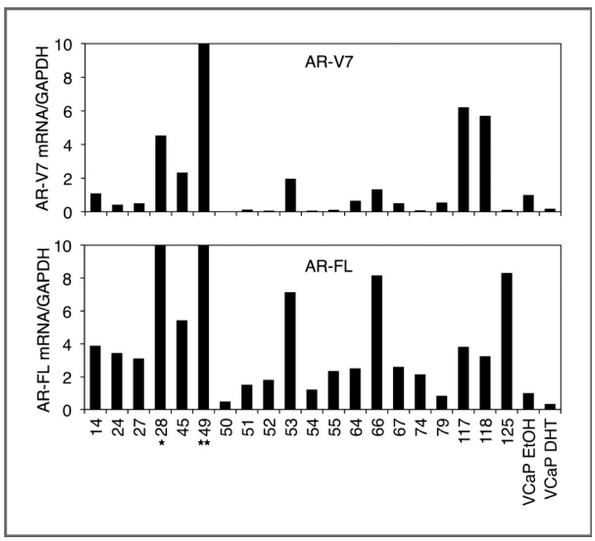

Figure 6. AR-V7 expression in CRPC patient samples. Expression of AR-V7 and AR-FL were assessed by qRT-PCR in 20 CRPC bone marrow biopsy tumor samples, with GAPDH coamplified as an internal control. The levels for each are normalized to those in androgen-starved VCaP cells (VCaP cells treated with ethanol vehicle control). The bottom panel shows the ratios of AR-V7 versus AR-FL, which are similarly normalized to the ratio in androgen-starved VCaP cells. *, AR-FL in sample 28 was 17.0-fold relative to androgen-deprived VCaP cells; **, AR-V7 and AR-FL in sample 49 were 14.0- and 860-fold, respectively, relative to those in the androgen-deprived VCaP cells.

was markedly higher than in androgen-deprived VCaP cells, suggesting that it could be making a more substantial contribution to AR activity in some tumors (Fig. 6, top; all levels are normalized to the level in androgen-deprived VCaP cells). However, these samples also had corresponding increases in AR-FL, indicating that the increase in AR-V7 may reflect primarily an increase in overall AR gene transcription rather than a marked shift in splicing toward AR-V7 (Fig. 6, bottom). However, it should be noted that the therapies in these patients did not include abiraterone, suggesting that substantial intratumoral androgens may be suppressing generation of AR-V7, and that ongoing studies of patients relapsing on abiraterone or enzalutamide may reveal higher levels of AR-V7 or other AR splice variants relative to AR-FL.

Discussion

Intratumoral androgen synthesis is now well established as a mechanism that contributes to AR reactivation after castration, but its role in resistance to CYP17A1 inhibitors or AR antagonists is not clear. Results in this study show that intratumoral levels of androstenedione, testosterone, and DHT are not restored in abiraterone-resistant VCaP xenografts. A recent study similarly found that androgen levels remained low in bone marrow aspirates from patients with abiraterone-resistant tumors (24). Importantly, although these findings indicate that full restoration of androgen synthesis is not a common mechanisms of abiraterone resistance, the AR may remain dependent on the low levels of androgen that are still being produced. Indeed, previous studies have shown that AR may become sensitized to low levels of androgen through a variety of mechanisms (30). Amongst the genes that were increased in the abiraterone-resistant VCaP xenografts, GATA2 was previously shown to cooperate with AR in the activation of multiple androgen-regulated genes (31). However, we did not observe increases in other well-characterized AR coactivators or decreases in AR corepressors. Interestingly, a negative regulator of the phosphoinositide 3-kinase pathway (PIK3IP1) was one of the most upregulated genes in the abiraterone-resistant xenografts. Recent studies show that the PI3 kinase pathway inhibition may enhance AR signaling (32, 33), but the basis for this effect seen in PTEN-deficient mouse models is not clear and studies in other models have yielded conflicting results (34–36). We also observed increased expression of BMX, a nonreceptor tyrosine kinase shown previously to enhance AR activity and to be increased in CRPC (37, 38). We recently reported that BMX enhances the activity of multiple receptor tyrosine kinases by phosphorylating a regulatory site in their kinase domains, but its role in CRPC remains to be established (39). Finally, expression of the mineralocorticoid receptor (NR3C2) was also increased, but its potential contribution to AR signaling remains to be determined.

A further mechanism implicated in resistance to androgen deprivation therapies is increased expression of constitutively active AR splice variants that have deleted the LBD (10, 14–20). Indeed, as observed here, previous reports found that AR variants were increased in prostate cancer xenografts after treatment with abiraterone or enzalutamide (10, 40). Analyses of our abiraterone-resistant VCaP xenografts showed that AR-V7 was the only consistently expressed AR variant. Expression of both AR-FL and AR-V7 transcripts were increased in the castration-resistant VCaP xenografts, and were further increased in the abiraterone-resistant xenografts. Significantly, the fold increase in AR-V7 was markedly more than for AR-FL, which suggested that there may be positive selection for cells with increased AR-V7. However, further studies showed that the increase in AR-V7 reflected rapid feedback mechanisms rather than selection for subclones with increased AR-V7. Consistent with our report showing that *AR* gene transcription is negatively regulated by agonist-liganded AR (21), we found that DHT rapidly decreased expression of both AR-FL and AR-V7. Moreover, we found that generation of AR-V7 was further suppressed by DHT through an additional mechanism that was dependent on AR-FL and required new protein synthesis. Significantly, a report that came out while this study was under review found that androgen deprivation could increase recruitment of certain splicing factors that enhanced splicing of AR pre-mRNA to AR-V7 (41). Further studies are needed to determine whether new proteins synthesized in response to DHT impair the recruitment of these splicing factors or suppress AR-V7 by other mechanisms, and whether they have broader roles in AR function.

Published OnlineFirst January 21, 2014; DOI: 10.1158/1078-0432.CCR-13-1863

Despite the marked fold increase in *AR-V7* mRNA during the development of castration and abiraterone resistance, AR-V7 mRNA remained at low levels compared with that of AR-FL (<1%). Moreover, although AR-V7 protein may be somewhat more stable than AR-FL under some conditions (29, 42), we found that AR-V7 protein was similarly present at very low levels relative to AR-FL in castration-resistant VCaP xenografts and in androgen-starved VCaP cells *in vitro*. As AR activity in the androgen-starved VCaP cells *in vitro* is markedly decreased, these observations indicate that AR-V7 expressed at these low levels is unlikely to be the major factor driving high-level AR activity in the castration- or abiraterone-resistant xenografts. Nonetheless, the functional analysis of AR-V7 in androgen-starved VCaP cells showed that it could make a substantial contribution to the residual basal AR activity under conditions where AR-FL is impaired. Therefore, we hypothesize that the rapid induction of AR-V7 immediately after androgen deprivation, mediated by both an increase in AR gene transcription and a decrease in androgen-regulated factors that suppress generation of the AR-V7 splice variant, represents a mechanism by which tumor cells retain low levels of AR activity needed for survival until more potent mechanisms emerge. Importantly, this would suggest that agents targeting AR splice variants may be most effective when used early in conjunction with androgen deprivation or antagonists that target the LBD, and that their efficacy may be markedly diminished if used later at relapse when additional mechanisms are driving AR activity. An exception may be in tumors expressing very high levels of AR splice variants relative to AR-FL. Although these tumors currently seem to be infrequent, and may occur primarily due to structural alterations in the *AR* gene (14, 18, 27, 43), they may become frequent as patients become resistant to more potent agents targeting the AR LBD.

Disclosure of Potential Conflicts of Interest

P.S. Nelson is a consultant/advisory board member for Janssen (Johnson and Johnson). S.P. Balk is a consultant/advisory board member for Astellas, Johnson and Johnson, and Tokai. No potential conflicts of interest were disclosed by the other authors.

Authors' Contributions

Conception and design: Z. Yu, C. Cai, S.P. Balk
Development of methodology: Z. Yu, S. Chen, A.G. Sowalsky, C. Cai
Acquisition of data (provided animals, acquired and managed patients, provided facilities, etc.): Z. Yu, A.G. Sowalsky, O. Voznesensky, E.A. Mostaghel, P.S. Nelson
Analysis and interpretation of data (e.g., statistical analysis, biostatistics, computational analysis): Z. Yu, A.G. Sowalsky, P.S. Nelson, C. Cai, S.P. Balk
Writing, review, and/or revision of the manuscript: Z. Yu, A.G. Sowalsky, E.A. Mostaghel, C. Cai, S.P. Balk
Administrative, technical, or material support (i.e., reporting or organizing data, constructing databases): Z. Yu, A.G. Sowalsky, O. Voznesensky, C. Cai, S.P. Balk
Study supervision: C. Cai, S.P. Balk

Acknowledgments

The authors thank Drs. Brett Marck and Alvin Matsumoto (University of Washington, Seattle, WA) for mass spectrometry assays, and Dr. Jun Luo (Johns Hopkins University, Baltimore, MD) and Dr. Chen-Lin Hsie (Dana-Farber Cancer Institute, Boston, MA) for AR-V7–specific qRT-PCR primers.

Grant Support

This work was supported by a Department of Defense Prostate Cancer Research Program Postdoctoral Training Award (W81XWH-12-PCRP-PTA to Z. Yu and A. Sowalsky), Idea Development Awards (W81XWH-11-1-0295, W81XWH-08-1-0414, and W81XWH07-1-0443 to S.P. Balk), DF/HCC-Prostate Cancer SPORE P50 CA090381 (to C. Cai and S.P. Balk), NIH K99 award CA166507 (to C. Cai), NIH P01 CA163227-01A1, and Prostate Cancer Foundation Challenge Award (S.P. Balk, E. Mostaghel, and P.S Nelson), PNW Prostate SPORE P50CA097186 and DOD PC093509 (P. Nelson and E. Mostaghel).

The costs of publication of this article were defrayed in part by the payment of page charges. This article must therefore be hereby marked *advertisement* in accordance with 18 U.S.C. Section 1734 solely to indicate this fact.

Received July 7, 2013; revised December 20, 2013; accepted January 9, 2014; published OnlineFirst January 21, 2014.

References

1. Cai C, Balk SP. Intratumoral androgen biosynthesis in prostate cancer pathogenesis and response to therapy. Endocr Relat Cancer 2011;18:R175–82.
2. Cai C, Chen S, Ng P, Bubley GJ, Nelson PS, Mostaghel EA, et al. Intratumoral de novo steroid synthesis activates androgen receptor in castration-resistant prostate cancer and is upregulated by treatment with CYP17A1 inhibitors. Cancer Res 2011;71:6503–13.
3. Locke JA, Guns ES, Lubik AA, Adomat HH, Hendy SC, Wood CA, et al. Androgen levels increase by intratumoral de novo steroidogenesis during progression of castration-resistant prostate cancer. Cancer Res 2008;68:6407–15.
4. Mohler JL, Gregory CW, Ford OH3rd, Kim D, Weaver CM, Petrusz P, et al. The androgen axis in recurrent prostate cancer. Clin Cancer Res 2004;10:440–8.
5. Montgomery RB, Mostaghel EA, Vessella R, Hess DL, Kalhorn TF, Higano CS, et al. Maintenance of intratumoral androgens in metastatic prostate cancer: a mechanism for castration-resistant tumor growth. Cancer Res 2008;68:4447–54.
6. Stanbrough M, Bubley GJ, Ross K, Golub TR, Rubin MA, Penning TM, et al. Increased expression of genes converting adrenal androgens to testosterone in androgen-independent prostate cancer. Cancer Res 2006;66:2815–25.
7. de Bono JS, Logothetis CJ, Molina A, Fizazi K, North S, Chu L, et al. Abiraterone and increased survival in metastatic prostate cancer. N Engl J Med 2011;364:1995–2005.
8. Ryan CJ, Smith MR, de Bono JS, Molina A, Logothetis CJ, de Souza P, et al. Abiraterone in metastatic prostate cancer without previous chemotherapy. N Engl J Med 2013;368:138–48.
9. Sartor O, Pal SK. Abiraterone and its place in the treatment of metastatic CRPC. Nat Rev 2013;10:6–8.
10. Mostaghel EA, Marck BT, Plymate SR, Vessella RL, Balk S, Matsumoto AM, et al. Resistance to CYP17A1 inhibition with abiraterone in castration-resistant prostate cancer: induction of steroidogenesis and androgen receptor splice variants. Clin Cancer Res 2011;17:5913–25.
11. Yuan X, Cai C, Chen S, Chen S, Yu Z, Balk SP. Androgen receptor functions in castration-resistant prostate cancer and mechanisms of resistance to new agents targeting the androgen axis. Oncogene 2013 Jun 10. [Epub ahead of print].
12. Cai C, Wang H, Xu Y, Chen S, Balk SP. Reactivation of androgen receptor-regulated TMPRSS2:ERG gene expression in castration-resistant prostate cancer. Cancer Res 2009;69:6027–32.
13. Loberg RD, St John LN, Day LL, Neeley CK, Pienta KJ. Development of the VCaP androgen-independent model of prostate cancer. Urol Oncol 2006;24:161–8.

Published OnlineFirst January 21, 2014; DOI: 10.1158/1078-0432.CCR-13-1863

14. Dehm SM, Schmidt LJ, Heemers HV, Vessella RL, Tindall DJ. Splicing of a novel androgen receptor exon generates a constitutively active androgen receptor that mediates prostate cancer therapy resistance. Cancer Res 2008;68:5469–77.
15. Dehm SM, Tindall DJ. Alternatively spliced androgen receptor variants. Endocr Relat Cancer 2011;18:R183–96.
16. Guo Z, Yang X, Sun F, Jiang R, Linn DE, Chen H, et al. A novel androgen receptor splice variant is up-regulated during prostate cancer progression and promotes androgen depletion-resistant growth. Cancer Res 2009;69:2305–13.
17. Hu R, Dunn TA, Wei S, Isharwal S, Veltri RW, Humphreys E, et al. Ligand-independent androgen receptor variants derived from splicing of cryptic exons signify hormone-refractory prostate cancer. Cancer Res 2009;69:16–22.
18. Li Y, Alsagabi M, Fan D, Bova GS, Tewfik AH, Dehm SM. Intragenic rearrangement and altered RNA splicing of the androgen receptor in a cell-based model of prostate cancer progression. Cancer Res 2011; 71:2108–17.
19. Sun S, Sprenger CC, Vessella RL, Haugk K, Soriano K, Mostaghel EA, et al. Castration resistance in human prostate cancer is conferred by a frequently occurring androgen receptor splice variant. J Clin Invest 2010;120:2715–30.
20. Watson PA, Chen YF, Balbas MD, Wongvipat J, Socci ND, Viale A, et al. Constitutively active androgen receptor splice variants expressed in castration-resistant prostate cancer require full-length androgen receptor. Proc Natl Acad Sci U S A 2010;107:16759–65.
21. Cai C, He HH, Chen S, Coleman I, Wang H, Fang Z, et al. Androgen receptor gene expression in prostate cancer is directly suppressed by the androgen receptor through recruitment of lysine-specific demethylase 1. Cancer Cell 2011;20:457–71.
22. Thorvaldsdottir H, Robinson JT, Mesirov JP. Integrative Genomics Viewer (IGV): high-performance genomics data visualization and exploration. Briefings in Bioinformatics 2011;14:178–92.
23. Cai C, Wang H, He HH, Chen S, He L, Ma F, et al. ERG induces androgen receptor-mediated regulation of SOX9 in prostate cancer. J Clin Invest 2013;123:1109–22.
24. Efstathiou E, Titus M, Tsavachidou D, Tzelepi V, Wen S, Hoang A, et al. Effects of abiraterone acetate on androgen signaling in castrate-resistant prostate cancer in bone. J Clin Oncol 2012;30:637–43.
25. Waltering KK, Helenius MA, Sahu B, Manni V, Linja MJ, Janne OA, et al. Increased expression of androgen receptor sensitizes prostate cancer cells to low levels of androgens. Cancer Res 2009;69:8141–9.
26. Hornberg E, Ylitalo EB, Crnalic S, Antti H, Stattin P, Widmark A, et al. Expression of androgen receptor splice variants in prostate cancer bone metastases is associated with castration-resistance and short survival. PloS one 2011;6:e19059.
27. Li Y, Hwang TH, Oseth LA, Hauge A, Vessella RL, Schmechel SC, et al. AR intragenic deletions linked to androgen receptor splice variant expression and activity in models of prostate cancer progression. Oncogene 2012;31:4759–67.
28. Zhang X, Morrissey C, Sun S, Ketchandji M, Nelson PS, True LD, et al. Androgen receptor variants occur frequently in castration resistant prostate cancer metastases. PLoS ONE. 2011;6:e27970.
29. Chan SC, Li Y, Dehm SM. Androgen receptor splice variants activate androgen receptor target genes and support aberrant prostate cancer cell growth independent of canonical androgen receptor nuclear localization signal. J Biol Chem 2012;287:19736–49.
30. Yuan X, Balk SP. Mechanisms mediating androgen receptor reactivation after castration. Urol Oncol 2009;27:36–41.
31. Wang Q, Li W, Liu XS, Carroll JS, Janne OA, Keeton EK, et al. A hierarchical network of transcription factors governs androgen receptor-dependent prostate cancer growth. Mol Cell 2007;27:380–92.
32. Carver BS, Chapinski C, Wongvipat J, Hieronymus H, Chen Y, Chandarlapaty S, et al. Reciprocal feedback regulation of PI3K and androgen receptor signaling in PTEN-deficient prostate cancer. Cancer Cell 2011;19:575–86.
33. Mulholland DJ, Tran LM, Li Y, Cai H, Morim A, Wang S, et al. Cell autonomous role of PTEN in regulating castration-resistant prostate cancer growth. Cancer Cell 2011;19:792–804.
34. Ha S, Ruoff R, Kahoud N, Franke TF, Logan SK. Androgen receptor levels are upregulated by Akt in prostate cancer. Endocr Relat Cancer 2011;18:245–55.
35. Lin HK, Hu YC, Yang L, Altuwaijri S, Chen YT, Kang HY, et al. Suppression versus induction of androgen receptor functions by the phosphatidylinositol 3-kinase/Akt pathway in prostate cancer LNCaP cells with different passage numbers. J Biol Chem 2003;278:50902–7.
36. Mellinghoff IK, Vivanco I, Kwon A, Tran C, Wongvipat J, Sawyers CL. HER2/neu kinase-dependent modulation of androgen receptor function through effects on DNA binding and stability. Cancer Cell 2004; 6:517–27.
37. Dai B, Chen H, Guo S, Yang X, Linn DE, Sun F, et al. Compensatory upregulation of tyrosine kinase Etk/BMX in response to androgen deprivation promotes castration-resistant growth of prostate cancer cells. Cancer Res 2010;70:5587–96.
38. Dai B, Kim O, Xie Y, Guo Z, Xu K, Wang B, et al. Tyrosine kinase Etk/BMX is up-regulated in human prostate cancer and its overexpression induces prostate intraepithelial neoplasia in mouse. Cancer Res 2006; 66:8058–64.
39. Chen S, Jiang X, Gewinner CA, Asara JM, Simon NI, Cai C, et al. Tyrosine kinase BMX phosphorylates phosphotyrosine-primed motif mediating the activation of multiple receptor tyrosine kinases. Sci Signal 2013;6:ra40.
40. Hu R, Lu C, Mostaghel EA, Yegnasubramanian S, Gurel M, Tannahill C, et al. Distinct transcriptional programs mediated by the ligand-dependent full-length androgen receptor and its splice variants in castration-resistant prostate cancer. Cancer Res 2012;72:3457–62.
41. Liu LL, Xie N, Sun S, Plymate S, Mostaghel E, Dong X. Mechanisms of the androgen receptor splicing in prostate cancer cells. Oncogene 2013 Jul 15. [Epub ahead of print].
42. Shafi AA, Cox MB, Weigel NL. Androgen receptor splice variants are resistant to inhibitors of Hsp90 and FKBP52, which alter androgen receptor activity and expression. Steroids 2013;78:548–54.
43. Li Y, Chan SC, Brand LJ, Hwang TH, Silverstein KA, Dehm SM. Androgen receptor splice variants mediate enzalutamide resistance in castration-resistant prostate cancer cell lines. Cancer Res 2013; 73:483–9.